

# Expression, purification and biological characterisation of IFN $\epsilon$

A thesis submitted for the degree of  
**Doctor of Philosophy**

By

**Sebastian A. Stifter**  
B. Biomed Sci. (Hons)

Centre for Innate Immunity and Infectious Diseases  
Monash Institute of Medical Research  
Monash University, Australia  
March 2015



**MONASH** University

**Notice 1**

*Under the Copyright Act 1968, this thesis must be used only under the normal conditions of scholarly fair dealing. In particular no results or conclusions should be extracted from it, nor should it be copied or closely paraphrased in whole or in part without the written consent of the author. Proper written acknowledgement should be made for any assistance obtained from this thesis.*

**Notice 2**

*I certify that I have made all reasonable efforts to secure copyright permissions for third-party content included in this thesis and have not knowingly added copyright content to my work without the owner's permission.*

---

## **Table of Contents**

Abstract .....	vii
Acknowledgements.....	ix
Declaration .....	x
Abbreviations.....	xi
List of Figures.....	xvi
Chapter 1 .....	xvi
Chapter 3.....	xvii
Chapter 4.....	xviii
Chapter 5.....	xix
List of Tables .....	xx
Chapter 1 .....	xx
Chapter 2.....	xx
Chapter 3.....	xx
Chapter 5.....	xx
Chapter 1 – Literature Review .....	2
1.1 Introduction .....	2
1.2 The Interferons.....	4
1.3 Type I IFNs .....	5
1.4 Evolution of type I IFNs .....	6
1.5 Transcriptional elements of type I IFN induction .....	9
1.6 Induction of type I IFNs .....	11
1.6.1 IRFs .....	11
1.6.1.1 IRF-1 .....	12
1.6.1.2 IRF-3 .....	12
1.6.1.3 IRF-7 .....	14
1.6.1.4 IRF-9 .....	14
1.6.2 TLRs .....	16
1.6.3 RLHs.....	17
1.6.4 NLRs.....	18
1.6.5 STING, IFI16 and other DNA sensors .....	19
1.6.6 Cell type specific mechanisms of induction.....	20
1.7 Type I IFN signal transduction.....	21
1.7.1 JAK-STAT Pathway.....	21

---

1.8 Biological activities of type I IFNs .....	24
1.8.1 Antiviral Activity .....	24
1.8.2 Antiproliferative Activity .....	26
1.8.3 Pro-apoptotic Activity.....	27
1.8.4 Immunoregulatory activity.....	29
1.9 Type I IFNs in reproduction .....	31
1.10 Structure of type I IFNs .....	32
1.10.1 IFN $\alpha$ .....	33
1.10.2 IFN $\beta$ .....	34
1.10.3 Potency of IFNs.....	35
1.10.4 Surface 'hot spots' determine IFN activity.....	37
1.10.5 Crystal structures of the IFN-Receptor complex .....	39
1.11 The female reproductive tract.....	41
1.11.1 Immune Cells in the FRT .....	43
1.11.1.2 T and B Lymphocytes.....	43
1.11.1.3 Uterine NK-cells .....	43
1.11.1.4 Dendritic cells and macrophages.....	44
1.11.2 IFN $\epsilon$ – A novel type I IFN.....	45
1.13 Overview and history of expression and purification of type I IFNs ....	48
1.14 Rationale and Aims .....	51
Aims:.....	52
Chapter 2 – Materials and Methods .....	53
2.1 DNA manipulations .....	53
2.1.1 Plasmid DNA extraction.....	53
2.1.2 Agarose gel electrophoresis .....	53
2.1.3 DNA extraction from agarose gels.....	54
2.1.4 Quantification of DNA samples.....	54
2.1.5 Restriction enzyme digestions .....	54
2.1.6 DNA Ligation .....	55
2.1.7 Codon Optimization of <i>Ifne1</i> .....	55
2.1.8 His <sub>6</sub> -tagged IFN cloning and bacmid generation.....	56
2.1.9 Tagless <i>Ifne1</i> cloning and bacmid generation.....	57
2.2 RNA Manipulation .....	59
2.2.1 RNA extraction using Qiagen kit.....	59
2.2.2 Extracting RNA using TRIsure.....	59
2.2.3 cDNA preparation.....	60
2.2.4 <i>Gapdh</i> PCR.....	60

---

2.2.5 Real-Time Polymerase Chain Reaction (RT-PCR) .....	61
2.3 Tissue Culture .....	62
2.3.1 Cell counting by trypan blue exclusion.....	62
2.3.2 Cell counting by Sysmex automated cell counter.....	63
2.3.3 Thawing of frozen cells.....	63
2.3.4 Freezing of cells .....	63
2.3.5 Adherent cell passaging .....	63
2.3.6 Suspension cell passaging .....	64
2.3.7 Hybridoma cell passaging .....	64
2.3.8 Hybridoma cell subcloning.....	64
2.3.9 Establishing viral titres.....	64
2.3.10 Mouse interferon antiviral assay .....	65
2.3.11 Human interferon antiviral assay .....	65
2.3.12 Scoring viral titre and interferon antiviral activity assays.....	66
2.3.13 Antiproliferative assay .....	66
2.3.14 MHC-I upregulation by type I Interferon.....	67
2.3.15 Preparing bone marrow derived macrophages .....	67
2.3.16 Stimulating primary spleen cells for flow cytometry.....	68
2.3.17 Insect Cell Transfections and P1 baculovirus generation.....	68
2.3.18 Amplification of recombinant baculovirus stock – P2 .....	69
2.3.19 Generation of high titre recombinant baculovirus – P3.....	69
2.3.20 Insect cell expressions .....	69
2.3.21 HEK293 transfection for N-terminal sequencing .....	70
2.3.22 RAW cell stimulation for protein lysates.....	71
2.3.23 IRG - Luciferase Assays.....	71
2.3.24 IFN $\epsilon$ mAb neutralisation .....	72
2.4 Protein Manipulations.....	73
2.4.1 Biotinylation of antibodies.....	73
2.4.2 SDS-PAGE (Sodium Dodecyl Sulfate – Polyacrylamide Gel Electrophoresis) .....	73
2.4.3 Coomassie blue staining of polyacrylamide gels .....	73
2.4.4 Western Blotting.....	74
2.4.5 Enhanced Chemiluminescence (ECL) Detection .....	74
2.4.6 Odyssey Detection .....	77
2.4.7 Bradford protein assay .....	77
2.4.8 Immobilizing metal affinity chromatography (IMAC).....	77
2.4.9 Size exclusion chromatography.....	78

---

2.4.10 Reverse Phase High Performance Liquid Chromatography (RP-HPLC).....	78
2.4.11 Removal of His <sub>6</sub> -tag by enterokinase digestion.....	79
2.4.12 Immunoaffinity Column preparation.....	80
2.4.13 Immunoaffinity column IFN $\epsilon$ purification.....	80
2.4.14 Determination of secondary fold by CD-Spectra.....	80
2.4.15 Temperature and pH stability tests.....	81
2.4.16 N-terminal protein sequencing.....	81
2.4.17 Surface Plasmon Resonance (SPR).....	81
2.4.18 Endotoxin Testing.....	82
2.5 Immunology Methods.....	82
2.5.1 Hybridoma supernatant ELISA.....	82
2.5.2 Flow cytometry.....	83
2.5.3 IFN $\epsilon$ immunoprecipitation using mAbs.....	84
2.5.4 IFN $\epsilon$ Immunohistochemistry.....	85
2.5.5 IFN $\epsilon$ ELISA.....	86
2.6 Animal handling.....	86
2.6.1 Immunizing mice for monoclonal antibodies.....	86
2.6.2 ELISA of sera from immunized mice.....	87
2.6.3 Mouse organ collection for histology.....	87
2.6.4 Mouse cycle determination.....	87
2.6.5 Mouse organ collection for RNA.....	88
2.6.6 Spleen collection for cell suspensions.....	88
Chapter 3 – Expression and Purification of IFN $\epsilon$ .....	89
3.1 Introduction.....	89
3.2 Results.....	91
3.2.1 Expression of IFN $\epsilon$ in Mammalian and Bacterial Hosts.....	91
3.2.2 Generation of recombinant His <sub>6</sub> -IFN $\epsilon$ baculovirus construct.....	92
3.2.3 Expression and purification of His <sub>6</sub> -IFN $\epsilon$ in insect cells.....	94
3.2.4 Removal of N-terminal His <sub>6</sub> purification tag by Enterokinase.....	96
3.2.5 Generation of untagged recombinant IFN $\epsilon$ baculovirus.....	97
3.2.6 Expression and purification of untagged IFN $\epsilon$ in insect cells.....	98
3.2.8 Generation of recombinant His <sub>6</sub> -IFN $\beta$ baculovirus construct.....	100
3.2.9 Expression and purification of His <sub>6</sub> -IFN $\beta$ in insect cells.....	101
3.2.10 Endotoxin testing of IFN $\epsilon$ and IFN $\beta$ .....	103
3.3. Discussion.....	104
3.4 Conclusion.....	112

---

Chapter 4 – Characterisation of recombinant IFN $\epsilon$ .....	113
4.1 Introduction .....	113
4.2 Results .....	115
4.2.1 Secondary structure determination of IFN $\epsilon$ expressed from an insect cell expression system .....	115
4.2.2 Glycosylation of IFNs produced from an insect cell expression system .....	116
4.2.3 Antiviral activity of IFN $\epsilon$ .....	117
4.2.4 Antiproliferative activities of IFN $\epsilon$ .....	118
4.2.5 Induction of interferon regulated genes in primary mouse bone marrow derived macrophages .....	119
4.2.6 IRG-Luciferase reporter assays .....	121
4.2.7 STAT1 phosphorylation .....	122
4.2.8 STAT3 phosphorylation .....	124
4.2.9 Physiochemical stability of IFN $\epsilon$ .....	125
4.2.10 Upregulation of MHC-I by IFN $\epsilon$ .....	126
4.2.11 Activation of immune cell subsets by IFN $\epsilon$ .....	127
4.2.12 <i>In vivo</i> gene induction by IFN $\epsilon$ .....	130
4.2.13 Antiviral activity of murine IFN $\epsilon$ on human cells .....	131
4.2.14 Antiproliferative activity of murine IFN $\epsilon$ on human cells .....	132
4.2.15 Gene induction of human IRGs by murine IFN $\epsilon$ .....	133
4.3 Discussion .....	135
4.4 Conclusion .....	144
Chapter 5 – Generation and characterisation of anti-IFN $\epsilon$ mAbs .....	145
5.1 – Introduction .....	145
5.2 Results .....	148
5.2.1 Generation of monoclonal antibodies against IFN $\epsilon$ .....	148
5.2.2 Anti-IFN $\epsilon$ hybridoma screening by supernatant ELISA .....	149
5.2.3 Anti-IFN $\epsilon$ mAbs exhibit different abilities to detect His <sub>6</sub> -IFN $\epsilon$ by western blot .....	151
5.2.4 Identifying IFN $\epsilon$ antibody pairs for ELISA .....	152
5.2.5 Optimising IFN $\epsilon$ ELISA .....	155
5.2.6 Immunohistochemistry using anti-IFN $\epsilon$ mAbs .....	157
5.2.7 Neutralising activity of IFN $\epsilon$ mAbs .....	158
5.2.8 Immunoprecipitation of IFN $\epsilon$ with monoclonal antibodies .....	159
5.2.9 Immunoprecipitation of IFN $\epsilon$ expressed in mammalian cells and N-terminal sequencing .....	161

---

5.3 Discussion.....	164
5.4 Conclusion .....	170
Chapter 6 – Discussion and Conclusions.....	171
Appendix A – Buffers and Reagents .....	181
Appendix B – Vector Maps .....	186
Appendix C – Monash PPU Report.....	190
Appendix D – Codon optimisation of murine <i>Ifne1</i> .....	193
Appendix E - N-terminal amino acid sequencing of tagless IFN $\epsilon$ .....	195
Appendix F – Prediction of IFN $\epsilon$ signal peptide cleavage site by SignalP software .....	196
Appendix G – Primer Sequences.....	197
Appendix H – N-terminal sequencing of native IFN $\epsilon$ expressed in HEK293 cells.....	199
Appendix I – MATF ELISA IFN $\epsilon$ optimisation .....	200
Appendix J – Immunohistochemistry of uterine sections stained with anti-IFN $\epsilon$ monoclonal antibody C3.....	204
Appendix K – Highly pure IFN $\epsilon$ obtained from a single immunoaffinity step	205
Appendix L – Published manuscripts .....	206
Bibliography.....	207

---

## **Abstract**

The interferons (IFNs) are a family of pleiotropic cytokines identified in 1957 based on their antiviral activity. There are three types of IFNs of which the type I IFNs are the largest family, comprising a number of subtypes such as  $\alpha$ ,  $\beta$ ,  $\epsilon$ ,  $\delta$  and  $\kappa$ , which code for 17 proteins in humans. In the years since their discovery, more biological activities have been attributed to them. We now know that type I IFNs have antiviral, antiproliferative, apoptotic and a host of immunoregulatory functions. Intriguingly, even though all type I IFNs signal via the same cell surface receptor, they have been found to elicit different biological activities, suggesting that while type I IFNs share an overlapping signalling pathway, their biological roles and functions are non-redundant.

In 2004, our laboratory identified a novel gene in the type I IFN locus predicted to be a type I IFN based on sequence homology and designated it IFN $\epsilon$ . Further work performed in our laboratory subsequently identified that IFN $\epsilon$  is produced constitutively in the reproductive tract and provides host immunity to reproductive tract infections caused by *Chlamydia muridarum* and Herpes Simplex Virus. As IFN $\epsilon$  was a recently discovered type I IFN, there were no commercial reagents available for its study. Therefore the aims of my project were to express and purify recombinant murine IFN $\epsilon$  to a level of purity suitable for definitive biological characterisation.

Using an insect cell expression system, I was able to successfully express His<sub>6</sub>-IFN $\epsilon$  however the purification protocol we developed proved unsuitable for purifying IFN $\epsilon$  as it was found to degrade during removal of the His<sub>6</sub> tag. We therefore immunized mice with His<sub>6</sub>-IFN $\epsilon$  and through differential screening, identified a number of IFN $\epsilon$  specific monoclonal antibodies. The anti-IFN $\epsilon$  antibodies proved successful in a number of applications including

---

western-blotting, immunohistochemistry and immunoprecipitation. Using immunoaffinity chromatography, we were subsequently able to purify tagless IFN $\epsilon$  and characterise its biological functions.

Although IFN $\epsilon$  demonstrated classical type I IFN activities such as antiviral, antiproliferative and immunoregulatory activities, these were 100 – 1000x less than IFN $\alpha$  and IFN $\beta$ . Among the key findings of this thesis however was that IFN $\epsilon$  required both type I IFN receptor subunits to induce the transcription of interferon regulated genes and therefore, this is the first account of IFN $\epsilon$  being a bonafide type I IFN. Another important discovery made was that cells of the uterine luminal epithelium are the main producers of IFN $\epsilon$  in mice. Although it was known that *Ifne1* was highly expressed in the reproductive tract, the exact site of expression remained elusive.

Overall, the work performed in this thesis resulted in the production and characterisation of highly pure recombinant mouse IFN $\epsilon$  as well as the generation of a number of anti-IFN $\epsilon$  monoclonal antibodies. These novel tools will enable us to study the role and function of IFN in greater detail and enhance our understanding of interferon biology and immunity.

---

## **Acknowledgements**

I'd like to thank my supervisors Paul and Nicky for taking me on as an honours student and then supporting me throughout my PhD. There were some tough times when I really questioned my project but Paul always managed to give me a motivational speech that would see me through it. I like to say that the man could sell ice to an Eskimo and I hope some of his optimism and passion has stuck to me. I also want to thank Nicky for keeping me sane throughout the years and making me feel good by reminding me that we produce millions of dollars worth of interferon each year. If only we could sell it...

Next I want to thank my co-workers from MIMR who over the years have become close friends. There was seldom a time I didn't enjoy lunch and all the obscene/silly/stupid/idiotic/bizarre things we talked about. Lou, Kevin, Ka Yee, Jodee, Gavin, Alec, Kathryn, Alistair you really made my time at MIMR special and memorable and I'm happy to have shared it with you guys. And no, I don't have food allergies! Give it a rest.

I'd like to thank my friends Flick, Dan, Oli, Jono, Tom and everyone else outside of work for getting me blind drunk when I needed it (which was often) and for supplying me with tasty food.

Last but not least I would like to thank my parents and my brother for supporting me from far away and being there when I needed them. I know it wasn't easy for them and I'm glad they gave me the freedom to pursue my own interests.

Thank you all!

---

## **Declaration**

This is to certify that this thesis contains no material that has been accepted for the award of any other degree or diploma in any university or other institution, and to the best of my knowledge, contains no material previously published or written by another person, except where due reference is made in the text of the thesis.

---

## **Abbreviations**

<b>°C</b>	Degrees celsius
<b>aa</b>	Amino acid
<b>APC</b>	Antigen presenting cells
<b>BMDM</b>	Bone-marrow derived macrophage
<b>bp</b>	Base pair
<b>CBB</b>	Coomassie brilliant blue
<b>CD</b>	Circular Dichroism
<b>CDK</b>	Cyclin dependent kinase
<b>cDNA</b>	Complementary DNA
<b>cGAS</b>	Cyclic GMP-AMP synthase
<b>CI</b>	Confidence intervall
<b>CIID</b>	Centre for Innate Immunity and Infectious Diseases
<b>CMV</b>	Cytomegalovirus
<b>CPE</b>	Cytopathic effect
<b>CpG</b>	2'-deoxyribo(cytidine-phosphate-guanosine)
<b>CSIRO</b>	Commonwealth Scientific and Industrial Research Organisation
<b>CV</b>	Column volumes
<b>DC</b>	Dendritic cell
<b>DNA</b>	Deoxyribonucleic acid
<b>dsRNA</b>	Double-stranded RNA
<b>EAE</b>	Experimental autoimmune encephalomyelitis
<b>EC</b>	Effective concentration
<b>EK</b>	Enterokinase
<b>ELISA</b>	Enzyme-linked immunosorbent assay
<b>EMCV</b>	Encephalomyocarditis virus
<b>EU</b>	Endotoxin units
<b>FACS</b>	Fluorescence-activated cell sorting

---

<b>FRT</b>	Female reproductive tract
<b>GAS</b>	Gamma-activated sequence
<b>HCl</b>	Hydrochloric acid
<b>hIFN</b>	human IFN
<b>His<sub>6</sub></b>	Hexahistidine tag
<b>HRP</b>	Horserraddish peroxidase
<b>Hrs</b>	hours
<b>HSV</b>	Herpes Simplex Virus
<b>Ig</b>	Immunoglobulin
<b>IFN</b>	Interferon
<b>IFNAR</b>	Interferon alpha receptor
<b>IFNGR</b>	Interferon gamma receptor
<b>IL</b>	Interleukin
<b>IMAC</b>	Immobilising metal affinity chromatography
<b>IP</b>	Immunoprecipitate
<b>IRF</b>	Interferon regulatory factor
<b>IRG</b>	Interferon regulated gene
<b>ISG</b>	Interferon stimulated gene
<b>ISGF3</b>	Interferon stimulated gene factor 3
<b>ISRE</b>	Interferon stimulated response element
<b>IU</b>	International unit
<b>IV</b>	Intravaginal
<b>JAK</b>	Janus Kinase
<b>Kb</b>	Kilobases
<b>kDa</b>	Kilodaltons
<b>KO</b>	Knock-out
<b>LAL</b>	Limulus amebocyte lysate
<b>LPS</b>	Lipopolysaccharide
<b>LTA</b>	Lipotechoic acid
<b>mAb</b>	Monoclonal antibody
<b>MAPK</b>	Mitogen-activated protein kinase

---

<b>MATF</b>	Monash Antibody Technologies Facility
<b>MDP</b>	Muramyl dipeptide
<b>MEF</b>	Mouse embryonic fibroblast
<b>mg</b>	Milligram
<b>MHC</b>	Major histocompatibility complex
<b>mIFN</b>	mouse IFN
<b>MIMR</b>	Monash Institute of Medical Research
<b>mM</b>	Millimolar
<b>MSP</b>	Mellitin signal peptide
<b>MTT</b>	Methylthiazolyldiphenyl-tetrazolium bromide
<b>MWCO</b>	Molecular weight cut-off
<b>NaOH</b>	Sodium hydroxide
<b>NDV</b>	Newcastle disease virus
<b>NFκB</b>	Nuclear factor κB
<b>Ni</b>	Nickel
<b>NIH</b>	National Institutes of Health
<b>NK</b>	Natural Killer
<b>Nm</b>	Nanometres
<b>NOD</b>	Nucleotide oligomerisation domain
<b>OAS</b>	Oligoadenylate synthase
<b>pAb</b>	polyclonal antibody
<b>PAGE</b>	Polyacrylamide gel electrophoresis
<b>PAMP</b>	Pathogen associated molecular pattern
<b>PAS</b>	Periodic Acid-Schiffs
<b>PBS</b>	Phosphate buffered saline
<b>PCR</b>	Polymerase chain reaction
<b>pDC</b>	Plasmacytoid dendritic cell
<b>PEC</b>	Peritoneal exudates cells
<b>PKR</b>	Protein kinase R
<b>pmol</b>	Picomoles
<b>PolyIC</b>	Polyinosinic-polycytidylic acid

---

<b>PPU</b>	Protein production unit			
<b>PRD</b>	Positive regulatory domain			
<b>PRR</b>	Pathogen Recognition Receptor			
<b>rIFN</b>	Recombinant IFN			
<b>RIG</b>	Retinoic-acid inducible gene			
<b>RLH</b>	RIG-like helicase			
<b>RNA</b>	Ribonucleic Acid			
<b>RP-HPLC</b>	Reverse-phase chromatography	high	performance	liquid
<b>RPM</b>	Revolutions per minute			
<b>RT</b>	Room temperature			
<b>RT-PCR</b>	Reverse-transcription PCR			
<b>RU</b>	Resonance units			
<b>SA</b>	Streptavidin			
<b>SDS</b>	Sodium dodecyl sulfate			
<b>SEV</b>	Sendai virus			
<b>SFV</b>	Semliki forest virus			
<b>siRNA</b>	Small interfering RNA			
<b>SLE</b>	Systemic Lupus erythematosus			
<b>SNP</b>	Single nucleotide polymorphism			
<b>SPR</b>	Surface Plasmon resonance			
<b>ssRNA</b>	Single stranded RNA			
<b>STAT</b>	Signal Transducer and Activator of Transcription			
<b>STING</b>	Stimulator of interferon genes			
<b>TBK1</b>	Tank-binding kinase 1			
<b>TBS</b>	Tris-buffered saline			
<b>TCID</b>	Tissue culture infectious dose			
<b>TFA</b>	Trifluoroacetic acid			
<b>TLR</b>	Toll-like Receptor			
<b>TNF<math>\alpha</math></b>	Tumor necrosis factor alpha			
<b>TRAIL</b>	TNF-related apoptosis-inducing ligand			

---

<b>TRIF</b>	TIR domain containing adaptor inducing interferon $\beta$
<b>U</b>	Unit
<b>V</b>	Volts
<b>VSV</b>	Vesicular stomatitis virus
<b><math>\mu</math>g</b>	Microgram
<b>WB</b>	Western blot
<b>WT</b>	Wild-type

---

## **List of Figures**

### **Chapter 1**

<b>Figure</b>	<b>Title</b>	<b>Page</b>
1.1	Sequence identity among mouse and human type I IFNs	ff5
1.2	The promoters of human <i>IFNB1</i> , murine <i>Ifna4</i> , <i>Ifna6</i> and <i>Ifna11</i> genes	ff9
1.3	Induction of type I IFNs	ff11
1.4	The type I IFN signalling pathway	ff21
1.5	Overlay of the crystal structures of human IFN $\alpha$ 2a and murine IFN $\beta$	ff33
1.6	The crystal structure of human IFN $\alpha$ 2a	ff33
1.7	Structural modelling of human IFN $\alpha$ 2 depicting side chains important for structural rigidity	ff33
1.8	Type I IFN ternary complex and receptor interaction	ff34
1.9	Comparison of the 3D structures of human IFN $\beta$ and mouse IFN $\beta$	ff35
1.10	Sequence alignment of human type I IFNs and locations of interferon activity “hot-spots”	ff37
1.11	3D Model of IFNAR1 – IFN $\alpha$ – IFNAR2 ternary structure	ff37

---

## Chapter 3

Figure	Title	Page
3.1	Trial expression of IFN $\epsilon$ in bacterial and mammalian expression systems by the Monash University Protein Production Unit and CSIRO	ff92
3.2	Flow char of His <sub>6</sub> -IFN $\epsilon$ cloning, expression and purification strategy	ff93
3.3	Nucleotide sequence alignment of murine <i>Ifne1</i> and gene optimised <i>Ifne1</i> sequences	ff93
3.4	Cloning of gene optimised <i>Ifne1</i> into the insect cell expression vector pFB-SHEK	ff94
3.5	Purification of His <sub>6</sub> -IFN $\epsilon$ by HisTrap Nickel Affinity Chromatography and analysis on SDS-PAGE	ff94
3.6	Size exclusion chromatography of nickel affinity purified His <sub>6</sub> -IFN $\epsilon$ and analysis on SDS-PAGE	ff95
3.7	His <sub>6</sub> -IFN $\epsilon$ incubated with EK-Max enterokinase resulted in non-specific digestion and degradation of His <sub>6</sub> -IFN $\epsilon$ protein	ff96
3.8	Flow chart of tagless IFN $\epsilon$ cloning, expression and purification strategy	ff97
3.9	Cloning of gene optimised <i>Ifne1</i> into pFB-MSP vector (tagless)	ff97
3.10	Purification of tagless IFN $\epsilon$ expresse from High Five insect cells	ff98
3.11	Size exclusion chromatography of tagless IFN $\epsilon$	ff99
3.12	Flow chart of His <sub>6</sub> -IFN $\beta$ cloning, expression and purification strategy	ff100
3.13	Cloning of <i>mlfnb1</i> into the baculoviral expression vector	ff100
3.14	The purification of recombinant IFN $\beta$ produced in insect cells	ff101

---

## Chapter 4

Figure	Title	Page
4.1	Circular Dichroism (CD) of recombinant IFN proteins	ff116
4.2	Analysis of carbohydrate content of recombinant type I interferons by Periodic Acid Schiffs (PAS) staining	ff117
4.3	Antiviral activity of murine type I interferons	ff119
4.4	Antiproliferative effect of murine type I interferons on the mouse macrophage cell lines RAW264.7	ff120
4.5	Induction of interferon regulated genes by murine type I interferons	ff121
4.6	Luciferase promoter activation induced by murine type I interferons	ff122
4.7	Phosphorylation of Tyrosine residue 701 of Signal Transducers and Activators of Transcription 1 (STAT1) following murine type I interferon treatment	ff123
4.8	Phosphorylation of Tyrosine residue 705 of Signal Transducers and Activators of Transcription 3 (STAT3) following murine type I interferon treatment	ff125
4.9	pH and temperature stability of recombinant murine type I IFNs	ff127
4.10	Upregulation of MHC Class I by type I IFNs	ff128
4.11	Upregulation of CD69 on CD4 <sup>+</sup> and CD8 <sup>+</sup> splenic cells by type I IFNs	ff129
4.12	Upregulation of CD69 on B220 <sup>+</sup> and NK1.1 <sup>+</sup> splenic cells by type I IFNs	ff130
4.13	Induction of IRGs by IFN $\epsilon$ treatment <i>in vivo</i>	ff131
4.14	Induction of IRGs in the vagina by IFN $\epsilon$ treatment in WT and IFN $\epsilon$ deficient animals	ff132
4.15	Antiviral activity of murine type I IFNs on human amniotic cells	ff133
4.16	Antiproliferative effect of murine IFN $\epsilon$ on human cells	ff133
4.17	Expression of interferon regulated genes in human cells induced by murine IFNs	ff134
4.18	Amino acid sequence alignment of type I IFNs and their conserved residues	ff138

---

## Chapter 5

<b>Figure</b>	<b>Title</b>	<b>Page</b>
5.1	IFN monoclonal antibody generation strategy	ff149
5.2	IFN $\epsilon$ serum ELISA of mice immunised with His <sub>6</sub> -IFN $\epsilon$	ff149
5.3	Anti-IFN $\epsilon$ Hybridoma supernatant ELISA	ff150
5.4	Western blotting of recombinant His <sub>6</sub> -IFN $\epsilon$ using $\alpha$ -IFN $\epsilon$ mAbs	ff152
5.5	Identification of IFN $\epsilon$ antibodies binding different epitopes of IFN $\epsilon$	ff154
5.6	Developing and optimising the IFN $\epsilon$ ELISA	ff156
5.7	Mouse uterine sections during estrus stage were stained with C3 anti-IFN $\epsilon$ antibody	ff158
5.8	Anti-IFN antibodies are able to neutralize the biological activity of IFN $\epsilon$ but not IFN $\beta$	ff159
5.9	Immunoprecipitation of recombinant tagless IFN $\epsilon$ with monoclonal antibodies	ff160
5.10	Immunoprecipitation of IFN $\epsilon$ expression in HEK293 cells and N-terminal Sequencing	ff162

---

## **List of Tables**

### **Chapter 1**

<b>Table</b>	<b>Title</b>	<b>Page</b>
1.1	Amino acid residues absolutely conserved among 35 IFN $\alpha$ species	ff34

### **Chapter 2**

<b>Table</b>	<b>Title</b>	<b>Page</b>
2.1	Antibodies used for western blotting	76
2.2	Antibodies used for flow cytometry	84

### **Chapter 3**

<b>Table</b>	<b>Title</b>	<b>Page</b>
3.1	Results of IFN $\beta$ expressed and purified from insect cell expression system	ff102

### **Chapter 5**

<b>Table</b>	<b>Title</b>	<b>Page</b>
5.1	Mean absorbance readings $\pm$ SD of the best conditions from Figure 5.6A and B (H3 : C3 data points taken from Figure 5.6B for comparison purposes)	ff156
5.2	Significance of absorbance readings at 6.25ng/ml compared to 0ng/ml. CI = confidence interval	ff156
5.3	Summary of 7 investigated monoclonal antibodies	163

---

Work carried out for this thesis contributed to the publications listed below and are attached in Appendix L:

Fung, K.Y., et al., Interferon-epsilon protects the female reproductive tract from viral and bacterial infection. *Science*, 2013. **339**(6123): p. 1088-92.

Stifter, S.A., et al., Purification and biological characterization of soluble, recombinant mouse IFNbeta expressed in insect cells. *Protein Expr Purif*, 2014. **94**: p. 7-14.

## **Chapter 1 – Literature Review**

### **1.1 Introduction**

The interferons (IFNs) are a large family of cytokines that can be separated into three distinct groups based on their sequence homology and the cell surface receptor they each use. The type I IFNs are the largest family, composed of over 8 members ( $\alpha$ ,  $\beta$ ,  $\epsilon$ ,  $\zeta$ ,  $\kappa$ ,  $\tau$ ,  $\sigma$ ,  $\omega$ ) and 17 proteins in humans including 13 IFN $\alpha$ s and one of each  $-\beta$ ,  $-\epsilon$ ,  $-\kappa$ ,  $-\omega$ . They were discovered by virtue of their antiviral activity over 50 years ago and since then many more biological activities have been attributed to them, including antiproliferative, immunoregulatory and apoptotic functions [1].

The elucidation of the signalling pathways involving pathogen recognition receptors (PRRs) such as the Toll-Like Receptors (TLRs) and RIG-like helicases (RLHs) has improved our understanding of how type I IFNs are produced. Specifically, we now know which compounds activate which pathway to lead to interferon production and importantly, how they can be modified for further study of interferons. PRR activation leads to the induction of transcription factors such as the family of interferon regulatory factors (IRFs) and Nuclear Factor  $\kappa$ B (NF $\kappa$ B) which are pivotal in promoting the complete type I interferon response [2].

The type I interferons are secreted from the cell and then act in an autocrine, paracrine and systemic manner via a heterodimeric cell surface receptor complex called interferon alpha receptor (IFNAR). Receptor engagement induces a signalling cascade involving the JAK-STATs and other pathways to induce or suppress interferon regulated genes (IRGs) [3, 4]. These IRGs are

responsible for the multiple biological effects of the interferons such as antiviral, antiproliferative and immunoregulatory activities.

Although the IFNs were one of the first cytokines to be discovered and one of the first pharmaceuticals to be produced using recombinant DNA technology [5], the differences in biological activity between individual interferons and indeed the existence of so many subtypes is less well understood. For example even though both IFN $\alpha$ 2 and IFN $\beta$  demonstrate similar antiviral and immunoregulatory activities *in vitro*, their therapeutic indications are different. IFN $\alpha$ 2 is used clinically for the treatment of Hairy cell leukaemia and viral hepatitis whereas IFN $\beta$  is used for the treatment of multiple sclerosis [6]. It has been proposed that each type I IFN engages the interferon receptor complex differently, therefore inducing different downstream signalling effects [7, 8]. The recent elucidation of the crystal structure of interferon in complex with its receptors indeed suggests that ligand specific interactions with the receptor dictate functional consequences [9]. Interestingly, discrimination of ligands by the receptor occurs via small differences in amino acid residues neighbouring conserved anchor points, highlighting the subtleties of the IFN receptor system. To further highlight the complexity of the IFN signalling system, other reports demonstrate that interferon activity also changes according to cell surface receptor density and dissociation time of the ligand from the receptor [10-12]. Clearly, the differential activities of IFNs are both ligand and cell dependent, emphasizing the need to investigate all members of the type I IFN family to not only characterise their mode of action but to also evaluate their therapeutic potential in disease states.

*Ifne1*, a novel gene discovered by the Hertzog group in the Centre for Innate Immunity and Infectious Diseases (CIID), is located in the type I IFN gene locus and is constitutively expressed in the female reproductive tract [13]. Our

group defined it as a type I IFN based on its sequence similarity to known type I IFNs and based on structural modelling of the encoded IFN $\epsilon$  protein [13]. Little is known about the function of this novel cytokine largely due to a limited number of reagents available for study. This literature review will give an overview of the type I interferon family and their function as pleiotropic immune cytokines. In particular, structure function relationships will be discussed to give a greater overview of how the IFNs mediate their multitude of biological activities.

## **1.2 The Interferons**

Interferons are a large group of proteins belonging to the class II helical cytokine superfamily. They are found exclusively in vertebrate species and were discovered and named after their ability to interfere with viral growth and replication [14]. IFNs can be categorized into three broad groups primarily based on their amino acid homology and on the type of receptor they each use. Type I IFNs ( $\alpha$ ,  $\beta$ ,  $\delta$ ,  $\epsilon$ ,  $\zeta$ ,  $\kappa$ ,  $\tau$ ,  $\omega$ ) signal through the heterodimeric receptor complex IFNAR [15], the type II IFN ( $\gamma$ ) mediates its actions through the interferon gamma receptor complex (IFNGR) [16] and the type III interferons ( $\lambda$ -1,2,3) signal through a receptor complex composed of a unique IFN $\lambda$ R1 receptor chain and the IL-10R $\beta$  subunit. [17, 18].

The singular type II interferon, IFN $\gamma$ , encoded by a gene located on chromosome 12 in humans (chromosome 10 in mice) signals via the interferon gamma receptor complex composed of two subunits, IFNGR1 and IFNGR2. Initially called immune interferon due to its specific expression and potent activity on immune cells (in contrast to type I IFNs which can be expressed by almost all nucleated cells [19]), we now know it is structurally

unrelated to type I IFNs and is produced by CD4 and CD8 T-cells and Natural killer (NK) cells following activation with mitogens such as phytohemagglutinin (PHA), IL-2 and IL-12 [5, 20].

A novel family of antiviral molecules was discovered in 2003 and termed IL-28/29 [18], however they have now been re-classified as type III interferons (IFN $\lambda$ ) [17]. Exhibiting antiviral activity, this family of genes is located on chromosome 19 and signal via a distinct cell surface receptor composed of IL-28R $\alpha$  (IFN $\lambda$ R1) and the IL-10R $\beta$  chain [17]. Like the type I IFNs, IFN $\lambda$ s are pathogen inducible however they appear to act in a more cell-type specific manner to elicit their biological function [21, 22].

Although each family of IFN binds a distinct receptor complex, they have all been shown to induce the JAK-STAT signalling pathway [5, 21]. This common signalling would explain why they all demonstrate some antiviral activity. As our research focus lies with type I interferons, this review will explore the evolution, induction, biological actions and structure function relationships of type I IFNs.

### **1.3 Type I IFNs**

The type I IFN family comprises 8 family members (- $\alpha$ , - $\beta$ , - $\epsilon$ , - $\kappa$ , - $\omega$ , - $\zeta$ , - $\tau$ , - $\sigma$ ) of which the latter three are found only in mice, ruminants and pigs, respectively [23, 24]. All type I IFN genes except IFN $\kappa$  are intronless and encode secreted proteins 165-166 amino acids (aa) in length [5] with the exception of IFN $\epsilon$  which is 185aa long. Structurally, they share between 20%-100% amino acid sequence identity to one another (Figure 1.1). The highest homology is observed in IFN $\alpha$  proteins with approximately 75% or greater amino acid identity between members [6, 25] and interestingly in humans, the

**A**

	<b>IFNT1</b>	<b>IFNW1</b>	<b>IFNA2</b>	<b>IFNA1</b>	<b>IFNA8</b>	<b>IFNA21</b>	<b>IFNA4</b>	<b>IFNA10</b>	<b>IFNB1</b>	<b>IFNE1</b>
<b>IFNT1</b>	100	56	49	52	51	52	53	53	33	36
<b>IFNW1</b>		100	61	57	59	57	58	59	31	31
<b>IFNA2</b>			100	82	82	81	81	80	34	33
<b>IFNA1</b>				100	77	81	80	79	30	36
<b>IFNA8</b>					100	81	81	80	30	32
<b>IFNA21</b>						100	92	91	31	34
<b>IFNA4</b>							100	96	32	34
<b>IFNA10</b>								100	32	34
<b>IFNB1</b>									100	37
<b>IFNE1</b>										100

**B**

	<b>ifnb1</b>	<b>ifne1</b>	<b>ifnk1</b>	<b>ifna4</b>	<b>ifna2</b>	<b>ifna1</b>	<b>ifna13</b>
<b>ifnb1</b>	100	23.3	21.59	26.04	26.01	28.32	29.48
<b>ifne1</b>		100	23.66	24.58	23.91	25.54	26.63
<b>ifnk1</b>			100	27.47	29.57	30.27	28.11
<b>ifna4</b>				100	85.95	80.43	81.52
<b>ifna2</b>					100	84.66	80.95
<b>ifna1</b>						100	87.83
<b>ifna13</b>							100

**Figure 1.1 Sequence identity among mouse and human type I IFNs.** The amino acid sequences of human (A) and mouse (B) type I IFNs were compared for their sequence identity using ClustalW2. Bovine IFN $\tau$  was also included in the alignment of human IFNs. Alignment scores include the signal peptides.

IFNA1 and IFNA13 genes encode identical proteins [26]. In mice, there is approximately 28% sequence identity between IFN $\alpha$ 1 and IFN $\beta$ , 23% identity between IFN $\epsilon$  and IFN $\beta$  and 25% identity between IFN $\alpha$ 1 and IFN $\epsilon$  (Figure 1.1). All type I IFN genes are localised on the short arm of chromosome 9 in humans and chromosome 4 in mice [13]. As stated previously, with the exception of the 14 IFN $\alpha$ 's each functional IFN protein is only encoded for by one gene in the IFN locus. The exact reason for the existence of so many type I IFNs and indeed, IFN $\alpha$  members, is currently unknown however one may postulate that differences in tissue expression, temporal expression and biological activity can account for the emergence of such a large gene family.

#### **1.4 Evolution of type I IFNs**

The type I IFN genes are thought to have evolved through duplication events 250-300 million years ago when the mammals and birds split from reptiles [27, 28]. The type I interferon locus is conserved among species and gives some clues as to the evolution of individual IFN genes. For example evolutionary analysis shows that an early common mammalian ancestor evolved separate IFNA and IFNB genes [29], yet for individual IFNA members speciation preceded gene duplication. In other words, each species evolved their large number of IFN $\alpha$  members independently of one another, an observation that is evidenced by the clustering of each species' IFN $\alpha$  subtypes [27-31]. This finding is remarkable, as it suggests the existence of a common evolutionary pressure that each species responded to the same way by evolving a repertoire of IFNA genes. In the context of IFN $\epsilon$ , IFN $\epsilon$ 's in different species appear to have evolved from IFN $\beta$  sometime at the beginning of mammalian evolution due to its presence in many mammalian species [32].

Furthermore over the last 5 years, with the availability of fish genomes, increasing evidence has mounted to conclusively determine the evolutionary history of the IFN system. Data from two independent groups suggests the common origin of all IFNs to have been an ancestral gene similar to type III interferons in fish [31, 33]. In accordance with this hypothesis, the early IFNs contained introns until a retroposition event either replaced or created the 'new' intronless IFN locus that through gene duplication events became what is now the type I IFN locus [34]. This hypothesis however is refuted by a more recent study which demonstrates that intron-containing type I and type III IFNs existed at the same time, suggesting that type I IFNs evolved to become intronless after the ancestral IFN system was duplicated [35]. With the aid of more recent structural information of the fish IFN families, it appears that although there exist multiple virus-inducible IFN subtypes in fish, these IFNs are structurally closely related to mammalian type I IFNs [36]. As such, the current evidence suggests that while these ancestral fish IFNs appear to be genetically more similar to type III IFNs, their structure bears more resemblance to mammalian type I IFNs. Although essential in terms of elucidating the evolution of the IFNs, these studies don't address the question as to why the type I interferons evolved to become the predominant antiviral system in amniotes and the significance of having the type I and type III IFN systems.

To address this question, Manry et al. undertook a comprehensive human genetic study investigating the evolutionary pressures on all three IFN systems in a number of geographic populations [37]. They found that the majority of type I IFN members were only subject to a small number of amino-acid altering mutations in the investigated populations, if any. These included IFNA2, IFNA5, IFNA6, IFNA8, IFNA13, IFNA14, IFNB1, IFNK1 and IFNW1.

Meanwhile IFNA1, IFNA4, IFNA7 and IFNA10 demonstrated higher levels of variants in populations, suggesting a relaxation of evolutionary pressure or redundancy in biological function. The latter would suggest that while once these IFNs served a specific function, the activities of other subtypes now overrides the need for a separate gene. Interestingly, IFNA10 and IFNE were both found to show high rates of homozygous nonsense mutations in some populations. The authors proposed that perhaps these genes may be undergoing pseudogenisation due to a lack or loss of selective pressure [37]. Although not a focus of this literature review, it is important to mention that the singular type II interferon, IFN $\gamma$ , demonstrated the lowest level of nucleotide diversity, suggesting that this gene performs non-redundant, indispensable functions. This of course raises the question of why there are so many type I IFNs (with similar functions) yet only a single type II IFN. Section 1.5 will aim to address this question by discussing the promoter elements of the type I IFNs.

Lastly, the presence of numerous gene copies of the same IFN subtype (IFN $\alpha$  for example) is proposed to be a result of the nature of type I IFN genes. As previously stated, all known mammalian type I interferon genes except IFN $\kappa$  are intronless, meaning that there cannot be splice-variants of the same gene to perform different functions. Therefore the gene is duplicated to perform a new function, which would reflect the differences in temporal expression and biological potencies observed among the type I IFNs [38]. Interestingly, whereas there are numerous IFN $\alpha$  subtypes, all other human (and mouse) type I IFNs are only represented once in the IFN locus. Although the importance of this has yet to be determined, it is plausible that the singular subtypes ( $\beta$ ,  $\kappa$ ,  $\epsilon$ ,  $\omega$ ) perform specific and conserved functions that have not

required the evolution of multiple gene copies. This certainly appears to be the case for IFN $\epsilon$ , which will be discussed in more detail in Chapter 1.12.

## 1.5 Transcriptional elements of type I IFN induction

To understand how the type I IFNs are induced one must first consider the make-up of their promoters and promoter elements to fully grasp the myriad ways that interferons are transcriptionally regulated. The singular IFN $\beta$  gene and its promoter have undergone the most scrutiny and will therefore be described in most detail in this section. The promoters of other type I IFN members will be discussed alongside to provide suitable comparisons.

The promoter region responsible for virus induced *IFNB* gene induction is found within approximately 120base pairs (bp) of the transcription start site [39, 40]. There are four positive regulatory domains (PRDs) within this promoter region of the *IFNB* gene, termed PRD I-IV (Figure 1.2A). Of these, PRD I and III are binding sites for IRFs while PRD II is the binding site for nuclear factor- $\kappa$ B (NF $\kappa$ B) and PRD IV binds the transcription factor AP-1. In contrast, some *IFNA* genes have so far only been shown to contain PRD I and III like promoter elements and are therefore not under the control of NF $\kappa$ B and AP1 (Figure 1.2B) [41].

The IRF binding sites are critical for the transcriptional activation of IFN $\beta$  upon virus stimulation, as mutations in these promoter sites results in a reduction of IFN $\beta$  inducibility by virus [42]. Furthermore, *IFNB* gene induction is controlled incrementally by the number of bound regulatory factors and as such, maximal *IFNB* gene activation is seen when all promoter elements are engaged [43]. One of the unique elements of the *IFNB* promoter is the presence of a NF $\kappa$ B binding site [44, 45]. The transcription factor NF $\kappa$ B has been shown to have

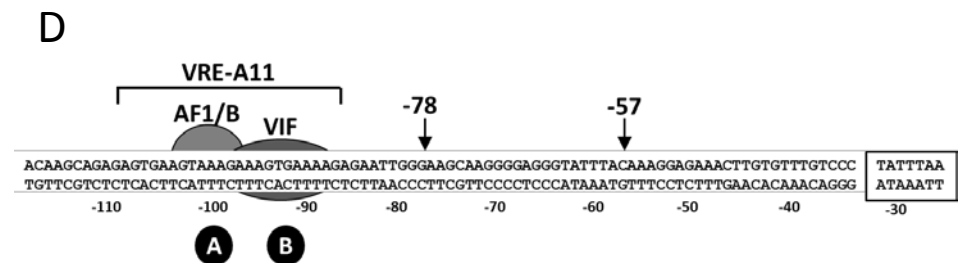
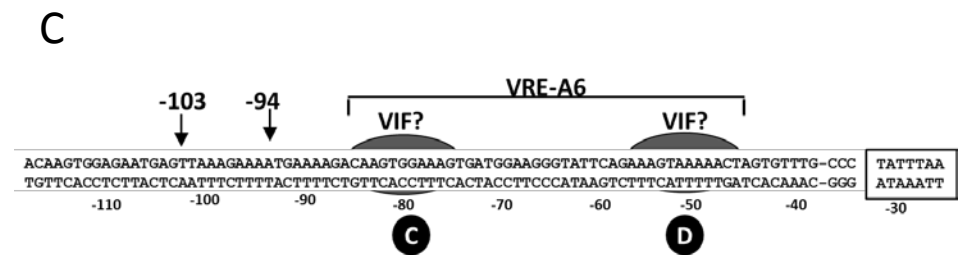
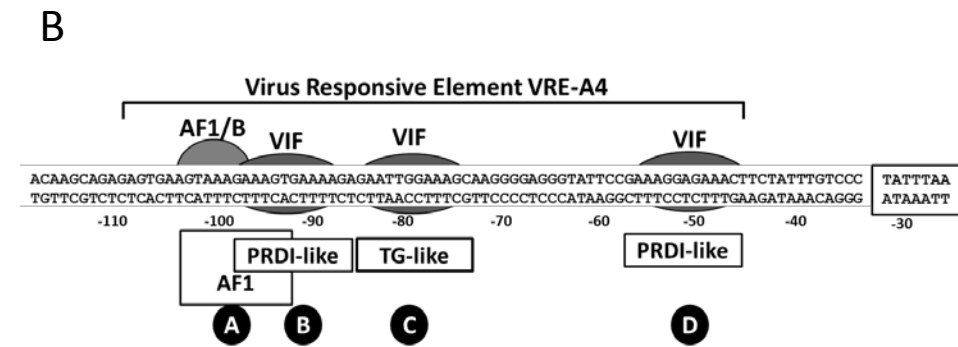
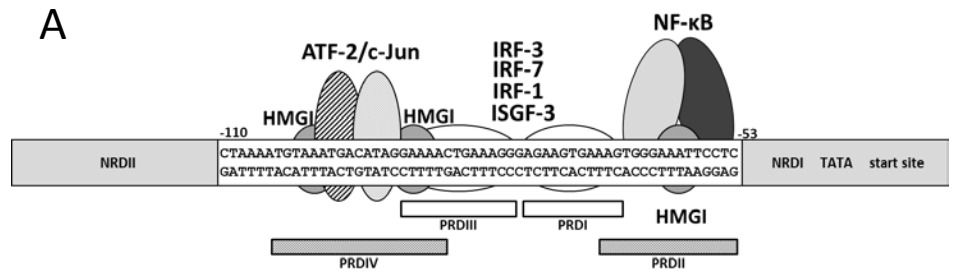


**Figure 1.2 The promoters of human *IFNB1*, murine *Ifna4*, *Ifna6* and *Ifna11* genes.** (A) The human *IFNB1* promoter and the regulatory factors that bind it. NF $\kappa$ B binds PRDII; IRFs bind to PRDI and PRDIII; ATF-2/c-Jun (AP-1) binds to PRDIV; HMGI binds AT-rich regions and is constitutive. Numbers indicate the nucleotide number relative to the transcription start site (B-D) The proximal promoter regions of murine *Ifna4* (B), *Ifna6* (C) and *Ifna11* (D). Binding motifs are depicted as black circles with letters A-D. VIF, virus inducible factor. Large arrows and nucleotide numbers indicate point mutations that disrupt binding motifs. Numbers below the sequences indicate the nucleotide number relative to the transcription start site. Figure adapted from Doly et al., 1998 [52].

important functions in inflammation, stress responses, cell cycle control and regulation and is activated by viruses, bacterial cell wall components such as Lipopolysaccharide (LPS) and pro-inflammatory cytokines (eg. TNF $\alpha$ ) to induce IFN $\beta$  [46-48]. As mentioned previously, maximal induction of *IFNB* occurs when all regulatory elements are bound and therefore the binding of NF $\kappa$ B is required for highest IFNB gene expression [49].

In contrast to the single *IFNB* promoter, *IFNA* promoters have been studied much less due to the presence of the many subtypes, which all demonstrate distinct transcriptional activity in different cell types [50]. Of the IFN $\alpha$ s, the human *IFNA1* and mouse *Ifna4* promoters have been studied in most detail due to their relatively early and high expression during viral infection compared to other *IFNA* genes [51-53]. At a molecular level, the promoters of these two genes are most alike *IFNB*, that is, they contain a virus responsive element composed of multiple PRDI-like sequences (but still lack the NF $\kappa$ B and AP-1 sites) [50, 54] (Figure 1.2B). This is in stark contrast to mouse *Ifna11* and *Ifna6* for example, which demonstrate no PRDI-like motifs and instead contain few virus inducible regions [54] (Figure 1.2C and 1.2D). In addition, *Ifna11* is poorly induced by viruses due to a nucleotide substitution in one of its virus inducible motifs that disrupts this transcription factor binding site [55]. Much like the *IFNB* promoter, maximal transcription of *IFNA* genes is dependent on the number of bound transcription factors. However, as many *IFNA* genes only demonstrate few and even weak virus inducible promoters, in most virally infected cells their maximal expression is not comparable to that of *IFNB* or *IFNA1/Ifna4* (with the exception of plasmacytoid dendritic cells, as discussed in the next section) [56]. Instead, their expression is highest during the positive feedback stage of type I IFN signalling and involves interferon stimulated response element (ISRE) sites, which are found in the promoters of

*IFNA* genes [50, 57, 58]. Section 1.6.1 will aim to further describe the induction mechanisms mediated by interferon regulatory factors and the contribution of each IRF member to type I IFN gene induction.

## **1.6 Induction of type I IFNs**

The induction of type I IFNs by pathogens has been known since their initial discovery, however only with the elucidation of Toll Like Receptor (TLR) and RIG Like Helicase (RLH) signalling has a more exact mechanism been described. Furthermore, the family of NOD like receptors (NLRs) have recently been implicated as another cytosolic sensor of bacterial components to induce the production of type I IFNs. This section will describe how the TLR, RLH, NLR and other pathways signal to induce type I IFN production (Figure 1.3).

### **1.6.1 IRFs**

Type I IFN induction occurs largely via IRFs, a 9-membered family of proteins sharing high homology in their DNA binding domain [59, 60]. The activities of individual IRFs depends on the conditions of activation, but it has been found that IRF-1, IRF-3, IRF-5 and IRF-7 activate type I IFN genes, while IRF-2 represses them [61]. Immediate virus induced production of IFNs by IRF-3 occurs in most cell types, whereas high IFN $\alpha$  producing cells (namely plasmacytoid dendritic cells) express IRF-7 constitutively [62] and are therefore able to mount a rapid IFN response without the need for prior IFN $\beta$  production via IRF-3 signalling [63, 64]. The latter effect is known as interferon priming and describes a positive feedback signalling system whereby the induction of the early response IFN $\beta$  and IFN $\alpha$ 1 (IFN $\alpha$ 4 in mice) leads to the

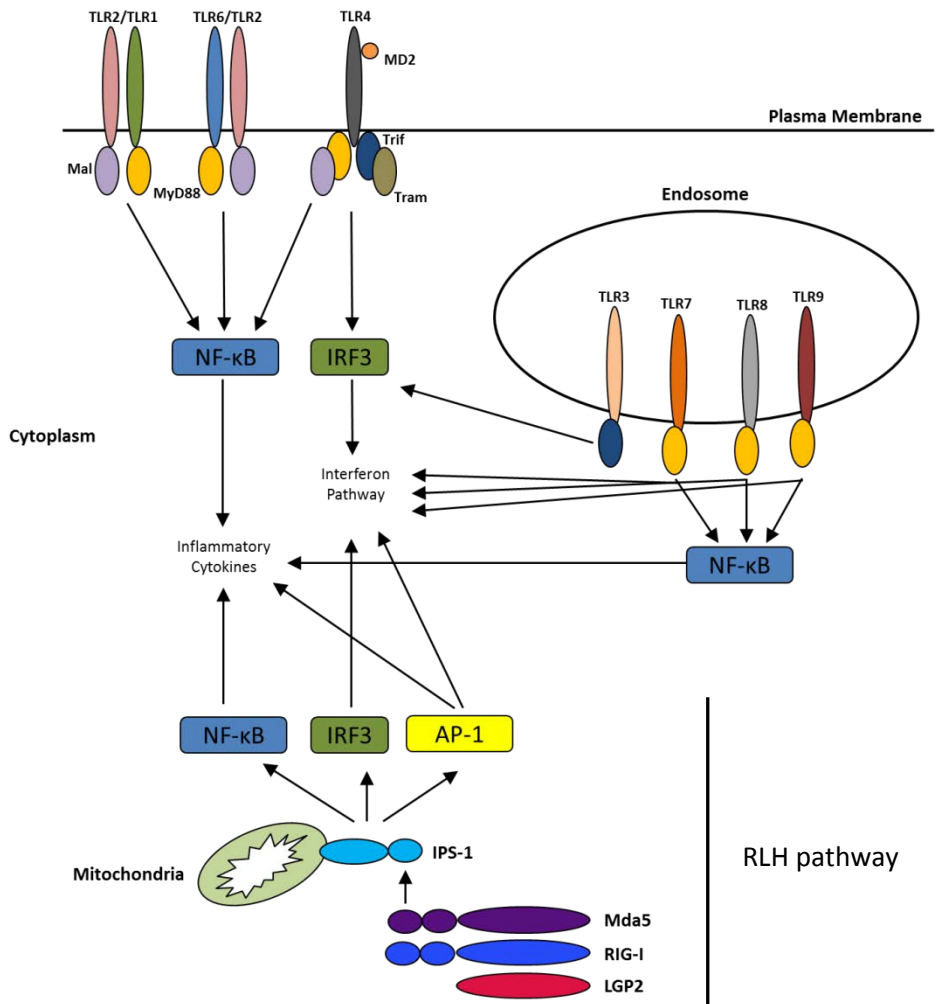


**Figure 1.3 Induction of type I IFNs.** The type I interferons are induced following pathogen associated molecular pattern recognition by pathogen recognition receptors, here depicted as belonging to the TLR and RLH families. Figure adapted from MacKichan et al., 2005 and Kawai and Akira, 2006.

production of an interferon induced state in cells, dramatically increasing IFN $\alpha$  gene production [58, 65].

Most of the IRFs have been knocked-out in mice and this has been pivotal in the characterisation of the individual contributions of IRF family members to type I IFN induction.

#### 1.6.1.1 IRF-1

The first discovered and archetypal interferon regulatory factor is IRF-1. It was discovered as a nuclear protein able to bind the PRD-I element in the *Irf1* promoter in the mouse fibroblast L929 cell line and induce *Irf1* gene transcription [42, 66]. Furthermore, IRF-1 was able to induce the transcription of interferon regulated genes such as *ISG15* and *IFNs* and has been shown to be of key importance in the antiviral response [67, 68]. Surprisingly, while IRF-1 null mouse embryonic fibroblasts (MEFs) produced dramatically lower levels of IFN $\alpha$  and IFN $\beta$  in response to the synthetic dsRNA analogue polyI:C than wild type MEFs, the same cells infected with Newcastle Disease Virus (NDV) produced levels of type I IFN virtually identical to wild type cells [69]. Furthermore, priming of IRF-1 null MEFs with IFN $\beta$  completely restored IFN $\alpha$  production in response to polyI:C, implying that while IRF-1 is important in dsRNA induced type I IFN production, there are other mechanisms in place to confer redundancy following infection with live virus. While the role of IRF-1 in type I IFN induction may not be critical, IRF-1 has been shown to be a key regulator of the antiviral response due to its broad acting activity to induce antiviral effector genes [70].

### 1.6.1.2 IRF-3

IRF-3 is central to the induction of type I IFNs, particularly the early subtypes IFN $\beta$ , human IFN $\alpha$ 1 and mouse IFN $\alpha$ 4 [71]. Importantly, IRF-3 demonstrates constitutive expression in all cell types, emphasizing its role in immediate IFN induction [56, 72]. Early IFN production is best explained by comparing the structure of promoters of type I IFNs produced rapidly (IFN $\beta$  and human IFN $\alpha$ 1 or mouse IFN $\alpha$ 4) to promoters of IFNs produced predominantly in the primed, feedback stage (human IFN $\alpha$ 2 and IFN $\alpha$ 10 for example).

The human *IFNA1* promoter exhibits three IRF binding sites, termed B, C and D. Binding site B is conserved in all *IFNA* species and recognises IRF-3 and IRF-7 equally. Site C is found only in the promoter of *IFNA1* and has higher affinity for IRF-3 than IRF-7. Site D favours IRF-7 in all *IFNA* species except *IFNA1*, in which IRF-3 is bound more strongly [56]. One can deduce that *IFNA1* is strongly induced by IRF-3 signalling due to the presence of three strong IRF-3 binding sites instead of just one as found in other *IFNA* genes. Indeed, *in vitro* infection of human cells with Sendai virus has shown that *IFNA1* and *IFNB* are the only type I IFNs induced immediately and highly due to the presence of IRF-3 binding sites [56]. In line with this, reconstitution of IRF-3 and IRF-7 doubly deficient MEFs with IRF-3 restored IFN $\beta$  to wild type levels following NDV infection. In contrast, IRF-7 reconstitution only restored approximately 50% of wild type IFN $\beta$  levels. To highlight the preference of IRF-7 compared to IRF-3 in most *IFNA* promoters [56], only reconstitution of IRF-7, but not IRF-3 in IRF-3/IRF-7 null MEFs was able to restore IFN $\alpha$  production after NDV infection [73].

Clearly, while IFN $\beta$  can be induced by multiple IRFs including IRF-3 and IRF-7 [73, 74] a loss of IRF-3 not only results in diminished IFN $\beta$  production after virus challenge but its absence also shifts IFN $\beta$  expression from immediate to

late production and severely impairs the IFN priming effect normally seen [73]. Thus, the production of IFN $\beta$  and IFN $\alpha$ 1 in unprimed cells is critically dependent on IRF-3.

### 1.6.1.3 IRF-7

IRF-7 is not only a principal type I IFN inducer but is itself highly induced following interferon treatment [58]. As explained previously, the expression of IFN $\alpha$  subtypes is largely dependent on the positive feedback phase of IFN signalling and is in no small part due to the expression of IRF-7 [56, 58]. Interestingly, *Irf7* null mice demonstrate a clear impairment in both IFN $\alpha$  and IFN $\beta$  induction in fibroblasts, pDCs and conventional DCs following virus challenge [74]. The finding that IFN $\beta$  production was significantly impaired in virus infected *Irf7*<sup>-/-</sup> mouse fibroblasts is unexpected given that a large body of work in previous reports provided a strong bias for IRF-3, and not IRF-7, in the production of IFN $\beta$  [56, 58, 73, 75]. Interestingly however, recent work in human cells contradicts the findings of *Irf7* in the mouse model. Steinhagen et al. have shown that siRNA knock-down of IRF-7 in human pDCs had no effect on IFN $\beta$  production following CpG DNA stimulation, the same TLR9 ligand used in the studies describing *Irf7* deficient mice [74, 76, 77]. Instead, IRF-5 was found to be critical for the induction of IFN $\beta$  following CpG DNA stimulation [76]. These findings suggest that the human and mouse IRF-IFN systems, while highly conserved, demonstrate subtle differences that necessitate a more flexible hypothesis which also considers the cell type and IFN inducing stimulus. However regardless of the contradictory evidence of the importance of IRF-7 in IFN $\beta$  induction, IRF-7 is a key transcription factor required for the production of IFN $\alpha$  subtypes from both primed and unprimed (pDC) cells.

#### 1.6.1.4 IRF-9

The most characterised role of IRF-9 is as a subunit of the interferon stimulated gene factor 3 (ISGF-3) transcription factor complex, which is induced following type I IFN receptor engagement [78]. Upon activation, ISGF-3 binds to the promoter of IRGs to induce their transcription and establish the antiviral state (described further in 1.7). In this context, IRF-9 is of utmost importance as MEFs and macrophages isolated from *Irf9*<sup>-/-</sup> mice demonstrate defective type I IFN production following NDV infection [57]. This defect was stronger for IFN $\alpha$  than IFN $\beta$  gene expression, which was only marginally reduced compared to WT cells. Furthermore, IFN $\beta$  induction kinetics did not change in *Irf9*<sup>-/-</sup> cells, suggesting that the immediate IFN $\beta$  response in MEFs and macrophages is not ISGF-3 dependent [57]. The authors obtained practically identical results in *Stat1* and *Ifnar1* deficient cells, highlighting that only IFN $\alpha$  production was critically dependent on the IFN signalling feedback loop.

Overall, the picture of IRF involvement in type I IFN induction can be summarised as follows: In most cells, viral infection leads to the production of IFN $\beta$  and IFN $\alpha$ 1 by IRF-3, which are secreted from the cell and bind the type I IFN receptor. Upon receptor binding and activation, ISGF-3 forms and translocates to the nucleus to induce the expression of antiviral genes, including IFN $\alpha$  subtypes and IRF-7. Due to increased availability of IRF-7, the IFN expression profile changes to also include the multiple IFN $\alpha$ s. The exception to this model occurs in pDCs as they constitutively express IRF-7 [62]. In these cells, IFN $\alpha$  and IFN $\beta$  induction is activated immediately and simultaneously and does not require a priming step. While perturbations in the described IRFs are somewhat compensated by redundancy, the absence of

either is enough to imbalance the IFN expression profile and leads to sub-optimal conditions to combat infection.

### **1.6.2 TLRs**

The TLRs are a family of pathogen recognition receptors (PRRs) comprising 10 members in humans and 12 in mice [79]. TLR 1, 2, 4, 5, 6 and 10 are found on the surface of cells whereas TLR 3, 7, 8 and 9 are expressed in the endosome. Each TLR recognises a different pathogen associated molecular pattern (PAMP), resulting in the expression of inflammatory cytokines via two distinct pathways, the MyD88 dependent or MyD88 independent pathway (Figure 1.3) [80].

In the context of interferon induction, TLR2, 3, 4, 7, 8 and 9 have all been shown to result in IFN gene expression via activation of IRFs [2]. Dissection of this signalling axis demonstrated that TLRs 7, 8 and 9, upon activation by their respective ligands, interact with MyD88 in the cytoplasm, which in turn directly binds to IRF-7 [81]. IRAK1 and IKK $\alpha$  are also found in this complex and upon receptor activation, phosphorylate IRF-7 which then translocates to the nucleus [82]. Importantly, the MyD88-TLR9 interaction does not lead to IRF-3 activation [81] and helps explain why IRF-7 is the primary IRF responsible for IFN induction in response to CpG DNA [74]. This also explains why Honda et al. [74] found IRF-7 to be the master regulator of IFN $\alpha$  and IFN $\beta$  production, as TLR9 is primarily expressed on pDCs [83] and furthermore their IFN inducing stimulus for many of their experiments was CpG DNA and thus IRF-7 specific. This example outlines how the use of single purified IFN inducers while aiding in describing induction mechanisms may be misleading when trying to relate back to pathogens themselves, which can express multiple PAMPs.

In contrast to the TLRs utilising MyD88, TLR3 (the ligand of which is dsRNA) stimulates the induction of IFN $\beta$  independently of MyD88 by a signalling pathway involving TRIF and the kinases IKK-i and TBK1 which phosphorylate IRF-3 [84, 85]. Importantly, not only viral PAMPs such as single or double stranded RNA lead to interferon induction. Lipopolysaccharide (LPS), a gram negative bacterial cell wall component and lipotechoic acid (LTA), a gram positive cell wall component, potently induce IFN $\beta$  via TLR4 and IFN $\alpha$  via TLR2, respectively [86, 87].

### **1.6.3 RLHs**

TLRs are not the only viral nucleic acid sensing molecules. In fact TLRs 3, 7, 8 and 9, the viral recognition TLRs, are inadequate at sensing viral RNA already present in the cytoplasm due to their endoplasmic localisation. In 2004, a novel family of intracellular RNA sensors termed the RIG-I like helicases (RLH) were discovered and characterised [88].

The RLHs are found exclusively in the cytoplasm and include three members; retinoic acid-inducible gene 1 (RIG-I), melanoma differentiation-associated protein 5 (MDA-5) and LPG-2. Recently, the complex interplay of viral RNA recognition by this family was elucidated and presents new insights into how the human body recognises invading viruses and leads to type I IFN production [89]. To briefly summarise, RIG-I preferentially recognises single stranded (ss) RNA and is only weakly activated by short double stranded (ds) RNA (~1kb length) whereas MDA-5 recognises long dsRNA (~3-4kb) [90, 91]. This nucleic acid “sensing” by RIG-I and MDA-5 also reflects in the viruses they each detect. RIG-I is a principal detector of ssRNA viruses (Sendai Virus, Hepatitis C Virus) or viruses with short dsRNA intermediates (reovirus)

whereas MDA-5 senses long dsRNA viral genomes (EMCV, reovirus) [88, 92]. The binding of viral RNA to the repressor domain of the molecule results in a conformational change that allows two caspase activation and recruitment domains (CARDs) to interact with another CARD on IFN $\beta$  promoter stimulator 1 (IPS-1), a mitochondrion bound protein, to induce downstream signalling and IFN induction (Figure 1.3) [93, 94]. The importance of IPS-1 in cytoplasmic viral sensing was demonstrated in *Ips1* null mice, which essentially produce no IFN $\alpha$  or IFN $\beta$  following NDV, VSV, SeV and EMCV infections [93]. As IPS-1 interacts directly with the kinase responsible for phosphorylating IRF-3, TBK1-IKK $\epsilon$ , perturbances in MDA-5, RIG-I or IPS-1 signalling therefore lead to diminished IFN production via loss of IRF-3 dimerisation [88, 93, 95].

LPG-2, the third member of the RLHs lacks CARD domains and is believed to be a regulator of RIG-I signalling, having exhibited both positive and negative regulatory activities following viral infections [96].

#### 1.6.4 NLRs

Nucleotide-binding oligomerization domain (NOD) proteins are a recently discovered group of cytosolic PRRs that have been shown to recognise bacterial peptidoglycan break-down products [97]. Intracellular bacteria such as *L. monocytogenes* and *M. tuberculosis* have been shown to induce IFN $\beta$  in mouse macrophages [98-100]. Type I interferon expression in these cases is dependent on NOD2 and its adaptor molecule RIP2. Interestingly, the well-studied NOD2 ligand MDP alone is not sufficient to induce IFN $\beta$  transcription [99], suggesting that a synergistic effect between NOD and other PRRs is required for type I IFN production using this pathway.

### 1.6.5 STING, IFI16 and other DNA sensors

Among a number of newly discovered cytoplasmic DNA sensor is stimulator of interferon genes (STING) [101-103]. STING localizes to the endoplasmic reticulum and was discovered by screening potential cDNA clones for their ability to activate the IFN $\beta$  promoter [101]. Importantly, IFN $\beta$  was produced in response to transfected poly:dAdT (a synthetic DNA molecule) and was found to be critically dependent on TBK-1 and IRF-3 dimerisation [101, 103]. Herpes simplex virus, Sendai virus, *Listeria monocytogenes* and VSV were all shown to induce IFN production in a STING dependent manner. Furthermore, *Tmem173* (the gene coding for STING) deficient mice demonstrated sharply reduced survival following HSV-1 and VSV infection compared to wild type mice, providing *in vivo* relevance [102]. Interestingly, STING is able to interact with IPS-1 and RIG-I to potentiate IFN production, suggesting that there is significant cross-talk between cytoplasmic nucleotide sensors [104].

Another recently discovered cytoplasmic DNA sensor is IFI16, which is part of the broader family of p200 proteins. The p200-family of proteins is so named due to a conserved 200 amino acid domain (also known as HIN-200 domain) that allows the binding of single and double stranded DNA [105]. The p200 protein family is conserved in both humans and mice and a seminal study by Unterholzner et al. found that IFI16 was able to upregulate the expression of *IFNB* in response to cytoplasmic dsDNA [106]. Interestingly, the IFN $\beta$  inducing ability of IFI16 was found to be dependent on the presence of STING, as *Tmem173* deficient bone marrow derived macrophages did not produce IFN $\beta$  after transfection of dsDNA or HSV-1 infection.

In addition to STING and IFI16, other DNA sensors play a role in the induction of type I IFNs. These include proteins such as cGAS [107, 108], DAI [109] and LRRFIP1 [110]. Although their mechanisms of action will not be discussed in this review, it is important to understand that new IFN inducing pathways are being identified with important roles in viral and bacterial infections.

### **1.6.6 Cell type specific mechanisms of induction**

As summarised in the previous paragraphs, type I IFN expression is largely induced by the recognition of pathogens or pathogen associated molecules. There are a number of exceptions that are important to mention at this point in time, namely IFN $\kappa$ , IFN $\tau$  and IFN $\epsilon$ . IFN $\kappa$  was discovered following high throughput cDNA sequencing and was found to be highly expressed in epidermal keratinocytes [111]. While IFN $\kappa$  expression in keratinocytes is constitutive, mRNA levels can be further increased by virus, dsRNA, IFN $\beta$  and IFN $\gamma$  treatment [111] suggesting that the IFN $\kappa$  promoter contains similar regulatory elements as found in other type I IFN promoters. Follow up studies have also demonstrated low IFN $\kappa$  expression in dendritic cells and purified peripheral blood monocytes that could be further increased by IFN $\gamma$  treatment, indicating that the expression of IFN $\kappa$  wasn't completely exclusive to keratinocytes [112]. Recent work has demonstrated associations between *IFNK* promoter single nucleotide polymorphisms (SNPs) and increased SLE skin pathology, indicating a tissue specific role in disease for this type I IFN [113]. While the factors responsible for keratinocyte specific expression have not yet been identified, IFN $\kappa$  highlights that some type I IFN genes can be under the control of tissue regulators but also still remain virus inducible.

Although IFN $\tau$  and IFN $\epsilon$  will be discussed at length in sections 1.9 and 1.12, respectively, it is important to mention them at this point as their expression is regulated in a manner unlike other type I IFNs. Neither are inducible by viruses, PAMPs or via type I IFN signalling but instead demonstrate expression restricted to the female reproductive tract [13, 24, 114]. IFN $\epsilon$  in particular demonstrates no conventional type I IFN inducing sequences such as ISRE, STAT, NF $\kappa$ B or IRF sites in its proximal promoter region [114]. However while the function and biological activities of IFN $\tau$  have been characterised in detail [24], the role of IFN $\epsilon$  is not fully known and current work including this thesis aims to address this shortcoming.

## **1.7 Type I IFN signal transduction**

As IFNs are secreted cytokines, they must bind to a cell surface receptor to elicit their biological activities. The predominant signalling pathway activated by type I IFNs is the Janus kinase (JAK)- Signal Transducer and Activator of Transcription (STAT) pathway (Figure 1.4) although it should be noted that p38 MAPK and CrkL signalling pathways are also activated following IFN stimulation [115].

### **1.7.1 JAK-STAT Pathway**

The type I interferons signal exclusively through a common cell surface receptor, composed of two subunits, IFNAR1 and IFNAR2 [5]. IFN binds to the high affinity subunit IFNAR2 followed by the recognition and signalling receptor subunit IFNAR1. The binding of IFN to the receptor results in the activation of receptor associated Janus kinase family members TYK2 and JAK1 via reciprocal phosphorylation, which in turn phosphorylate and activate

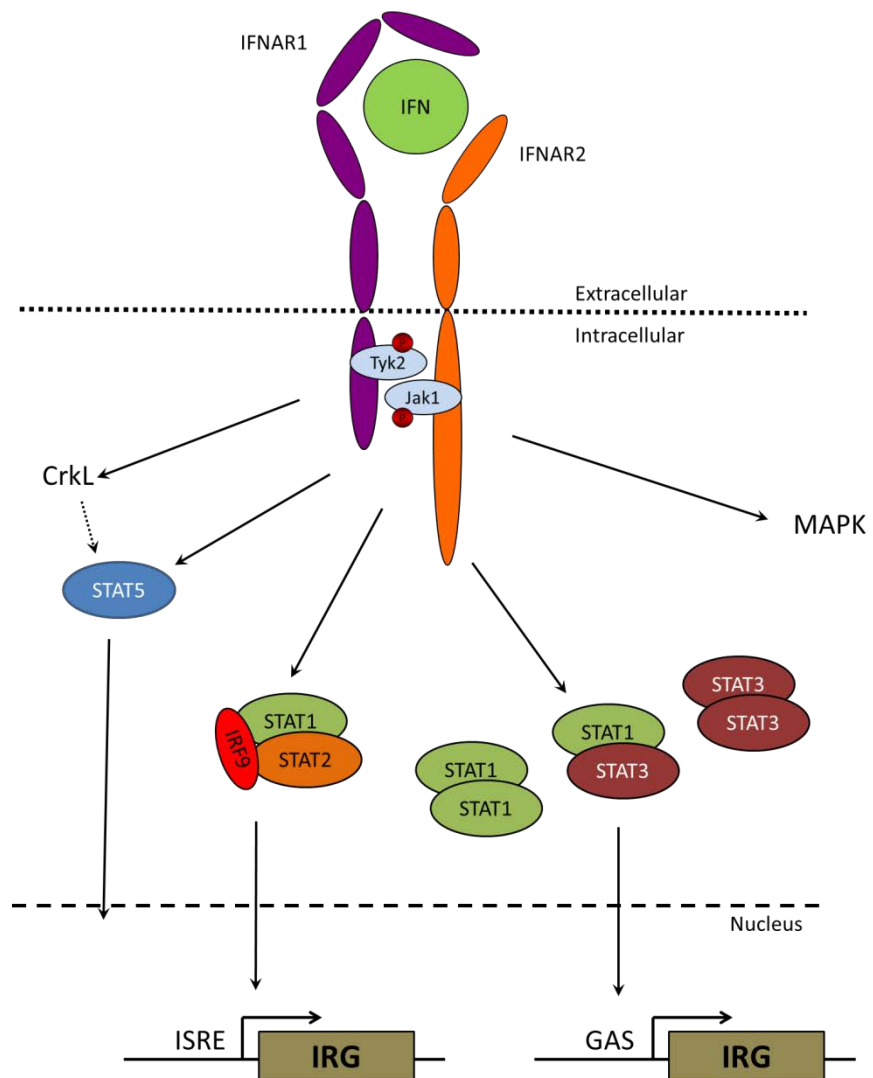


**Figure 1.4 The type I IFN signalling pathway.** A diagram of the intracellular signalling pathway of type I IFNs following receptor engagement. Type I IFN (Bright green) binds the two surface receptors, leading to the initiation of the intracellular signalling cascade. The receptor associated Tyk2 and Jak1 are phosphorylated, which leads to phosphorylation and dimerisation of STAT molecules. These translocate to the nucleus where they initiate the transcription of interferon regulated genes. STAT1/STAT2/IRF9 denotes the signalling molecule ISGF-3.

latent cytoplasmic transcription factors known as STATs [116]. Activated STATs homo and heterodimerise before translocating to the nucleus to induce the transcription of genes common to interferon signalling. The best described signalling molecule of type I interferons is ISGF-3, a trimeric transcription factor composed of STAT1, STAT2 and IRF-9 [117].

ISGF-3 recognises a specific sequence called the interferon stimulated response element (ISRE) in the promoter of IRGs and induces their transcription. In addition to ISREs, IRG promoters can also contain gamma-activated sequence (GAS) elements which are recognised by various STAT dimers, for example STAT1:STAT1, STAT1:STAT3 and STAT3:STAT3. These dimers are often called gamma-activated factors as they are the principal IFN $\gamma$  transcription factors (but are still formed in type I IFN signalling) [118]. Intriguingly, some IRG promoters contain either ISREs or GAS elements or sometimes both, no doubt an important feature when considering the plethora of biological responses elicited by type I interferons [119].

STATs are critical for IFN signalling, as *Stat1* null mice demonstrate virtually no induction of IRGs and succumb to sublethal viral challenge [120]. Importantly, rare human STAT1 alleles with loss of function mutations lead to increased susceptibility to viral and mycobacterial infections [121, 122]. Type I IFN signalling has also been found to be greatly reduced when STAT2 is absent [123]. This suggests that not only is the STAT2 containing ISGF-3 a principal mediator of type I IFN signalling but that STAT1 or STAT3 are not capable of compensating the loss of ISGF-3 or STAT2 [123].

The role of STAT3 in IFN signalling is less well defined due to the unavailability of *Stat3* null mice, which demonstrate embryonic lethality [124]. Interestingly, ablation of STAT3 in adult tissues does not lead to antiviral

deficiencies as observed with STAT1 or STAT2, suggesting it may not be necessary for the antiviral response [125]. On the other hand one study reported that reconstitution of the IFN resistant Daudi cell line with functional STAT3 sensitised the cells to IFN induced antiviral activity [126]. In addition, a separate study found that activation of STAT3 from a cytokine independent fusion construct lead to anti-hepatitis C virus activity in liver cells, indicating that it does in fact contribute to IFN induced antiviral activity [127]. More recent work however has indicated that STAT3 may be a negative regulator of the interferon induced antiviral response, as MEFs and macrophages with reduced STAT3 levels produced elevated levels of IRGs and IFNs following viral challenge compared to control cells [128]. Although there does not appear to be a clear consensus on the contribution of STAT3 to the IFN response, what has become apparent is that the actions of STAT3 are cell type and tissue dependent [125]. More targeted STAT3 ablation via tissue specific knock-outs for example may provide a better indication for the role of this transcription factor in type I IFN signalling.

STAT5 is another STAT family member that has been demonstrated to play a role in type I IFN signalling. STAT5 exists as a number of isoforms and early studies found that STAT5a and STAT5b were predominantly activated following type I IFN stimulation in the form of homo and heterodimers [129]. Intriguingly, STAT5a and STAT5b are not activated equally in all cell types as type I IFN induced STAT5b activation was readily observed in cervical epithelial cells but not in fibroblasts [130]. In terms of the type I IFN response, STAT5 was found to be important for the complete IFN induced transcriptional activation, as STAT5a and STAT5b deficient MEFs demonstrated a reduced ability to induce GAS element dependent luciferase activity [131]. Interestingly, STAT5b was also found to form a heterodimer with the molecule

CrkL that bound to specific GAS elements in the promoters of IRGs [132]. Loss of CrkL was found to lead to a reduction in GAS activation, indicating that the STAT5-CrkL dimer plays a non-redundant role in IRG transcription and can't be compensated for by STAT5 homodimers [133]. Although providing evidence that there is a role for STAT5 in transcriptional regulation more work is required to determine if STAT5 is essential to the type I IFN response during infection.

## **1.8 Biological activities of type I IFNs**

The type I IFNs were initially discovered based on their antiviral activity and have since been shown to also exhibit antiproliferative and immunoregulatory activities [14, 134, 135]. This section will aim to outline the canonical biological activities of type I IFNs and the downstream signalling mediators responsible for the observed activities.

### **1.8.1 Antiviral Activity**

The hallmark biological action of IFNs is their ability to interfere with the replication of viruses in infected cells. This antiviral response occurs fairly rapidly and acts as an immediate barrier against viral infections usually lasting hours to days after the initial insult [136-138]. The antiviral state is induced by a subset of IRGs responsible for blocking protein synthesis, promoting RNA cleavage, inhibiting transcription and affecting viral secretion [1]. An example of blocking translation is the dsRNA dependent protein kinase R (PKR), a serine-threonine kinase that is constitutively expressed and synthesised in an inactive form [115]. Binding of PKR to dsRNA for example blocks *de novo* protein synthesis by preventing the factor eukaryotic translation initiation factor

2 (eIF2 $\alpha$ ) to recycle [139, 140]. PKR knock-out studies showed a significantly decreased antiviral response against both herpes simplex virus 1 and encephalomyocarditis virus [141].

2'5'-OAS is another antiviral IRG that is activated in the presence of dsRNA to activate RNase L, which cleaves both viral and cellular ssRNA [142]. Although the inadvertent blocking of host protein synthesis by cleaving cellular ssRNA may be considered counter-productive towards an antiviral response, mice lacking 2'5'-OAS have increased susceptibility against viral infections [115].

One of the earliest induced proteins following type I IFN signalling is interferon stimulated gene 15 (ISG15), a 15kDa ubiquitin homologue [143]. Unlike ubiquitin, which attaches to proteins and targets them for degradation, ISG15 appears to act as an activator and has also been shown to prevent virus-mediated degradation of IRF-3 [144, 145]. Although >100 proteins have been postulated to be targets of ISGylation, the precise mechanisms and molecular outcomes of ISGylation are not known [146]. Importantly, *Isg15*<sup>-/-</sup> mice are more susceptible to influenza, herpes and sindbis virus infections, indicating that ISG15 contributes to the type I IFN induced antiviral state [147].

MxA, a protein belonging to the family of GTPases, is transcriptionally activated upon viral infection by ISGF-3 and binds viral polymerases and viral ribonucleoproteins to inhibit viral replication [148]. Interestingly, most laboratory mouse strains lack functional Mx1 due to naturally occurring mutations. This results in a natural susceptibility to influenza virus infection which is rescued when Mx1<sup>+</sup> is re-introduced [149].

Although thousands of IRGs have been identified since the discovery of the IFNs, it has been technically challenging to discern the contribution of individual IRGs in the interferon mediated antiviral response. Schoggins et al.

have addressed this issue by utilising a FACS based assay in which individual IRGs were cloned into a fluorescent protein expressing lentiviral vector. These lentiviral vectors, together with various viruses were then used to co-infect human cell lines [70]. Their results demonstrated that some IRGs (IRF-1, MDA5 and RIG-I for example), can have broad antiviral actions against many viruses yet some IRGs (IFI6 and OASL) produce targeted antiviral activity against certain viruses. Interestingly, the authors found a synergistic antiviral effect of co-transfected IRGs, indicating that the antiviral activity produced by interferons is more than the sum of individual gene contributions.

### **1.8.2 Antiproliferative Activity**

In addition to antiviral activity, interferons also demonstrate antiproliferative functions, although the exact mechanism of action is not as well defined as the antiviral response. Interferon mediated growth arrest can occur at all stages of the cell cycle although it is most commonly observed at the G1 phase [150]. This antiproliferative effect is modulated by the expression of cell-cycle regulators such as cyclin dependent kinase (Cdk) inhibitors, *c-myc*, the retinoblastoma protein and the E2F family of transcription factors [151]. In the first instance, a number of groups showed that stimulation of mouse and human cells with IFN $\alpha$  resulted in the induction of a multitude of Cdk inhibitors such as p15, p27, p19<sup>Ink4d</sup> and p21<sup>Cip1</sup> [151-153]. These inhibitors lower the kinase activity of the cyclin/Cdk complex, which is a primary regulatory molecule for cell cycle progression in eukaryotes.

c-Myc is a proto-oncogenic transcription factor with expression in tissues demonstrating high proliferative potential. The chromosomal translocation of c-Myc to one of the three chromosomes carrying antibody encoding genes is

responsible for the progression of human Burkitt's lymphoma [154]. Furthermore, high c-Myc levels are also seen in a multitude of leukaemic cell lines. Einat et al. found that stimulation of the Daudi cell line (isolated from a Burkitt's lymphoma patient) with IFN $\alpha$  demonstrated a marked reduction in c-Myc messenger RNA, resulting in G0/G1 growth arrest [155]. Importantly however, while c-Myc mRNA is downregulated by type I IFNs in Daudi cells, other cancer cell lines sensitive to the antiproliferative effect of IFN $\beta$  overexpressing c-Myc showed no correlation between the growth arrest and c-Myc mRNA levels [156]. This suggests that c-Myc mRNA downregulation by type I IFNs is important for the antiproliferative activity in some but certainly not all cells overexpressing c-Myc. This aspect is highlighted further on in section 1.10.3.

An interesting finding is that the antiproliferative actions of IFNs are only maintained as long as interferon signalling is present, in contrast to the antiviral state which can be maintained in the absence of IFN [157]. This is significant when considering that upon prolonged IFN $\alpha$  exposure, cells undergo growth arrest followed by apoptosis [158]. This phenomenon might be a protective mechanism to ensure viral clearance without being self-destructive.

### **1.8.3 Pro-apoptotic Activity**

One of the mechanisms by which type I interferons are proposed to exert their anti-tumor activity is via the ability to induce apoptosis. Broadly speaking, IFNs have been shown to induce the activation of caspases, a family of proteases which follow a signal cascade to induce apoptosis in target cells [159]. This pathway is known as the intrinsic pathway and involves a loss of mitochondrial

membrane potential and cytochrome c release, targeting the cells for programmed cell death [160]. In addition, IFNs have also been shown to repress the expression of antiapoptotic genes such as Bcl-xL and Bcl-2, demonstrating a multi-factorial approach to inducing cell death [161]. The critical role of Bcl-2s in IFN induced apoptosis was shown as overexpression of Bcl-2 in interferon treated cells virtually conferred apoptotic resistance [162].

Type I interferons have also been shown to induce the expression of the tumor suppressor gene p53 and its target genes Mdm2 and CD95 [163]. Although apoptosis decreased in response to blocking CD95 and p53, apoptosis still occurred, highlighting that multiple apoptotic pathways are induced following IFN treatment [164].

Cell surface death receptors such as CD95/Fas and TNF related apoptosis inducing ligand (TRAIL) are interferon inducible genes implicated in interferon induced apoptosis [165, 166]. Intriguingly, this effect appears to be IFN subtype and cell specific as IFN $\alpha$  has been shown to induce both TRAIL and Fas in multiple myeloma cells whereas TRAIL induction was poor in melanoma cells. In contrast, IFN $\beta$  preferentially induced TRAIL in melanoma and ovarian carcinoma cells when compared to IFN $\alpha$  [167, 168]. One can hypothesise that it is these subtle differences that account for the different pharmaceutical indications of IFN formulations.

It is clear that type I interferons, either directly or indirectly activate virtually every apoptotic effector pathway. Intriguingly, IFN induced apoptosis is seen quite late after treatment (>48hrs), suggesting that the apoptotic effect is induced by intermediates rather than directly by IFNs [165, 169]. It is likely that this serves the function to allow immediate interferon effects such as antiviral

and antiproliferative activities to take hold to clear the insult before a more drastic approach is taken.

#### **1.8.4 Immunoregulatory activity**

The type I interferons demonstrate a remarkable number of immunoregulatory activities including the ability to activate natural killer (NK) cells, T- and B- cells and induce the maturation and differentiation of dendritic cells (DCs) [134, 170-172]. These functions are critical for both innate and adaptive immune systems as mice deficient in parts of the interferon signalling pathway demonstrate increased immune phenotypes [173].

One of the first immunoregulatory functions of type I interferons discovered was their ability to activate NK-cells [171, 174]. ‘Classical’ NK-cells are non-T cells that seek out target cells and elicit their cytotoxic function by the release of Granzyme B and perforin into the target cells [175]. This activity however is not restricted to viral infections as IFN activated NK-cells also demonstrate potent anti-tumor activity [176]. Importantly, type I IFNs and STAT1 are critical molecules for NK-cell activity as a loss of STAT1 in mice significantly reduced NK-cell lytic potential [173, 177].

A broader function of type I interferons in the immune response is their capacity to upregulate the expression of MHC class I protein on the surface of cells [178]. This leads to an increase in antigen presentation, thereby promoting adaptive immune responses elicited by T-cells [179].

Type I IFNs have been shown to have a profound effect on the humoral response by directly promoting enhanced antibody production from B-cells and inducing isotype switching [172, 180]. The latter effect was mediated by

IFN $\alpha/\beta$  activated dendritic cells, further demonstrating the capacity of type I IFNs to link the innate and adaptive immune responses. Interestingly, IFN $\alpha/\beta$  treatment of murine splenic B-cells protected from apoptosis in a dose dependent manner [181]. This observation is in direct contrast with the finding that interferons induce apoptosis in a number of malignant cell lines as outlined previously. Therefore this further suggests that the effects associated with type I IFN treatment are highly cell dependent.

Type I IFNs have been shown to have a profound immunoregulatory effect on T-cells [134]. T-cells are rapidly activated in response to antigen and just as rapidly undergo apoptosis [182]. Type I IFNs were found to be a potent survival factor for activated T-cells (of both CD4 and CD8 lineages), as *in vivo* activated T-cells were able to be cultured significantly longer *in vitro* in the presence of type I IFN compared to IFN $\gamma$  [183]. Also, type I IFN was found to directly inhibit the apoptotic signal induced by CD95/Fas in activated human T-cells [184]. Moreover Tough et al. found that IFN induced proliferation of memory CD8 cells, however this effect was later found to be indirect through the actions of IL15, an IRG [185, 186]. Critically, type I IFN was found to directly confer the signal resulting in antigen-specific T-cell expansion and subsequent effector and memory cell generation, as mice deficient in IFNAR1 demonstrated a 100-fold reduced memory T-cell pool compared to wild type mice [187].

Lastly, type I IFN was found to regulate lymphocyte egress from lymphoid organs, virtually shutting down lymphocyte trafficking in these organs [188, 189]. The purpose of this is to ensure maximal exposure of antigen-specific cells to antigen presenting cells in lymph organs, resulting in their activation [190].

## 1.9 Type I IFNs in reproduction

As outlined in section 1.8, the IFNs have a broad range of ‘classical’ biological activities. Interestingly, in some species certain type I IFNs have a much more specialised function.

Of all the currently known IFNs, the trophoblast (pre-placenta) interferons ( $\tau$  and  $\delta$ ) are the most unusual. Although sharing high sequence similarity with human and mouse IFN $\alpha$  (~50%) [191, 192], their predominant function is in maternal recognition of the conceptus and maintenance of pregnancy in a number of ungulate species such as cattle, sheep and goats. [193, 194]. A striking feature of IFN $\tau$  that differentiates it from classical type I IFNs is its inability to be induced by viruses and instead is under the control of Ets2, a member of the Ets family of transcription factors which are important in the regulation of proliferation, differentiation and apoptosis of a variety of tissues and cell types [195, 196]. Importantly, IFN $\tau$  acts on the maternal uterine system by serving as the principal signal secreted by the developing conceptus that maintains the corpus luteum, a cellular body that secretes progesterone to signal the endometrium to maintain pregnancy [197]. Despite the apparent difference in function compared to the virally inducible IFNs, IFN $\tau$  still signals via the canonical type I IFN receptor to induce STAT activation [198].

Perhaps somewhat unexpectedly, IFN $\tau$  demonstrates antiviral activity comparable to that of IFN $\alpha$  *in vitro* even though there is no indication of it being functional as an antiviral cytokine in the uterine environment [199]. Interestingly IRGs common to the antiviral response such as CXCL10, ISG15 and MX1 can be measured in the endometrium of cattle treated with IFN $\tau$  *in vivo* [200], implying that IFN $\tau$  could also have antiviral activity *in vivo*. IFN $\tau$  was also found to exhibit other hallmark type I interferon activities *in vitro* such

as antiproliferative and immunoregulatory effects, suggesting that the canonical type I IFN activities of IFN $\tau$  are still present even though the cytokine serves a different biological function in ruminants [38].

While in humans, chorionic gonadotropin is responsible for maintaining the corpus luteum and is secreted by the trophoblast at around day 8 of pregnancy, the trophoblast does have the capability of secreting IFN $\alpha$  and IFN $\beta$  [193, 201, 202]. However this IFN was found to be virus inducible as IFN $\alpha$ , - $\beta$  or - $\omega$  subtypes and therefore does not appear to contribute to human pregnancy like IFN $\tau$  does in ungulates.

A number of studies found elevated levels of IFN activity in human cord blood, maternal blood, seminal plasma, amniotic fluid and foetal blood in the absence of apparent infection, however it was not determined which cells expressed this interferon. More importantly the studies couldn't exclude the possibility of the presence of pathogenic stimuli at some stage [203, 204]. A separate study found elevated level of IFN $\alpha$  in pregnant mothers with a history of Herpes Simplex Virus 2 (HSV-2) infection [205], indeed implying that IFN activity in human pregnancy is likely to result from infection. Thus far, any evidence for a role of type I interferon in human pregnancy appears to be limited to its function as a pathogen inducible cytokine with no unique properties specific to the reproductive tract.

## **1.10 Structure of type I IFNs**

The determination of crystal structures of type I IFNs pointed out their relation to the family of helical cytokines, which include members such as growth hormone and interleukin-6, both cylindrical globular proteins composed of 4  $\alpha$ -helices [206, 207]. Interferons are slightly different from these cytokines in that

they carry an additional helix, which has important functions in receptor binding.

Crystal structures of hIFN $\alpha$ , hIFN $\beta$ , mIFN $\beta$  and ovIFN $\tau$  are available and indicate remarkable structural conservation, even across species [207-210] (Figure 1.5). More significantly, these structural findings also assisted in the characterization of individual residues important in protein folding and receptor-ligand interactions [211] [6], which will be discussed in more detail later in this section.

### **1.10.1 IFN $\alpha$**

Type I IFNs demonstrate a remarkably conserved structure considering sequence identity can be as low as 21% (Figure 1.1). This conserved structure allows all type I IFNs to signal via a common cell surface receptor. A feature common to type I IFNs are cysteine residues which in IFN $\alpha$ 's are involved in two disulfide bonds; Cys 1-Cys 98 and Cys 29-Cys 139 [206] (Figure 1.6 and 1.7). The importance of the cysteine residues in IFN $\alpha$  is highlighted in Cys29 or Cys139 mutants, which show dramatically reduced biological activity and the surrounding residues are believed to be fundamental in receptor binding [6]. Furthermore, loss of the disulphide bonds either by treatment with reducing agents or from incorrect folding lead to protein aggregation and complete loss of activity [212, 213], highlighting the importance of the disulphide bonds for the function of IFNs.

In addition to the cysteine residues, sequence analysis of 35 separate IFN $\alpha$  species identified 25 absolutely conserved residues, the majority of which are responsible for maintaining the structural framework of the molecule as they

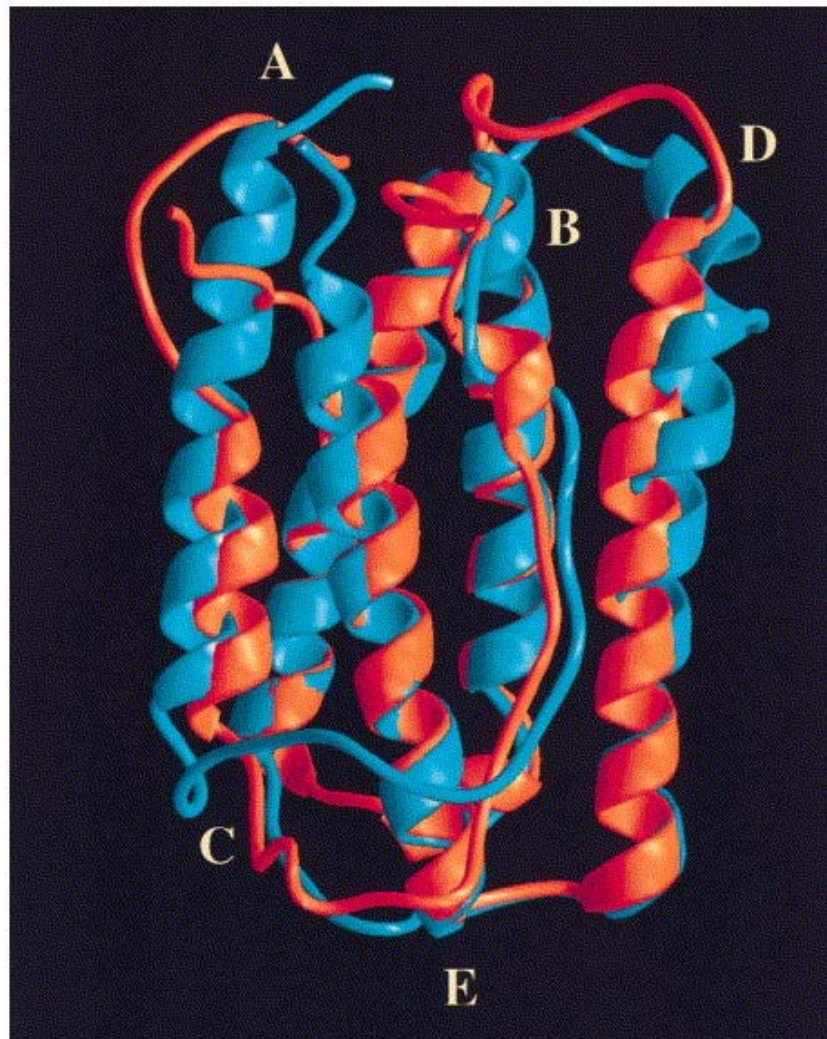


**Figure 1.5 Overlay of the crystal structures of human IFN $\alpha$ 2a and murine IFN $\beta$ .** Ribbon models of the crystal structures of human IFN $\alpha$ 2a (orange) and murine IFN $\beta$  (blue) were overlaid to highlight the conserved structure adopted by type I IFNs. Letters denote the  $\alpha$ -helices of human IFN $\alpha$ 2a. Figure was taken from Klaus et al., 1997 [213].

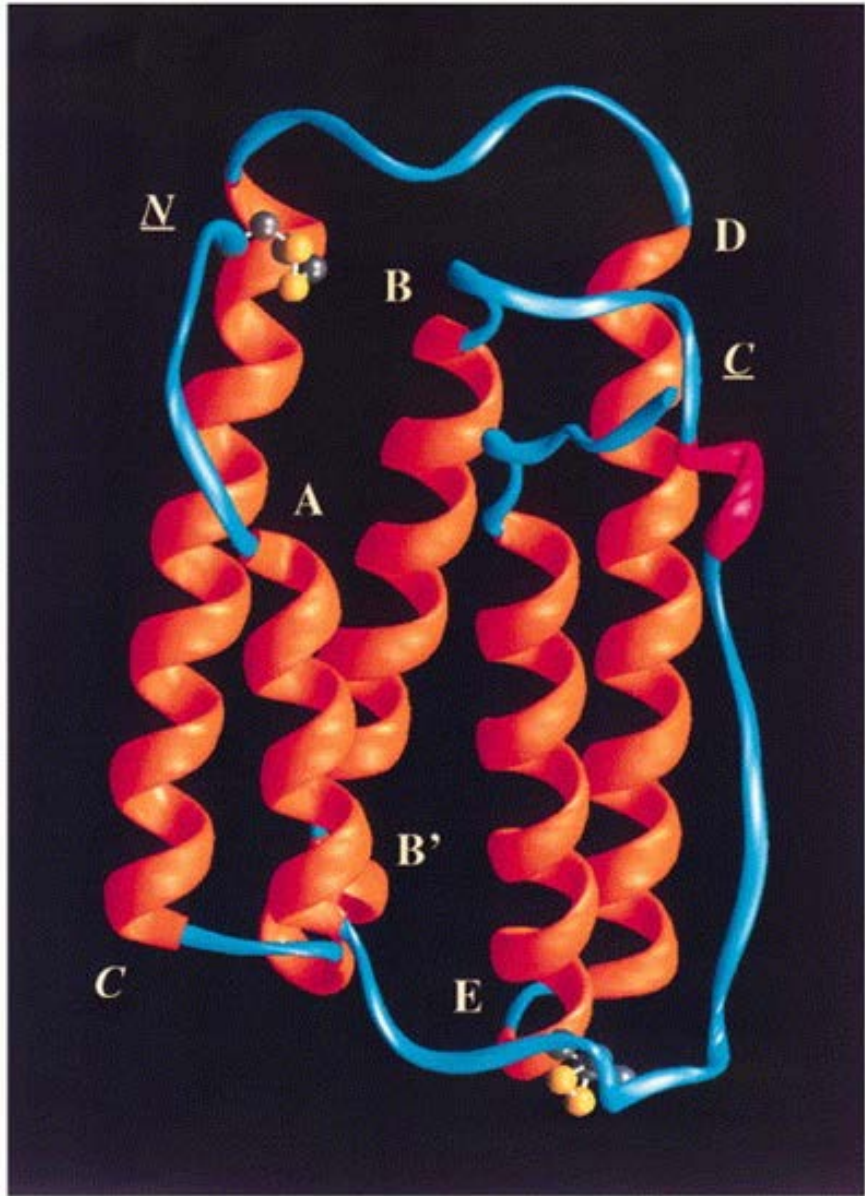


**Figure 1.6** The crystal structure of human IFN $\alpha$ 2a. A ribbon model of the crystal structure of human IFN $\alpha$ 2a, depicting the  $\alpha$ -helices in orange and the connecting loops highlighted in blue. The letters denote the  $\alpha$ -helices. Underlined letters denote the N- and C-terminal ends of the molecule. The two disulfide bonds are portrayed as ball and sticks. Figure taken from Klaus et al., 1997 [213].

are important in the formation of the  $\alpha$ -helices and disulphide bonds [210] (Table 1.1 and Figure 1.7).

Furthermore, site directed mutagenesis of critical residues in hIFN $\alpha$ 2a lead to the identification of proposed binding sites for the IFN receptor complex [214-216]. These sites are believed to be patches of conserved hydrophobic residues, namely 29-35, 78-95 and 123-140 [216]. Importantly, these residues fall within the absolutely conserved amino acids described above (Table 1.1). Indeed, the recent elucidation of the interferon ternary complex (an IFN $\alpha$ 2 mutant bound to IFNAR1 and IFNAR2) has demonstrated five patches of contact between the IFN molecule and the receptor chains (Figure 1.8) [9]. Importantly, all regions previously reported to be sites of interaction were validated in the ternary complex crystal structure. For instance Waite et al. found that mutating residues 26, 27, 31, 32, 34, 35 and 37 in IFN $\alpha$ 4 did not significantly affect biological activity [214], which from the crystal structure data can be seen are not sites that interact with the receptor (Figure 1.8). On the other hand, mutating Leu30, Arg33 and Phe36 resulted in a dramatic decrease in activity and we now know these sites are not only conserved in all IFN $\alpha$  species [210], but they also are involved in receptor binding [9].

### 1.10.2 IFN $\beta$

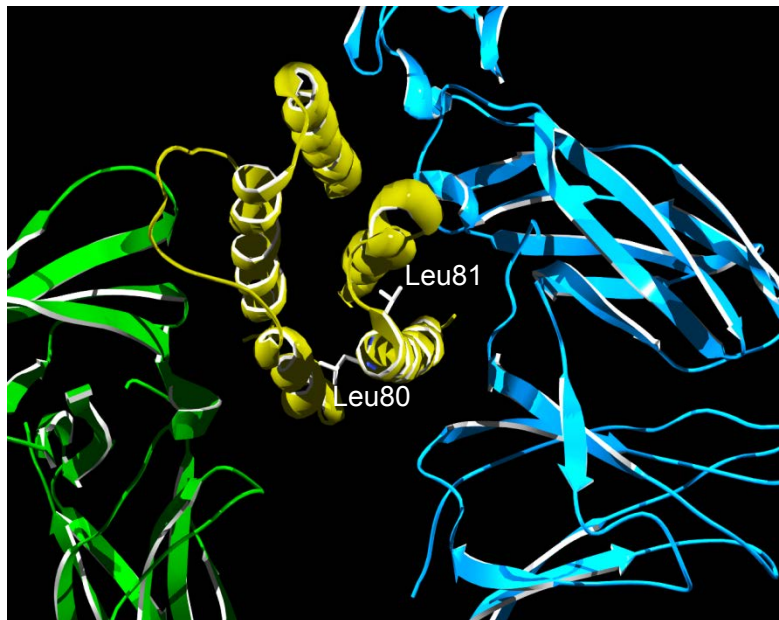
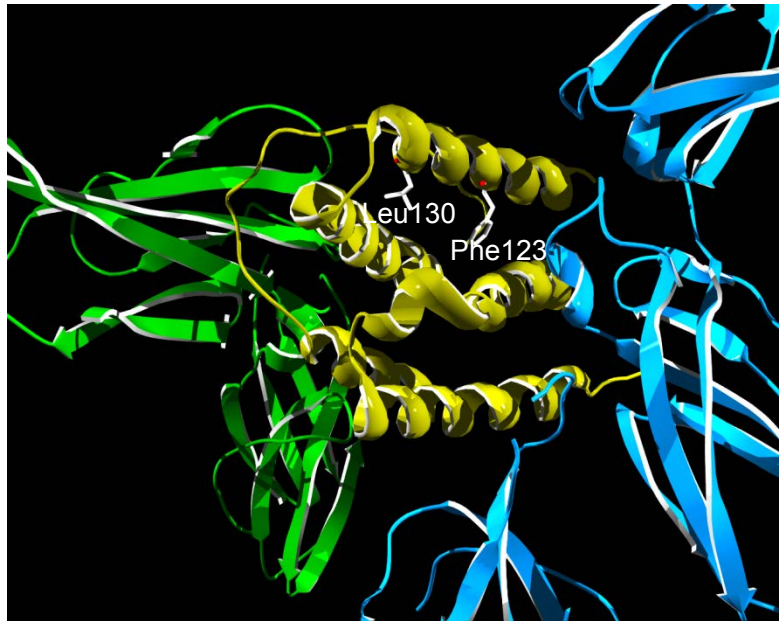
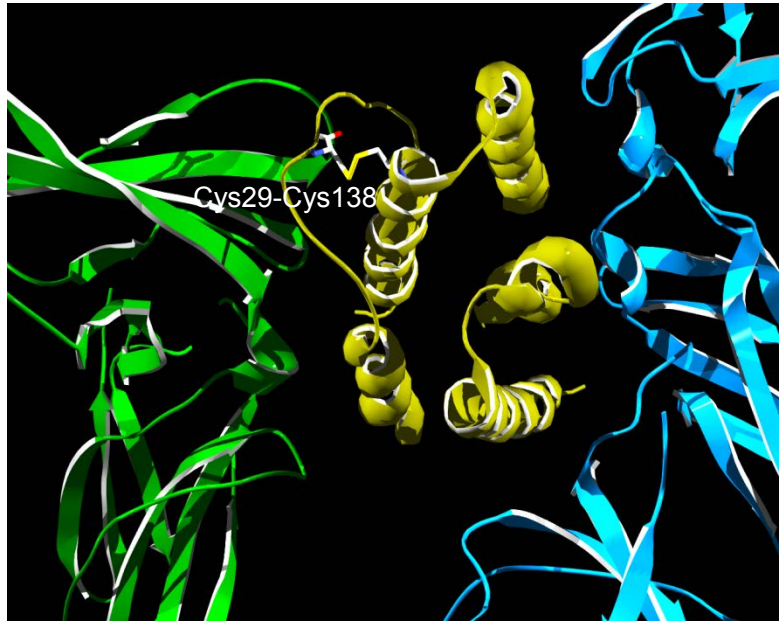
hIFN $\alpha$ 's and hIFN $\beta$  share approximately 30% sequence similarity (Figure 1.1) and IFN $\beta$  also demonstrates similar homology to other type I interferon members. Unlike hIFN $\alpha$ s, hIFN $\beta$  only contains the disulfide bond Cys31-Cys141 (equivalent to Cys29-Cys138 in IFN $\alpha$ ) and X-ray crystallography studies of human and murine IFN $\beta$  show a remarkable structural conservation across species [29, 210]. In light of this structural conservation, it is surprising

Table 1.1. Amino acid residues absolutely conserved among 35 IFN $\alpha$  species

Residue	Location	Putative Role
Cys1	N terminus	Disulfide bond
Leu3		
Leu9		
Ser28	AB loop	Receptor interaction
Cys29		Disulfide bond
Arg33	AB loop	Receptor interaction
Phe36	AB loop	Packing against helix D
Gln46	AB loop	
Gln61	Helix B	
Leu80	Helix C	Helix packing
Leu81	Helix C	Helix packing
Cys98	Helix C	Disulfide bond
Gln101	Loop CD	
Leu110	Helix D	
Tyr122	Helix D	Packing against AB loop
Phe123	Helix D	Helix packing
Arg125	Helix D	Receptor interaction
Leu130	Helix D	Helix packing
Cys138	Helix E	Disulfide bond
Ala139	Helix E	Helix packing
Trp140	Helix E	Helix packing
Glu141	Helix E	Salt bridge
Ala145	Helix E	
Arg149	Helix E	
Ser154	Helix E	Helix stabilizing

Table reproduced from Klaus et al., 1997 [209].

**Figure 1.7 3D modelling of human IFN $\alpha$ 2 depicting side chains important for structural rigidity.** Images showing the 3D structure of the type I receptor in complex with IFN $\alpha$ 2. Some of the side chains important for structural rigidity as described in Table 1.1 are highlighted as wireframe molecules and annotated. Of note, side chains important for structural rigidity face inwards. Blue, IFNAR1; Green, IFNAR2; Gold, IFN $\alpha$ 2. Structural modeling was done using PDB Viewer software.



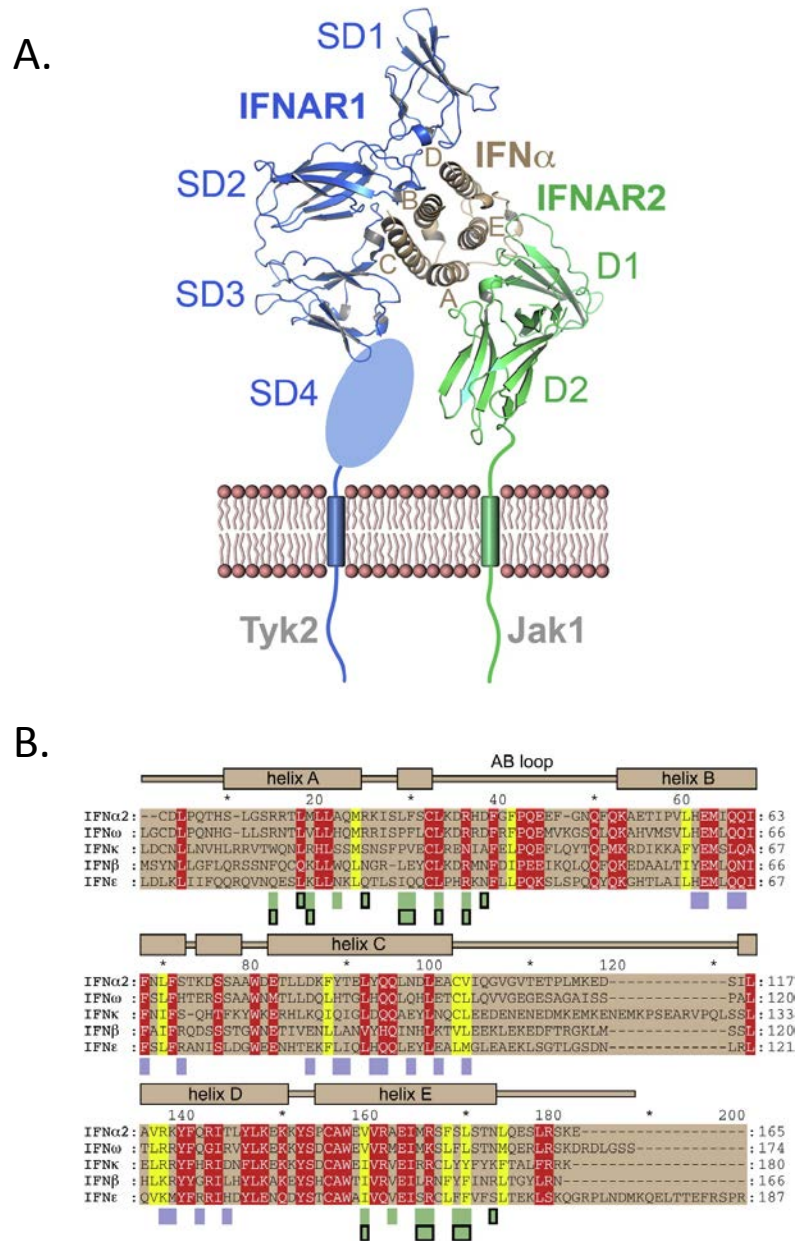


**Figure 1.8 Type I IFN ternary complex and receptor interaction.** A) Ribbon model of the crystal structure of the type I IFN ternary receptor complex (IFNAR1ECD, IFN $\alpha$ 2 mutant ligand and IFNAR2ECD). Domains of each receptor are indicated as either SD or D. IFN ligand helices are indicated as A, B, C, D and E. The crystal structure was resolved without the membrane proximal domain of IFNAR1, here depicted as an oval. B) Sequence alignment of human type I IFN family members and secondary structure elements (on top of sequences). Invariant residues are colored red, conservative substitutions are colored yellow. Receptor interacting residues are in rectangles below the alignment and are: blue, IFNAR1 interaction; green, IFNAR2 interacting. Outlined rectangles mark interacting residues in the IFN $\alpha$ 2/IFNAR2 binary complex. Figures from Thomas et al., 2011 [9].

to see that murine IFN $\beta$  only has a single cysteine residue in the mature protein at residue 17. While the complete lack of a disulfide bond apparently has little effect on the structure of mIFN $\beta$ , a mutant generated to mimic hIFN $\beta$  with the intact Cys31-Cys141 disulfide bond does demonstrate a 10-fold increase in antiviral activity compared to the wild-type form [217]. Perhaps the reason for the absence of a disulfide bond in mIFN $\beta$  is as simple as there being no evolutionary need for higher antiviral activity in mIFN $\beta$ .

Apart from the disulfide bond, the most noteworthy difference between human and murine IFN $\beta$  is the presence of a small but distinct sixth helix in the murine model, termed Helix CD, which comprises the residues 102 to 108 [209] (Figure 1.9). As there is no resolved 3D structure of mIFN $\alpha$ , it is yet to be determined whether or not helix CD is also present in IFN $\alpha$ s, and whether or not it has significance in receptor binding and biological activity.

### 1.10.3 Potency of IFNs

Small mutations in the protein coding sequence, rather than gross conformational changes are hypothesised to influence the individual activities of IFN $\alpha$  subtypes [216, 218, 219]. Antiviral activity is the hallmark feature of IFNs and therefore *in vitro* antiviral activity is often used to determine the potency of interferons. These vary quite considerably among individual IFNs and are also dependant on the cell type the assay is carried out in [220-222]. As such, IFN $\alpha$ 8 appears to exhibit the highest antiviral activity in most cell lines tested whereas IFN $\alpha$ 1 has the lowest [221, 223]. Interestingly, all therapeutic forms of IFN $\alpha$  are either derived from IFN $\alpha$ 2 or from an IFN $\alpha$  consensus sequence [6, 224-227], which is likely due to IFN $\alpha$ 2's high antiviral activity [221, 228]. In addition to antiviral activity IFNs also possess

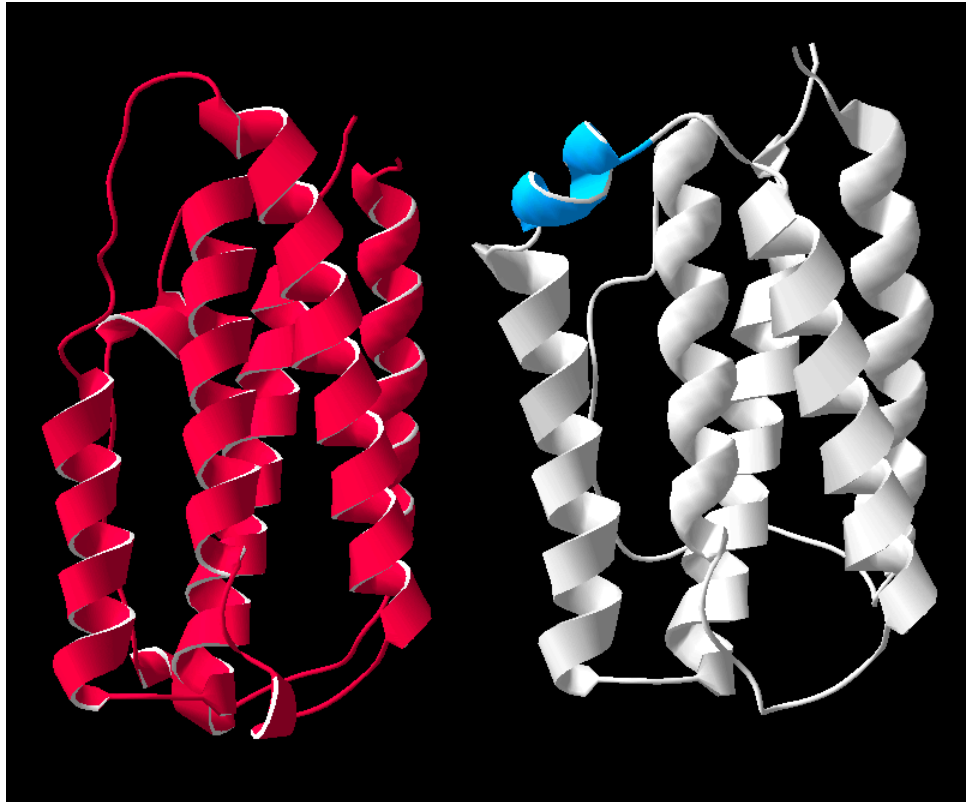


**Figure 1.9 Comparison of the 3D structures of human IFN $\beta$  and mouse IFN $\beta$ .** The three dimensional structures of human (red) and murine (white) IFN $\beta$  were compared using the resolved structures (PDB:1AU1 and PDB:1WU3, respectively). The blue helix highlights Helix CD in mouse IFN $\beta$ , which is absent in human IFN $\beta$ . Structural modeling was done using PDB Viewer software.

antiproliferative and immunoregulatory functions and much like antiviral activity, each IFN demonstrates varying abilities to activate NK-cells. IFN $\alpha$ 2, -8 and -10 for example are potent activators of NK-cells, whereas IFN $\alpha$ 7 demonstrates virtually no effect and is believed to enable IFN $\alpha$ 7 to negatively regulate NK-cell activation [229]. It should be mentioned however that this is an isolated report of such a vast difference in a specific biological activity and needs to be examined more closely.

Interestingly, IFN $\beta$  demonstrates significantly higher antiproliferative activity compared to other type I IFNs [135, 223, 230]. A comprehensive study conducted by Borden et al. found that out of 25 different cell lines, IFN $\beta$  was able to inhibit the growth by more than 20% in 88% of the cells after 120 hours [135]. In contrast, at 120hours an IFN $\alpha$  mix was only able to inhibit cell growth by more than 20% in 36% of cells. While in this study a mix of IFN $\alpha$  proteins was used, later studies have also demonstrated that the antiproliferative activity of recombinant IFN $\beta$  far exceeds that of any other recombinant IFN $\alpha$  subtype [223]. Unlike IFN induced antiviral activity, in which the gene products and cellular mediators are well characterised, less is known about the components and pathways that elicit the antiproliferative effect and indeed why IFN $\beta$  is so much more potent than IFN $\alpha$ . Sanceau et al. found that while IFN $\alpha$ 2 and IFN $\beta$  were similarly effective at inducing tyrosine phosphorylation on STAT1, only IFN $\beta$  induced serine phosphorylation on STAT1 [231]. Furthermore, the authors also found that ISGF-3 was more efficiently formed following IFN $\beta$  than IFN $\alpha$ 2 stimulation. This is interesting as a more recent study has found that IRF-9, a key component of ISGF-3 is essential for the antiproliferative effect of IFN $\alpha$ 2 [232]. It is thus possible that the increased antiproliferative activity of IFN $\beta$  is in part due to a stronger assembly or recruitment of ISGF-3 compared to IFN $\alpha$ .

These differences in activity among interferons are interesting when considering their close structural conservation and their common use of the single heterodimeric interferon receptor. More recent work has addressed this phenomenon by examining the structure/function relationship of the IFN molecule to its receptor. The next section of this literature review will address our current knowledge of how receptor binding affects IFN activity.

#### **1.10.4 Surface ‘hot spots’ determine IFN activity**

The different biological efficacies observed among IFN $\alpha$  subtypes has been attributed to the relative binding affinities of each molecule for the common type I IFN receptor [216, 223]. IFN mutagenesis studies demonstrated the presence of ‘hot-spots’ on the surface of IFN $\alpha$ 2 that were important for receptor affinity and biological activity [216]. Interestingly, the 28 residues that were mutated within these hot spots are all near the interferon receptor binding sites (Figure 1.10 and Figure 1.11), yet don’t directly interact with the receptor. With the exception of 3 residues, they also did not include the critically conserved residues described before (Table 1.1), suggesting that small mutations in these areas are responsible for the different biological potencies seen within the IFNs. Indeed, sequence alignment of IFN subtypes shows subtle mutations in these residues among some IFN $\alpha$  subtypes (Figure 1.10). Importantly, many of these residues are not homologous in IFN $\beta$  and thus may account for the much higher antiproliferative activity of IFN $\beta$ .

What these mutagenesis studies also found was a direct correlation between binding affinity and antiviral and antiproliferative activity [216, 219] such that the stronger the binding affinity of the IFN with IFNAR2, the higher the biological activity [219]. Indeed, a further study investigating the biological

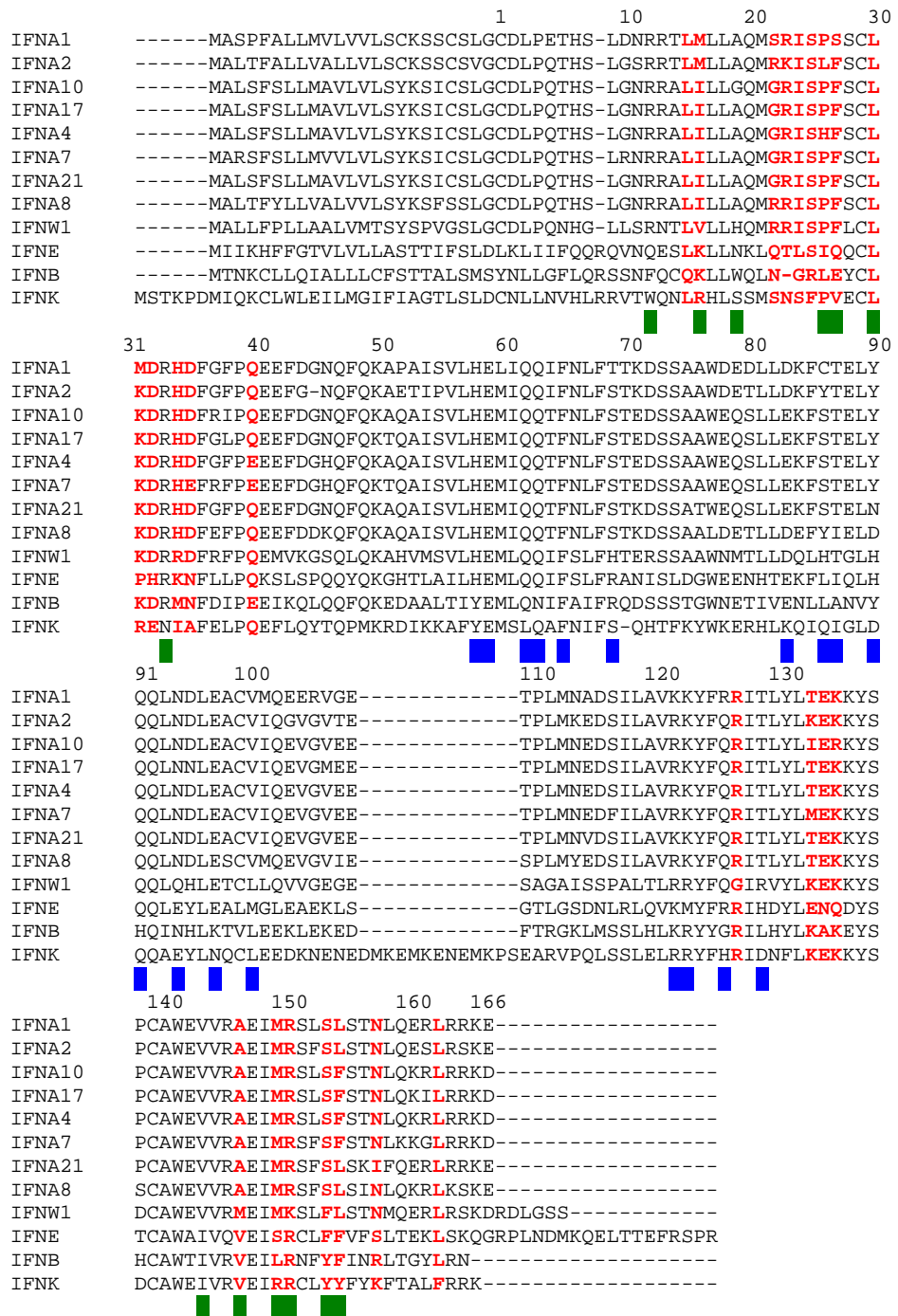
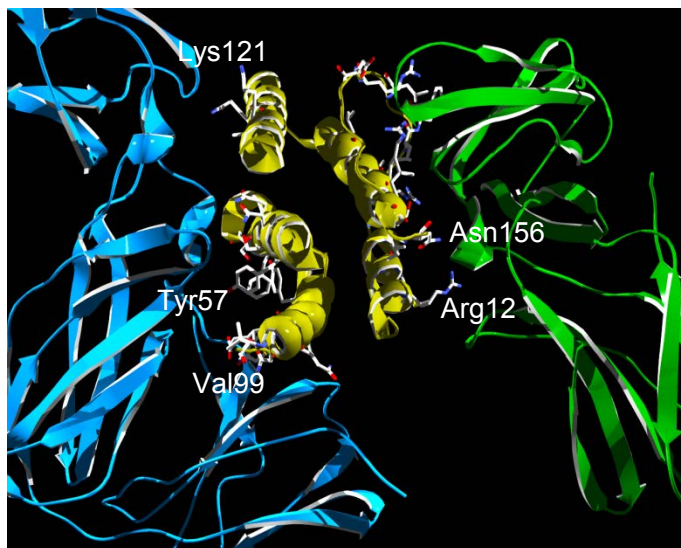
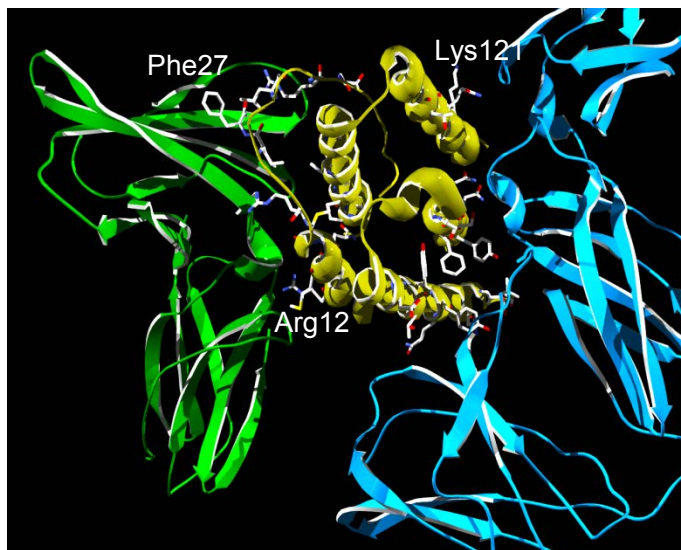
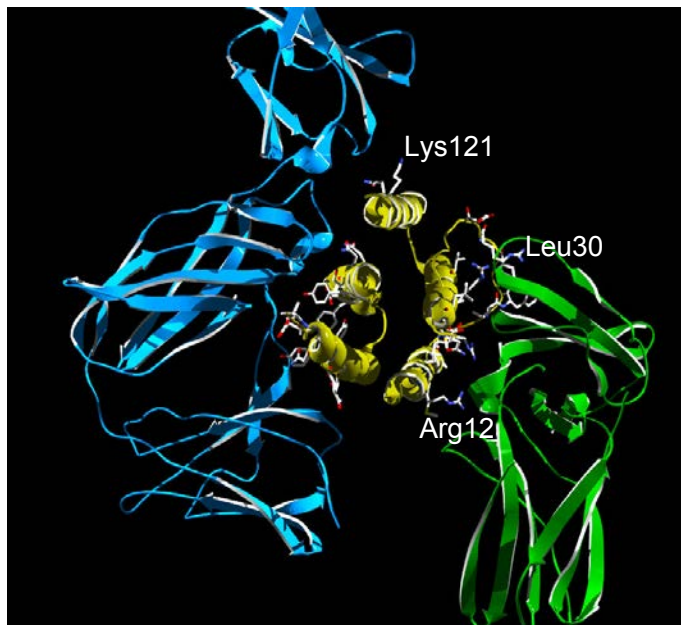


**Figure 1.10** Sequence alignment of human type I IFNs and locations of interferon activity “hot-spots”. The amino acid sequences of human type I IFNs were aligned using ClustalW2 and the locations of amino acid residues mutated in Klaus et al [209] are highlighted in red. Numbers indicate amino acid residues where 1 is the mature start site of IFN $\alpha$ 1/2. Colored boxes below the sequences denote the amino acid residues that directly interact with the receptors. Green boxes, IFNAR2 interactions; Blue boxes, IFNAR1 interactions.

**Figure 1.11 3D Model of IFNAR1 – IFN $\alpha$  – IFNAR2 ternary structure.** 3D structural images depicting human IFN $\alpha$ 2 in complex with its receptors IFNAR1 and IFNAR2. Residues important for binding the IFN receptors as shown in Figure 1.10 are highlighted here as individual wireframe molecules with some residues annotated. Of note, amino acid sidechains important for receptor interaction point towards the receptor subunits. Blue, IFNAR1; Green, IFNAR2; Gold, IFN $\alpha$ 2. Structural modeling was done using PDB Viewer software.



activities and binding affinities of all IFN $\alpha$  subtypes found that there was a direct correlation between receptor binding affinity and antiproliferative activity, showing that the studies with mutant IFN $\alpha$  subtypes also reflect what happens with the naturally occurring subtypes [223]. What is most interesting however is that Lavoie et al. also found that antiviral activity correlated best with IFNAR2 affinity alone, whereas antiproliferative activity correlated best with the relative affinity to both receptor subunits [223]. This indeed suggests that affinity towards IFNAR1 could dictate the strength of the antiproliferative effect.

The above hypothesis is further supported by a study in which hIFN $\alpha$ 2 was mutated to elicit similar biological activities as hIFN $\beta$  [230]. Residues H57, E58 and Q61 were changed to alanines, forming the triple mutant called HEQ, which demonstrated IFNAR1 binding affinities over 35-fold higher than wild type IFN $\alpha$ 2 (IFN $\beta$  was 50-fold) while maintaining the same binding affinity for IFNAR2. The mutations were also associated with an increase in antiviral and antiproliferative activities, supporting the hypothesis that relative binding affinities of IFN subtypes towards the receptors correlate with differential responses [230].

Recent studies have revealed the stability of the interferon/receptor ternary complex to be vital in eliciting the differential actions of the IFNs by discerning weak and rapid from strong and prolonged receptor engagement [10, 233]. These studies made use of another IFN $\alpha$ 2 mutant called YNS, which had the following mutations; H57Y, E58N and Q61S [233]. In this work, the YNS mutant had IFNAR1 binding affinities 60-fold greater than WT IFN $\alpha$ 2 and 3-fold greater than IFN $\beta$ , resulting in higher biological activities directly relative to the increased binding affinity. Furthermore, this YNS mutant was found to have much decreased dissociation rates from IFNAR1 compared to WT

IFN $\alpha$ 2, meaning the mutant bound the receptor much longer. In a follow up study using the YNS mutant, the biological activities of IFNs were found to be dictated by the overall binding strength to both receptor subunits rather than individual receptor affinities [10]. Therefore the model proposes that low concentrations of weaker binding IFNs are largely responsible for the antiviral effect whereas high concentrations of a tighter binding IFN lead to an antiproliferative and apoptotic response [10].

This hypothesis is further supported by Moraga et al. *who* demonstrated that the different biological potencies of IFN $\alpha$ 2 and IFN $\beta$  are only evident at low receptor levels [11]. Using cells engineered to express higher levels of IFNAR1 and IFNAR2, the authors found that while IFN $\alpha$ 2 was indeed less potent at eliciting an antiproliferative response compared to IFN $\beta$  in cells expressing low levels of receptors, IFN $\alpha$ 2 was just as, if not more biologically active than IFN $\beta$  in the presence of abundant cellular receptors. The proposed model is that the lower binding affinities of IFN $\alpha$ 2 to the receptors compared to IFN $\beta$  allow it to sequentially activate multiple receptors, therefore triggering more downstream signalling. In other words, when cell surface receptors are in abundance, the differential activities of type I IFNs are lost.

#### **1.10.5 Crystal structures of the IFN-Receptor complex**

Recently, the interferon ternary complex was crystallised, which resulted in a greater understanding of the receptor-ligand interactions required for differential IFN signalling [9]. This study proposed that IFNAR1 undergoes a conformational change upon encountering its ligand, resulting in the N-terminal SD1 domain to contact more residues on the IFN molecule. This leads to the stabilization of the ternary complex and thus successful

transphosphorylation of intracellular JAK1 and TYK2 to initiate the downstream signalling cascade. Evaluating how drastic the conformational change in IFNAR1 is following ligand binding is still unknown as the structure of unbound IFNAR1 has not yet been determined. In addition, it was also found that as the IFNAR1 extracellular domain is twice the size of IFNAR2, ligand binding residues are distributed over a greater surface of the receptor and thus individual contributions from each residue can lead to 'fine-tuning' of the interferon response by small changes in binding affinity.

Thus, similar to previous studies, it was found that while antiviral and antiproliferative activities were both influenced by binding affinity, this effect was more obvious for antiproliferative activity. The authors concluded that the antiproliferative effect is a more 'tunable' process, as maximal antiviral activity was seen with intermediate affinities while antiproliferative activity required high affinities to reach a maximal effect [9]. A likely reason for this effect is the nature of the response observed. Sustained antiproliferative activity leads to apoptosis and tissue damage, therefore requiring much tighter control to avoid unnecessary damage. When considering the interferon response as a whole, different IFN subtypes and their relative binding affinities to the receptors therefore tightly control the duration and strength of the biological response [10]. One can hypothesise that perhaps the interferons evolved to contain so many subtypes as a means of self-regulation, that is, to dampen a response that may otherwise lead to uncontrolled damage.

Although the IFNs are thought to signal only via an interaction that includes both receptor subunits, recent work performed in our laboratory demonstrates that a binary complex of IFNAR1 and IFN $\beta$  leads to functional signalling [234]. Mouse IFN $\beta$  was shown to bind to IFNAR1 in an IFNAR2 independent manner with nanomolar affinity. Importantly, comparison of the IFN $\beta$ -IFNAR1

and ternary complex crystal structures shows that while broadly speaking the same areas of IFNAR1 bind the ligand, the docking angle is slightly different in the IFN $\beta$ -IFNAR1 ternary complex. This results in a closer interaction of the receptor with the ligand, namely helices C, CD and D. As mentioned previously in 1.10.2, a unique feature of mouse IFN $\beta$  is the presence of Helix CD, which appears to be absent in other type I IFNs and could therefore be an integral part of this interaction. As the cytoplasmic regions of both receptors are required for JAK-STAT signalling, it is unsurprising to see that STAT phosphorylation and conventional IRG induction do not occur in this model of IFN signalling. Instead, a small subset of genes were induced that are known to be involved in the pathogenesis of septic shock, such as *Trem1* and *Tgm2* [234]. The authors then found that while WT and IFNAR2 deficient mice succumb to LPS challenge, IFNAR1 deficient mice are resistant, indicating that the IFN $\beta$ -IFNAR1 complex may also be functional in cells that have both receptor subunits. It would be interesting to see if other type I IFNs share this unconventional receptor engagement and whether or not cells lacking IFNAR2 can be found in the body.

### **1.11 The female reproductive tract**

As mentioned in Chapter 1.9, the type I IFNs have been implicated in the female reproductive tract (FRT). While their function in humans does not appear to be necessary for reproduction as seen with ungulate species, the cells of the FRT are able to produce and respond to type I IFNs [235, 236]. As IFN $\epsilon$  is exclusively and constitutively expressed in the FRT, this section will address the physiology and cellular components of this unique site.

The FRT comprises the organs necessary for successful reproduction and survival of a species. Structurally, the vagina and ectocervix (which projects into the vagina) are lined by stratified squamous epithelium whereas the endocervix (projecting into the uterus), uterus and fallopian tubes are lined by columnar epithelial cells [237]. Importantly, the columnar epithelial cells are hormonally regulated and important for implantation of the embryo, while the stratified squamous epithelium of the lower FRT serves a more protective function [238]. Significantly, both upper and lower FRT cells when grown in culture are polar and demonstrate the formation of tight junctions, which has been shown to be critical for the antimicrobial function of the FRT [237].

Lining the uterus is the endometrium, which serves as the implantation site for the developing embryo. The endometrium is highly regenerative and undergoes cyclical cellular and structural changes according to the female menstrual cycle. The menstrual cycle is controlled by the female sex hormones estrogen and progesterone, which control the proliferation and vascularisation of the endometrium. Three phases constitute the 28 day cycle; proliferative, secretory and menstrual. During the proliferative phase, the endometrium undergoes rapid cellular proliferation under the control of estrogen. Once ovulation (the release of an oocyte from the ovary) occurs, progesterone starts to be produced which results in the endometrial lining to become secretory in preparation for blastocyst implantation. The menstrual phase occurs in the absence of implantation and is the process by which the thick, blood vessel rich endometrium sloughs off.

In contrast to humans, most other mammals including mice undergo an estrous cycle. A key feature of the mouse estrous cycle is the lack of a menstrual phase and instead, the shed endometrial layer is re-absorbed. Also unlike the human menstrual cycle, the estrous cycle in mice lasts only 4-5

days and is separated into four distinct phases; pro-estrus, estrus, post-estrus and di-estrus. Similarly to humans, hormonal fluctuations occur during the cycle such as that estrogen levels are highest during estrus and progesterone is highest at di-estrus. In the estrous cycle, cellular proliferation and growth is most active during pro-estrus and estrus.

Interestingly for such a highly regenerative process, a vast array of immune mediators are present during the cycle that facilitate this function. The endometrium and uterus have been shown to contain large numbers of T-cells, B-cells, macrophages and even a specific population of NK-cells known as uterine NK (uNK) cells [238, 239].

### **1.11.1 Immune Cells in the FRT**

#### **1.11.1.2 T and B Lymphocytes**

Approximately 6-20% of cells in the reproductive tract are leukocytes with the uterus having the highest number per gram of tissue [240]. In the cycling female, 30-60% of these leukocytes are T-lymphocytes whereas approximately only 10% are B-cells. These T and B cells are organised into lymphoid aggregates where the B-cells make up the core, surrounded by T-cells. As pregnancy progresses, these aggregates disappear and overall less T-cells are present in pregnant endometrium compared to non-pregnant [241].

#### **1.11.3 Uterine NK-cells**

uNK-cells (CD16<sup>-</sup> CD56<sup>bright</sup>) are phenotypically different from peripheral NK-cells (CD16<sup>+</sup> CD56<sup>dim</sup>) however it is not entirely known how these cells are

selected [242]. The level of uNK-cells changes during the cycle and they become the dominant leukocyte population (approx 70%) during decidualization, the stage at which the endometrium is ready for implantation [243]. In humans, uNK-cells slowly diminish as pregnancy progresses into the third trimester whereas in rodents uNK-cells are present throughout gestation although they show signs of apoptosis and loss of membrane potential [241]. Mice deficient in NK cells produce viable offspring however these are smaller than wild type littermates. In addition, studies have shown that NK-cells in the decidua secrete factors that lead to the activation of endothelial cells [244]. Interestingly, progesterone has been found to be required for the continual viability of uNK-cells, differentiating these cells again from their circulating counterparts.

Although a clear function for NK-cells in pregnancy has not been observed, dysregulated levels of NK-cells in females have been associated with recurrent loss of pregnancy, endometriosis and uterine and ovarian cancer, suggesting that the balance of NK-cells is crucial to maintain reproductive health [244].

#### **1.11.4 Dendritic cells and macrophages**

As in other tissues, dendritic cells and macrophages are also the primary antigen presenting cells (APCs) in the female genital tract [238]. Langerhans cells and submucosal DCs comprise the main populations of dendritic cells in the female reproductive tract and are found within the epithelium and the submucosa, respectively [245]. Interestingly, it was found that monocytes in the FRT of mice were dependent on sex hormones, as ovariectomised mice had reduced levels of monocytes compared to control mice [246]. In humans

on the other hand, it was found that immature DC numbers varied with the stage of the menstrual cycle and were higher in the follicular phase compared to the secretory phase [247]. Although studies as the ones mentioned previously have aimed at determining the levels of APCs in the reproductive tract during the cycle, the functional significance of these cellular changes is currently unknown [238].

### **1.12 IFN $\epsilon$ – A novel type I IFN**

Annotation of the human and mouse type I interferon loci by our group in 2004 led to the discovery of a novel gene with sequence similarity to the type I interferon family. Proposed to be a novel type I IFN, it demonstrates constitutive expression in the reproductive tract, particularly in the uterus and ovaries [13]. Protein modelling indicated that IFN $\epsilon$  has a three dimensional structure like other type I IFNs with sequence similarity between 25 and 30% to IFN $\alpha$ s and IFN $\beta$ , respectively [13]. An interesting feature of mouse IFN $\epsilon$  is that while it shares closer phylogeny with mIFN $\beta$  than mIFN $\alpha$  [13] it bears some features more similar to IFN $\alpha$ . For example IFN $\epsilon$  carries cysteine residues at position 29 and 139 like IFN $\alpha$ s, suggesting the presence of the conserved disulfide bond (see section 1.10). Uniquely, IFN $\epsilon$  also has an unpaired cysteine at position 151 however it is not known whether this residue affects the structure or activity of IFN $\epsilon$ .

In terms of tertiary structure, IFN $\epsilon$  has been modelled and shown to adopt an alpha helical bundle shape like other type I IFNs [13]. Interestingly human IFN $\epsilon$ , which is some 20aa longer than IFN $\alpha$ , has been proposed to contain a sixth  $\alpha$ -helix in the C-terminus termed Helix F. While certain residues in the C-terminus of type I IFNs are proposed to be important for receptor binding [9],

there is no published data to suggest how (or if) additional C-terminal residues would affect biological activity.

Peng et al. expressed and purified recombinant human IFN $\epsilon$  from *E. coli* and demonstrated low antiviral, antiproliferative and NK-cell activating activity when compared to hIFN $\alpha$ 2 [248]. Importantly, they demonstrated that rhIFN $\epsilon$  induced classical IRGs, suggesting that rhIFN $\epsilon$  elicited its actions via IFNAR. Oddly however, they hypothesised IFN $\epsilon$  to have a specialised function in the brain, a site they propose IFN $\epsilon$  is constitutively and exclusively expressed in. We and others however have not found significant expression in the brain but as mentioned previously, found highest expression in the FRT [13, 114].

In one study, hamster cells were engineered to express chimeric type I IFN receptors that contain the intracellular domains of the IFN $\gamma$  receptors, which the authors propose removes any bias of the stimulus. The cells were then transfected with vector constructs expressing different type I IFNs including IFN $\epsilon$  [249]. The results indicate that cells transfected with the IFN $\epsilon$  construct show STAT1 phosphorylation suggesting that IFN $\epsilon$  does indeed signal via the type I IFN receptor. Critically however, the authors did not quantify IFN $\epsilon$  in the conditioned supernatant and it is therefore difficult to correlate STAT1 activation in this artificial receptor model to biological activity [249].

Other studies showed that vaccinia-virus encoding IFN $\epsilon$  in its genome was able to upregulate the antiviral genes PKR and 2'5'-OAS *in vitro* and induce the cell surface markers CD69 and CD86 on B-cells [250]. Compared to the parental vaccinia virus vector, IFN $\epsilon$  expressing vaccinia virus was also able to reduce viral growth in L929 murine cells, demonstrating antiviral activity. While demonstrating other classic type I interferon activities such as the ability to induce CD69 on B-cells, the lack of quantification of IFN $\epsilon$  in these experiments

makes it difficult to compare the measured activities of IFN $\epsilon$  to IFN $\alpha$  and IFN $\beta$ . In a follow up study using the same vaccinia virus vectors, Yang et al. found a proposed role for IFN $\epsilon$  in mucosal immunity of the lung and gut. Here, the IFN $\epsilon$  encoding vaccinia virus was shown to induce elevated antigen specific T-cell responses *in vivo* and enhance their migration to gut mucosa [251]. Interestingly, the enhanced activation of these antigen specific T-cells appeared to be greater in mice infected with the vaccinia virus encoding IFN $\epsilon$  than in those infected with virus carrying IFN $\alpha$ 4 or IFN $\beta$ . As the gut is a primary site of HIV replication, the authors propose that using these vaccinia viruses encoding IFN $\epsilon$  could have a potential use in therapy for controlling HIV-1. Similar to previous studies however, the production of IFN $\epsilon$  protein by the vaccinia virus vectors was never confirmed and it is therefore difficult to correlate the reported biological activities with protein concentration.

Following on from our original study, we have recently demonstrated a unique role for IFN $\epsilon$  in protecting the female reproductive tract from the sexually transmitted diseases *Chlamydia muridarum* and HSV-2 [114]. Interestingly, IFN $\epsilon$  expression is regulated by hormones throughout the estrous cycle in mice (and equivalent stages in humans) and not PRRs as is the case for other type I IFNs. Work performed in this thesis contributed to this publication and demonstrated distinctly that recombinant mouse IFN $\epsilon$  was unable to induce IRGs in type I IFN receptor knock-out animals but was active in wild type animals. Furthermore, *C. muridarum* infected mice treated with recombinant mIFN $\epsilon$  demonstrated significantly reduced bacterial burden 3 days post infection. Importantly, this data for the first time, definitively demonstrated that IFN $\epsilon$  is a type I IFN as it requires both IFNAR1 and IFNAR2 to signal.

Thus far, IFN $\epsilon$  has been shown to be expressed exclusively and constitutively in the reproductive tract. Furthermore, while demonstrating classic type I

interferon activities such as antiviral and antiproliferative functions, these appear to be different when compared to IFN $\alpha$  and IFN $\beta$ . It is clear from these studies that a major obstacle for further study is the lack of available reagents. It is difficult to accurately determine the roles of IFN $\epsilon$  when biological activity cannot be related back to protein quantity. The work outlined in this thesis aims to address this issue by describing the production, purification and characterisation of recombinant murine IFN $\epsilon$ .

### **1.13 Overview and history of expression and purification of type I IFNs**

The first published report on the biological activity of interferons stems from Isaacs and Lindenmann in 1957, where the investigators infected chicken embryos with influenza A virus and noticed viral interference, the phenomenon by which material harvested from the infected chicken embryo could protect chorionic membranes of naive chicken eggs from viral infection [14]. Although this antiviral activity was attributed to a protein, or perhaps multiple proteins, it was difficult to say for certain as only partially purified material was available [252]. Amusingly, considering present day drug formulation standards, interferon used in initial human clinical trials and experiments was from a crude protein fraction reported to be less than 1% weight as interferon [253]. It took 18 more years for interferon to be purified to homogeneity, as reported by Knight [254]. In these experiments, mouse fibroblast L. cells were infected with MM virus (belonging to the group of encephalomyocarditis viruses) and the resulting supernatant purified by acidification, ammonium sulphate precipitation, gel filtration and ion exchange chromatography. For the first time, a specific biological activity was calculated for a homogenous formulation of interferon (IFN $\beta$ ). In continuation to these experiments, Knight

also documented that the antiviral and antiproliferative activities of human fibroblast interferon (IFN $\beta$ ) could be attributed to a single protein and not multiple molecules as was postulated at the time [255].

In 1979, both Rubinstein and colleagues and Zoon and colleagues were successful in the purification of human leukocyte/lymphoblastoid interferon to homogeneity, from Newcastle disease virus induced donor leukocytes and Namalwa (human Burkitt lymphoma cell line) cells, respectively [256, 257]. Where Rubinstein et al. employed the newly developed RP-HPLC method for the purification of IFN, Zoon et al. purified interferon by immunoaffinity column, gel filtration and ion exchange chromatography. When considering the protein yields achieved at present day with recombinant DNA technology it is difficult to fathom the scale of material required in the late 1970s. Rubinstein reports the use of 50-100 blood buffy coats weekly over a 9 month period to achieve an unpurified yield of  $10^9$ IU, which at a yield of  $1\mu\text{g}$  per 2L of human blood means approximately 2000L of blood was collected [256]. Considering some recombinant expression systems produce interferon in the  $10^{10}$ IU/L range [258, 259] the scale of this science appears unbelievable compared to present day standards. Still even more interesting however is the fact that purification schemes themselves have not changed much, even if yields have, highlighting the importance of these early experimental procedures.

The next leap in interferon science and indeed, science as a whole was the development of molecular biology and recombinant DNA technology. Here, mRNA from virus infected cells (or polyI:C) was isolated and transcribed to cDNA before being cloned en masse into *Escherichia coli* vectors [260]. Plasmid DNA containing interferon sequences were identified by radiolabelled  $^{32}\text{P}$ -cDNA probes [260]. To condense years worth of research into a single measurement, approximately  $1\text{-}2 \times 10^8$ IU of interferon could be produced from

a litre of bacterial culture, over 1000 fold more than previously generated from donor blood [261, 262]. Reviews written by the people who were present during these times encapsulate not only the amazing science performed but also describe the work in an astonishing amount of detail that I could never attempt to duplicate in this literature review [252, 253].

To date, interferons have been produced in virtually every expression host including bacterial, yeast and various mammalian systems. Purification schemes typically involve acidification (owing to the acid stability of IFNs [263]), ion exchange chromatography, size exclusion chromatography, hydrophobic interaction chromatography and immunoaffinity chromatography. Importantly, no single method appears to be used universally and is likely a reflection of the chosen expression system and subsequent cost of purification methods.

## **1.14 Rationale and Aims**

Type I IFNs have been studied extensively since their original discovery in 1957 [14]. Sequencing of the human and mouse genomes has allowed for the identification of and localisation of the type I IFN gene family. Located on human chromosome 9 and on the mouse chromosome 4, some 13 IFN $\alpha$  genes, 1 IFN $\beta$ , 1 IFN $\omega$ , 1 IFN $\epsilon$  and 1 IFN $\kappa$  were identified in humans (with additional gene members in other species).

Functional characterisation of these type I IFN isotypes has revealed major differences in their inducibility, tissue expression and biological activity [13, 111, 114, 223]. Importantly, structure-function studies of type I IFNs have demonstrated that the unique biological activities associated with each type I IFN are due to complex receptor-ligand interactions [9, 10, 12].

Our laboratory discovered a novel type I IFN in 2004 and since then, we have established an important immunological role for IFN $\epsilon$  in protecting mucosal surfaces such as the female reproductive tract from pathogens [114, 251]. Thus far, studies of IFN $\epsilon$  have been limited due to availability of high quality reagents. The rationale of my project therefore is to address this need and produce and characterise IFN $\epsilon$ .

**Aims:**

To express and purify recombinant IFN $\epsilon$  using a suitable expression system.

Characterise the biological activities of IFN $\epsilon$ , in particular receptor usage and signal transduction pathways.

Generate monoclonal antibodies against mouse IFN $\epsilon$  and determine their use as novel reagents for the study of IFN $\epsilon$ .

## **Chapter 2 – Materials and Methods**

### **2.1 DNA manipulations**

#### **2.1.1 Plasmid DNA extraction**

Small scale and large scale plasmid DNA extractions were performed using a QIAprep Spin Miniprep Kit (Qiagen) and a QIAGEN Plasmid Maxi Kit (Qiagen) respectively, according to the manufacturer's instructions. Briefly, bacterial cultures were grown overnight and the cell pellet harvested by centrifugation at 3000rpm for 5 minutes. Cells were resuspended in buffer P1 and lysed with buffer P2 and incubated for 5 minutes at room temperature. Neutralisation buffer was added and the sample mixed by inversion. For Mini-preps, samples were centrifuged for 15 minutes at 13,000rpm and then applied to mini-prep columns. Columns were washed with W1 wash buffer and DNA eluted in 50µl Milli-Q (MQ) H<sub>2</sub>O (Millipore). For Maxi-Preps, neutralised sample was filtered through filter columns into QiaMaxi columns. Columns were washed twice with Buffer W1 and sample eluted with elution buffer. DNA was precipitated with isopropanol and centrifuged for 60 minutes, 5000rpm at 4°C. The DNA pellet was washed with 70% Ethanol/H<sub>2</sub>O and DNA resuspended in 300µl MQ H<sub>2</sub>O. DNA was quantified as outlined in 2.1.4.

#### **2.1.2 Agarose gel electrophoresis**

To visualise DNA, 1 part DNA loading dye (Appendix A) was added to 5 parts sample and loaded on a 1% w/v agarose gel (Appendix) containing 1:30 dilution of SybrSafe (Life Technologies). The gel was electrophoresed in 1 x TAE buffer (Appendix) at 100 volts for 30 minutes. DNA visualisation was

performed by blue light illumination in a Safe Imager (Invitrogen) and images printed with a P90 video copy processor (Mitsubishi).

### **2.1.3 DNA extraction from agarose gels**

DNA fragments were run on 1% w/v agarose gels and excised using a scalpel blade under blue light. The DNA was purified from the gel slice using a QIAquick DNA Extraction Kit (Qiagen) according to the manufacturer's instructions. Briefly, the agarose slice was dissolved in buffer QG at 50°C for 10 minutes. 1 gel volume of isopropanol was added to the mixture and DNA bound to a QIAquick column by centrifugation at 13,000rpm for 1 minute. The column was washed with Buffer PE and DNA eluted in 30µl MQ H<sub>2</sub>O. DNA was quantified using Nanodrop as outlined in 2.1.4.

### **2.1.4 Quantification of DNA samples**

DNA quantification was performed using a NanoDrop ND-1000 spectrophotometer (Analytical Technologies). The instrument was calibrated using 2µl of MQ dH<sub>2</sub>O followed by 2µl of appropriate sample buffer as the blank. Concentration and purity of DNA was determined by a 2µl drop of sample measured at an absorbance of 230nm/260nm/280nm.

### **2.1.5 Restriction enzyme digestions**

Restriction enzyme digestions of DNA were performed according to the manufacturer's instructions (Promega). Briefly, a known quantity of DNA was diluted to a final volume of 50µl in 1x reaction buffer containing 0.1mg/ml acetylated BSA. Restriction enzyme was added at 1U/µg of DNA and the reaction incubated at 37° for 60 minutes or until all DNA was digested. Double digests were performed in the most suitable buffer as determined by Promega Methods with 1U/µg of DNA for each restriction enzyme.

### 2.1.6 DNA Ligation

DNA ligations were performed according to the manufacturer's instructions (Promega). Briefly, the required amounts of vector and insert DNA were calculated as follows:

$$\frac{\text{ng vector} \times \text{kb size of insert} \times \text{molar ratio of insert}}{\text{kb of vector}} = \frac{\text{ng insert required}}{\text{vector}}$$

All ligation reactions were performed with a insert:vector ratio of 3:1. Reactions contained 50ng vector, appropriate amount of insert, 1U T4 DNA ligase and 1x DNA ligase buffer in a total volume of 10µl. Ligation reactions were incubated overnight at 4°C. Simultaneous control reactions were prepared for each ligation reaction and contained no insert DNA to allow estimation of vector background self re-ligation.

### 2.1.7 Codon Optimization of *Ifne1*

The murine *Ifne1* gene was codon optimised for expression in insect cells by replacing rare or uncommonly used codons by insect cells with ones more frequently used. Additionally, the internal *BamHI* site at nucleotide positions 446-451 was modified from a G to C at position 447 to ensure future compatibility with restriction enzyme digestion. This mutation has no consequence on the amino acid sequence. The codon optimization was carried out by Kathryn Hjerrold (MIMR, Clayton, Australia). To ensure the codon optimised sequence was changed sufficiently, its codon adaptation index (CAI) was compared to the native gene using [http://www.genscript.com/cgi-bin/tools/rare\\_codon\\_analysis](http://www.genscript.com/cgi-bin/tools/rare_codon_analysis). The native gene's CAI was 0.71 whereas the codon optimised *Ifne1* sequence was 0.81. A CAI of 1.0 is considered ideal for increased protein expression and any CAI over 0.8 is considered good for expression. Codon optimized *Ifne1* was ordered from Genscript and was delivered as pUC57-*Ifne1* vector.

### 2.1.8 His<sub>6</sub>-tagged IFN cloning and bacmid generation

4µg pUC57-*lfne1* was digested with *Bam*HI and *Hind*III restriction enzymes according to 2.1.5 in order to release the *lfne1* fragment. 5µg of pFB-SHEK was digested with *Bam*HI and *Hind*III according to 2.1.5 and heat inactivated at 65°C for 15 minutes. pFB-SHEK was a kind gift from Dr Hugh Reid (Monash University, Clayton, Australia). 4 units of thermosensitive alkaline phosphatase (Promega) was added to the pFB-SHEK reaction and incubated at 37°C for 15 minutes. TSAP enzyme was irreversibly inactivated by incubating the mixture at 74°C for 15 minutes. The pUC57-*lfne1* and pFB-SHEK digestions were electrophoresed on 1% w/v agarose gel as described in 2.1.2 and purified as described in 2.1.3. *lfnb1* was amplified using pFB-*lfnb*-fwd and pFB-*lfnb*-rev primers (Appendix G) from genomic C57Bl/6 DNA. *lfne1* or *lfnb1* insert was ligated into open pFB-SHEK vector according to 2.1.6 and 2µl of ligation mix subsequently transformed into 50µl competent cells (Bioline) by conventional heat shock method. Ampicillin resistant clones were picked from LB agar plates, grown up and DNA extracted according to 2.1.1. Sanger sequencing with pFB-seq primer (Appendix G) confirmed the correct insertion of *lfne1* or *lfnb1* into pFB-SHEK. pFB-SHEK containing either *lfne1* or *lfnb1* was electroporated into ΔCC E.coli containing bacmid [264] by electroporation using a 0.1cm cuvette with the following settings: 2kV, 25µFD, 200ohms. Single colonies were isolated on LB agar containing 50µg/ml Kanamycin, 10µg/ml Tetracycline, 34µg/ml Chloroamphenicol, 7µg/ml Gentamicin, 50µg/ml X-Gal and 1mM IPTG and visually screened for blue/white colour selection. White colonies were picked and subjected to colony PCR with M13 forward and reverse primers (Appendix G) to ensure successful bacmid recombination with the following parameters:

Temperature	Time
95°C	3 minutes
95°C	45 seconds
55°C	45 seconds
72°C	5 minutes
72°C	5 minutes

} 35 cycles

Successful recombination was indicated by an amplified PCR product of size 2.4kb when visualised on 1% w/v agarose gel. Selected clones were amplified and maxi-prepped according to 2.1.1.

### 2.1.9 Tagless *Ifne1* cloning and bacmid generation

pFB-MSP vector was linearised with *EcoRI* and *HindIII* according to 2.1.5. pFB-MSP was a kind gift from Kathryn Hjerrold (MIMR). 2.5 units of thermosensitive alkaline phosphatase (Promega) was added to the pFB-MSP reaction and incubated at 37°C for 15 minutes. TSAP enzyme was irreversibly inactivated by incubating the mixture at 74°C for 15 minutes. Linearised pFB-MSP was separated and agarose gel purified as described in 2.1.3. Codon optimised *Ifne1* was amplified by Pfu PCR using pUC57-*Ifne1* as a template with primers pFB-MSP-*Ifne*-fwd and pFB-MSP-*Ifne*-rev (Appendix G) with the following parameters:

Temperature	Time
95°C	5 minutes
95°C	30 seconds
56°C	30 seconds
72°C	50 seconds
72°C	5 minutes

} 35 cycles

The amplified PCR product was excised from 1% w/v agarose as described in 2.1.3 and digested with *Hind*III followed by *Mfe*I according to 2.1.5. Digested *lfne1* insert was subsequently column purified according to the manufacturer's instructions (Qiagen). *lfne1* was ligated into open pFB-MSP vector with T4 ligase as described in 2.1.6. The ligated vector was transformed into competent *E. coli* (Bioline) by standard heat shock method and Ampicillin resistant clones screened by colony PCR for *lfne1* positive colonies with pFB-MSP-*lfne*-fwd and pFB-MSP-*lfne*-rev primers (Appendix G) using the following parameters:

Temperature	Time
95°C	5 minutes
95°C	30 seconds
56°C	30 seconds
72°C	50 seconds
72°C	5 minutes

} 35 cycles

Positive clones were Sanger sequenced with pFB-seq primer (Appendix G) to ensure correct and in-frame insertion of *lfne1* into the vector. Electroporation of  $\Delta$ CC *E. coli* and successful recombination of bacmid was carried out as described previously in 2.1.8. Selected clones were amplified and maxi prepped according to 2.1.1.

## **2.2 RNA Manipulation**

### **2.2.1 RNA extraction using Qiagen kit**

RNA was extracted from cells using RNeasy columns according to the manufacturer's instructions (Qiagen). Briefly, 350µl of Buffer RLT containing β-mercaptoethanol was directly added to cells and the cells scraped with a cell scraper (TPP). The lysate was homogenised by passing through a 20-gauge needle 10 times. 350µl of 70% ethanol was added to the lysate and the mixture transferred to an RNeasy spin column. The sample was centrifuged for 15s at 8000g and the flowthrough discarded. The column was washed with 700µl Buffer RW1 and centrifuged for 15s at 8000g and the flowthrough discarded. The column was washed twice with 500µl Buffer RPE by centrifugation. RNA was eluted by addition of 30µl RNase-free water to the column and centrifugation for 1 minute at 8000gs. RNA was stored frozen at -80°C until used.

### **2.2.2 Extracting RNA using TRIsure**

RNA from snap frozen mouse organs was prepared using TRIsure according to the manufacturer's instructions (Bioline). Briefly, mouse organs were weighed and 1ml of TRIsure added per 100mg of tissue. Organs were thoroughly homogenized on an Ika Ultra Turrax T25 (Crown Scientific) homogenizer and the homogenate frozen on dry ice. Tissue homogenates were stored at -80°C until used. Frozen homogenates were thawed at room temperature, 0.2ml of chloroform added per 1ml of TRIsure reagent and mixed thoroughly. Following centrifugation for 15 minutes at 12,000g, 4°C, the upper aqueous phase was transferred to a fresh 1.7ml microcentrifuge tube and RNA precipitated with 0.5ml of isopropyl alcohol per 1ml of TRIsure. The sample was centrifuged for 15 minutes, 12,000g, 4°C and the RNA pellet washed with 75% Ethanol/DEPC H<sub>2</sub>O. The RNA was pelleted for 5 minutes,

7,200g, 4°C, allowed to air-dry and then resuspended in an appropriate volume of DEPC H<sub>2</sub>O (Appendix A) at 55°C for 10 minutes. All RNA was stored at -80°C until used.

### **2.2.3 cDNA preparation**

cDNA was synthesized from 2µg of total RNA unless otherwise indicated. Genomic DNA was removed by treating RNA with 2µl DNase I (Promega) in the presence of 2µl M-MLV 5x Reaction buffer diluted in a final volume of 10µl nuclease free water. This reaction was incubated at 37°C for 45 minutes. The reaction was stopped by addition of 1µl stop solution (Promega) and incubation at 65°C for 15 minutes. Each reaction was incubated with 500ng of random hexamers (Promega) at 70°C for 5 minutes and then cooled to 4°C on ice. RNA in each sample was reverse transcribed in a solution containing; 4µl M-MLV 5X Reaction Buffer, 2µl 10mM dNTP (Bioline), 1µl RNasin Plus RNase inhibitor (Promega), 7µl DEPC H<sub>2</sub>O (Appendix A) and 1µl M-MLV Reverse Transcriptase at 37°C for 1 hour. The reverse transcriptase (RT) enzyme was inactivated by incubating the reaction at 70°C for 15 mins. Genomic DNA contamination was measured by performing control reactions in parallel in the absence of reverse transcriptase.

### **2.2.4 *Gapdh* PCR**

*Gapdh* (glyceraldehyde-3-phosphate dehydrogenase) PCR was performed on cDNA samples from both RT+ and RT- samples to determine quality of cDNA and genomic contamination of RT- control samples. Reactions were carried out in a total volume of 25µl containing 1U of GoTaq DNA polymerase (Promega), 5µl of 5X GoTaq buffer, 0.2µM of each 5' and 3' *Gapdh* primers (Appendix) and 0.2mM dNTPs (Promega). PCR was carried out using a MyCycler Thermal Cycler (Bio-Rad) using the following parameters:

Temperature	Time
95°C	3 minutes
95°C	30 seconds
55°C	30 seconds
72°C	1 minute
72°C	7 minutes

} 35 cycles

PCR products were visualised by electrophoresis on 1% w/v agarose gels as described in section 2.1.2.

### 2.2.5 Real-Time polymerase chain reaction (RT-PCR)

RT-PCR was performed with Taqman probes or SYBR green labelled primers (see Appendix G for primer sequences). cDNA was diluted 1/10 in MQ H<sub>2</sub>O and aliquoted in triplicate into a 384well plate (Applied Biosystems). For TaqMan RT-PCR, 0.5µl of VIC-labelled 18S probe, 0.5µl of FAM-labelled target probe, 5µl of Universal Master Mix and 2µl MQ-H<sub>2</sub>O were added to each well of the triplicate sample. For Sybr RT-PCR, 0.2µl of 10µM forward primer, 0.2µl of 10µM reverse primer, 5µl of SYBR Magic Master Mix and 2.6µl of MQ-H<sub>2</sub>O were added to each well of the triplicate sample. Plates were sealed with MicroAmp™ optical adhesive film and subjected to polymerase chain reaction on a 7900HT Fast Real-Time PCR system (Applied Biosystems) with the following parameters:

Temperature	Time
50°C	2 minutes
95°C	10 minutes
95°C	15 seconds
60°C	1 minute

} 40 cycles

For SYBR Green RT-PCRs, the following dissociation step was included:

Temperature	Time
95°C	15 minutes
60°C	15 minutes
95°C	15 minutes

The expression level of all genes was normalised against the expression of the housekeeping gene 18S. Data analyses were performed using the  $\Delta\Delta C_t$  method [265].

## 2.3 Tissue Culture

All mammalian cell tissue culture incubations were performed in a humidified incubator at 37°C, 5% CO<sub>2</sub>.

### 2.3.1 Cell counting by trypan blue exclusion

Cell number and viability of samples was determined by trypan blue exclusion. 10µl of cells were mixed with 10µl of Trypan blue (Appendix A) and cells counted on a haemocytometer. Viability was determined as the number of trypan blue negative cells divided by total cells.

### **2.3.2 Cell counting by Sysmex automated cell counter**

Automated cell counts were performed using a Sysmex KX-21N automated cell counter according to the manufacturer's instructions (Sysmex Corporation). Briefly, 100µl of homogeneous cell suspension was aliquotted into a 1.7ml microcentrifuge tube and the sample aspirated into the cell counter.

### **2.3.3 Thawing of frozen cells**

Cells were removed from liquid nitrogen storage and thawed immediately in a water bath at 37°C. 9ml of the appropriate complete media was added and the cells pelleted at 1000rpm for 5 minutes. Cells were resuspended in pre-warmed complete media (Appendix A) and transferred to a 75cm<sup>2</sup> tissue culture flask (BD Falcon) and incubated. The media was changed after 24 hours and the cells returned to the incubator for 2 days.

### **2.3.4 Freezing of cells**

Cells to be frozen down were cultured to approximately 80% confluence and then trypsinised as described in 2.3.5. Resuspended cells were pelleted at 1000rpm for 5 minutes and the cell pellet gently dislodged by tapping. Cells were resuspended in FCS containing 10% v/v DMSO, aliquotted into cryovials (Greiner Biosciences), transferred to a Mr Freeze (Invitrogen) and placed at -80°C for 24 hours. Cells were subsequently transferred to liquid nitrogen for permanent storage.

### **2.3.5 Adherent cell passaging**

Adherent cell lines were passaged according to standard protocols. Briefly, growth media was removed and the cells washed with PBS (Gibco). 1ml or 2ml TrypLE (Invitrogen) was added to a T75 flask or T175 flask, respectively and the cells returned to 37°C for 5 minutes. The flask was tapped to dislodge

cells and complete media added to 10ml. Cells were split at a 1:10 ratio into fresh media unless otherwise indicated.

### **2.3.6 Suspension cell passaging**

The YAC-1 moloney leukemia virus transformed mouse cell line (ATCC) was passaged by 1:10 split into fresh RPMI media containing 10% v/v FCS (Invitrogen) and 1% v/v Pen/Strep every other day. Cells were maintained between  $2 \times 10^5$  cells/ml and  $2 \times 10^6$  cells/ml.

### **2.3.7 Hybridoma cell passaging**

Hybridoma cell lines were initially received from MATF in 20% v/v FCS Hybridoma Media (Appendix A). Cells were passaged by 1:10 split into fresh 20% FCS Hybridoma Media and subsequently adapted to 10% v/v FCS Hybridoma Media by stepwise passage into lower %FCS Hybridoma Media.

### **2.3.8 Hybridoma cell subcloning**

Subcloning of hybridoma cell lines ensures monoclonality of clones and was carried out on  $\alpha$ -IFN $\epsilon$  mAb clones H3, G2 and C3. Briefly, cells were grown to >80% confluence in 6-well tissue culture plates and their healthiness gauged microscopically. Cell counts were performed by trypan blue exclusion as outlined in 2.3.1. Subcloning was performed by dilution of cells to 5 cells/ml in 10% v/v FCS Hybridoma Media and 200 $\mu$ l was aliquotted into each well of a 96-well tissue culture plate. Cells were incubated until colony formation became visible. Once cells reached confluence (12-14 days post seeding), a supernatant ELISA was performed to determine antibody secretion status. Positive clones were expanded and frozen as previously described in 2.3.4.

### **2.3.9 Establishing viral titres**

Mouse L929 cells (L. cells) supplied by the American Type Tissue Collection (ATCC) were seeded into each well of a 96-well tissue culture plate at a

density of  $2 \times 10^4$  cells per well in 180 $\mu$ l of 3%FCS/RPMI. Cells were then incubated for 24 hours at 37°C, 5% CO<sub>2</sub>. The following day, stock Semliki Forest Virus (SFV) was diluted 1:10 in reduced serum RPMI and 20 $\mu$ l added to the first column of the 96-well plate. Serial log<sub>10</sub> dilutions were then performed across the plate and the 96-well plate incubated for 72 hours. After the incubation, cytopathic killing was measured visually and the dose at which 50% of cells were found to be dead was calculated as the (Tissue Culture Infectious Dose 50) TCID<sub>50</sub>.

### **2.3.10 Mouse interferon antiviral assay**

Antiviral assays were performed as previously described [266]. Briefly, mouse L929 cells were seeded into each well of a 96-well plate at a density of  $2 \times 10^4$  cells per well in 180 $\mu$ l of 3%FCS/RPMI. Four hours post seeding, cell attachment was confirmed by microscopic evaluation. Mouse interferon standard (NIH – Gu02-901-511) was diluted to a stock concentration of 250IU/ml using 3%FCS/RPMI media and 90 $\mu$ l aliquotted into duplicate wells. Protein samples to be tested for antiviral activity were diluted in reduced serum RPMI media at the indicated concentrations and 90 $\mu$ l aliquotted into duplicate wells. Serial  $\frac{1}{2}$  log dilutions were performed on the samples and the tissue culture plate incubated for 16 hours. The following day, media was removed from the wells and SFV diluted to the TCID<sub>50</sub> + log<sup>2</sup> in 3%FCS/RPMI. Virus was added to all sample containing wells and a virus control well. 3%FCS/RPMI was added to an unstimulated control well and the 96-well plate incubated for 72 hours.

### **2.3.11 Human interferon antiviral assay**

Human interferon antiviral assays were performed like the mouse assays, except WISH cells were challenged with EMCV diluted to the TCID<sub>50</sub> + log<sup>2</sup>. The NIH interferon standard used was Ga23-901-532.

### **2.3.12 Scoring viral titre and interferon antiviral activity assays**

After the indicated incubation times, the 96-well plate was examined microscopically for cell death where a value of 0 denoted no cell death and 4 equalled complete death. For viral titres, a value of 2 represented the TCID<sub>50</sub> which was the dilution at which 50% of the cells were dead. Interferon antiviral activity was calculated as previously reported [267]. Briefly, all wells underwent microscopic viability scoring as mentioned above. The interferon reference standard was used to calculate an average standard log titre and calibration factor. Each sample was normalized using the calibration factor and the international units (IU) of antiviral activity calculated. Average antiviral activity for any sample was calculated from three independent experiments.

### **2.3.13 Antiproliferative assay**

The antiproliferative effect of interferons was determined in RAW 264.7 mouse macrophage cells as previously described [266] and HeLa human cervical cancer cells. For each assay  $4 \times 10^3$  cells were seeded in a volume of 100 $\mu$ l into a 96 well plate. Serially diluted interferon samples in 100 $\mu$ l were then added to each well, in duplicate, and incubated. After 72hours, 20 $\mu$ l of 5mg/ml MTT (Appendix A) was added to each well, the plate wrapped in aluminium foil and returned to 37°C, 5% CO<sub>2</sub> for 3 hours. Following this incubation, the cell supernatant was aspirated and 100 $\mu$ l of DMSO (Sigma Aldrich) added to each well. MTT crystals were dissolved by gentle swirling of the plate and the absorbance measured at 590nm on a FLUOstar OPTIMA plate reader.

To calculate the % proliferation, a baseline absorbance reading of  $4 \times 10^3$  cells was taken and subtracted from all readings. Each interferon containing well was then compared to an unstimulated control. The equation used is shown below:

$$\% \text{ proliferation} = \frac{(\text{stimulated} - \text{baseline})}{(\text{unstimulated} - \text{baseline})} \times 100$$

#### **2.3.14 MHC-I upregulation by type I Interferon**

Mouse T-cell lymphoma YAC-1 cells were seeded in triplicate into each well of a 96 well plate at a density of  $2 \times 10^4$  cells/well in a volume of 100 $\mu$ l. IFN was diluted to 2x final concentration in 100 $\mu$ l of complete RPMI (Appendix A) and added to cells for 24 hours. Following stimulation, flow cytometry was performed on cells according to 2.5.2.

#### **2.3.15 Preparing bone marrow derived macrophages**

Bone marrow derived macrophages (BMDMs) were prepared from wild-type, *Ifnar1*<sup>-/-</sup> and *Ifnar2*<sup>-/-</sup> mice off the C57Bl/6 background as previously described [114]. Briefly, mice were anaesthetised according to institutional guidelines (MMCAF) and the femurs collected under aseptic conditions and placed in PBS (Gibco). All subsequent handling of cells was performed in a laminar flow safety cabinet (BTR Environmental). Muscle tissue was removed and the bones rinsed in 70% ethanol. The ends of the femurs were removed and the bone marrow flushed with 5ml complete RPMI using a 21 gauge needle. Cells were spun at 1000rpm for 5 minutes and resuspended in complete RPMI containing 20% v/v L-cell conditioned media (Appendix A). 1 10cm x 10cm non-adhesive tissue culture plate (Sarstedt) was used per mouse and cells incubated at 37°C, 5% CO<sub>2</sub>. After 5 days, 5ml of additional complete RPMI media containing 20% v/v L-cell conditioned media was added to cells and incubated for a further 24 hours. Cells were then counted and seeded at  $2.5 \times 10^6$  cells/well of a 6-well plate and incubated prior to being stimulated with IFN.

### **2.3.16 Stimulating primary spleen cells for flow cytometry**

Spleen cell suspensions were created as outlined in 2.6.6. For stimulations,  $1 \times 10^6$  cells were seeded in each well of a 96 well plate in a volume of 100 $\mu$ l. 2x the desired concentration of IFN was prepared and 100 $\mu$ l added to each well containing cells. Cells were incubated for 24 hours and stained with fluorochrome-conjugated antibodies for analysis by flow cytometry as described in 2.5.2.

### **2.3.17 Insect Cell Transfections and P1 baculovirus generation**

*Spodoptera frugiperda* (Sf9) cells were seeded in a 6-well plate at a density of  $1 \times 10^6$  cells per well in 2ml of 1mg/L Gentamicin supplemented SF900-II media and left to adhere for 1 hour in a humidified 27°C incubator. During the incubation, DNA transfection mix was prepared. 95 $\mu$ l and 80 $\mu$ l of antibiotic free SF900-II media were aliquotted into microcentrifuge tubes for the transfection mix and DNA mix, respectively. Each transfection mix tube received 5 $\mu$ l of Cellfectin (Invitrogen) and each DNA mix tube received 20 $\mu$ l of undiluted recombinant Bacmid. Transfection and DNA tube contents were then combined, gently mixed and incubated at room temperature for 40 minutes.

Media from the adhered Sf9 cells was aspirated and washed once with antibiotic free SF900-II media. 800 $\mu$ l of antibiotic free SF900-II media was then added to the cells. Prepared DNA transfection mix was added dropwise to the cells, gently mixed and incubated for 5 hours in a humidified 27°C incubator. Following this incubation, the media was aspirated and replaced with 2ml of Gentamicin supplemented SF900-II media and further incubated for 4 days. Infection of Sf9 cells with recombinant baculovirus was confirmed microscopically by the identification of enlarged, virus laden cells. P1

baculovirus stock was harvested by aspiration of the supernatant and stored at -80°C, supplemented with 2% v/v FCS.

### **2.3.18 Amplification of recombinant baculovirus stock – P2**

Following insect cell transfections and P1 virus generation, recombinant baculovirus was amplified by infecting Sf9 cells at a concentration of  $1 \times 10^6$  cells/ml in Gentamicin supplemented SF900-II media with previously generated P1 virus at 1:100 final volume. Infected cells were then incubated for 4 days in a shaking incubator at 27°C. P2 recombinant baculovirus was harvested by pelleting cells for 10 minutes, 3000rpm at room temperature. P2 baculovirus stock was stored at -80°C in 8ml tubes supplemented with 2% v/v FCS.

### **2.3.19 Generation of high titre recombinant baculovirus – P3**

Following P2 baculovirus generation, recombinant baculovirus was further amplified by infecting Sf9 cells at a concentration of  $1 \times 10^6$  cells/ml in Gentamicin supplemented SF900-II media with P2 virus at 1:100 final volume. Infected cells were then incubated for 7 days in a shaking incubator at 27°C. P3 recombinant baculovirus was harvested by pelleting cells for 10 minutes, 3000rpm at room temperature. P3 baculovirus stock was stored at 4°C in sterile tissue culture flasks protected from light.

### **2.3.20 Insect cell expressions**

Recombinant proteins were expressed in HighFive™ cells (Tichoplusia ni egg cell homogenate cell line BTI-TN-5B1-4, Life Technologies). High Five cells were seeded at a density of  $1.8 \times 10^6$  cells/ml in sterile tissue culture grade Erlenmeyer flasks and infected with P3 high-titre recombinant baculovirus at 1:10 final volume. Protein expression was carried out at 27°C in a shaking incubator for 48 hours. Insect cell supernatant containing recombinant protein

was harvested by centrifugation at 1000rpm for 15 minutes at 4°C, followed by a subsequent centrifugation step at 5000rpm for 15 minutes at 4°C. All centrifugation steps were carried out in sterile, endotoxin free 50ml conical tubes (Becton Dickinson). Clarified insect cell culture supernatant was supplemented with 1mM PMSF, loaded into previously boiled and equilibrated 10,000MWCO dialysis tubing (Pierce Thermo) and dialysed for 16 hours against TBS pH8.0 (Appendix A) at 4°C with stirring.

### **2.3.21 HEK293 transfection for N-terminal sequencing**

HEK293 cells were seeded in complete DMEM (Appendix A) at  $1 \times 10^6$  cells in a 10cm sterile tissue culture dish and incubated for 24 hours. Transfections with pCMV-Ifne-lres-mCitrine (Appendix B.4) were carried out with Fugene6 according to the manufacturer's instructions (Promega). Briefly, Fugene6 transfection reagent was diluted in DMEM media (Gibco) and incubated for 5 minutes at room temperature. 2µg of plasmid DNA was mixed in a ratio of 1:3 with Fugene6 and incubated at room temperature for 20 minutes. Transfection mix was added drop-wise to cells and the cells returned to 37°C, 5% CO<sub>2</sub> for 72hours.

Supernatant from transfected cells was harvested and filtered through a 0.2µm syringe filter (Sartorius). Bovine immunoglobulins were pre-cleared by incubating the supernatant with 500µl Protein G beads for 4 hours at 4°C on a rocking platform. 60µg of anti-IFNε antibody H3 or isotype control was added to the supernatant and incubated on a tube roller at 4°C overnight. The following day, 60µl of Protein G beads were added and incubated for 4h at 4°C. Protein G resin was collected by centrifugation at 1000rpm for 5 minutes at 4°C. Resin was washed three times with 1ml PBS (Appendix A) prior to resuspending the Protein G beads in 20µl 5 x SDS-PAGE Loading Dye (Appendix A).

### **2.3.22 RAW cell stimulation for protein lysates**

RAW 264.7 cells were plated at a density of  $1 \times 10^6$  cells/well in a 6 well plate and incubated for 24 hours. The cells were stimulated with interferon at the indicated concentrations for the indicated amount of time. Following stimulation, supernatants were aspirated with a vacuum pump and the cells washed with 1ml ice cold PBS (Appendix A). PBS was aspirated and the cells lysed in 80 $\mu$ l/well KalB lysis buffer (Appendix A) with mechanical scraping. Lysates were transferred to microcentrifuge tubes and placed on a rotating wheel at 4°C for 30 minutes. Cell debris was pelleted at 14,000rpm for 5mins at 4°C and the cleared lysate transferred to pre-chilled microcentrifuge tubes. 30 $\mu$ l of SDS-PAGE loading dye (Appendix A) was added to each sample and boiled for 5 minutes at 95°C. Samples were kept frozen at -20°C until used.

### **2.3.23 IRG - Luciferase Assays**

Luciferase assays were carried out in an immortalized IFNAR1 null MEF cell line [268] or in HEK293-ISRE cells.

IFNAR1 null MEFs were diluted to a final concentration of  $2 \times 10^4$  cells/ml and transfected in triplicate with the following constructs per well; 30ng of ISRE-luciferase reporter (Stratagene) or ISG15-luciferase reporter, 100ng of TK-renilla, 1ng of IFNAR1 and 369ng of pEF-Bos. Per well, 1.25 $\mu$ l FuGene 6 was mixed with 20 $\mu$ l of DMEM (no additives) and incubated with plasmid DNA for 30 minutes at room temperature. Following this incubation, transfection mix was added to the cells and 1ml aliquoted into each well of a 24 well plate and incubated at 37°C for 24 hours. The cells were stimulated with interferon and returned to the incubator for a further 8 hours. Cell supernatants were aspirated and cells scraped in 200 $\mu$ l of Reporter Lysis Buffer (Promega) with a cell scraper (TPP). 80 $\mu$ l of lysed cells were transferred to an opaque 96-well plate in duplicate for luciferase and TK renilla readings. 100 $\mu$ l of Luciferase

substrate (Promega) or 200µl of TK-renilla substrate (Appendix A) were added to their corresponding wells and the luminescence read in a FLUOStar Optima plate reader (BMG Labtech). Relative luciferase activity was determined as the relative activity of stimulated compared to unstimulated readings following TK-renilla transfection control correction.

HEK293 cells stably expressing an ISRE driven luciferase reporter were seeded at a density of  $2 \times 10^4$  cells in a 96 well plate in a total volume of 100µl and incubated for 24 hours. Interferon diluted in 100µl of complete DMEM was then added to cells in triplicate and incubated for 16 hours at 37°C, 5% CO<sub>2</sub>. Cells were lysed in 50µl Reporter Lysis Buffer (Promega) for 10 minutes and 20µl of lysate transferred to an opaque 96-well plate. 30µl of reconstituted Luciferase substrate reagent (Promega) was added to each well and the luminescence read on a FLUOStar Optima plate reader. Relative luciferase activity was determined as the ratio of light units of stimulated samples compared to unstimulated samples.

#### **2.3.24 IFNε mAb neutralisation**

Antibody neutralisation experiments were performed using either antiviral activity assays (2.3.10) or MEF Luciferase assays (2.3.23). IFNε at the indicated concentration was incubated with antibody at the indicated concentration at room temperature for 4 hours. Samples were added to the assays and continued as described for the respective assay.

## **2.4 Protein Manipulations**

### **2.4.1 Biotinylation of antibodies**

Antibodies were biotinylated according to the manufacturer's instructions (Thermo Scientific). Antibody was dialysed into 0.1M sodium bicarbonate buffer overnight at 4°C and the absorbance measured at A280nm by Nanodrop using an extinction coefficient of 1.5. Easylink NHS Biotin (Thermo Scientific) was dissolved in DMSO (Sigma Aldrich) at the same concentration as antibody and added to the antibody at a ratio of 0.12ml of reagent per ml of antibody. The sample was incubated for 4 hours at room temperature protected from light and subsequently dialysed against PBS (Appendix A) overnight at 4°C. Dialysed antibody was harvested, filter sterilised and the protein concentration determined by Bradford assay as described in 2.4.7. Biotinylated antibodies were stored at 4°C protected from light.

### **2.4.2 SDS-PAGE (Sodium Dodecyl Sulfate – Polyacrylamide Gel Electrophoresis)**

Protein samples were boiled at 95°C with 5x SDS-PAGE loading dye (Appendix A) for 5 minutes and separated on SDS-PAGE gels with 5% SDS-PAGE stacking gels (Appendix A). The percentage of polyacrylamide varied depending on the protein of interest and is indicated. Gels were cast and run using the Bio-Rad ProteanII system at 100 volts in SDS-PAGE running buffer (Appendix A) for 90-120 minutes. Molecular weight was determined by running Prestained protein ladder (NEB) alongside protein samples.

### **2.4.3 Coomassie blue staining of polyacrylamide gels**

Protein bands separated on SDS-PAGE were visualised with Coomassie Brilliant blue (CBB) stain (Appendix A). Gels were destained in H<sub>2</sub>O containing

40% ethanol and 7.5% glacial acetic acid on a rocking platform. Following destaining, gels were heat sealed in plastic sleeves and scanned.

#### **2.4.4 Western Blotting**

All western blotting was performed using the wet transfer technique. Immobilon-P Polyvinylidene fluoride (PVDF) membrane (Millipore) was primed in 100% Methanol for 5 seconds and washed in MQ dH<sub>2</sub>O. The primed membrane, filter paper and fibre pads were soaked in transfer buffer (Appendix) for 5 minutes. The SDS-PAGE gel and PVDF membrane were packed with a piece of filter paper on each side and placed in between two fiber pads. This was placed into a transfer cassette (BioRad) with the SDS-PAGE gel being closest to the cathode. The closed transfer cassette was placed into the electrode assembly together with a frozen cooling unit and submerged in transfer buffer in a transfer tank (Bio-Rad). The tank was surrounded with ice while transferring at 100v for 60-75 minutes.

#### **2.4.5 Enhanced Chemiluminescence (ECL) Detection**

Following protein transfer the PVDF membranes were placed into roller tubes (Sarstedt) and incubated with 5% w/v milk solution (Appendix A) for 1 hour at 4°C on a roller mixer. Primary antibody was diluted in fresh 5% w/v milk solution and incubated with the PVDF membrane at RT for 1hr. The antibodies used in this project are outlined in Table 2.1. The membranes were subsequently washed 3 x 5mins in PBST (Appendix A) and incubated with secondary antibody diluted in 5% w/v milk solution at RT for 1hr. All membranes underwent a final 3 x 5min wash in PBST before visualization.

Each membrane was visualized by 2 minute incubation with 600µl of SuperSignal West Pico Chemiluminescent Substrate (Pierce). Membranes were placed inside a Hypercassete (Amersham) and exposed to CL-X Posure

Film (Pierce) until bands appeared. An AGFA CP1000 developer was used to develop the films.

**Table 2.1 Antibodies used for western blotting**

1° Ab	Dilution	Source	2° Ab	Dilution	Source	Detection Method
pStat1-Y701	1:1000	Cell Signalling Technologies	Polyclonal $\alpha$ -rabbit IgG-IRDye 800CW	1:2000	Rockland	Odyssey (InfraRed)
pStat3-Y705	1:1000	Cell Signalling Technologies	Polyclonal $\alpha$ -rabbit IgG-IRDye 800CW	1:2000	Rockland	Odyssey (InfraRed)
Total Stat1	1:1000	Cell Signalling Technologies	Polyclonal $\alpha$ -rabbit IgG-IRDye 800CW	1:2000	Rockland	Odyssey (InfraRed)
Total Stat3	1:1000	Cell Signalling Technologies	Polyclonal $\alpha$ -rabbit IgG-IRDye 800CW	1:2000	Rockland	Odyssey (InfraRed)
$\beta$ -tubulin	1:1000	Abcam	Polyclonal $\alpha$ -mouse IgG-IRDye 800CW	1:2000	Rockland	Odyssey (InfraRed)
Actin	1:1000	Cell Signalling Technologies	Polyclonal $\alpha$ -mouse IgG-IRDye 800CW	1:2000	Rockland	Odyssey (InfraRed)
Mouse $\alpha$ -mIFN $\epsilon$ clone H3	1:1000 (1 $\mu$ g/ml)	In-house	Polyclonal rabbit $\alpha$ -mouse IgG	1:1000	Dako	ECL
Polyclonal rabbit $\alpha$ -IFN $\epsilon$	1:50,000	In-house	Polyclonal goat $\alpha$ -rabbit IgG	1:1000	Dako	ECL
Mouse $\alpha$ -His <sub>6</sub>	1:1000	Cell Signalling Technologies	Polyclonal rabbit $\alpha$ -mouse IgG	1:1000	Dako	ECL

#### **2.4.6 Odyssey Detection**

Following protein transfer the PVDF membranes were placed into roller tubes (Sarstedt) and incubated with Odyssey blocking buffer (Licor) for 1 hour at 4°C on a roller mixer. Primary antibody was diluted in fresh Odyssey blocking buffer and incubated with the PVDF membrane overnight at 4°C on a roller mixer. The antibodies used in this project are outlined in Table 2.1. The membranes were subsequently washed 3 x 5mins in PBST (Appendix A) and incubated with secondary antibody diluted in Odyssey blocking buffer at RT for 1hr. All membranes underwent a final 3 x 5min wash in PBST before visualization. Each membrane was visualized on an Odyssey Infrared Western Blot Imager (Licor).

#### **2.4.7 Bradford protein assay**

Protein concentrations were determined by standard Bradford colorimetric protein assay according to the manufacturer's instructions (Bio-Rad). 5µl of sample was aliquotted in duplicate in a 96-well plate and PBS added to a final volume of 200µl. 50µl of Protein Assay dye (Bio-Rad) was added to each sample well including the BSA control wells and mixed until a colour change occurred. The 96-well plate was then read by a FLUOstar<sup>+</sup> Optima plate reader (BMG Labtech) at an absorbance of 590nm, where the concentration of protein was determined using a BSA standard curve between 0.5µg and 10µg per well.

#### **2.4.8 Immobilizing metal affinity chromatography (IMAC)**

Dialysed insect cell culture supernatant containing recombinant His<sub>6</sub>-tagged protein was filtered through 0.8µm syringe filters (Sartorius) using a 50ml sterile syringe (Beckton Dickinson). Following filtration, sterile Imidazole was added to a final concentration of 20mM and mixed. IMAC was performed for

24 hours at 4°C with the aid of a recirculating peristaltic pump (MasterFlex) using Ni<sup>+</sup> Sepharose Fast Flow 6 resin (GE) at a volume of 1ml wet bed resin per 1L of dialysed culture supernatant. Ni<sup>+</sup> resin was washed with 10 column volumes (CV) of chilled IMAC wash buffer (Appendix A) and recombinant His<sub>6</sub>-tagged protein eluted stepwise with 1CV chilled IMAC elution buffer (Appendix A) per fraction. Protein containing fractions were detected spectrophoretically using a NanoDrop ND-1000 (Analytical Technologies) and by SDS-Coomassie and Western Blot. Fractions containing the protein of interest were dialysed or buffer exchanged into TBS pH8.0 (Appendix A).

#### **2.4.9 Size exclusion chromatography**

All size exclusion chromatography was carried out on an Akta PrimePlus System (GE Healthcare) with either a Superdex S200 16/60 gel filtration column or a Superdex S75 column (GE Healthcare), as indicated. Samples to be purified were concentrated to approximately 4ml using spin concentrators at 4°C, 6000rpm and filtered through a 0.22µm syringe filter to remove particulates. Samples were resolved with TBS pH8.0 containing 10% v/v glycerol at 1ml/min and fractions collected with an Akta Prime Plus Wavelength Monitor and Fraction Collector (GE Healthcare). Protein containing fractions were confirmed spectrophoretically by NanoDrop and analysed by SDS-Page and Western Blotting.

#### **2.4.10 Reverse Phase High Performance Liquid Chromatography (RP-HPLC)**

RP-HPLC was carried out on an Agilent 1100 Modular RP-HPLC system using ChemStation software (Agilent). Recombinant protein was acidified to pH2.0 using concentrated trifluoroacetic acid (TFA - Merck) and centrifuged at 10,000rpm for 5 minutes at 4°C to remove particulates. The sample was

injected onto a Phenomenex Jupiter C5 10 $\mu$ m prep column attached to a guard column (Phenomenex) via a 10ml loop. The sample was resolved using the following gradient settings:

Time	% Buffer B	Flow Rate
20mins	0	3ml/min
80mins	100%	3ml/min
100mins	100%	3ml/min

1.5ml fractions were collected into Axygen 96well collection plates and peak containing fractions transferred to sterile 1.7ml microcentrifuge tubes. Buffer containing organic solvent was evaporated by centrifugation under vacuum for 16 hours at room temperature. Dried samples were resuspended in 1 part 0.05% TFA/H<sub>2</sub>O, 8 parts H<sub>2</sub>O and mixed thoroughly. Once resuspended, the sample was neutralised in 1 part 10x Hepes Buffer (Appendix A). Resuspended samples were stored at 4°C until used.

#### **2.4.11 Removal of His<sub>6</sub>-tag by enterokinase digestion**

IMAC purified His<sub>6</sub>-IFN $\beta$  protein was digested using EKMax Enterokinase according to the manufacturer's instructions (Invitrogen). Briefly, EKMax enzyme was added to His<sub>6</sub>-IFN $\beta$  at a concentration of 1Unit/20 $\mu$ g of protein. The sample was then placed on a rotating wheel at 4°C for 18 hours. The activity of enterokinase was stopped by the addition of Imidazole to 100mM final concentration. Successful fusion tag removal was determined by western blotting against His<sub>6</sub> and by molecular weight shift on 15% SDS-PAGE stained with Coomassie Brilliant Blue.

#### **2.4.12 Immunoaffinity Column preparation**

The AminoLink immunoaffinity column was prepared according to the manufacturer's instructions (Thermo Scientific). To summarise briefly, 5mg of purified H3 anti-mIFN $\epsilon$  was diluted in pH10 Citrate-Carbonate coupling buffer and added to 1ml AminoLink Agarose beads. The coupling reaction was catalysed by Sodium Cyanoborohydride and the remaining active sites blocked with 1M Tris pH7.4 solution. The resulting  $\alpha$ -IFN $\epsilon$  immunoaffinity column (hereafter called IFN $\epsilon$  mAb column) was washed extensively with PBS pH7.2 (Thermo Scientific) prior to use. The efficiency of coupling was determined to be greater than 99% by A280nm absorbance of pre-column and post-column samples.

#### **2.4.13 Immunoaffinity column IFN $\epsilon$ purification**

Recombinant untagged IFN $\epsilon$  protein dialysed into TBS pH8.0 was filtered through a 0.8 $\mu$ m syringe filter (Sartorius) and loaded onto the IFN $\epsilon$  mAb column for two cycles at room temperature by gravity flow. Following supernatant loading, the column was washed with 10CV of TBS pH8.0 (Appendix A) and IFN $\epsilon$  protein eluted stepwise with 1/2 CV fractions of 100mM Glycine pH3.0. Collected fractions were immediately neutralised in 1/10<sup>th</sup> elution volume with 1M Tris pH8.0 and buffer exchanged by addition of 1/10<sup>th</sup> final volume of 10x TBS pH8.0 (Appendix A). Protein containing fractions as determined by A280nm absorbance were supplemented with 10%v/v Glycerol and stored at 4°C until used. The IFN $\epsilon$  mAb column was stored in PBS pH7.2 (Thermo Scientific) supplemented with 0.05% Sodium Azide between uses.

#### **2.4.14 Determination of secondary fold by CD-Spectra**

Circular Dichroism experiments were performed according to standard protocols on a Jasco J815 CD Spectrophotometer. Each sample measured

contained 40µg of protein in a final volume of 300µl. Final graphs were generated using GraphPad Prism.

#### **2.4.15 Temperature and pH stability tests**

The temperature and pH stability of interferons was evaluated by antiviral activity assay as described in section 2.3.10. For temperature stability, interferon was placed at 55°C for 90 minutes prior to the antiviral assay and chilled at 4°C before adding to cells. For pH stability, interferon was acidified to pH2 using hydrochloric acid (HCl - Merck) and incubated at 4°C overnight. The following morning, the pH was neutralised to pH8.0 using sodium hydroxide (NaOH) and the sample added to cells. Each experiment contained control IFN samples and temperature/pH treated samples.

#### **2.4.16 N-terminal protein sequencing**

Samples were run on a 15% SDS-PAGE gel and transferred to PVDF membrane as described in section 2.4.4 with the exception that the transfer was carried out in CAPS buffer (Appendix A). Following protein transfer, the membrane was washed 3 times for 5 minutes in MQ H<sub>2</sub>O and then stained for 5 minutes with 0.025% Coomassie Blue R250 dissolved in a 40% Methanol solution on a rocking platform. The membrane was destained in a 50% Methanol solution for 10-15 minutes or until the background became light blue. Protein bands of interest were cut out and sent to the Monash University Proteomics facility for N-terminal sequencing.

#### **2.4.17 Surface Plasmon Resonance (SPR)**

All SPR was carried out on a BIAcore 3000 (GE Healthcare) by Dr Travis Beddoe (Monash University, Clayton, Australia) according to standard methods [269]. Anti-mouse IgG antibody was immobilised to a CM5 chip according to the manufacturer's instructions (GE Healthcare). 100µg H3 α-

IFN $\epsilon$  antibody was washed across the chip at 50 $\mu$ l/min, followed by 10 $\mu$ g IFN $\epsilon$ . Secondary  $\alpha$ -IFN $\epsilon$  antibody was injected at a flow rate of 50 $\mu$ l/min. Final response was calculated by subtracting the response achieved from a blank run in which no secondary antibody was added. Graphs were generated in GraphPad Prism.

#### **2.4.18 Endotoxin Testing**

Expressed recombinant interferons were tested for endotoxin contamination by Limulus amoebocyte lysate (LAL) assay according to the manufacturer's instructions (Genscript). Briefly, samples were diluted to 1 $\mu$ g/ml in endotoxin free water. LAL was added to each sample and incubated for 45 minutes at 37°C. Following incubation, chromogenic substrate was added to each sample and incubated at 37°C for 6 minutes. Color-stabilizers 1-3 were added in succession and the absorbance of each sample read at 545nm. Endotoxin levels were calculated compared to a standard curve of *E. Coli* endotoxin standard and presented as EU/ $\mu$ g.

## **2.5 Immunology Methods**

### **2.5.1 Hybridoma supernatant ELISA**

Each well of a Nunc Immunosorbent plate was coated with 0.1 $\mu$ g of antigen diluted in NaHCO<sub>3</sub> and incubated for 2 hours at room temperature. Unbound antigen was washed off with 300 $\mu$ l of PBST in three repeated washes. 3% BSA/PBST was prepared and each well blocked in 200 $\mu$ l for 1 hour at room temperature. The plate was again washed three times with PBST. 50 $\mu$ l of undiluted hybridoma culture supernatant was added to each well and the plate sealed and incubated overnight at 4°C. The following morning, all wells were washed three times with PBST. Rabbit anti mouse HRP-labelled antibody

(Dako) was diluted 1:1000 in PBS and 50µl added to each well for 1hour at room temperature. The plate was washed 5 times with PBST and all remaining liquid removed by repeated tapping against a paper towel. TMB substrate was prepared according to the manufacturer's instructions (Thermo) and 100µl added to each well an incubated at room temperature until colour change became apparent. The chromogenic reaction was stopped by addition 50µl of 2M NaSO<sub>4</sub> to each well. The absorbance was measured at 450nm on a FLUOStar Optima plate reader (BMG Labtech). Readings approximately 3x the background were considered significant.

### **2.5.2 Flow cytometry**

Cells to be analysed for surface antigen expression were prepared as described previously (2.3.14 and 2.3.16). Cells were pelleted at 1000rpm for 5 minutes and resuspended in 100µl 2%FCS/PBS containing 2.5µg/ml of anti-mouse CD16/32 Fcy III/II receptor blocking antibody (BD Bioscience) to prevent non-specific antibody binding. Cells were incubated for 15 minutes on ice and subsequently washed 2x with 2%FCS/PBS. Cells were centrifuged at 1000rpm for 5 minutes, the supernatant discarded and cells resuspended in 100µl of antibody cocktail mix (Table 2.2). All antibodies were purchased from Becton Dickinson.

**Table 2.2 Antibodies used for flow cytometry**

Cocktail	Antibodies	Concentration
T-cells	CD8-biotin (APC)	1/200
	CD4-FITC	1/200
	CD69-PE	1/200
B and NK-cells	NK1.1-biotin (APC)	1/200
	B220-FITC	1/200
	CD69-PE	1/200
MHC-1 stain	H2kd-PE	1/200

For T-cell, B-cell and NK-cell staining, IgG2a-PE at a concentration of 1/200 was used instead of CD69-PE as an isotype control. For MHC-1 staining, IgG2a-PE at a concentration of 1/200 was used instead of H2kd-PE as an isotype control. All flow cytometry data acquisition was performed on a FACSCantoll (BD Biosciences). Flow cytometry analysis was performed using FlowJo 7.6.5 Software (Tree Star).

### **2.5.3 IFN $\epsilon$ immunoprecipitation using mAbs**

5ml of insect cell supernatant containing recombinant IFN $\epsilon$  protein was incubated with 10 $\mu$ g of purified anti-IFN $\epsilon$  mAbs overnight on a rotating wheel at 4°C. The following day, 40 $\mu$ l of a 50% Protein G Sepharose slurry was added to each sample and placed on a rotating wheel at 4°C for 2 hours. Protein G Sepharose was pelleted by centrifugation at 1000rpm for 5 minutes at 4°C. Sepharose beads were washed three times in 1ml of ice cold PBS before being resuspended in 30 $\mu$ l of 5x SDS-PAGE Loading Dye (Appendix A). Samples were boiled for 5 minutes at 95°C and proteins separated on SDS-PAGE for Coomassie staining and Western blotting.

#### **2.5.4 IFN $\epsilon$ Immunohistochemistry**

IFN $\epsilon$  immunohistochemistry was performed on 4 $\mu$ m thick paraffin embedded tissue sections. Sections were de-waxed in Xylene and re-hydrated in ethanol series from 100% Ethanol to 70% Ethanol before being placed in tap water. Antigen retrieval was performed using 10mM Citrate Buffer pH6.0 in a Dako Cytomation pressure cooker set at 125°C for 5 minutes followed by 90°C for 10 seconds. Slides were removed and allowed to cool to room temperature before proceeding with the immunostaining. Staining wells were created with a PAP pen and the tissue blocked in 3% Normal Goat Serum (Vector Technologies) diluted in PBST (Appendix) for 45 minutes at room temperature. Mouse anti-IFN $\epsilon$  antibodies were diluted to 10 $\mu$ g/ml in blocking buffer and evenly dispersed onto the sections with a micropipette. Staining was carried out at 4°C for 18hours.

Following staining, slides were washed 3x 5mins in PBST (Appendix) before incubation with biotin-conjugated goat  $\alpha$ -mouse IgG secondary antibody (Vector Technologies) diluted 1/250 in 3% Normal Goat Serum in PBST for 1 hour at room temperature in a humidified box. Slides were washed 2 x 5mins in PBST followed by a 5 minute wash in PBS. Endogenous peroxidases were inactivated by immersion of the slides in a mixture of 0.3% hydrogen peroxide in methanol for 30 minutes at room temperature. Slides were washed 4 x 5 mins in PBST and incubated for 30 minutes in ABC HRP-conjugate (Vector Technologies). Slides were washed 4 x 5 mins in PBS and stained with DAB substrate (Vector Technologies) until staining became apparent. The staining was stopped by submersion of slides in water and subsequently counterstained with haematoxylin where indicated.

### **2.5.5 IFN $\epsilon$ ELISA**

IFN $\epsilon$  ELISAs were performed according to standard sandwich ELISA protocols. Briefly, capturing antibody at the indicated concentration was plated in a total volume of 100 $\mu$ l of NaHCO<sub>3</sub> in a 96 well immunosorbent plate (Nunc) and incubated overnight at 4°C. The plate was washed 4 x with PBST (Appendix A) and then blocked for 2 hours at room temperature in 10%FCS/PBS. The plate was washed 4 x in PBST and 100 $\mu$ l of IFN $\epsilon$  standard or sample added to wells for 2 hours at room temperature. The plate was washed 4 x with PBST and 100 $\mu$ l detection antibody diluted in blocking buffer at the indicated concentration added to each well for 1 hour at room temperature. The plate was washed 4 x with PBST and each well incubated with Streptavidin-horse raddish peroxidase (SA-HRP) diluted 1:2500 in blocking buffer for 30 minutes at room temperature. The plate was washed 8 x with PBST and 100 $\mu$ l of TMB Substrate (Thermo Scientific) added to each well. Reactions were stopped by addition of 100 $\mu$ l 2M NaSO<sub>4</sub> and the plates read at 450nm on a FLUOStar Optima plate reader (BMG Labtech).

## **2.6 Animal handling**

All animal experimental procedures and breeding were performed with approval from the institutional animal ethics committee (MMC-A). Unless otherwise stated, all animal procedures were carried out by myself. Animal handling training was completed at the Monash Medical Centre Animal Facilities (MMCAF).

### **2.6.1 Immunizing mice for monoclonal antibodies**

6 week old *Ifne1* null mice were injected intraperitoneally (I.P) with IFN $\epsilon$  immunogen mixture fortnightly for 6 weeks. The IFN $\epsilon$  immunogen mixture

comprised of (per injection, per mouse); 8µg boiled His<sub>6</sub>-IFNε, 8µg intact IFNε, 10µl CpG oligonucleotides, 100ul Sigma Adjuvant System (Sigma-Aldrich), 45µl PBS (Gibco). Immunogen mixture was warmed to 37°C prior to injection into mice. Mice received a final booster injection 4 days prior to splenectomy. All mouse injections were performed by Dr. Niamh Mangan (MIMR, Clayton, Australia).

### **2.6.2 ELISA of sera from immunized mice**

Mice used to generate monoclonal antibodies were cheek bled prior to immunogen injection and again one week after the final injection. The collected blood was allowed to clot for 15 minutes at room temperature in a microcentrifuge tube and then centrifuged at 4000rpm for 12 minutes at 4°C. The serum layer was collected and delivered to Monash Antibodies Technology Facility to be tested for immunogenicity against IFNε.

### **2.6.3 Mouse organ collection for histology**

6-12 week old mice were euthanized by asphyxiation and cervical dislocation and organs surgically removed. Organs were placed into tissue cassettes and immediately submersed in buffered formalin (Amber Scientific). Following 24hours at 4°C, cassettes were transferred into 70% ethanol and stored at 4°C until processed. All tissue processing, embedding and sectioning was carried out by the MIMR Histology Facility.

### **2.6.4 Mouse cycle determination**

To determine the female cycle stage in adult mice, standard reproductive tract swabbing was performed. A cotton swab was wetted in PBS (Gibco) and the mouse vagina swabbed. Cells were streaked onto a microscope slide and allowed to dry. Cell staining was performed with Modified Wright-Giemsa Stain (Sigma Aldrich) and the stage of cycle determined by cell populations present.

### **2.6.5 Mouse organ collection for RNA**

6-12 week old mice were euthanized by asphyxiation and cervical dislocation and organs surgically removed. The organs were placed into sterile microcentrifuge tubes and immediately snap frozen in liquid nitrogen. Snap frozen samples were stored at -80°C until used.

### **2.6.6 Spleen collection for cell suspensions**

6-12 week old mice were euthanized by asphyxiation and cervical dislocation and spleens surgically removed. Spleens were placed into chilled PBS (Gibco) until cell suspensions were created. Spleen cells were isolated by mincing spleens through a 70µm fine cell strainer (Becton-Dickinson) with 5ml of complete RPMI. Cells were pelleted at 1000rpm for 5 minutes and the supernatant removed. 2ml of red blood cell lysis buffer (Appendix A) was added and cells incubated for 5 minutes at room temperature. Cells were washed twice in complete RPMI and resuspended in 10ml of complete RPMI before performing cell counts on a Sysmex automated cell counter as previously described in 2.3.2.

## **Chapter 3 – Expression and Purification of IFN $\epsilon$**

### **3.1 Introduction**

The interferons are a large family of cytokines that have been studied extensively since their discovery in 1957 [14]. They demonstrate a number of biological functions including antiviral, antiproliferative and immunoregulatory activities. The most well characterised interferons are human IFN $\alpha$ 2 and IFN $\beta$  and this is reflected in their use as therapeutics for a number of indications as outlined in Chapter 1.

Although the interferons were described in 1957, it took almost another 30 years for them to be purified to homogeneity. In addition, with the advent of recombinant DNA technology large quantities of interferon could be produced for study. Importantly, until this point interferon formulations were impure and some of the biological activities attributed to interferons could not actually be validated due to the low quantity and purity of end product [252].

IFN $\epsilon$  is a novel type I interferon discovered by our group and has been the focus of extensive study with the use of *Ifne1* null animals [13, 114]. While these studies demonstrate a clear function for IFN $\epsilon$  in maintaining reproductive tract homeostasis, it is challenging to determine the exact biological activities of the molecule itself without a pure preparation of protein. As IFN $\epsilon$  is a novel cytokine, commercial companies do not include it in their available list of products and as such, recombinant protein needs to be produced in order to fully study its biological functions. Therefore the aim of this chapter was to express recombinant murine IFN $\epsilon$  and purify it for use in biological studies. To assist in the characterisation process, recombinant

murine IFN $\beta$  was expressed and purified alongside IFN $\epsilon$ . As IFN $\beta$  has been extensively characterised, it would serve as a control for the expression system used and as a comparison for measurements of biological activities.

## 3.2 Results

### 3.2.1 Expression of IFNε in Mammalian and Bacterial Hosts

Recombinant interferons have a long standing history of being expressed in bacterial and mammalian expression systems [259, 261]. Each expression system has its advantages and disadvantages. Bacterial expression hosts are ideal for producing high yields of recombinant protein cheaply and reproducibly. A drawback to this is the potential for the expressed protein to form inclusion bodies, which are insoluble aggregates of protein that need to be denatured and refolded. There are a number of ways to overcome inclusion body formation. Varying time, temperature and induction conditions often aids in increasing the soluble protein fraction. An alternative approach is the use of fusion partners to increase solubility. The small ubiquitin like modifier (SUMO) tag is one such solubility tag that has shown great potential in increasing the proportion of soluble protein [270]. To test the effect of SUMO on the solubility of IFNε, the DNA sequence coding for *Ifne1* was inserted into the pET-SUMO vector (Appendix B.1) and sent to the Monash University Protein Production Unit (PPU) for trial expression in 8 different *E. coli* cell lines at two different temperatures, 20°C and 28°C. Figure 3.1A highlights the results of the trial expression in the five highest expressing cell lines. Although a band was observed at the expected size of 33kDa, the low yields resulted and the co-purification of a number of other proteins were a problem. Furthermore, western blotting for the N-terminal His<sub>6</sub> tag revealed breakdown products originating from the C-terminal end of the protein. The full PPU report is attached in Appendix C. Collectively, these data indicated that although successful, expression in bacterial cells resulted in too low a yield of soluble protein to continue.

A second widely used expression system for the production of interferons are mammalian cells, specifically HEK293 derived cells [259]. To investigate the ability to express IFN $\epsilon$  in mammalian cells, the *Ifne1* gene was cloned into two vectors suitable for mammalian expression (Appendix B.2 and B.3). The pTT22 system has been shown to produce in excess of hundreds of milligrams per litre of recombinant hIFN $\alpha$ 2b and was therefore an ideal candidate for IFN $\epsilon$  expression [259]. pTT22 vector was a kind gift of Dr. Yves Durocher (BRI, Montreal, Canada). Similarly, pkCMVintPolyli has been used successfully for the expression of murine IFNs *in vivo* and *in vitro* with yields reaching 1 milligram per litre [271]. pkCMVintPolyli was a kind gift of Prof. Cassandra Berry (Murdoch University, Perth, Australia). The two mammalian *Ifne1* expression vectors were sent to CSIRO for expression trials by transient transfection into suspension grown HEK293 cells. Expression culture supernatants were analysed by SDS-PAGE and Western blotting for IFN $\epsilon$  using a polyclonal anti-IFN $\epsilon$  antibody (generated by Dr. Helen Cumming) and compared to a known quantity of His<sub>6</sub>-IFN $\epsilon$  produced in insect cells (see 3.2.3) (Figure 3.1B). A faint band was visible in the reduced sample from the pTT22 expression however the quantity was lower than what was seen in the well containing 10ng of His<sub>6</sub>-IFN $\epsilon$ . The cells transfected with pkCMVintPolyli-*Ifne1* vector demonstrated no observable protein by SDS-PAGE Western blot either at reducing or non-reducing conditions. Together, these findings suggested that this mammalian expression host was not suitable for the production of recombinant murine IFN $\epsilon$ .

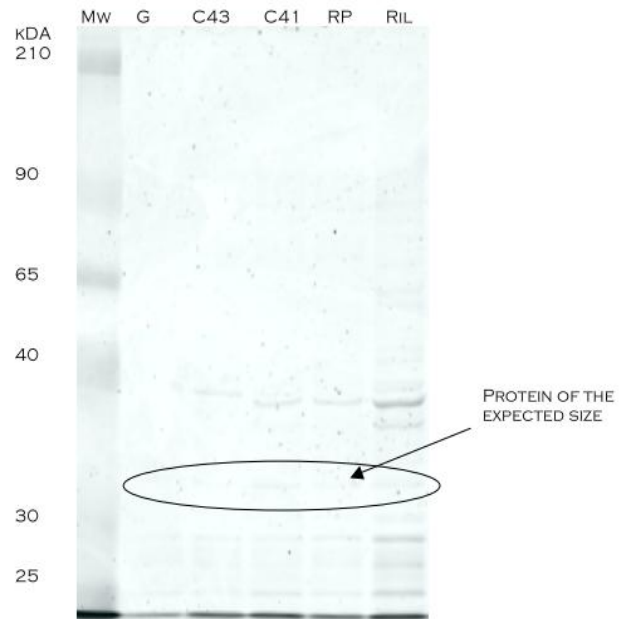
### 3.2.2 Generation of recombinant His<sub>6</sub>-IFN $\epsilon$ baculovirus construct

Another commonly used expression system for the large scale production of recombinant proteins is the baculovirus expression system. Yields are

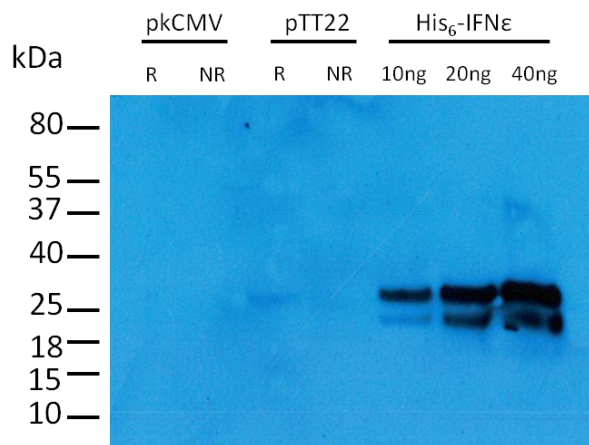
**Figure 3.1. Trial expression of IFN $\epsilon$  in bacterial and mammalian expression systems by the Monash University Protein Production Unit and CSIRO. A)** A western blot of nickel-affinity purified pET-SUMO-Ifne1 trial expressions performed in different *E. coli* strains stained with an  $\alpha$ -His antibody. The bacterial vector pET-SUMO-Ifne1 was trialled for its expression in a number of *E. coli* cell lines at varying conditions as outlined in the report attached in Appendix. *E. coli* strains: G, BL21(DE3) Gold; C43, C43(DE3); C41, C41(DE3); RP, BL21-CodonPlus-RP; RIL, BL21-CodonPlus-RIL

**B)** A western blot of culture supernatant from mIFN $\epsilon$  expressed in eukaryotic cells. Two mammalian expression vectors were transiently transfected into HEK293E cell-lines and supernatant analysed for secreted protein by western blotting using a polyclonal anti-IFN $\epsilon$  antibody. R, reduced sampled; NR, non-reduced sample. Compared to His $_6$ -IFN $\epsilon$ , the secreted product is only barely detectable in the reduced supernatant transfected with pTT22-Ifne1. Supernatants from cells transfected with pCMVpolyli-Ifne $\epsilon$  showed no band at the predicted size. His6-IFN $\epsilon$  was protein expressed from insect cells used as a positive control for the western blots.

A.



B.



typically lower than achievable in bacterial or mammalian expression systems and as a result baculovirus expression systems are less cost effective for the production of large amounts of recombinant protein. A major advantage compared to bacterial expression systems however is that insect cells are eukaryotic and therefore post-translational modifications and correct folding are possible. Furthermore, expression is carried out in serum free, low protein containing media which simplifies downstream protein purification. Importantly, published data and work performed in our laboratory indicated that a baculovirus expression system was suitable for the production and purification of IFNs and receptors [272-274].

The cloning and expression strategy of His<sub>6</sub>-IFN $\epsilon$  is described in Figure 3.2 which follows standard protocols as described in Chapter 2. To generate the pFastBac donor construct the gene optimised codon sequence of murine *lfne1* (see Figure 3.3) was cloned downstream of a hexahistidine tag and enterokinase cleavage site of the modified pFastBac-SHEK vector (from here on described as pFB-SHEK) as described in Chapter 2.1.9. pFB-SHEK was a kind gift of Dr. Hugh Reid (Monash University, Melbourne, Australia). The *lfne1* gene was codon optimised for expression in insect cells by substituting rare or infrequently used codons for the most highly used codons, theoretically enabling the highest level of expression. The methods used for codon optimization are described in Chapter 2.1.7. Codon optimisation is routinely used to increase recombinant protein yield and has a proven track record [275-277]. Comparing the native *lfne1* sequence to codon optimised *lfne1*, only 77% sequence identity remained. When comparing the Codon Adaptation Index (CAI) of each gene, the native gene had a CAI of 0.71 whereas the codon optimised gene had a CAI of 0.81. The CAI is a scale of the suitability for high protein expression level in any given organism. A CAI of

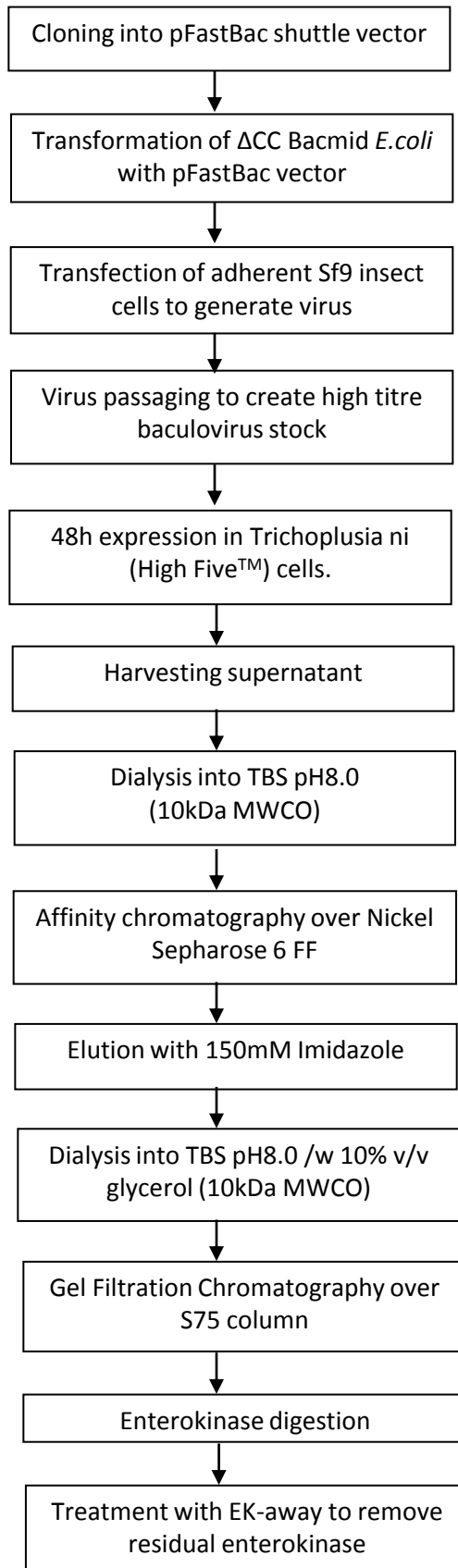


**Figure 3.2 Flow chart of His<sub>6</sub>-IFN<sub>ε</sub> cloning, expression and purification strategy.** A flowchart outlining the steps undertaken for cloning *Ifne1* into the baculovirus expression system and subsequent expression and purification of His<sub>6</sub>-IFN<sub>ε</sub> recombinant protein.



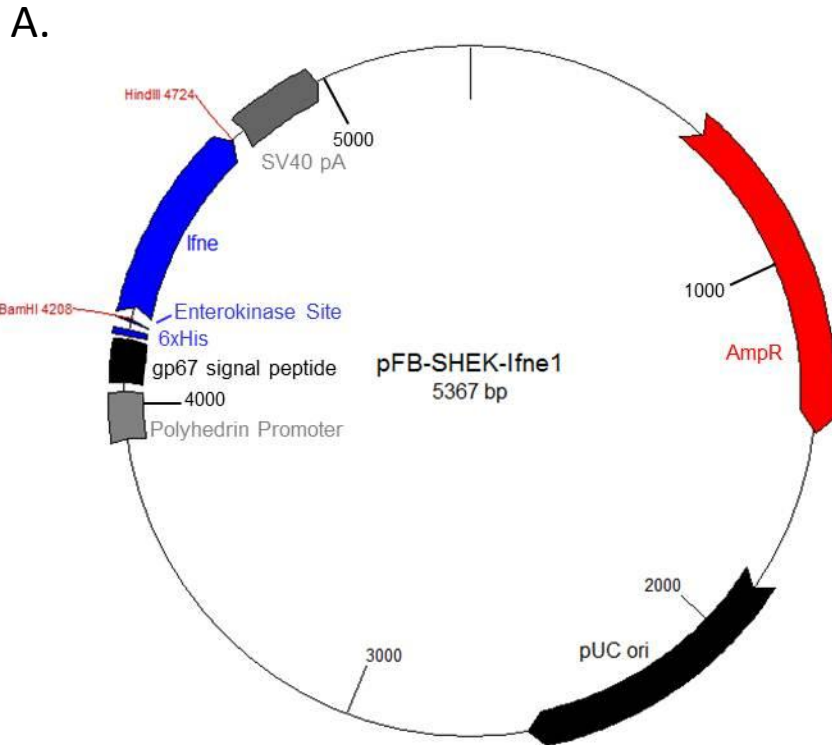
1.0 is considered ideal and >0.8 is rated as good for expression (Appendix D). Thus, the codon optimised *lfne1* gene should be beneficial in increasing expression yields from insect cells.

The presence of the *lfne1* gene in the resulting pFB-SHEK-*lfne1* vector (Figure 3.4A) was confirmed by Sanger sequencing and the vector subsequently electroporated into chemically competent ΔCC bacmid containing *E. coli* [264]. The bacmid is a baculovirus shuttle vector and is needed for generation of the recombinant bacmid by transposition of the gene of interest from the pFB-SHEK vector. The presence of gene insert and correct orientation was confirmed by polymerase chain reaction. High titre recombinant baculovirus stock was generated as outlined in Chapter 2.

### 3.2.3 Expression and purification of His<sub>6</sub>-IFNε in insect cells

HighFive™ insect cells (Invitrogen) were used for the expression of recombinant IFNε as outlined in Chapter 2.3.20. HighFive™ cells have been shown to be more suitable for the expression of secreted protein products compared to Sf9 cells [278]. Figure 3.4B illustrates the predicted IFNε protein product as expressed by HighFive™ cells. The resulting recombinant IFNε protein contains an N-terminal His<sub>6</sub> tag for purification, followed by an enterokinase cleavage site which allows for the removal of the purification tag with only a two amino acid overhang.

Following expression, conditioned insect cell culture supernatant was dialysed into TBS pH8.0 and passed over a nickel affinity column. Bound proteins were recovered by gradient elution with imidazole and the resulting fractions analysed by SDS-PAGE and western blot (Figures 3.5 B and C). The nickel affinity elution chromatogram demonstrated a major elution peak and trailing



B.

```

MLLVNQSHQGFNKEHTSKMVSAIVLYVLLAAAAHSAFAAHHHHHHGSGSDDDDDKGSPKRIPFLW
                                     ↓
MNRESLQLLKLPPSSSVQQLAHRKNFLLPQQPVSPHQYQEGQVLAVVHEILQQIFTLLQTHGTMGI
WEENHIEKVLAALHRQLEYVESLGGLNAAQSGGSSAQNRLRQIKAYFRRIHDYLENQRYSSCAWIIV
QTEIHRMFFVFRFTTWLSRQDPDP
  
```

**Figure 3.4 Cloning of gene optimised *Ifne1* into the insect cell expression vector pFB-SHEK.** A) Vector map of construct used to generate recombinant bacmid. The gene optimised *Ifne1* sequence was cloned into pFB-SHEK with BamHI and HindIII restriction enzymes. *Ifne1* expression is under the control of the polyhedron promoter. The vector map was generated in GENTle. B) The sequence of the predicted IFNε protein product as expressed by High Five insect cells. Italics denote the gp67 signal peptide, the bold font shows the enterokinase site, the underlined sequence is the mature form of mIFNε. Arrow indicates where the signal peptide is cleaved; arrow head, enterokinase cleaves after the lysine. Vector map was prepared using GENTle Software.

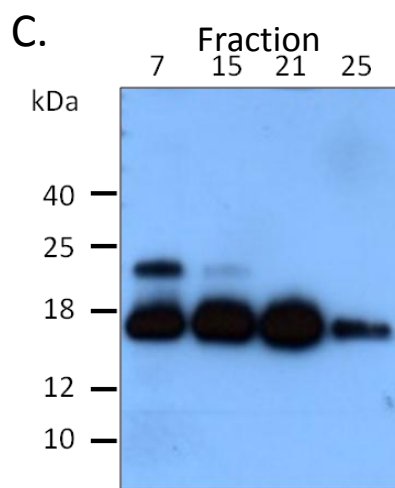
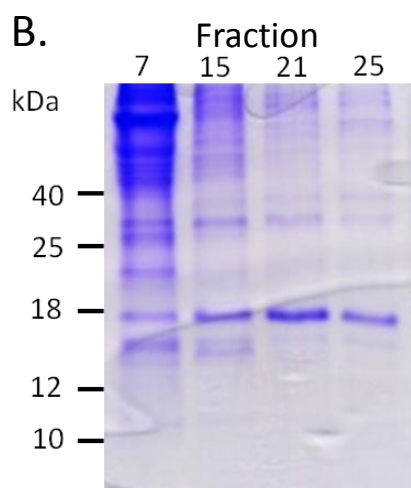
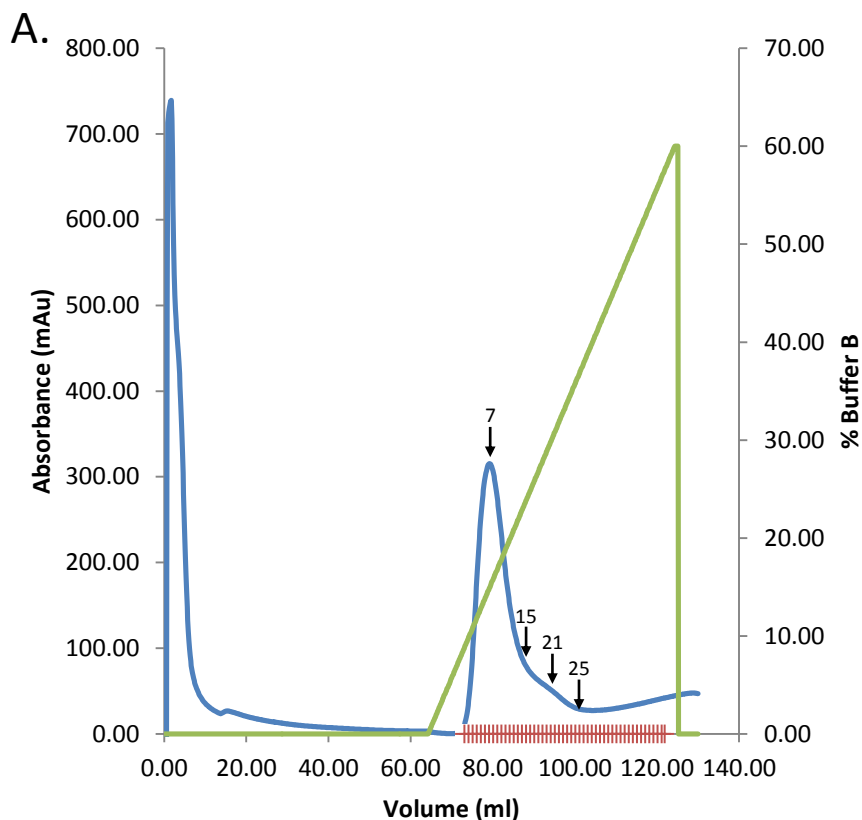


**Figure 3.5 Purification of His<sub>6</sub>-IFN<sub>ε</sub> by HisTrap Nickel Affinity Chromatography and analysis on SDS-PAGE.** Clarified insect cell expression supernatant was recirculated over HisTrap resin at 4°C, followed by elution using a gradient of Imidazole from 20mM to 1M. **A)** The chromatogram of the nickel affinity purification. A major peak with a trailing shoulder was observed on the chromatogram and all fractions were collected for SDS-PAGE analysis. Arrows indicate fractions analysed by SDS-PAGE. Blue line: Absorbance at 280nm; green line, concentration of Buffer B; red lines on x-axis, collected fractions. Chromatography fractions were visualised on 15% SDS-PAGE gels stained with **B)** Coomassie brilliant blue and **C)** after western blotting using a polyclonal anti-IFN<sub>ε</sub> antibody. A protein of expected size (~18kDa) was found to elute as early as Fr7 (peak) and increase in concentration by Fr 21 (shoulder). IFN<sub>ε</sub> specific western blotting using a polyclonal antibody confirmed the presence of IFN<sub>ε</sub> throughout the elution profile.

shoulder (Figure 3.5A). Analysis of the fractions by SDS-PAGE visualised with Coomassie brilliant blue (Figure 3.5B) and IFNε specific western blot (Figure 3.5C) demonstrated the presence of a band at ~18kDa in all investigated elution fractions which increased in intensity by Fraction 21, the sample corresponding to the peak of the resolved shoulder on the chromatogram. The predicted size of His<sub>6</sub>-IFNε expressed from insect cells was calculated to be 21.6kDa [279] and therefore the apparent size is smaller than expected. IFNε specific western blotting using a polyclonal antibody however confirmed the presence of IFNε protein in fractions of interest and the band in Fraction 21 appeared to be more intense than the remaining fractions (Figure 3.5C). These data indicated that the protein of interest was present in the trailing shoulder. Conversely, the major elution peak demonstrated a much fainter 18kDa band with excess high molecular weight proteins.

To reduce contaminating proteins and increase purity, only fractions 15-25 were pooled, dialysed against TBS pH8.0 containing 10% v/v glycerol and resolved by size exclusion chromatography on a Superdex S200 column. The gel filtration chromatogram highlights three resolved peaks (Figure 3.6A) which correspond to the void volume (Peak 1 – Fraction 6), high molecular weight contaminant protein (Peak 2 – Fraction 15) and IFNε (Peak 3 – Fraction 26). These fractions were analysed by SDS-PAGE visualised with Coomassie Brilliant Blue and the fractions corresponding to peak 3 were found to contain a band at 18kDa and a second fainter band at ~36kDa. In our experience, high concentrations of IFNα have led to the formation of an IFN dimer (unpublished data) and if this was happening for IFNε would correspond to the second band observed at 36kDa. Western blotting using an anti-IFNε antibody would confirm this hypothesis. Overall, this process enabled us to produce approximately 300μg of His<sub>6</sub>-IFNε protein per litre of culture. This was

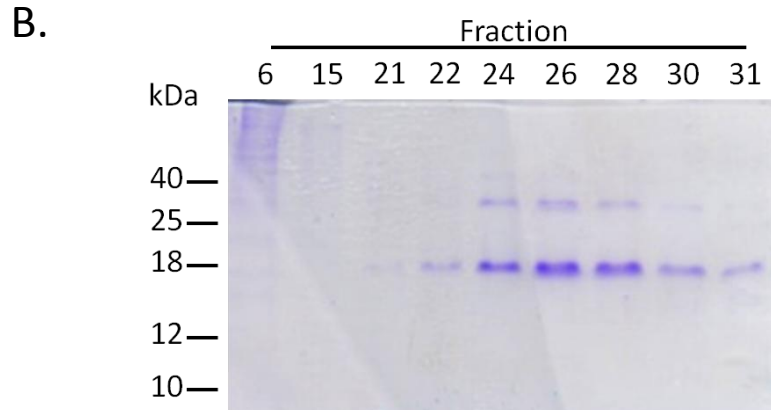
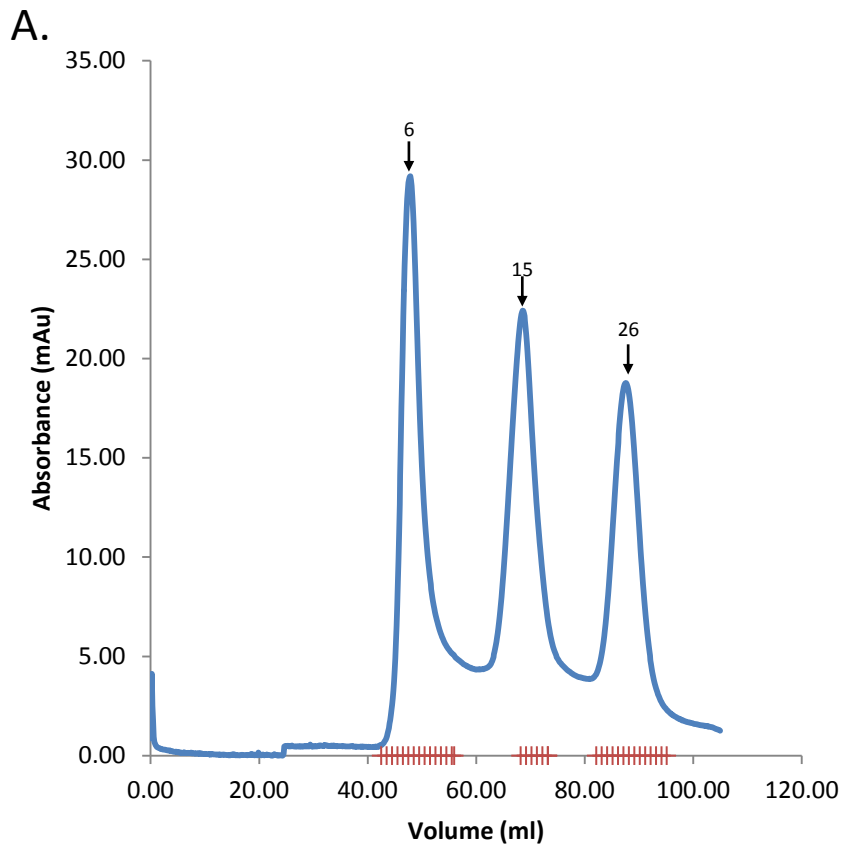


**Figure 3.6 Size exclusion chromatography of nickel affinity purified His<sub>6</sub>-IFN $\epsilon$  and analysis on SDS-PAGE. A)** A chromatogram of nickel-affinity purified IFN $\epsilon$  purified by gel filtration chromatography. His<sub>6</sub>-IFN $\epsilon$  purified from nickel affinity chromatography was separated by size on a Superdex S200 gel filtration column and peak containing fractions collected. Three peaks were observed and correspond to the void volume of the gel filtration column (Peak 1), a high molecular weight contaminant found in insect cell expressions (Peak 2) and a protein of the expected size of His<sub>6</sub>-IFN $\epsilon$  (Peak 3). Arrows indicate peak containing fraction numbers. Blue line, absorbance at 280nm; red lines on x-axis, collected fractions. **B)** Analysis of the collected fractions by SDS-PAGE stained with Coomassie Brilliant Blue revealed that Peak 3 contained a major protein band of the expected size of IFN $\epsilon$  and an unknown higher molecular weight protein.

the highest expression level we had obtained for IFN $\epsilon$ , demonstrating the suitability of the system for the production of IFN $\epsilon$ .

### **3.2.4 Removal of N-terminal His<sub>6</sub> purification tag by Enterokinase**

The recombinant IFN $\epsilon$  protein was produced with an N-terminal His<sub>6</sub> tag for purification by metal affinity chromatography. In order to fully characterise IFN $\epsilon$  and avoid possible aberrant biological activities from the N-terminal purification tag, we attempted to remove the His<sub>6</sub> tag by treatment with enterokinase (EK). Enterokinase is a human digestive enzyme that has found widespread use in protein biochemistry due to its highly specific and unique cleavage site [280]. EK cleaves proteins following the lysine in the sequence Asp-Asp-Asp-Asp-Lys, making it an ideal enzyme for the removal of fusion partners.

In order to investigate the ability of EK to remove the N-terminal His<sub>6</sub> tag from IFN $\epsilon$ , 10 $\mu$ g of nickel affinity chromatography purified His<sub>6</sub>-IFN $\epsilon$  was incubated with varying doses of EK-Max enzyme for either 5 or 24 hours at 22°C. The resulting digestions were then analysed by SDS-PAGE visualised with Coomassie Brilliant Blue (Figure 3.7). Undigested protein was found to migrate as two protein bands at 20kDa and 23kDa. Following incubation of His<sub>6</sub>-IFN $\epsilon$  with 1U of EK-Max for either 5h or 24h, no protein band at the expected size was observed. Instead, degradation products were visible at sizes <10kDa indicating non-specific degradation of recombinant His<sub>6</sub>-IFN $\epsilon$ . This degradation was less following incubation with 0.1U and 0.01U of EK-Max, demonstrating a dose response effect. A band shift of the protein of interest was observed following treatment with 0.01U of EK-Max, indicating cleavage of the N-terminal tag. The band intensity however decreased,

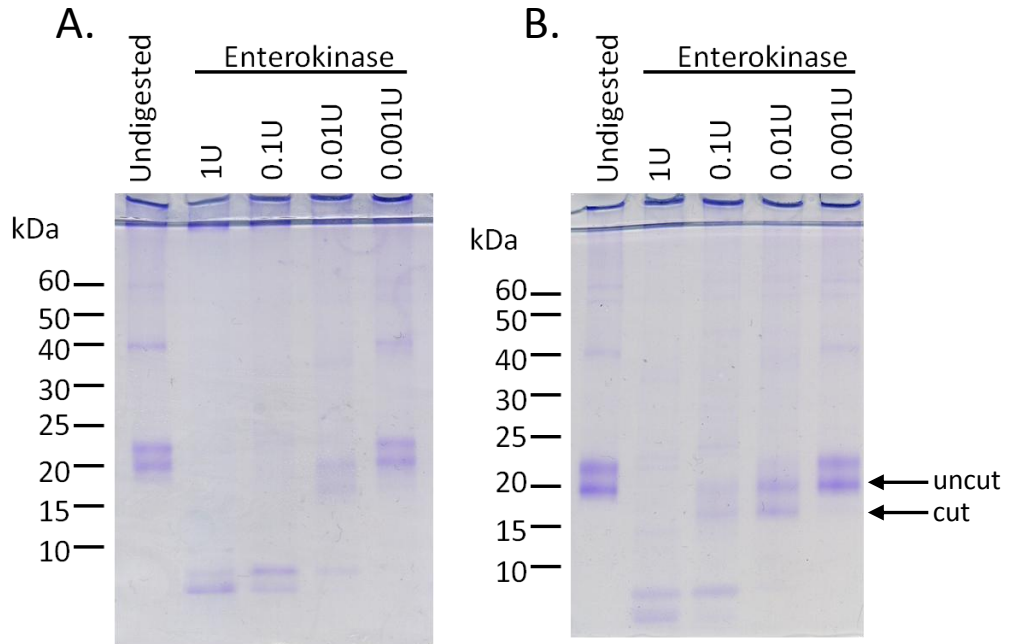


**Figure 3.7 His<sub>6</sub>-IFN $\epsilon$  incubated with EK-Max enterokinase resulted in non-specific digestion and degradation of His<sub>6</sub>-IFN $\epsilon$  protein.** A total of 10ug of recombinant protein purified by nickel affinity chromatography was incubated with varying doses of EK-Max enzyme at room temperature for **A) 5 hours** and **B) 24 hours** and analysed on 15% SDS-PAGE stained with CBB. Compared to untreated protein, enterokinase treated protein was found to be partially digested at low concentrations of EK-Max (0.01U) and completely absent at higher concentrations (0.1-1U). Arrows indicate the sizes corresponding to uncut and cut His<sub>6</sub>-IFN $\epsilon$ .

suggesting a loss of product during the digestion step. Further reduction of the concentration of EK-Max to 0.001U per 10 $\mu$ g of protein resulted in no apparent molecular weight change of the band of interest, suggesting the enzyme concentration was insufficient to catalyse the cleavage reaction. These data demonstrate that the removal of the N-terminal purification tag is only partially effective and can result in non-specific degradation of the protein of interest.

### 3.2.5 Generation of untagged recombinant IFN $\epsilon$ baculovirus

In order to overcome the difficulty of removing a fusion tag from a recombinant protein and the potential for degradation, a different expression strategy was adopted once monoclonal antibodies were available (see Chapter 5) (Figure 3.8). The *Ifne1* gene was cloned into a pFastBac donor vector lacking a purification tag and the secreted protein purified with a monoclonal antibody generated against His<sub>6</sub>-IFN $\epsilon$  (Chapter 5).

The codon optimised *Ifne1* gene was inserted into the pFastBac donor vector pFB-MSP by directional cloning using the restriction enzymes *EcoRI*, *MspI* and *HindIII*. The *EcoRI* site in pFB-MSP forms a compatible overhang with the *MspI* site at the 5' end of the *Ifne1* insert and is destroyed in the subsequent ligation reaction. pFB-MSP was derived from the parental pFastBac vector and was modified to contain the honeybee mellitin signal peptide as a secretion signal instead of the gp67 signal peptide (Figure 3.9A). pFB-MSP was a kind gift from Kathryn Hjerrild (MIMR, Clayton, Australia). Sanger sequencing confirmed the correct insertion and orientation of the *Ifne1* gene and Bacmid containing  $\Delta$ CC *E.coli* cells were transformed with the pFB-MSP-*Ifne1* vector by electroporation. Polymerase chain reaction was used to

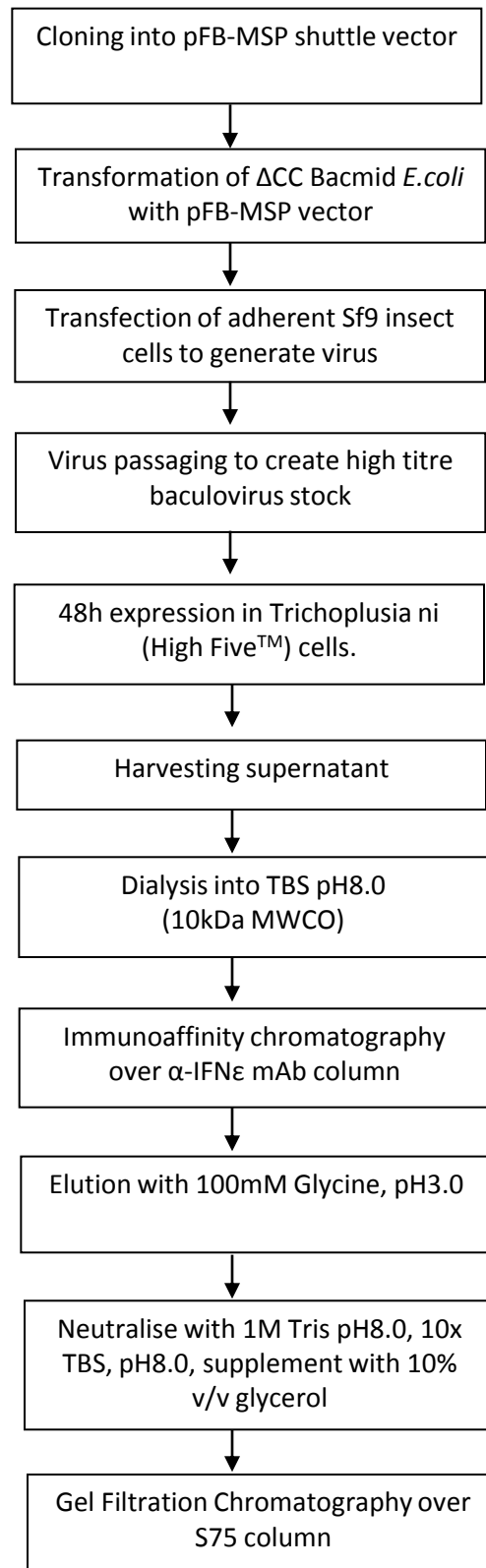


**Figure 3.8 Flow chart of tagless IFNε cloning, expression and purification strategy.** A flowchart outlining the steps undertaken for cloning codon optimised *Ifne1* into the baculovirus expression system and subsequent expression and purification of tagless IFNε recombinant protein.

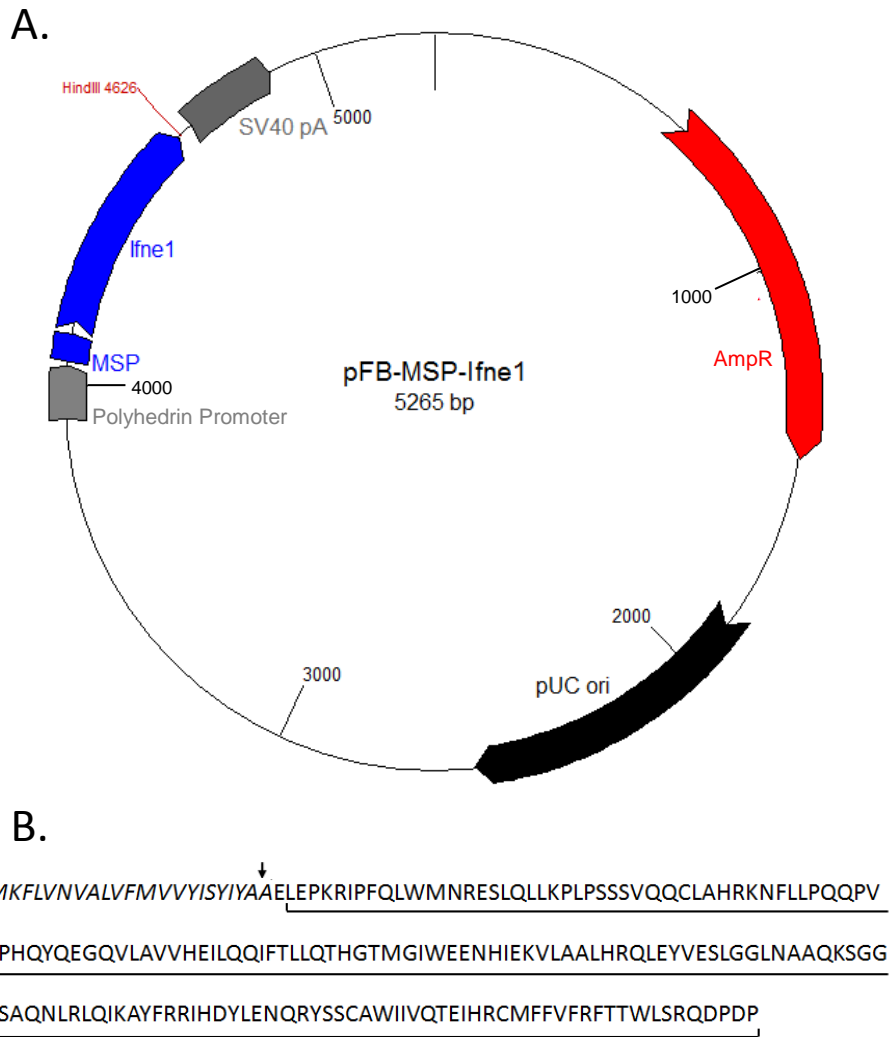


**Figure 3.9 Cloning of gene optimised *Ifne1* into pFB-MSP vector (tagless).** **A)** Vector map of the construct used to generate recombinant bacmid. The gene optimised *Ifne1* sequence was cloned into pFB-MSP with HindIII and MspI restriction enzymes, the latter of which is lost during cloning. *Ifne1* expression is under the control of the polyhedron promoter. The vector map was generated in GENTle **B)** The sequence of the predicted IFNε protein product as expressed by HighFive™ insect cells. Italics denote the honeybee mellitin signal peptide, the underlined sequence is the mature form of mIFNε. Arrow indicates where the signal peptide is cleaved. Vector map was prepared using GENTle Software.

confirm the transposition of the untagged *Ifne1* expression cassette into the parental bacmid. Recombinant untagged *Ifne1* bacmid was amplified in selective LB broth and purified by maxi prep before transfection into adherent Sf9 insect cells. Successful transfection and virus generation was confirmed microscopically by an increase in cell diameter and granular appearance 72 hours post transfection and high titre virus stocks produced as outlined in Chapter 2.3.19. The predicted protein product using this expression strategy is shown in Figure 3.9B.

### 3.2.6 Expression and purification of untagged IFN $\epsilon$ in insect cells

HighFive™ cells were infected with recombinant untagged IFN $\epsilon$  baculovirus and protein expressed for 48 hours as described in Chapter 2.3.20. The conditioned insect cell culture supernatant was harvested and dialysed against TBS pH8.0 prior to being loaded on an IFN $\epsilon$  immunoaffinity column. Proteins were eluted with 100mM Glycine pH3.0 buffer and immediately neutralised in 1M Tris pH8.0. Proteins were visualised by separating the eluted fractions on 15% SDS-PAGE and stained with Coomassie Brilliant Blue (Figure 3.10A). A major protein band of high purity was observed in Eluates 3-5 at approximately 20kDa which corresponds to the theoretical molecular weight of IFN $\epsilon$  expressed from this construct (calculated at 20.6kDa [279]). The presence of IFN $\epsilon$  in the elution fractions was confirmed by separating proteins on 15% SDS-PAGE and visualising by western blot specific for IFN $\epsilon$  (Figure 3.10B). IFN $\epsilon$  containing fractions were supplemented with 10% v/v glycerol due to its positive effects on protein stability [281] and proteins immediately stored at 4°C to reduce the chance of degradation.

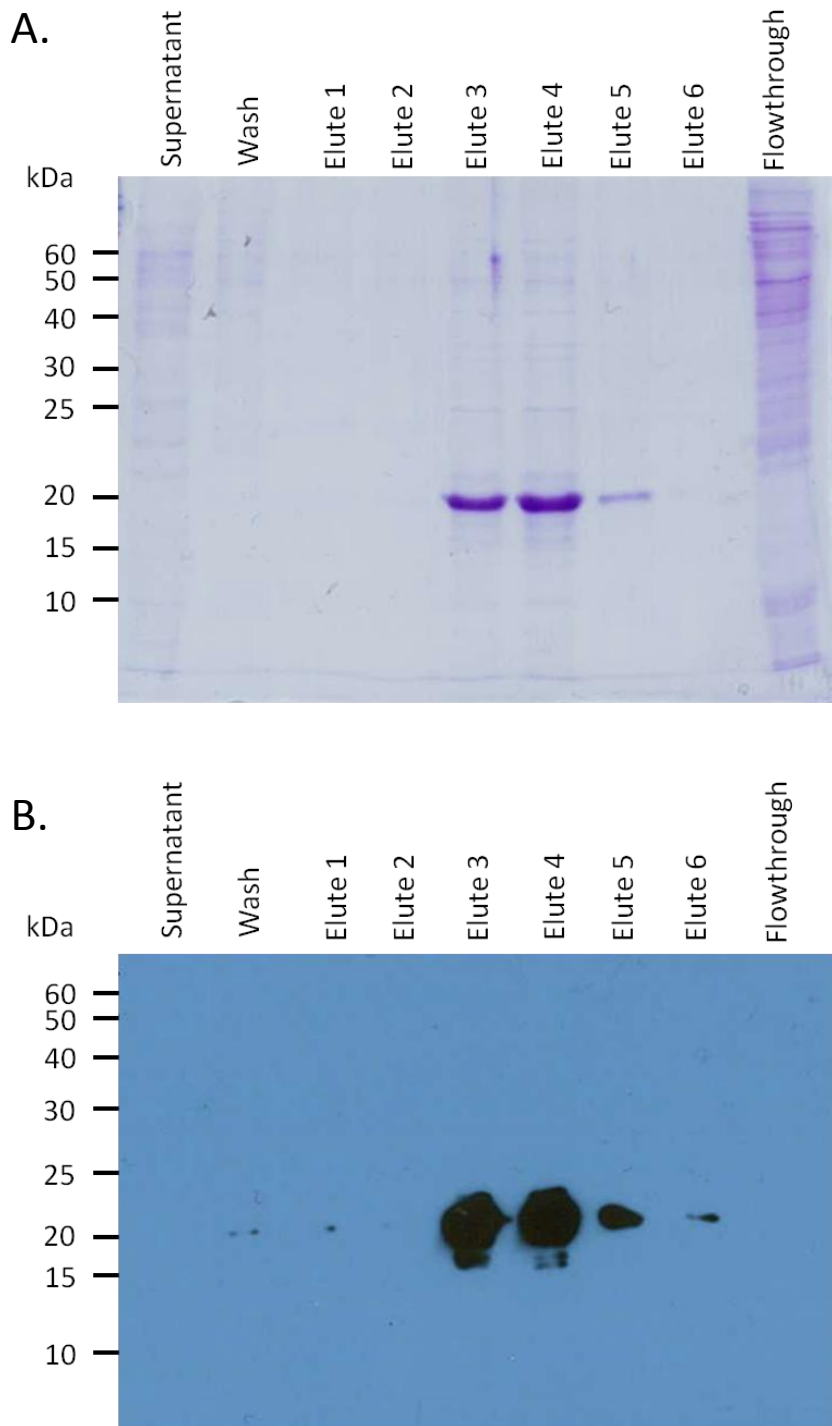


**Figure 3.10 Purification of tagless IFNε expressed from High Five insect cells.** Visualisation of IFNε purified using H3 anti-IFNε immunoaffinity chromatography by 15% SDS-PAGE **A)** stained with Coomassie brilliant blue and **B)** western blotting for mIFNε using H3 anti-IFNε mAb. Clarified insect cell expression supernatant was passed over the IFNε immunoaffinity column at room temperature by gravity flow and protein eluted with 100mM Glycine pH3.0. A major protein band at the expected size of IFNε (~20kDa) was observed in Eluates 3, 4 and 5 by both Coomassie staining and western blotting.

Recombinant untagged IFN $\epsilon$  was further purified by size exclusion chromatography on a Superdex S75 column using TBS pH8.0 containing 10% v/v glycerol (Figure 3.11). Four peaks were observed, where fractions 8, 11 and 16 comprised the peak containing fractions. Samples from the fourth peak were not collected. Due to the size of IFN $\epsilon$ , the third peak was postulated to contain IFN $\epsilon$  protein. Analysis of the collected fractions by SDS-PAGE stained with Coomassie Brilliant Blue revealed the presence of a major protein band at 20kDa in the third peak at Fraction 16 (Figure 3.11B). Fraction 8 was found to contain a faint band >60kDa and this corresponds to the void volume of the Superdex S75 resin. Fraction 11 contained a protein of ~35kDa. Subsequent visualisation of 2 $\mu$ g of protein by SDS-PAGE Coomassie pooled from Peak 3 revealed the presence of a single protein moiety migrating at 20kDa (Figure 3.11C). Furthermore, analysis of 0.1 $\mu$ g of this product by western blot using H3 anti-IFN $\epsilon$  monoclonal antibody indicated the presence of IFN $\epsilon$  at the expected size of 20kDa and corresponds to the same size as the protein seen on SDS-PAGE coomassie (Figure 3.11D). Unlike expression of His<sub>6</sub>-IFN $\epsilon$  (see Chapter 3.2.3), expression of tagless IFN $\epsilon$  did not appear to lead to the formation of dimers.

To ensure recombinant tagless IFN $\epsilon$  was expressed as anticipated (Figure 3.9B), the protein was separated on SDS-PAGE and transferred to PVDF membrane prior to N-terminal amino acid sequencing (see Chapter 2.3.16). The first six residues sequenced were AELEPK, which are the predicted start residues of the cloned IFN $\epsilon$  product (see Appendix E for full sequencing report).

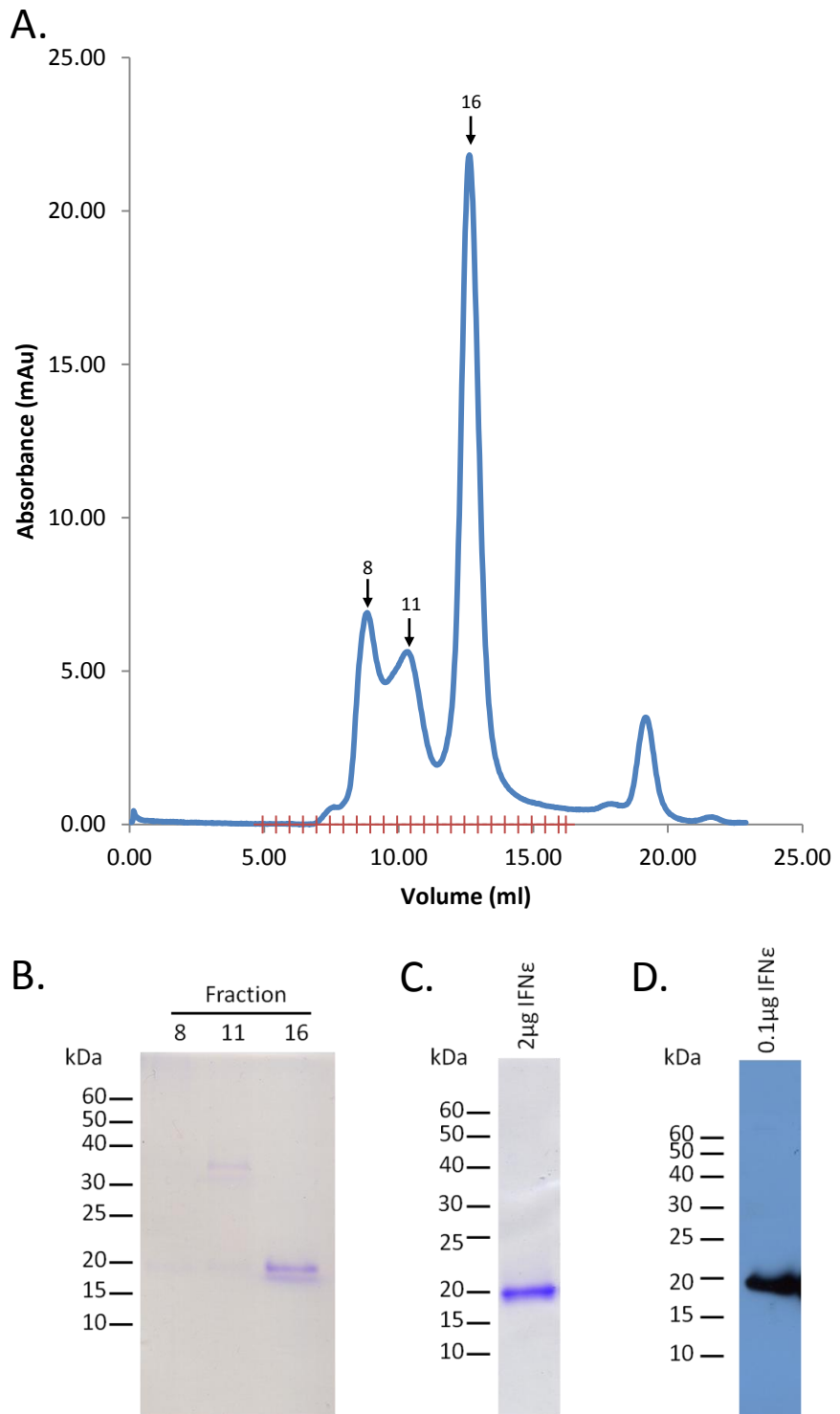


**Figure 3.11 Size exclusion chromatography of tagless IFN $\epsilon$ .** Recombinant IFN $\epsilon$  purified by immunoaffinity chromatography was resolved on a S75 Superdex column by size exclusion. **A)** Chromatograph of the IFN $\epsilon$  purification. Arrows indicate fractions analysed by SDS-PAGE. **B)** Analysis of collected fractions by SDS-PAGE stained with Coomassie Brilliant Blue. Fraction 16 contained a band of the expected size of IFN $\epsilon$  at  $\sim$ 20kDa. **C)** All fractions under the third peak were pooled and 2 $\mu$ g of protein visualised by SDS-PAGE stained with CBB revealed a homogenously pure product. **D)** Analysis of 0.1 $\mu$ g of the purified 20kDa product by western blot using H3 anti-IFN $\epsilon$  mAb.

### 3.2.8 Generation of recombinant His<sub>6</sub>-IFNβ baculovirus construct

To assist in the characterisation process of IFNε, it was important to validate the expression system using an early characterised type I IFN. We therefore expressed and purified recombinant mouse IFNβ from HighFive™ insect cells. The cloning and expression strategy of His<sub>6</sub>-IFNβ is summarised in Figure 3.12 and described in detail in Chapter 2. Due to the unavailability of sufficient amounts of IFNβ monoclonal antibodies to enable immunoaffinity chromatographic purification, the pFastBac donor construct carrying the murine *ifnb1* gene was generated by cloning the gene sequence coding for the mature IFNβ polypeptide downstream of a hexahistidine tag and enterokinase cleavage site of the modified pFB-SHEK vector as described in Chapter 2.1.8. Briefly, the *ifnb1* gene was amplified by PCR from mouse genomic DNA and inserted directly into pFB-SHEK by blunt-end ligation. The ligation mix was transformed into competent cells and resulting colonies screened for the correct insertion of *ifnb1* by PCR. PCR positive clones were sequenced by conventional Sanger sequencing to determine correct insertion and in-frame orientation. The resulting pFB-SHEK-*ifnb1* vector (Figure 3.13A) was transformed into competent ΔCC bacmid carrying *E. coli* by electroporation to generate the recombinant *ifnb1* bacmid. The presence of gene insert in the bacmid was confirmed by PCR. The recombinant *ifnb1* bacmid was then amplified by growth in LB broth containing selective antibiotics and bacmid DNA isolated by maxi-prep. Isolated bacmid DNA was transfected into adherent Sf9 insect cells to generate recombinant baculovirus and infectivity visually observed after 72 hours. High titre baculovirus stock was generated by amplifying virus in suspension grown Sf9 cells as described in Chapter 2.3.19.

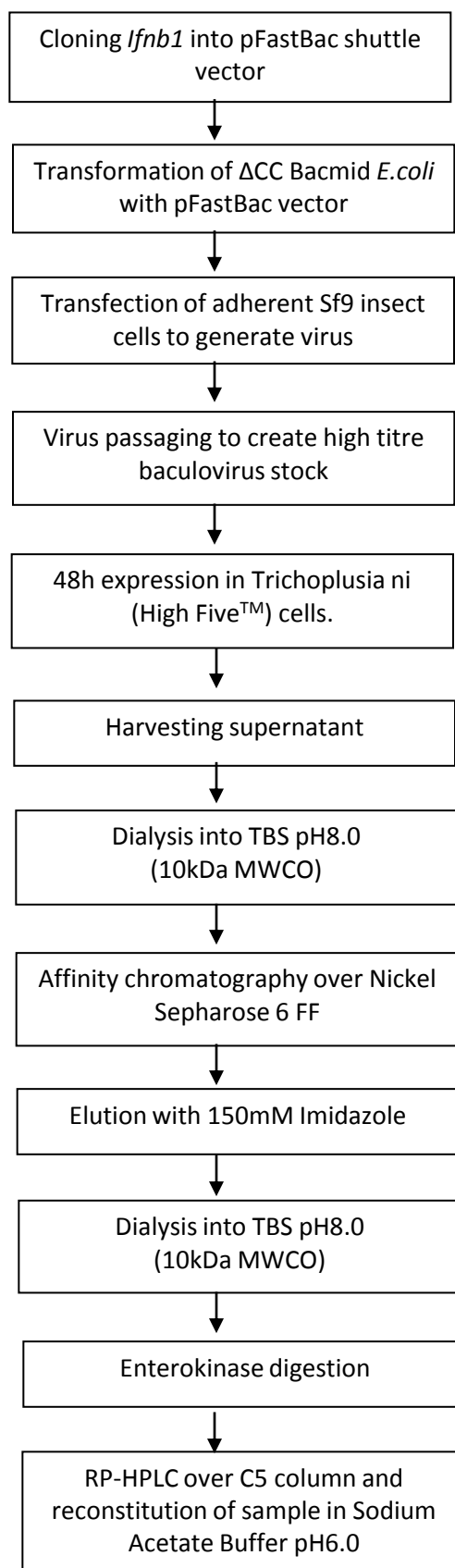
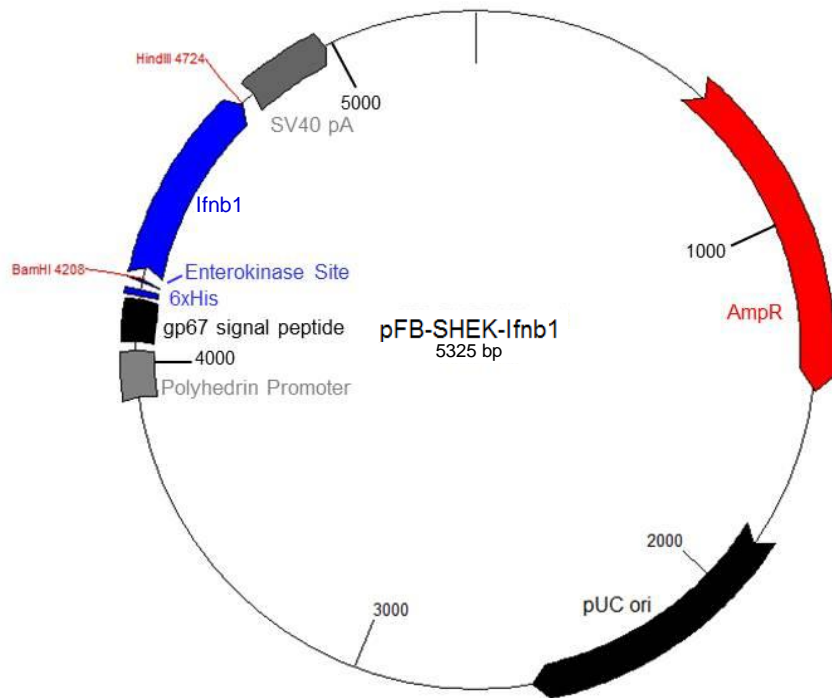


**Figure 3.12 Flow chart of His<sub>6</sub>-IFNβ cloning, expression and purification strategy.** A flowchart outlining the steps undertaken for cloning *Ifnb1* into the baculovirus expression system and subsequent expression and purification of His<sub>6</sub>-IFNβ recombinant protein.

A.



B.

```

MLLVNQSHQGFGNKEHTSKMVSAIVLYVLLAAAAHSFAAHHHHHHGSGSDDDDKGSYKQLQLQER
                                     ↓
TNIRKQELLEQLNGKINLTyrADFKIPMEMTEKMQKSYTAFAIQEMLQNVFLVFRNNFSSTGWNETI
VVRLLDELHQQTVFLKTVLEEKQEERLTWEMSSTALHLKSYWVRVQRYLKLKMKYNSYAWMMVRAEI
FRNFLIIRRLTRNFQN
    
```

**Figure 3.13 Cloning of *mIfnb1* into the baculoviral expression vector. A)** Recombinant pFB-SHEK-Ifnb1 vector map. The polyhedron promoter drives the expression of the *Ifnb1* gene. The vector map was generated in GENTle. **B)** The amino acid sequence of the predicted IFN $\beta$  product as secreted by the High Five insect cells. Italics denote the gp67 signal peptide, the bold font shows the enterokinase site, the underlined sequence is the mature form of mIFN $\beta$ . Arrow, indicates where the signal peptide is cleaved; arrow head, Enterokinase cleaves after the lysine. Vector map was prepared using GENTle Software.

### 3.2.9 Expression and purification of His<sub>6</sub>-IFN $\beta$ in insect cells

HighFive<sup>TM</sup> cells were infected in culture with recombinant IFN $\beta$  baculovirus and expression carried out for 48 hours as described in Chapter 2.3.20. Figure 3.13B describes the predicted His<sub>6</sub>-IFN $\beta$  protein product as expressed by HighFive<sup>TM</sup> cells. The resulting recombinant His<sub>6</sub>-IFN $\beta$  protein contains an N-terminal His<sub>6</sub> tag for purification, followed by an enterokinase cleavage site which allows for the removal of the purification tag with enterokinase enzyme.

Following expression, conditioned insect cell culture supernatant was dialysed into TBS pH8.0 and passed over a nickel affinity column. Bound proteins were recovered by elution with 150mM imidazole and the resulting fractions analysed by SDS-PAGE visualised with Coomassie Brilliant Blue (Figure 3.14A). A major protein band was visible at ~24kDa in the elution fractions and corresponds to the expressed His<sub>6</sub>-IFN $\beta$  protein. The theoretical molecular weight of His<sub>6</sub>-IFN $\beta$  is 21.6kDa however murine IFN $\beta$  is known to be expressed as a glycoprotein [282], which may account for the difference in size between the predicted and the observed molecular weights (also see Chapter 4).

The His<sub>6</sub> purification tag was removed by incubation of His<sub>6</sub>-IFN $\beta$  recombinant protein with enterokinase as described in Chapter 2.4.11. Briefly, 1U of enterokinase was sufficient to digest 20 $\mu$ g of protein for 16hours at 4°C. These conditions were determined to be the optimal parameters from a series of optimization experiments carried out previously. The enterokinase activity was neutralised by incubation with 100mM Imidazole and the sample acidified to pH2.0 with concentrated trifluoroacetic acid (TFA) prior to injection onto a C5 RP-HPLC column. Proteins were resolved with an acetonitrile gradient from 0 to 90% in the presence of 0.1% TFA as described in Chapter 2.3.10. Organic solvent was removed by evaporation on a speedy-vac overnight and

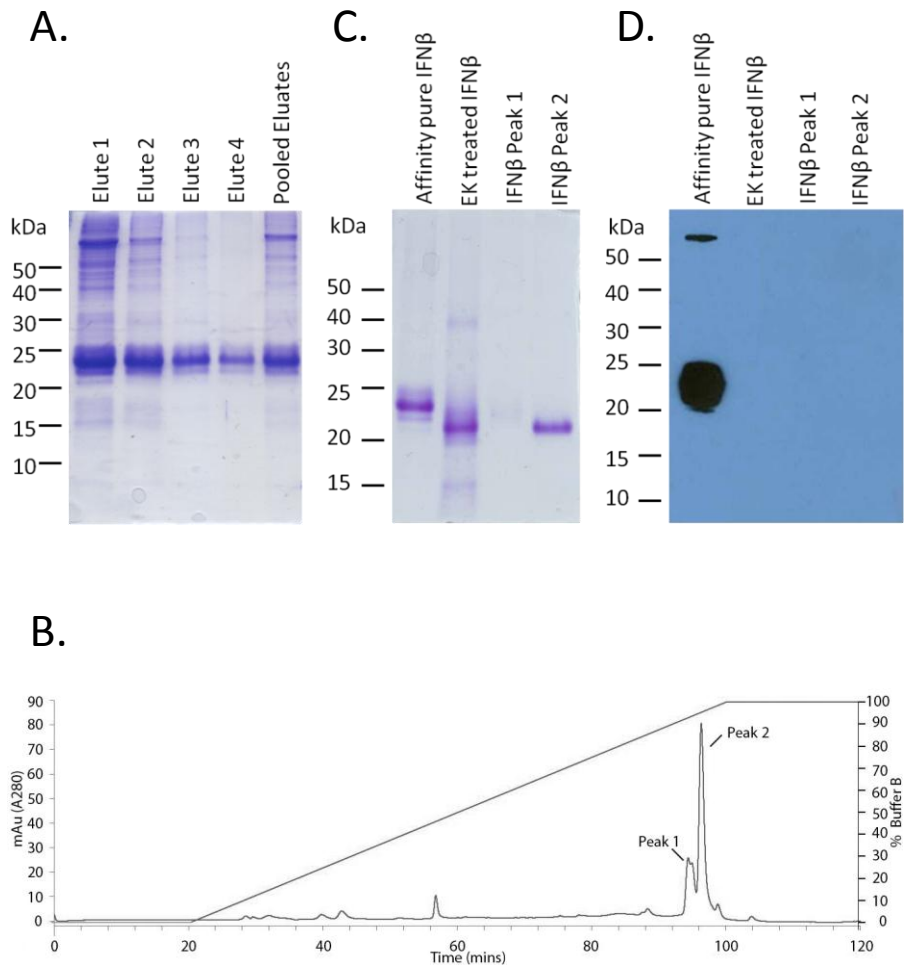


**Figure 3.14 The purification of recombinant IFN $\beta$  produced in insect cells by a two step method** **A)** SDS-PAGE stained with Coomassie Brilliant blue (CBB) of nickel affinity chromatography of His $_6$ -IFN $\beta$  purified from insect cell supernatant. **B)** RP-HPLC chromatogram of IFN $\beta$  purification. Nickel affinity purified and EK-Max treated IFN $\beta$  was injected onto a Phenomenex C5 RP-HPLC column and the protein resolved using a linear gradient of Acetonitrile, 0.1% TFA. **C)** SDS-PAGE stained with CBB of EK-Max digestion of His $_6$ -IFN $\beta$  and RP-HPLC purified IFN $\beta$  **D)** Western blot against His $_6$  of EK-Max digested His $_6$ -IFN $\beta$  and RP-HPLC purified IFN $\beta$ .

the sample resuspended in Hepes buffer (Appendix A). The chromatogram of IFN $\beta$  purified by RP-HPLC demonstrated two distinct peaks which resolved at 90% and 93% Buffer B, respectively (Figure 3.14B).

The enterokinase digested and subsequent RP-HPLC purified samples were analysed on 15% SDS-PAGE visualised with Coomassie Brilliant Blue (Figure 3.14C). Enterokinase digested His<sub>6</sub>-IFN $\beta$  underwent a clear shift in molecular weight from ~24kDa to ~21.5kDa and corresponds to the loss of the His<sub>6</sub> purification tag and enterokinase cleavage site. Visualising the two peaks collected from the RP-HPLC on 15% SDS-PAGE stained with Coomassie Brilliant Blue demonstrated a protein migrating at ~23kDa collected from the first peak and a major protein moiety at ~21.5kDa from the second peak. No other protein bands were observed in the peak containing fractions, indicating very high purity of protein.

To confirm the removal of the N-terminal His<sub>6</sub> purification tag, affinity purified His<sub>6</sub>-IFN $\beta$ , enterokinase digested His<sub>6</sub>-IFN $\beta$  and samples from each RP-HPLC peak were analysed by western blotting using a His<sub>6</sub> specific antibody (Figure 3.14C). The lane containing affinity purified His<sub>6</sub>-IFN $\beta$  demonstrated a His<sub>6</sub> positive band at ~24kDa, corresponding to His<sub>6</sub> tagged IFN $\beta$  as expressed by insect cells. Enterokinase treated IFN $\beta$  and RP-HPLC purified IFN $\beta$  were not positive for His<sub>6</sub> by western blot, suggesting that the N-terminal His<sub>6</sub> purification tag was successfully removed by the enterokinase treatment.

To confirm the suitability of the insect cell expression system in producing biologically active interferon, fully purified IFN $\beta$  activity was measured in an antiviral assay and found to be practically identical to the published activity of  $2 \times 10^8$  international units (IU)/mg (Table 3.1).

**Table 3.1.** Results of IFN $\beta$  expressed and purified from insect cell expression system

Purification Step	Total Protein (mg)	Volume (ml)	Activity (IU/ml)	Specific Activity (IU/mg)	Total Activity (IU)	Fold Enrichment	Yield (%)
Supernatant	40	200	7.9x10 <sup>5</sup>	3.95x10 <sup>6</sup>	1.58x10 <sup>8</sup>	1.00	100
Dialysed Supernatant	34.65	210	6.3x10 <sup>5</sup>	3.82x10 <sup>6</sup>	1.32x10 <sup>8</sup>	0.97	84
Ni Sepharose FF	0.31	4	2.57x10 <sup>7</sup>	3.32x10 <sup>8</sup>	1.03x10 <sup>8</sup>	83.95	65
RP-HPLC His <sub>6</sub> -IFN $\beta$	0.31	0.5	1.31x10 <sup>8</sup>	2.11x10 <sup>8</sup>	6.55x10 <sup>7</sup>	53.49	41
RP-HPLC, EK treated IFN $\beta$ <sup>a</sup>	0.28	0.8	7.25x10 <sup>7</sup>	2.07x10 <sup>8</sup>	5.80x10 <sup>7</sup>	52.44	37

<sup>a</sup> RP-HPLC, EK treated IFN $\beta$  was an independent experiment and is not consecutive to prior purifications listed.

### **3.2.10 Endotoxin testing of IFN $\epsilon$ and IFN $\beta$**

Endotoxin is a bacterial membrane product known to activate NF $\kappa$ B and induce type I IFN production [283]. To minimise any potential of such stimulus, samples were tested for their endotoxin concentration as described in Chapter 2.4.18. IFN $\epsilon$  and IFN $\beta$  were both found to contain endotoxin concentrations below the sensitivity range of the assay at less than 0.1 Endotoxin Units (EU)/ $\mu$ g.

### 3.3. Discussion

The interferons were among the first proteins to be expressed from recombinant hosts and due to their therapeutic applications have been produced in virtually every expression system. The choice of expression system is important for a multitude of reasons and needs to be carefully selected based on the type of investigation being performed. For example crystallographic studies require large amounts of pure protein, preferably lacking glycosylation and thus bacterial expression hosts are favoured. In addition, for these studies, endotoxin concentration is not a major concern. In contrast, proteins expressed for clinical purposes need to be highly pure, have a long shelf life and need to adhere to strict guidelines regarding purity and pyrogenicity. Although bacterial expression hosts are used for many pharmaceutical products, mammalian expression hosts such as chinese hamster ovary (CHO) cells and Human embryonic kidney (HEK) cells are beginning to gain favour as they produce products containing post-translational modifications such as glycosylation, which can affect their stability, pharmacokinetics and pharmacodynamics [259, 284, 285].

Unfortunately there are no predictive programs available to determine how well a protein would express in any given host organism and thus the expression of each protein needs to be determined empirically. Although there exists vast information on the expression of interferons, the novel type I interferon, IFN $\epsilon$  has only been documented to be expressed in a bacterial host [248]. Furthermore the IFN $\epsilon$  produced by Peng *et al.* was the human homologue, which only bears 50% sequence homology with murine IFN $\epsilon$  and is likely to have different expression and purification characteristics. This chapter outlines how recombinant murine IFN $\epsilon$  expression was trialled in a number of expression hosts with varying degrees of success and finally

expressed and purified to homogeneity using a baculovirus insect cell expression system.

Initially bacterial expression was trialled. The SUMO fusion tag was selected as it had been used successfully for the production of cytokines and the specificity of SUMO fusion tag cleavage was an attractive option to produce native protein [270, 286]. I attempted expression in a number of bacterial host strains suitable for mammalian gene expression and optimised conditions in regards to time, temperature and inducing IPTG concentration. Although successful, possible breakdown products were observed in all investigated conditions and the expression vector was given to the Monash University Protein Production Unit (PPU) for a more comprehensive expression trial. Following expression in 7 host cells suitable for difficult to express proteins, only a small amount of recombinant IFN $\epsilon$  was produced. Furthermore, the PPU also observed multiple protein moieties, indicating that either the fusion protein was unstable or perhaps an endogenous bacterial protease was causing protein degradation. Prematurely halted protein translation is often seen when expressing mammalian genes in bacteria due to the presence of rare codons in the gene. Bacteria often lack the genes required to express certain tRNAs that are more common in eukaryotic cells and thus translation often stops when a rare codon is reached. Although possible, it is unlikely that this occurred here, as the vector was trialled in a number of bacterial cell lines complemented with the genes necessary to produce rare tRNAs. It is plausible that an endogenous bacterial enzyme recognised a motif in the expressed protein to cleave it. However this would not explain the presence of both full length fusion protein and degraded protein. If indeed an endogenous enzyme was present, one would expect only the shorter protein product. Regardless of the degradation products observed, the final yield of SUMO-IFN $\epsilon$  was

exceptionally low. It is difficult to determine the exact reasons behind this and in the interests of continuing on, mammalian expression was investigated next.

We investigated two different mammalian expression vectors as both had demonstrated success in the expression of interferons [259, 271]. Furthermore an advantage to using mammalian expression systems is that expression can be trialled quickly by transient transfection before generating stable cell lines. Expression trials were performed by CSIRO as they had the necessary transfection reagents and equipment for suspension grown mammalian cells.

Western blotting of expression culture supernatant indicated that only the pTT22 vector had been successful in producing IFN $\epsilon$  although the yield was very low. In mammalian cells, low expression yield can be difficult to explain. While we did not investigate the *Iine1* mRNA levels following transfection, the promoters in our vectors have resulted in high level production of other proteins in the past [259, 271]. Importantly, while gene transcription may have been high, translation could still have been affected. For example even though *Iine1* was cloned into the expression vectors with its own Kozak consensus sequence, this might not be an ideal sequence for optimum translation. Furthermore, the transcribed *Iine1* mRNA may not be stable and degrade prematurely. Indeed, one published report highlights how TNF $\alpha$  stabilises *Iine1* mRNA and it is plausible that mRNA degradation might explain the low expression yields observed [287].

Interestingly, IFN $\epsilon$  was not seen in the non-reduced sample from the pTT22 expression and only in the reduced sample. This is most commonly observed when a protein forms aggregates that would normally not enter the gel but

instead remain in the stacking gel. Reducing the sample breaks the aggregates and allows the protein to fully enter the gel. Aggregates can arise due to a number of reasons such as exposed hydrophobic pockets, aberrant glycosylation [288] and are also often observed at higher protein concentrations. In this instance it is possible that certain regions of the mature IFN $\epsilon$  protein bear a strong charge that facilitate the formation of aggregates even at low protein concentrations. This would mean that regardless of yield, the isolation of pure protein would remain a challenge and thus a different expression system was investigated.

The baculovirus/insect cell expression system was trialled for two reasons. One, it has been published that interferons had been successfully produced from insect cells [272, 273, 289]. Additionally in our laboratory we routinely produce both subunits of the interferon receptor from insect cells and subsequently have also been able to produce significant quantities of IFN $\alpha$ 1 using the same expression protocol (unpublished data). Prior to cloning *Ifne1* into the pFB-SHEK shuttle vector, I codon optimised the sequence for expression in insect cells. Although I did not compare optimised to unoptimised DNA sequences in terms of final protein yield, published data indicates that codon optimisation is of benefit [275]. The pFB-SHEK vector itself was chosen because, as previously mentioned, we've had good results expressing the interferon receptors and IFN $\alpha$ 1 and also because the introduced enterokinase cleavage site would allow us to remove the N-terminal purification tag with only two extra amino acid residues remaining. This would allow characterisation of recombinant mouse IFN $\epsilon$  as a near native protein, important when considering this is the first report of its characterisation.

Our results clearly demonstrate that we were able to express recombinant murine IFN $\epsilon$  using insect cells and purify it by immobilising metal affinity chromatography. We were further able to purify the protein by size exclusion chromatography although the IFN $\epsilon$  fractions did contain a second band of approximately twice the molecular weight of IFN $\epsilon$ . The samples were denatured at 95°C prior to visualisation on SDS-PAGE and should therefore not be protein dimers however in the past we've seen a similar phenomenon with RP-HPLC pure recombinant IFN $\alpha$ 1 produced from *P. pastoris* (unpublished data). Furthermore, human IFN $\beta$  has been demonstrated to form inactive oligomers at certain ionic strengths [290], which could potentially explain the multimerisation observed here. Although unlikely, the N-terminal hexahistidine purification tag could also affect protein chemistry and facilitate enhanced multimerisation. Indeed, this has been documented to occur for other recombinant proteins and may provide a possible explanation for the results seen [291].

In order to fully characterise IFN $\epsilon$  as a native protein, it was important to remove the N-terminal purification tag which was made up of 16 amino acid residues. Following EK treatment IFN $\epsilon$  appeared to degrade nonspecifically, particularly at high concentrations of enterokinase. The IFN $\epsilon$  protein sequence does not contain other canonical enterokinase cleavage sites and therefore it is difficult to determine where or how the protein is degraded. The observed protein degradation appeared to be enzyme concentration dependent, suggesting that it was an enzyme specific effect and not caused by another variable such as temperature or time. Although 0.01 Units of enzyme for every 10 $\mu$ g of protein appeared to be successful in removing the purification tag, there was an associated reduction in band intensity, suggesting a significant loss of product associated with the enzymatic reaction. Further lowering the

concentration of enterokinase did not result in a molecular weight shift, implying that the concentration was too low to catalyse the reaction. To summarise the expression of His<sub>6</sub>-IFN $\epsilon$ , even though purification tags are commonly used for recombinant protein expression, their removal is often associated with loss of function or protein degradation [292, 293]. Importantly, enterokinase has been found to not exhibit high stringency towards its cleavage site and is able to recognise other cryptic sites [280, 293]. Such factors can often not be accounted for before empirically testing them. Thus, while a baculovirus expression system appeared to produce sufficient quantities of IFN $\epsilon$ , a different purification strategy needed to be devised to produce tagless recombinant protein.

Importantly, alongside cloning and expressing IFN $\epsilon$  using this strategy, we were also expressing IFN $\beta$ . The idea behind expressing both proteins was that we could directly compare the biological activities of the two type I IFN family members expressed under the same conditions. Unlike IFN $\epsilon$  however, using the His<sub>6</sub>-tag expression method and enterokinase treatment worked for IFN $\beta$ . As such, His<sub>6</sub>-IFN $\beta$  was successfully expressed and partially purified by nickel affinity chromatography. Enterokinase was used at a concentration of 1 unit per 20  $\mu$ g of protein to successfully remove the N-terminal purification tag. This result further illustrates that the degree of success seen with fusion tag removal is highly protein dependent and can provide different results with proteins of the same family such as type I IFNs. To purify IFN $\beta$  to homogeneity, RP-HPLC was utilised. RP-HPLC is a common method used for the purification of proteins, and was in part developed for the purification of interferons [170, 253, 294]. Importantly, the biological activity of IFN $\beta$  expressed in the insect cell expression system was the same as reported in the literature, demonstrating that the expression system was suitable for the

production of biologically active type I interferon. Given these findings, we now had to identify an expression and purification protocol that would avoid the use of enzymes to generate tagless IFN $\epsilon$ .

Producing tagless, or 'native' recombinant protein is ideal in that it allows for characterisation of a form as it would be produced from host cells. The major bottleneck for this becoming common practice is that downstream protein purification needs to be specifically tailored to the protein's biochemical or immunological properties - To this end, His<sub>6</sub>-IFN $\epsilon$  protein was used to inject mice to raise monoclonal antibodies against IFN $\epsilon$  (as outlined in Chapter 5). The codon optimised *Ifne1* gene was then inserted into a pFastBac shuttle vector designed to produce a near tagless protein, with only two extra amino acid residues at the N-terminus. Analysis of the expression and purification of tagless IFN $\epsilon$  by SDS-PAGE stained with Coomassie demonstrated high purity and yield of IFN $\epsilon$  purified using this strategy. In many instances, purity was estimated to exceed 90% in a single purification step (See Figure 3.10a). To ensure absolute purity of product, tagless IFN $\epsilon$  was further purified by size exclusion chromatography to yield homogenous protein. The resulting protein was determined to be chromatographically pure and below 0.1EU/ $\mu$ g of endotoxin and suitable for characterisation studies including biological activities.

In order to ensure that the secreted protein product was as expected and did not suffer from N-terminal amino acid changes, the purified recombinant protein was sequenced. The N-terminal amino acid residues corresponded to the predicted protein product. Although the IFN $\epsilon$  produced in this baculovirus expression system did carry two additional amino acids at the N-terminus, we believed that this would not affect biological activity as N-terminal

modifications such as hexahistidine tags on other type I IFNs did not affect specific activity [266].

### **3.4 Conclusion**

This chapter outlined the expression and purification of murine IFN $\epsilon$  for the first time. We initially trialled the more commonly used expression systems with little success. Baculovirus expression proved successful however my efforts to remove the purification tag resulted in unanticipated protein breakdown, requiring me to develop a different purification strategy. To this end, monoclonal antibodies were raised against His<sub>6</sub>-IFN $\epsilon$  and used to purify an untagged form of IFN $\epsilon$  expressed in insect cells for comparative purposes. This expression and purification method proved highly efficient in isolating highly pure recombinant murine IFN $\epsilon$ . To aid in the characterisation of IFN $\epsilon$ , IFN $\beta$  was expressed and purified to homogeneity from insect cells. Both proteins were shown to have endotoxin concentrations lower than 0.1EU/ $\mu$ g, which is equal to or lower than commercial cytokine preparations. Taken together, with the production and purification of recombinant IFN $\epsilon$  and IFN $\beta$ , the characterisation of this novel IFN was now possible. In Chapter 4, I investigate the biochemical and biological properties of mouse IFN $\epsilon$  for the first time.

## **Chapter 4 – Characterisation of recombinant IFNε**

### **4.1 Introduction**

Type I interferons are a large family of alpha-helical cytokines composed of approximately 20 individual proteins, forming many subtypes ( $\alpha$ ,  $\beta$ ,  $\epsilon$ ,  $\kappa$ ,  $\omega$ ,  $\tau$ ,  $\zeta$ ,  $\delta$ ). All type I interferons characterised to date signal via the canonical type I interferon receptor, composed of the subunits IFNAR1 and IFNAR2 [5]. Since their discovery over 50 years ago, the type I interferon signalling mechanisms have been well characterised. As outlined in Chapter 1, the JAK-STAT pathway is activated upon interferon-receptor engagement, resulting in homo and hetero-dimerisation of STAT molecules and translocation to the nucleus. There, STATs in the form of dimers or as the type I interferon specific transcription factor ISGF-3 bind to the promoter of interferon regulated genes (IRGs) to regulate their transcription. Ultimately, IRGs are responsible for the plethora of biological activities of type I IFNs, which include antiviral, antiproliferative and immunoregulatory actions.

IFNε was postulated to be a novel type I interferon based on its chromosomal location and sequence similarity to the other IFN family members. Studies since then have established its role in reproductive tract homeostasis and its function as a mucosal cytokine able to elicit adjuvant properties [114, 251]. Thus far, the study of IFNε has been sparse due to a lack of available reagents. Studies have either made use of unpurified IFNε expressed from adenoviral vectors or poorly documented recombinant protein [248, 250]. As described in Chapter 3, I have successfully expressed and purified recombinant mouse IFNε to homogeneity for the first time using an insect cell

expression system. Endotoxin levels were undetectable (less than 0.1EU/ $\mu$ g). As most commercial companies only guarantee endotoxin at less than 1EU/ $\mu$ g, we felt that not even detecting any endotoxin in our assay with a lower sensitivity of 0.1EU/ $\mu$ g of protein was suitable for our characterisation studies. Furthermore, endotoxin concentrations of 0.1EU to 1EU have been found to elicit very weak immune activation in human peripheral blood mononuclear cells and murine macrophages as measured by proinflammatory cytokine release [86, 295]. To compare the functions and signalling mechanisms of novel IFN $\epsilon$ , I also expressed and purified murine IFN $\beta$  from insect cells which will be used alongside in functional assays as a direct comparison. This will give me an opportunity to characterise the biological activities of this novel murine cytokine for the first time.

Biological activities of IFN $\epsilon$  to be investigated include antiviral, antiproliferative and immunoregulatory functions which are signature characteristics of type I IFNs (refer to Chapter 1). Furthermore, I will investigate the signalling pathways activated by IFN $\epsilon$ , in particular the use of the canonical type I interferon receptor and the downstream signalling mechanisms of STAT activation ultimately resulting in IRG transcription.

These findings will provide the necessary groundwork to not only define the novel IFN $\epsilon$  as a type I IFN but to establish its *in vitro* biological activities and signalling mechanisms. This information, together with existing knowledge about the unique tissue expression of IFN $\epsilon$  will allow us to more closely examine the cellular targets of IFN $\epsilon$  signalling.

## 4.2 Results

### 4.2.1 Secondary structure determination of IFN $\epsilon$ expressed from an insect cell expression system

Although we expect correct folding of mammalian proteins expressed in eukaryotic cells, we wanted to obtain evidence that the interferons expressed from the baculoviral expression system were folded correctly. Gross structural differences such as changed secondary structure would indicate that the expression system would be unsuitable for the expression of a properly folded recombinant form of IFN $\epsilon$ . Although IFNs have been expressed from insect cells in the past [272-274], it was necessary to ensure thorough characterisation steps of this novel cytokine were performed. To examine the secondary structure, circular dichroism (CD) was utilised. CD is a process by which secondary structure can be investigated by measuring the absorbance of light at the peptide bond. Proteins rich in  $\beta$ -sheets or  $\alpha$ -helices have distinctly separate wavelength profiles/spectra [296]. These profiles are easily discernible when comparing IFNAR2, a  $\beta$ -sheet protein, to type I IFNs,  $\alpha$ -helical proteins (Figure 4.1). IFN $\alpha$ 1 formed two minima peaks of  $y = -1,827$  and  $y = -1,676$  at 208nm and 221nm respectively, indicative of  $\alpha$ -helical secondary structure [296]. Likewise, IFN $\beta$  produced from insect cells demonstrated a near identical profile, again indicating an  $\alpha$ -helical fold, commensurate with what we know about the structure of type I IFNs. IFN $\epsilon$  demonstrated the same wavelength profile of 2 minima peaks (at 208nm and 221nm), however at reduced magnitude compared to IFN $\alpha$  and IFN $\beta$ , which was determined to be a consequence of lower protein concentration. To compare, IFNAR2 exhibited only a single minima of  $y = -863$  at 215nm, which is the wavelength profile exhibited by proteins rich in  $\beta$ -sheets [296]. To investigate if the shape of the profile could be altered, IFN $\epsilon$  was boiled and observed that the previously

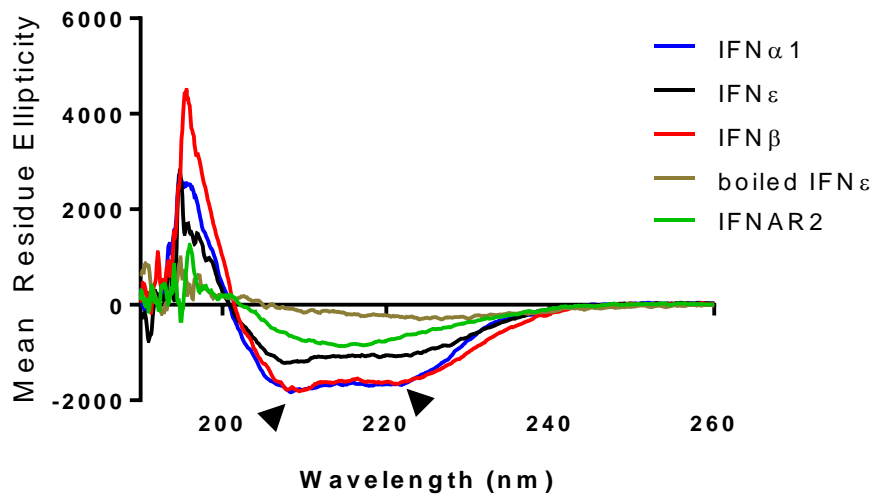


**Figure 4.1 Circular Dichroism (CD) of recombinant IFN proteins.** The CD spectra of IFN $\alpha$ 1, IFN $\beta$  and IFN $\epsilon$  were compared and found to demonstrate the classical double minima peaks (arrowheads) associated with  $\alpha$ -helical proteins. IFNAR2, a protein rich in  $\beta$ -sheets, only demonstrated one minima peak. Boiled IFN $\epsilon$  showed no discernable secondary structural characteristics indicating a loss of secondary fold. Data denotes the mean readings from one experiment performed in duplicate. N=2.

observed shape was lost. Instead, the wavelength profile was changed to become an almost straight line, indicating a loss of secondary structure following protein denaturation. These data indicate that recombinant murine IFNs expressed from insect cells including IFN $\epsilon$ , form an  $\alpha$ -helical secondary structure and are therefore folded as the native type I IFNs.

#### **4.2.2 Glycosylation of IFNs produced from an insect cell expression system**

Type I interferons are glycoproteins, meaning they carry carbohydrate side chains [297]. Many murine type I IFNs, including IFN $\alpha$ 1 and IFN $\beta$  have been shown to be *N*-glycosylated but not *O*-glycosylated [282]. Glycosylation sites vary in number from 1 (in IFN $\alpha$ 1) to 3 (in IFN $\beta$ ) and are conserved at position 78 of the mature protein (amino acid residue 76 in IFN $\beta$ ) [282]. Computational prediction of *N*-linked glycosylation sites in IFN $\beta$  coincide with experimental findings, suggesting that the software can be used to potentially identify glycosylation sites [298]. Analysis of IFN $\epsilon$  using this software showed no putative *N*-linked glycosylation sites and is consistent with published predictions [282]. The glycosylation of proteins can also be determined experimentally via staining with periodic acid-Schiff's stain (PAS) [297, 299]. 2 $\mu$ g of IFN $\alpha$ 1, His<sub>6</sub>-IFN $\beta$ , IFN $\epsilon$  and IFNAR1 were separated on SDS-PAGE and transferred to PVDF membrane for PAS staining or the polyacrylamide gel stained with Coomassie Brilliant Blue (CBB) (Figure 4.2). As seen by the PAS blot (top panel), all the proteins investigated demonstrated some degree of glycosylation and PAS positive bands correlated with the protein sizes seen on polyacrylamide gels stained with CBB (bottom panel). IFN $\alpha$ 1 expressed from the methylotropic yeast *P. pastoris* demonstrated the highest level of glycosylation, followed by IFNAR1 expressed using the baculoviral expression

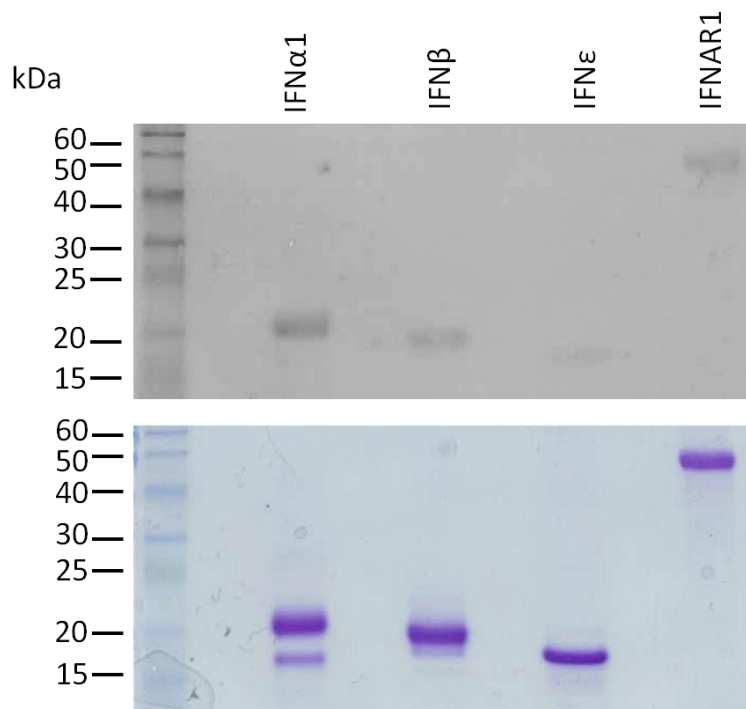


**Figure 4.2 Analysis of carbohydrate content of recombinant type I interferons by Periodic Acid Schiffs (PAS) staining.** To analyse the carbohydrate content of investigated type I interferons, 2 $\mu$ g of each investigated protein were separated on SDS-PAGE and transferred to PVDF membrane and stained with PAS (top panel) or SDS-PAGE gels stained with Coomassie brilliant blue (bottom panel). IFN $\alpha$ 1 demonstrated the most highly PAS positive band, followed by IFNAR1. IFN $\beta$  demonstrated only light PAS staining whereas IFN $\epsilon$  was only weakly positive. The Coomassie stained SDS-PAGE confirms protein loading.

system. IFN $\alpha$ 1 and IFNAR1 protein were kindly provided by Dr. N.A. de Weerd. His<sub>6</sub>-IFN $\beta$  also demonstrated positive PAS staining, although at much reduced levels when compared to IFN $\alpha$ 1 or IFNAR1. A very faint PAS positive band was present in the IFN $\epsilon$  protein, suggesting that IFN $\epsilon$  expressed from insect cells is lightly glycosylated. One point to consider is that not all carbohydrate molecules are detectable by PAS staining as aldehyde containing sugars such as glucose, galactose, mannose and sialic acids are oxidised more readily by the PAS reaction. Regardless, the PAS staining is among the most commonly used methods for the rapid detection of glycoproteins.

#### **4.2.3 Antiviral activity of IFN $\epsilon$**

The most widely characterised and most well-known biological activity of the type I IFNs is their antiviral activity. It was this observation that first generated interest in the study of IFNs [14]. Type I IFNs are the principal antiviral cytokine produced by virtually all cells in the body in response to viral (and also bacterial) infection. Intriguingly, studies have shown that the specific antiviral activities (the amount of interferon activity per milligram of protein) between IFN molecules (particularly IFN $\alpha$  species) can differ almost 1000 fold [282]. I therefore investigated IFN $\epsilon$  for this principal biological activity according to a standard cytopathic effect inhibition assay [300]. L929 cells were stimulated with IFNs overnight and subsequently challenged with Semliki Forest Virus for 72 hours as described in Chapter 2. Cytopathic effect was scored visually and also by staining of viable cells with MTT [301]. A reference standard from NIH was used in all experiments to calibrate subsequent readings.

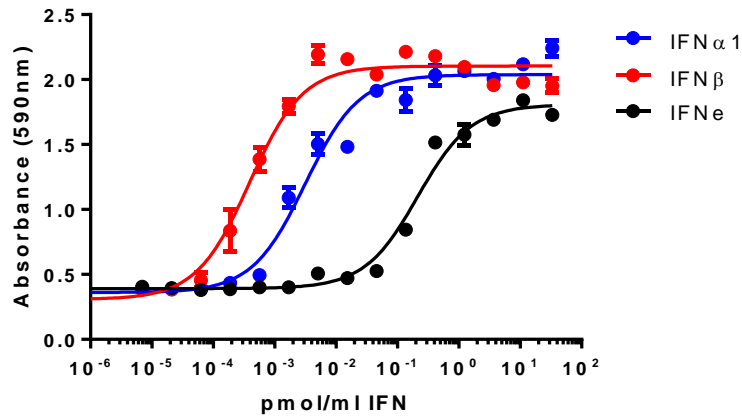
As seen in Figure 4.3A, the cytopathic inhibition effect elicited by the investigated IFNs followed a sigmoidal dose response. IFN $\alpha$ 1 and IFN $\beta$  exhibited EC<sub>50</sub> values of 0.003pmol/ml (95%CI: 0.0022 - 0.0045) and 0.00039pmol/ml (95%CI: 0.00028 - 0.00054) respectively, in this assay. The EC<sub>50</sub> is a measure of the concentration of compound required to elicit a response 50% of maximal activity. Interestingly IFN $\epsilon$  exhibited lower antiviral efficacy, resulting in an EC<sub>50</sub> of 0.214pmol/ml (95%CI: 0.163 – 0.281). These data show that IFN $\epsilon$  is approximately 100-fold less active than IFN $\alpha$ 1 and 1000-fold less active than IFN $\beta$  in this assay.

A more common method for expressing the specific antiviral activity of IFNs is described as international units (IU) per milligram of protein, where one IU is the concentration of interferon required to protect 50% of infected cells from cytopathic effect [302]. This is calculated by comparison to an international reference standard to maintain accuracy between assays and sites. Using this assay, it was determined that IFN $\epsilon$  had a specific antiviral activity of  $2.1 \pm 0.3 \times 10^5$  IU/mg, compared to  $2.4 \pm 0.2 \times 10^7$  IU/mg for IFN $\alpha$ 1 and  $2.2 \pm 0.6 \times 10^8$  IU/mg for IFN $\beta$  (Figure 4.3B). Therefore IFN $\epsilon$  demonstrated a 120-fold and 1000-fold lower specific antiviral activity compared to IFN $\alpha$ 1 and IFN $\beta$ , respectively.

#### 4.2.4 Antiproliferative activities of IFN $\epsilon$

Among the earliest discovered properties of IFNs was their potential to inhibit the proliferation of cells, particularly tumour cell lines [155, 156]. Although the exact signalling mechanisms leading to growth arrest aren't as well defined as those responsible for the antiviral effector functions, interferon mediated growth arrest has been shown to occur predominantly at the G1 phase due to

A.



B.

Interferon	Specific Activity (IU/mg)
IFN $\alpha$ 1	2.4 $\pm$ 0.2 x10 <sup>7</sup>
IFN $\beta$	2.2 $\pm$ 0.6 x10 <sup>8</sup>
IFN $\epsilon$	2.1 $\pm$ 0.3 x10 <sup>5</sup>

**Figure 4.3 Antiviral activity of murine type I interferons. A)** A dose response curve of mouse L929 fibroblast cells stimulated with interferons for 16 hours and then challenged with Semliki Forest Virus (SFV) for 72hours. The inhibition of cytopathic effect (CPE) by IFNs was measured compared to NIH reference standard GU-02-901-511. Cell viability was assessed by MTT staining and used to calculate the EC<sub>50</sub>. IFN $\alpha$ 1, 0.003pmol/ml (95%CI: 0.0022 - 0.0045); IFN $\beta$  0.00039pmol/ml (95%CI: 0.00028 - 0.00054); IFN $\epsilon$ , 0.214pmol/ml (95%CI: 0.163 – 0.281). Data points are the mean of an experiment performed in duplicate as a representative of three independent experiments. **B)** A table of antiviral specific activity of investigated IFNs expressed as international units (IU) per milligram of protein. 1IU was the concentration of interferon required to inhibit 50% of the CPE. Data was acquired from at least 3 independent experiments.

many possible (and cell type specific) mechanisms including the actions of cdk inhibitors, downregulation of c-Myc RNA and E2F family of transcription factors (see section 1.8.2). To investigate the antiproliferative functions of IFN $\epsilon$ , RAW264.7 murine macrophage cells were seeded in combination with increasing doses of IFNs and cellular proliferation measured 72hours post seeding by MTT dye staining. To compare the antiproliferative effect, IFN $\alpha$ 1 and IFN $\beta$  were analysed alongside as positive controls.

As seen in Figure 4.4, treatment with each IFN resulted in a dose-dependent reduction in proliferation. IFN $\beta$  exhibited the highest antiproliferative effect, with as little as 0.054pmol/ml (95%CI: 0.034 – 0.088pmol/ml) sufficient to inhibit 50% of cell growth. IFN $\alpha$ 1 demonstrated 50% growth inhibition at 1.33pmol/ml (95%CI: 0.984 – 1.806pmol/ml). IFN $\epsilon$  demonstrated the weakest antiproliferative activity with 50% growth inhibition observed at 291.9pmol/ml (95%CI: 49.43 – 745.3pmol/ml). Therefore IFN $\alpha$ 1 is approximately 25 times less active than IFN $\beta$  and IFN $\epsilon$  is ~5000x and ~220x less active than IFN $\beta$  and IFN $\alpha$ 1, respectively, in this anti-proliferative assay.

#### **4.2.5 Induction of interferon regulated genes in primary mouse bone marrow derived macrophages**

The biological functions of type I IFNs are in part elicited at the transcriptional level through the induction of genes. Interferon signalling has been shown to result in the transcription of thousands of genes responsible for the antiviral, antiproliferative and immunoregulatory properties of these cytokines [67, 303]. Of these, *Isg15*, *Irf7* and *Oas1a* are amongst the best characterised and are highly induced. To investigate whether IFN $\epsilon$  activated these genes, bone marrow derived macrophages (BMDMs) from C57Bl/6 wild type, *Ifnar1*<sup>-/-</sup> and

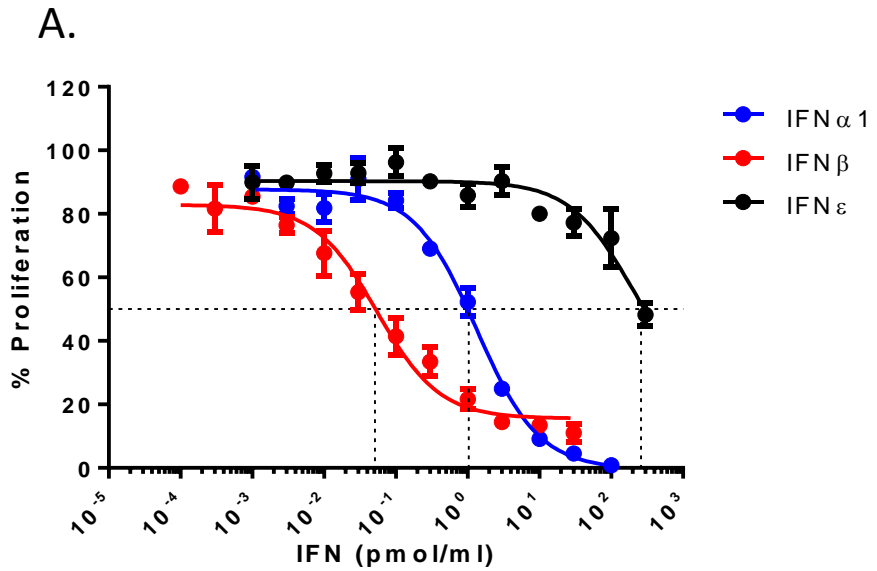


**Figure 4.4. Antiproliferative effect of murine type I interferons on the mouse macrophage cell line RAW264.7.** A dose response curve of the antiproliferative effect of mouse IFNs on RAW264.7 cells.  $2 \times 10^4$  cells were stimulated with IFNs for 72 hours the proliferation measured by MTT staining. % Proliferation was calculated by comparing the  $OD_{590}$  reading of IFN stimulated cells with unstimulated cells. The  $EC_{50}$  of each IFN are indicated by the dotted lines and were calculated to be: IFN $\alpha$ 1 1.33pmol/ml (95%CI: 0.984 – 1.806); IFN $\beta$  0.054pmol/ml (95%CI: 0.034 – 0.088); IFN $\epsilon$  291.9pmol/ml (95%CI: 49.43 – 745.3). Data points denote the mean  $\pm$  SEM of 3 independent experiments performed in duplicate.

*Ifnar2*<sup>-/-</sup> mice were stimulated with 5pmol/ml of IFN $\alpha$ 1, IFN $\beta$  or IFN $\epsilon$ . RNA was extracted from the cells and cDNA synthesised as outlined in Chapter 2. qRT-PCR was performed using TaqMan probes as outlined in Chapter 2 and gene expression normalised to the expression of 18S. Gene induction was expressed relative to the level of gene expression in unstimulated cells.

As can be seen in Figure 4.5, stimulation with IFN $\alpha$ 1, IFN $\beta$  or IFN $\epsilon$  led to the induction of *Isg15*, *Irf7* and *Oas1a* mRNA expression in wild-type BMDMs. Interestingly, levels of gene induction in wild-type mice were comparable among the IFN subtypes. For example *Oas1a* was induced approximately 15-fold with IFN $\alpha$ 1 and 17-fold with IFN $\beta$  and IFN $\epsilon$ . This trend was also seen with *Irf7*, where stimulation with either of the three IFNs led to approximately 40-fold gene induction over unstimulated controls. Gene expression following IFN treatment was highest for *Isg15* and reached approximately 500-600 fold relative to unstimulated cells.

Induction of these genes was also investigated in *Ifnar1*<sup>-/-</sup> and *Ifnar2*<sup>-/-</sup> BMDMs to determine whether or not IFN $\epsilon$  would signal via the canonical type I interferon receptor complex. Compared to wild-type BMDMs, gene induction following IFN $\epsilon$  treatment was completely ablated in either receptor null cells, indicating that induction of *Isg15*, *Irf7* and *Oas1a* required both receptor subunits. The same loss of gene induction was also seen following treatment of receptor null cells with IFN $\alpha$ 1 and IFN $\beta$ .

The gene induction results presented here are in contrast to the different biological activities of IFN $\epsilon$  compared to IFN $\alpha$ 1 and IFN $\beta$  so far (see 4.2.3 and 4.2.4). This may reflect the ability of BMDMs to respond to IFNs differently compared to the other cells used in this thesis and this will be discussed further in Section 4.3 and Chapter 6. In addition, as outlined in 1.8.1, work by

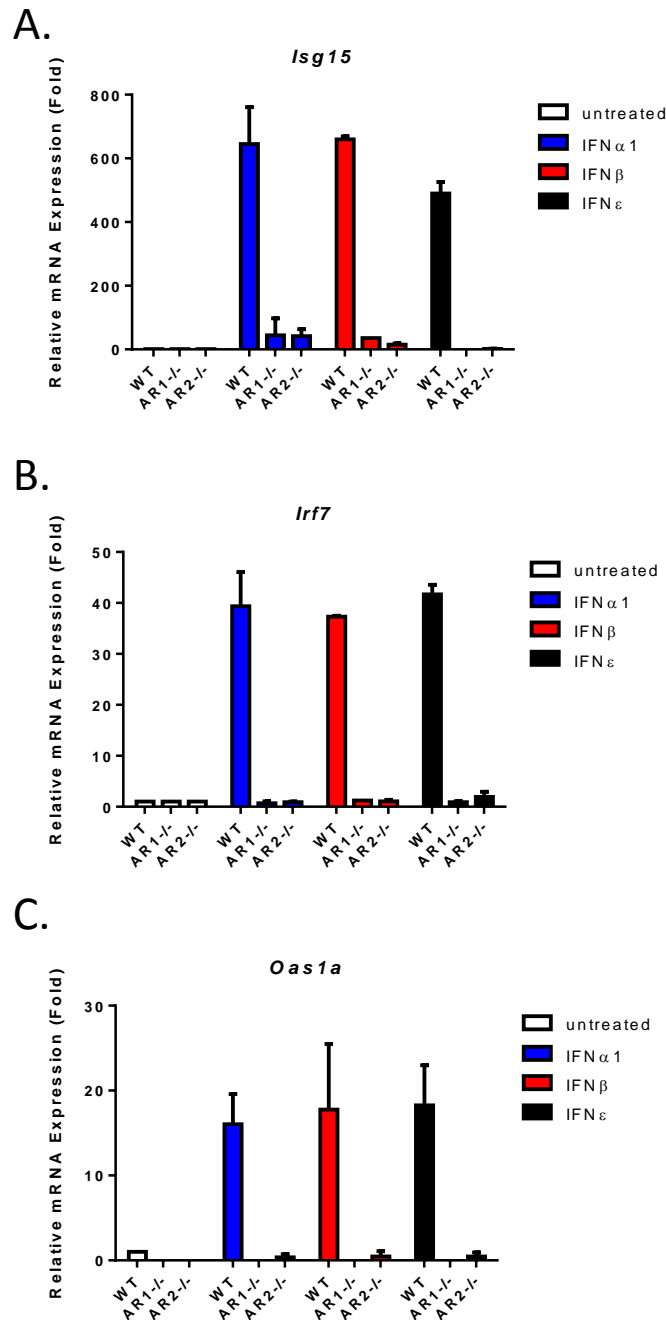


**Figure 4.5 Induction of interferon regulated genes by murine type I interferons.** Histograms of genes induced by type I interferons. Primary bone marrow derived macrophages (BMMs) from wild type (WT), IFNAR1 null (AR1<sup>-/-</sup>) and IFNAR2 null (AR2<sup>-/-</sup>) mice were stimulated with 5pmol/ml of purified IFN $\alpha$ 1, IFN $\beta$  or IFN $\epsilon$  and gene induction measured by qRT-PCR using TaqMan probes and are presented relative to *18S* expression. All investigated interferons were found to induce the classical IRGs **A)** *Isg15*, **B)** *Irf7* and **C)** *Oas1a* in wild type BMMs. This gene induction was ablated in BMMs lacking either of the type I interferon receptor subunits, IFNAR1 or IFNAR2. Data presents mean  $\pm$  SD of 2 independent experiments performed in triplicate.

Schoggins et al. indicates that individual IRGs have synergistic properties [70] and as such the measurement of individual IRGs may not reflect the total anti-viral response. Another explanation could be that the concentrations of IFN $\alpha$ 1 and IFN $\beta$  used in these experiments reached saturating concentrations and therefore need to be titrated to accurately compare the differential gene induction activities in this cell type.

#### 4.2.6 IRG-Luciferase reporter assays

The type I IFNs signal via the JAK-STAT signalling pathway by either activating the transcription factor complex ISGF-3 or via homo and heterodimers of other STAT molecules. As shown in 4.2.5, IFN $\epsilon$  was able to induce the expression of a number of IRGs in WT cells. In order to develop a more reproducible and easier to use *in vitro* assay, a luciferase reporter assay was developed. A synthetic promoter containing 5 ISRE sites has become a common method for investigating type I IFN signalling functions and is potently induced by type I IFNs [268]. For comparison, we also performed these reporter experiments using the 1,000bp proximal promoter sequence of ISG15 as it would contain more than just ISRE regulatory elements and thus may serve as a useful reporter for IFN signalling. The ISG15-luciferase vector was a kind gift from Prof. Paula Pitha (Johns Hopkins, Maryland, USA). The luciferase assay was performed with MEFs as outlined in 2.3.23.

IFN $\epsilon$  induced the ISRE promoter in a dose dependent manner (Figure 4.6A), reaching a relative luciferase activity of 7.4-fold over unstimulated cells using 30pmol/ml. In contrast, IFN $\beta$  was found to induce the ISRE promoter 10-fold at all concentrations tested, suggesting that 0.3pmol/ml, the lowest concentration investigated, was sufficient to maximally induce ISRE. IFN $\epsilon$  was

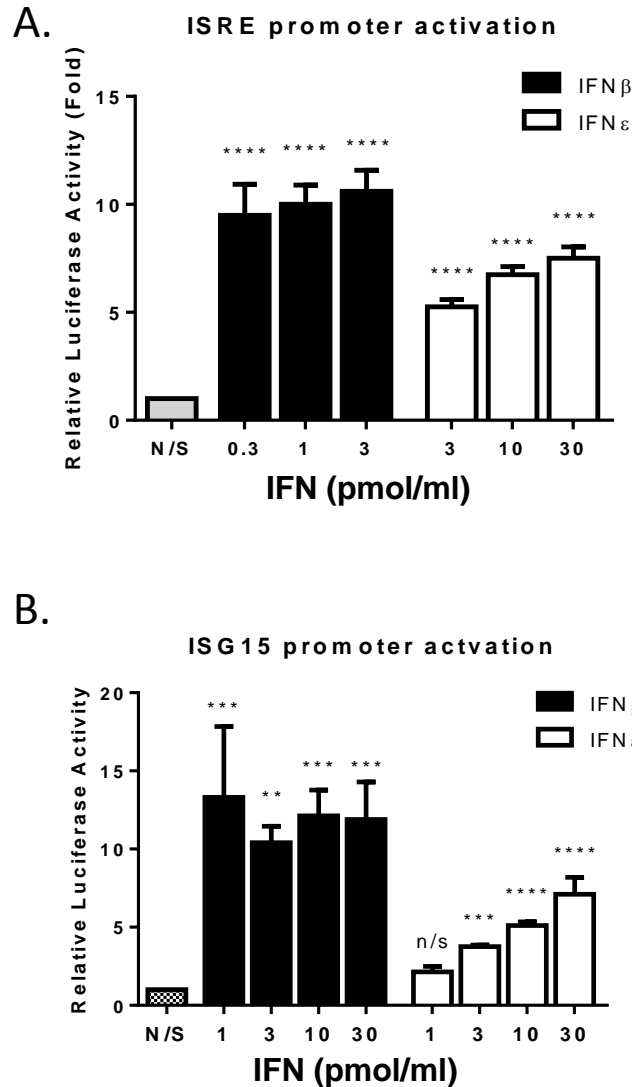


**Figure 4.6 Luciferase promoter activation induced by murine type I interferons.** Histograms of the relative luciferase activity produced by promoters driven by type I IFN signalling. The ability of type I interferons to induce the luciferase reporter gene under the control of **A)** ISRE and **B)** *Isg15* promoters was evaluated in an immortalised mouse embryonic fibroblast cell line. Cells were transfected and stimulated for 8 hours with IFNs. Luciferase activity was expressed relative to transfected TK-Renilla and compared to unstimulated control cells. IFN $\epsilon$  was found to induce ISRE and *Isg15* promoters however to a reduced level when compared to IFN $\beta$ . Data are presented as the mean  $\pm$  SD of an experiment performed in triplicate as a representative experiment. The experiments were repeated at least three times. \*\*,  $p < 0.01$ ; \*\*\*,  $p < 0.001$ ; \*\*\*\*,  $p < 0.0001$ . Statistical analyses were performed using one way ANOVA and represent significance of stimulated compared to unstimulated samples.

able to induce ISRE in this reporter assay, suggesting that it signalled via ISGF-3 however with weaker potency when compared to IFN $\beta$ .

Similar to ISRE, IFN $\epsilon$  induced the ISG15 promoter in a dose dependent manner (Figure 4.6B). This result was expected as IFN $\epsilon$  had already been shown to induce *Isg15* gene transcription in BMDMs (Chapter 4.2.5). The highest response in this assay was seen when cells were treated with 30pmol/ml IFN $\epsilon$ , which reached 6.9-fold induction compared to unstimulated cells. Stimulation with IFN $\beta$  yielded similar results as found in Figure 4.6A. At concentrations between 1 and 30pmol/ml of IFN $\beta$ , the *Isg15* promoter was activated maximally and reached 12-fold compared to unstimulated cells. This work therefore demonstrates that while IFN $\epsilon$  elicits a dose dependent increase in ISG15 promoter activation, high concentrations of IFN $\epsilon$  are required to induce this gene as optimally as IFN $\beta$ .

#### 4.2.7 STAT1 phosphorylation

As shown in Chapter 4.2.6, IFN $\epsilon$  was able to induce the transcription of an ISRE-luciferase reporter construct, indicating the use of ISGF-3. To further investigate the kinetics of STAT activation, RAW264.7 macrophage cells were stimulated with IFN $\alpha$ 1, IFN $\beta$  or IFN $\epsilon$  and the cellular lysates analysed for phosphorylation of tyrosine residue 701 on STAT1 by western blot.

As seen in Figure 4.7A, phosphorylation of STAT1-Y701 was observed with as little as 0.03pmol/ml of IFN $\alpha$ 1 following 30 minutes of stimulation. The western blot band corresponding to STAT1 increased in intensity with higher doses of IFN $\alpha$ 1, indicative of a dose response effect. Stimulation of RAW264.7 cells with IFN $\beta$  also led to phosphorylation of tyrosine 701, however this effect was only seen at concentrations above 0.1pmol/ml (Figure

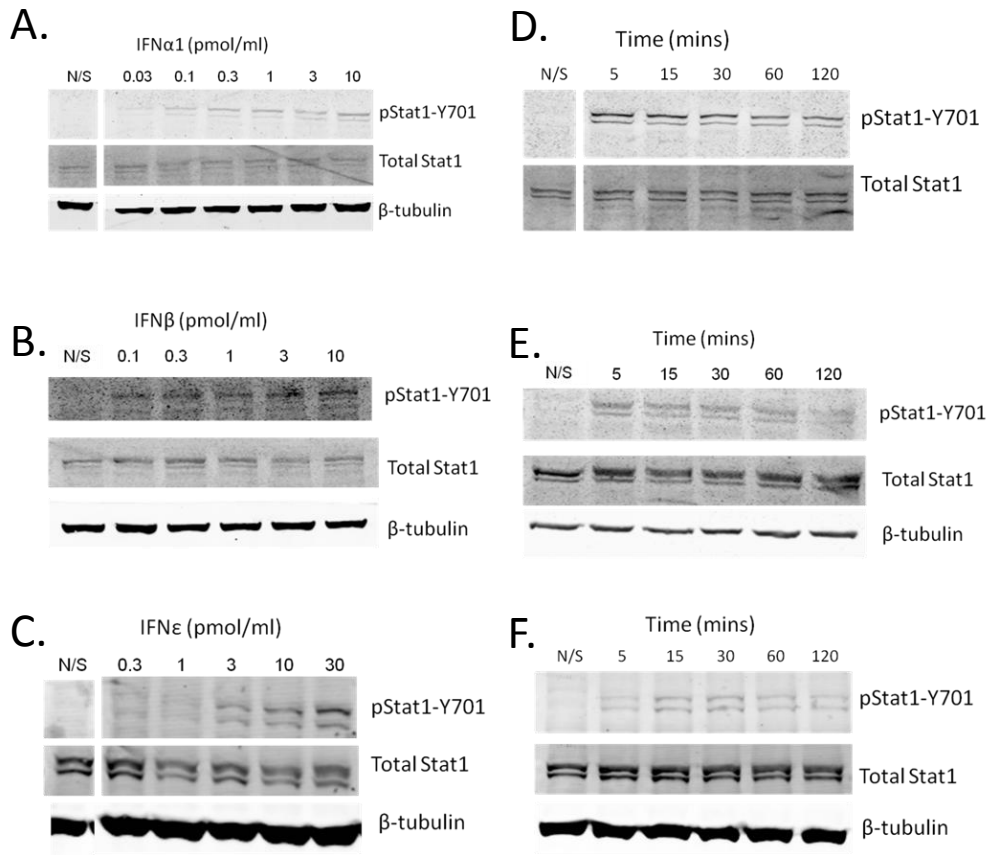


**Figure 4.7 Phosphorylation of Tyrosine residue 701 of Signal Transducers and Activators of Transcription 1 (STAT1) following murine type I interferon treatment.** Western blots of cell lysates probed using anti-pStat1-Y701, anti-Stat1 and anti- $\beta$ -tubulin antibodies. The mouse macrophage cell line RAW264.7 was stimulated with either IFN $\alpha$ 1, IFN $\beta$  or IFN $\epsilon$  and cellular protein extracts evaluated for tyrosine phosphorylation by western blotting against pStat1-Y701. Phosphorylation was measured following dose response (A-C) and time course (D-F) experiments. Data is representative of at least 2 experiments.

4.7B). Similarly to IFN $\alpha$ 1, a dose responsive effect was also seen with IFN $\beta$ . In contrast to IFN $\alpha$ 1 and IFN $\beta$ , phosphorylation of Y701 on STAT1 following IFN $\epsilon$  treatment required a dose of 3pmol/ml or higher, demonstrating a 30-100-fold reduced ability to phosphorylate tyrosine 701 compared to IFN $\alpha$ 1 and IFN $\beta$  (Figure 4.7C). Increasing the dose of IFN $\epsilon$  resulted in an increase in western blot band intensity, indicating a dose response effect.

To further characterise the activation of STAT1 by IFNs, a time course was performed to investigate the kinetics of STAT1 activation (Figures 4.7D-F). RAW264.7 cells were stimulated with 10pmol/ml of IFN and cells harvested 5, 15, 30, 60 and 120 minutes after stimulation and the lysates analysed for STAT1 phosphorylation at tyrosine 701 residue by western blot. Rapid and highest tyrosine 701 phosphorylation was seen with both IFN $\alpha$ 1 and IFN $\beta$  after 5 minutes of stimulation (Figures 4.7D and E, respectively). Band intensity decreased over the time-course with residual activation present even after 120 minutes. In contrast, even though stimulation with IFN $\epsilon$  resulted in rapid phosphorylation after 5 minutes, peak phosphorylation levels were not seen until 15-30 minutes, suggesting a slower maximal activation rate (Figure 4.7F). Phosphorylation levels decreased after 60 and 120 minutes with residual phosphorylation still present at 120 minutes.

Together, the activation of STAT1 by IFN $\epsilon$  was found to be some 30- to 100-fold less potent than IFN $\alpha$ 1 or IFN $\beta$ . Furthermore, the time taken to reach maximum phosphorylation levels of STAT1 was longer after IFN $\epsilon$  stimulation compared to IFN $\alpha$ 1 and IFN $\beta$ . As STAT1 complexes with STAT2 and IRF-9 to form the transcription factor ISGF-3, the results above compliment the data obtained in Chapter 4.2.6.

#### 4.2.8 STAT3 phosphorylation

Since IFNs signal via STAT1 and STAT3 homo or hetero-dimers, RAW 264.7 macrophage cells were treated with IFN $\alpha$ 1, IFN $\beta$  or IFN $\epsilon$  and the cell lysates examined for STAT3 phosphorylation at Tyrosine 705 via western blot.

Following 30 minutes of stimulation, phosphorylation of Y705 on STAT3 became apparent starting with 0.3pmol/ml of IFN $\alpha$ 1 and increasing in a dose dependent manner (Figure 4.8A). Similar phosphorylation of STAT3 Y705 was observed with IFN $\beta$  treatment, where 0.1pmol/ml was the lowest concentration able to phosphorylate STAT3. Increasing doses of IFN $\beta$  again resulted in more pronounced phosphorylation, indicating a dose response effect. In contrast, phosphorylation of STAT3 Y705 by IFN $\epsilon$  was only seen with doses above 10pmol/ml, indicating that IFN $\epsilon$  was approximately 100-fold less potent at inducing STAT3 phosphorylation at tyrosine residue 705 than IFN $\alpha$ 1 or IFN $\beta$ . Although there are faint bands in 0.3, 1 and 3 pmol/ml IFN $\epsilon$ , these do not differ in intensity to the unstimulated sample. A similar basal level of STAT3 phosphorylation at Y705 can also be seen in the IFN $\alpha$ 1 experiment (Figure 4.8A), suggesting that there could be low levels of basal STAT3 phosphorylation present.

Like STAT1, a time course was performed by stimulating RAW 264.7 cells with 10pmol/ml of IFN and cells harvested 5, 15, 30, 60 and 120 minutes after stimulation. Cellular lysates were analysed for phosphorylated tyrosine 705 on STAT3 by western blot. As expected, rapid phosphorylation was observed after 5 minutes of IFN $\alpha$ 1 treatment and remained at maximal intensity until 30 minutes (Figure 4.8D). Phosphorylation decreased by 60 minutes and was almost absent by 120 minutes post-treatment. Stimulation of cells with IFN $\beta$  resulted in a similar finding. STAT3 was phosphorylated as early as 5 minutes after treatment and remained strong until 30 minutes (Figure 4.8E).

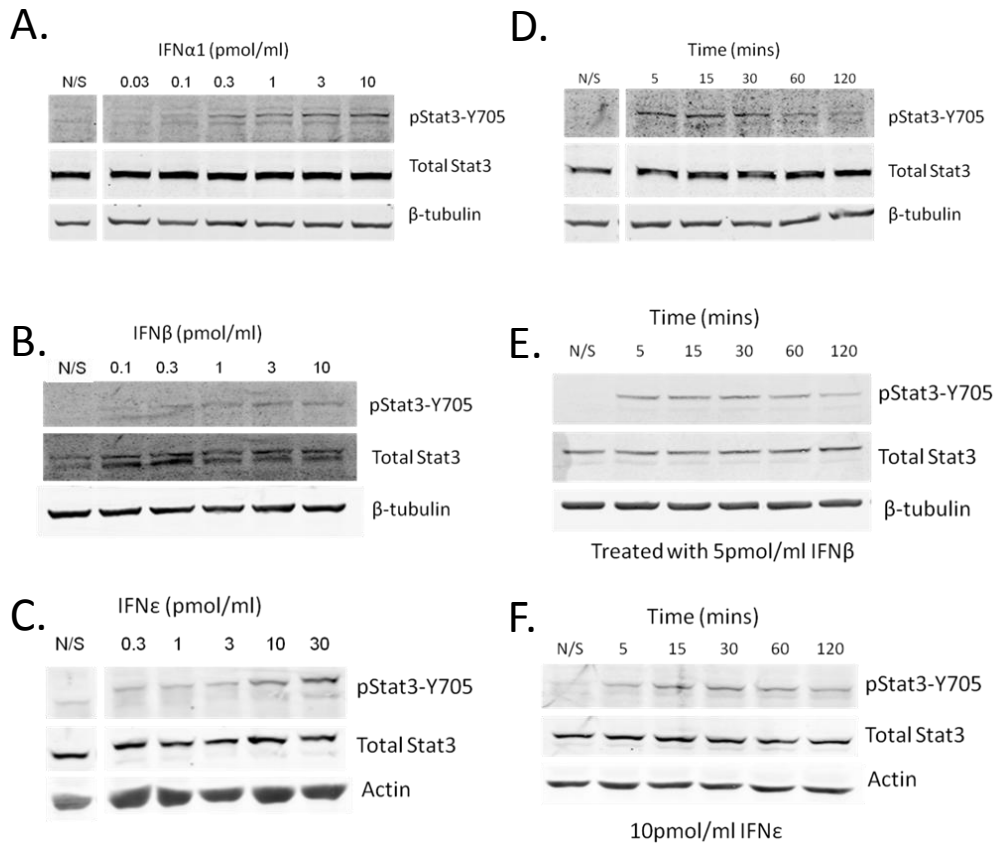


**Figure 4.8 Phosphorylation of Tyrosine residue 705 of Signal Transducers and Activators of Transcription 3 (STAT3) following murine type I interferon treatment.** Western blots of cell lysates probed using anti-pStat3-Y705, anti-Stat3, anti- $\beta$ -tubulin and anti-Actin antibodies. The mouse macrophage cell line RAW264.7 was stimulated with either IFN $\alpha$ 1, IFN $\beta$  or IFN $\epsilon$  and cellular protein extracts evaluated for tyrosine phosphorylation by western blotting against pStat3-Y705. Phosphorylation was measured following dose response (**A-C**) and time course (**D-F**) experiments. Data is representative of at least 2 experiments.

Phosphorylation was found to decrease by 60 minutes with residual phosphorylation present after 120 minutes. IFNε was able to induce phosphorylation of tyrosine 705 on STAT3 as early as 5 minutes and as seen with STAT1, the western blot band intensity increased until reaching a peak at 30 minutes post treatment (Figure 4.8F). Signal intensity decreased by 60 minutes and was reduced but still present by 120 minutes post stimulation.

Overall, IFNε stimulation leads to lower and slower phosphorylation of STAT3 compared to IFNα1 and IFNβ. Phosphorylation seems to wane at a similar rate among the three IFNs, suggesting that the phosphorylation of STAT3 by IFNε is not prolonged even if maximal phosphorylation occurs at a later time compared to IFNα1 and IFNβ.

#### **4.2.9 Physiochemical stability of IFNε**

The type I IFNs share a number of physiochemical properties that have not only aided characterisation, but have also benefited their purification. Among these properties are heat and acid stability [263]. Before recombinant DNA technology, a common method for producing IFN was to infect cells in culture with virus [254]. The resulting cell culture supernatant would contain interferon and also virus. To inactivate virus, the supernatant was acidified to pH2.0 and stored overnight at 4°C. The following day, the sample was pH neutralised and either used or further purified. An added benefit of acidification was that acid labile proteins would precipitate and thus increase final purity. It was also found that type I IFNs would remain biologically active following treatment at 56°C and this method was also employed to inactivate virus [263]. These observations were among the first that differentiated between the type I IFNs, IFNγ and the more recently discovered type III interferons, which are acid

labile [304]. To investigate the physiochemical properties of IFN $\epsilon$ , IFNs were diluted 1:100 in complete RPMI media and acidified to pH2.0 with concentrated hydrochloric acid (HCl) and stored at 4°C overnight. Following incubation, 5M sodium hydroxide was added to neutralise the sample. To test heat stability, IFNs were incubated at 55°C for 90 minutes. The degree of inactivation was determined by cytopathic effect inhibition between treated and untreated samples assayed at the same time.

As seen from Figure 4.9A, acidification of either IFN $\alpha$ 1, IFN $\beta$  or IFN $\epsilon$  to pH2.0 resulted in no significant loss of biological activity in any of the type I IFNs, as reported. In terms of temperature stability, only IFN $\beta$  biological activity was found to be significantly reduced following heat treatment at 55°C, with a 126 fold reduction in biological activity (Figure 4.9B).

Overall, these data indicate that IFN $\epsilon$  is both acid and heat stable as has been reported for type I IFNs previously.

#### **4.2.10 Upregulation of MHC-I by IFN $\epsilon$**

Among the immunoregulatory properties of type I IFNs is their ability to upregulate the expression of major histocompatibility complex 1 (MHC-I) [178]. This allows for an increased potential of antigen presentation to T-cells, which recognise the presented epitope and their subsequent activation. To determine if IFN $\epsilon$  demonstrated this particular immunoregulatory property, YAC-1 suspension cells were stimulated for 24 hours with increasing doses of IFN and analysed by flow cytometry for MHC-I H-2<sup>Kb</sup> cell surface expression. YAC-1 cells are a Moloney murine leukemia virus induced lymphoma cell line traditionally used to evaluate NK-cell activity *in vitro* [305]. Importantly, YAC-1

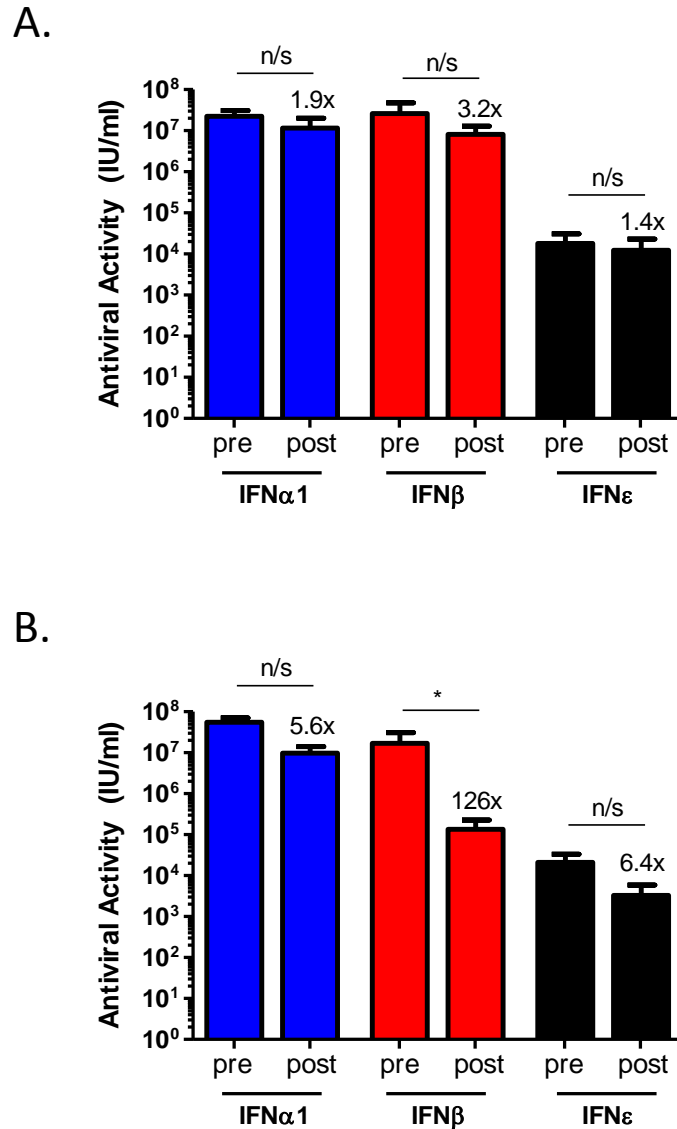


**Figure 4.9 pH and temperature stability of recombinant murine type I IFNs.** Histograms of the antiviral activity as measured by a cytopathic effect inhibition assay on L929 cells challenged with Semliki Forest Virus. **A)** Type I interferons were acidified to pH2.0 with concentrated HCl and incubated overnight at 4°C. The pH was neutralised with sodium hydroxide before samples were analysed for their antiviral activity. **B)** Type I interferons were incubated at 55°C for 90 minutes prior to measuring the antiviral activity. Numbers indicate fold decrease in activity post treatment compared to pre treatment. Data is presented as mean  $\pm$  SEM of 4 independent experiments. \*,  $p < 0.05$ ; n/s, not significant. Statistical analyses were performed using Student's t-test.

cells in response to IFN have been reported to upregulate the cell surface expression of MHC-I [306, 307].

As expected, IFN $\alpha$ 1 and IFN $\beta$  treatment resulted in a dose-dependent increase of MHC-I cell surface levels compared to an unstimulated control (Figure 4.10). 0.3pmol/ml of either IFN $\alpha$ 1 or  $\beta$  was sufficient to induce a 3-fold induction of MHC-I, increasing to 5-fold with 30pmol/ml in a dose-dependent manner. Interestingly, there was no difference in the potential to upregulate MHC-I between IFN $\alpha$  and IFN $\beta$  treated cells at any dose investigated. The ability of IFN $\epsilon$  to increase MHC-I expression was less compared to IFN $\alpha$  or IFN $\beta$ . 0.3pmol/ml IFN $\epsilon$  was only sufficient to increase expression by 1.3-fold over unstimulated controls; this increased to 2.8-fold with 100pmol/ml of IFN $\epsilon$ . Therefore, IFN $\epsilon$  is more than 300-fold less potent in inducing similar levels of MHC-I expression compared to IFN $\alpha$  or IFN $\beta$ , commensurate with the differential biological activities described above.

#### **4.2.11 Activation of immune cell subsets by IFN $\epsilon$**

Type I IFNs have a well-documented ability to activate immune cells (Chapter 1.8.4). They induce the survival and proliferation of T cells, induce isotype switching of B cells and potently activate NK-cells [134, 172, 175]. For this study, immune cell activation was broadly measured on all investigated cell types by CD69 expression. CD69 is a transmembrane c-type lectin strongly induced by type I IFNs such as IFN $\alpha$  and IFN $\beta$  and has been widely used as an activation marker for T and B lymphocytes [181, 188, 308-310]. To examine the ability of IFN $\epsilon$  to activate immune cells, single cell suspensions were prepared from spleens of wild-type C57Bl/6 mice and treated for 24 hours with equivalent doses of IFN $\alpha$ 1, IFN $\beta$  or IFN $\epsilon$ . Untreated cells were

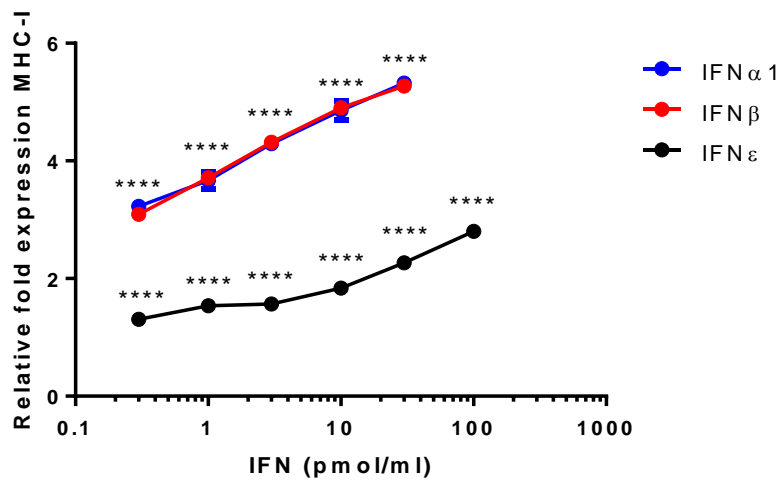


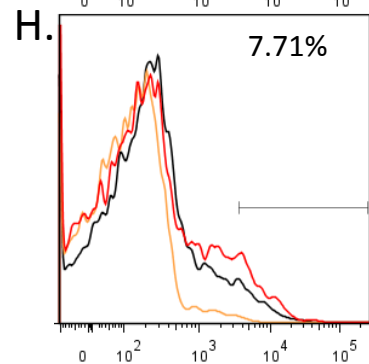
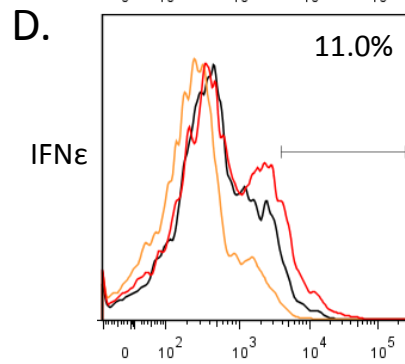
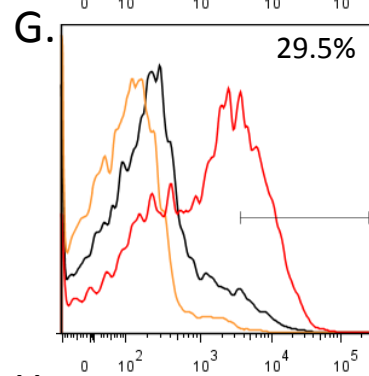
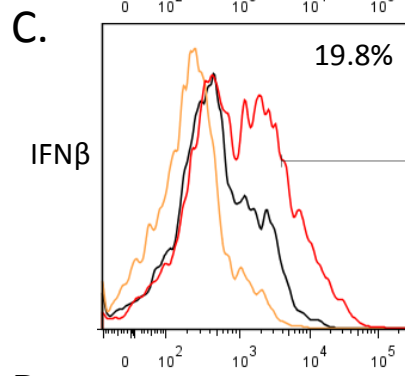
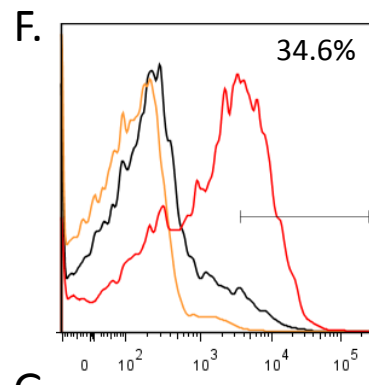
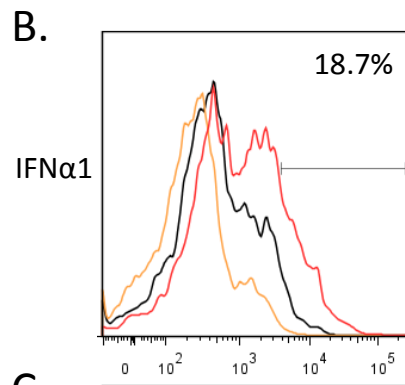
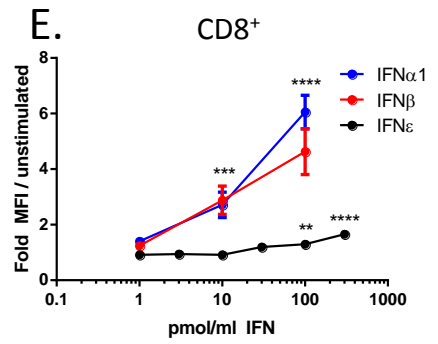
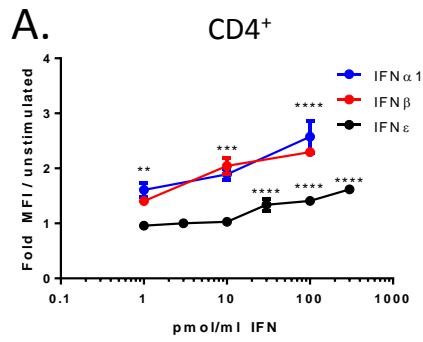
**Figure 4.10 Upregulation of MHC Class I by type I IFNs.** A graph demonstrating the effect of type I IFNs on the expression of MHC-I. The ability of recombinant murine type I IFNs to upregulate the expression of Major Histocompatibility Complex I (MHC-I) was investigated by stimulation of mouse YAC-1 cells with recombinant type I interferons. Cell surface levels of MHC-I were measured by flow cytometry and made relative to unstimulated control cells. Data is presented as mean  $\pm$  SD of a representative experiment performed in triplicate. The experiment was repeated three times. \*\*\*\*,  $p < 0.0001$ . Statistical analyses were performed using one way ANOVA and represent significance of stimulated compared to unstimulated samples.

included for comparison. Cells were stained with antibodies against CD4, CD8, B220, NK1.1 and CD69 and analysed by flow cytometry, as outlined in Chapter 2.5.2. For analysis, CD69 expression was examined following gating of CD4<sup>+</sup>, CD8<sup>+</sup>, B220<sup>+</sup> and NK1.1<sup>+</sup> cells.

As seen in Figure 4.11A, the expression of CD69 on CD4<sup>+</sup> cells increased in a dose-dependent manner in response to treatment with each IFN. While concentrations of up to 10pmol/ml of IFNε were not sufficient to significantly increase CD69 expression, IFNε at a concentration of 30pmol/ml induced CD69 expression 1.3-fold and reached a maximum of 1.6-fold at 300pmol/ml, relative to unstimulated cells. In contrast, treatment with IFNα1 and IFNβ demonstrated approximately 1.5-fold increase in CD69 expression over unstimulated cells at 1pmol/ml which increased to 2.5-fold with 100pmol/ml. Histograms in Figure 4.11B-D show the percentage of cells positive for CD69 when stimulated with 100pmol/ml of each IFN and appropriate isotype controls are included for comparison. 18.7%, 19.8% and 11% of CD4<sup>+</sup> cells stained positive for CD69 following IFNα1, IFNβ and IFNε treatment, respectively.

The dose-response profiles of CD69 expression on CD4<sup>+</sup> and CD8<sup>+</sup> cells treated with IFNε were comparable (Figure 4.11A/E). However, the extent of CD69 upregulation was greater on CD8<sup>+</sup> cells than CD4<sup>+</sup> cells treated with IFNα1 and IFNβ at all doses tested (e.g. Fold MFI IFNα1 compared to unstimulated at 100pmol/ml, 2.57 CD4<sup>+</sup> vs 6.05 CD8<sup>+</sup>). 30pmol/ml IFNε was the lowest dose shown to induce CD69 expression (1.2-fold over unstimulated) while 1.7-fold induction of CD69 was observed at the highest concentration tested (300pmol/ml). IFNα1 and IFNβ were more potent at inducing CD69 expression on CD8<sup>+</sup> cells than IFNε. 1pmol/ml of IFNα1 or IFNβ led to approximately 1.4-fold induction of CD69 expression over unstimulated cells, which increased to 6-fold and 5-fold at 100pmol/ml for

**Figure 4.11 Upregulation of CD69 on CD4<sup>+</sup> and CD8<sup>+</sup> splenic cells by type I IFNs.** Graphs of the effect of type I IFNs on the induction of CD69 on the surface of cells.  $1 \times 10^6$  spleen cells were stimulated with IFN $\alpha$ 1 - $\beta$  or - $\epsilon$  for 24h and the expression of CD69 measured by flow cytometry on CD4<sup>+</sup> (**A-D**) and CD8<sup>+</sup> cells (**E-H**). **A** and **E**) Fold CD69 induction was calculated using the MFI of stimulated samples compared to unstimulated control cells. Data is expressed as mean  $\pm$  SD of an experiment performed in triplicate. The experiment was performed three times. \*\*,  $p < 0.01$ ; \*\*\*,  $p < 0.001$ ; \*\*\*\*,  $p < 0.0001$ . Statistical analyses were performed using one way ANOVA and represent significance of stimulated compared to unstimulated samples. **C-D** and **F-H**): Representative histograms of cells treated with 100pm/ml IFN. Bar indicates the gate where 5% of unstimulated cells stained positive for CD69. Percentage indicates percentage of cells positive for CD69. Black line, unstimulated cells; yellow line, isotype control; red line, IFN stimulated.

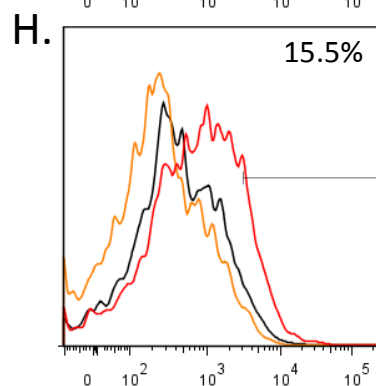
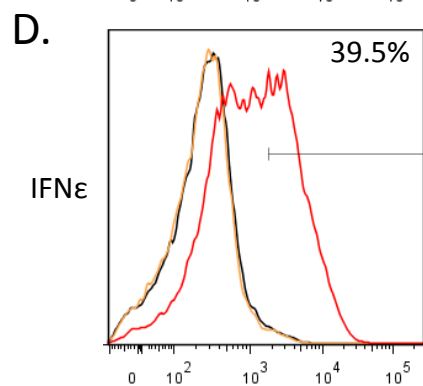
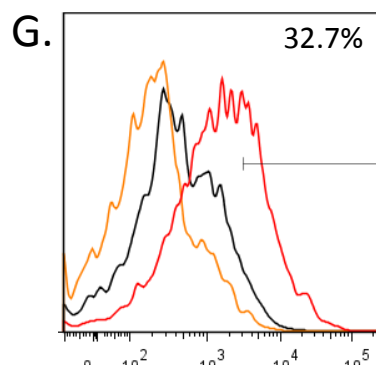
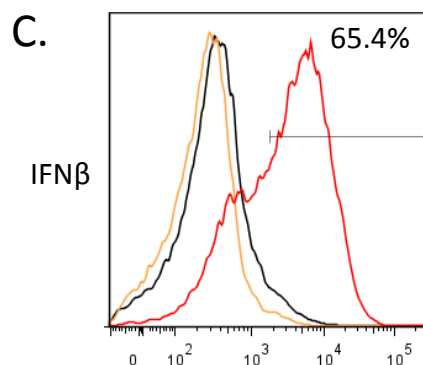
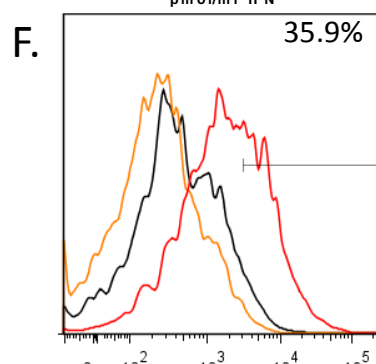
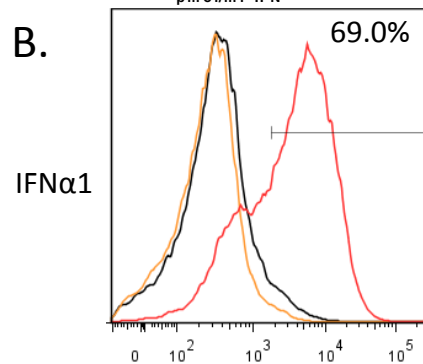
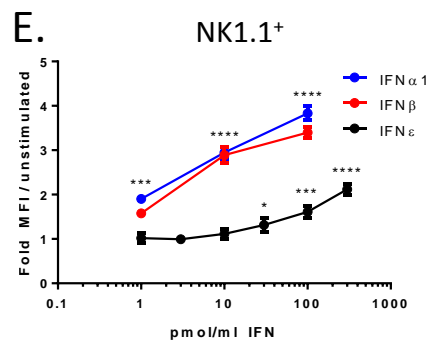
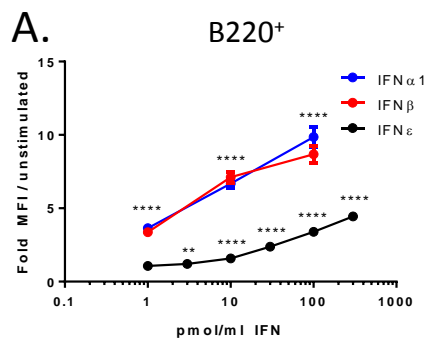


IFN $\alpha$ 1 and IFN $\beta$ , respectively. Representative histograms in Figure 4.11F-H indicate the percentage of cells positive for CD69 when stimulated with 100pmol/ml of IFNs. 34.6%, 29.5% and 7.71% of CD8<sup>+</sup> cells expressing CD69 following IFN $\alpha$ 1, IFN $\beta$  and IFN $\epsilon$  treatment, respectively. These results indicate that IFN $\epsilon$  was able to enhance the expression of the activation marker CD69 on CD4<sup>+</sup> and CD8<sup>+</sup> cells in a dose-dependent manner but to a lesser extent than IFN $\alpha$ 1 and IFN $\beta$ . These data demonstrate that an equivalent surface expression of CD69 is reached with 1pmol/ml of IFN $\alpha$ 1 or IFN $\beta$  and 300pmol/ml of IFN $\epsilon$ , therefore indicating that IFN $\epsilon$  is approximately 300 times less active than IFN $\alpha$ 1 and IFN $\beta$ .

IFN $\epsilon$  had a more pronounced effect on CD69 upregulation on B220<sup>+</sup> cells and NK1.1<sup>+</sup> cells than T cells (Figure 4.12). IFN $\epsilon$  was able to induce a dose-dependent increase in CD69 expression on B220<sup>+</sup> cells reaching 4.5-fold over unstimulated controls at 300pmol/ml. IFN $\alpha$ 1 and IFN $\beta$  demonstrated a much higher biological response than IFN $\epsilon$  with maximal CD69 expression on B220<sup>+</sup> cells reaching 9.5-fold and 8.5-fold over unstimulated cells for IFN $\alpha$ 1 and IFN $\beta$ , respectively at 100pmol/ml. IFN $\epsilon$  at a concentration of 100pmol/ml induced CD69 3.5-fold however only 1pmol/ml of IFN $\alpha$ 1 or IFN $\beta$  was required for the same level of induction, highlighting that 100x more IFN $\epsilon$  protein is required to elicit the same effect as IFN $\alpha$ 1 and IFN $\beta$ . Representative histograms of cells stimulated with 100pmol/ml IFN demonstrate that 69%, 65.4% and 39.5% of B220<sup>+</sup> cells treated with IFN $\alpha$ 1, IFN $\beta$  and IFN $\epsilon$  respectively, expressed CD69 (Figure 4.12B-D).

Similarly, CD69 expression was upregulated on NK1.1<sup>+</sup> cells by IFN $\epsilon$  reaching a maximal fold induction of 2.1 at 300pmol/ml (Figure 4.12E). IFN $\alpha$ 1 and IFN $\beta$  had a more potent effect compared to IFN $\epsilon$ , inducing CD69 expression on NK1.1<sup>+</sup> cells 3.8-fold and 3.4-fold, respectively at 100pmol/ml. As a

**Figure 4.12 Upregulation of CD69 on B220<sup>+</sup> and NK1.1<sup>+</sup> splenic cells by type I IFNs.** Graphs of the effect of type I IFNs on the induction of CD69 on the surface of cells.  $1 \times 10^6$  spleen cells were stimulated with IFN $\alpha$ 1 - $\beta$  or - $\epsilon$  for 24h and the expression of CD69 measured by flow cytometry on B220<sup>+</sup> (A-D) and NK1.1<sup>+</sup> cells (E-H). A) and E) Fold CD69 induction was calculated using the MFI of stimulated samples compared to unstimulated control cells. Data is expressed as mean  $\pm$  SD of an experiment performed in triplicate. The experiment was performed three times. \*,  $p < 0.05$ ; \*\*,  $p < 0.01$ ; \*\*\*,  $p < 0.001$ ; \*\*\*\*,  $p < 0.0001$ . Statistical analyses were performed using one way ANOVA and represent significance of stimulated compared to unstimulated samples. C-D and F-H): Representative histograms of cells treated with 100pm/ml IFN. Bar indicates the gate where 5% of unstimulated cells stained positive for CD69. Percentage indicates percentage of cells positive for CD69. Black line, unstimulated cells; yellow line, isotype control; red line, IFN stimulated.



percentage, IFN $\alpha$ 1 induced CD69 on 35.9%, IFN $\beta$  on 32.7% and IFN $\epsilon$  on 15.5% of NK1.1<sup>+</sup> cells (Figure 4.12F-H).

The data from these experiments clearly demonstrate that IFN $\epsilon$  is able to induce the expression of CD69 on the surface of T, B and NK-cells. Consistent with previous findings in this thesis however, an equal biological effect was only seen with a 100 - 300-fold excess of IFN $\epsilon$  protein compared to IFN $\alpha$ 1 and IFN $\beta$ .

#### **4.2.12 *In vivo* gene induction by IFN $\epsilon$**

As shown in 4.2.5, IFN $\epsilon$  was able to induce the transcription of IRGs *in vitro*. To evaluate the *in vivo* potency of IFN $\epsilon$  we felt it was vital to also analyse the expression of IRGs following varying routes of *in vivo* administration. All *in vivo* injections were performed by N.E. Mangan (MIMR). 200pmol of IFN $\epsilon$  was injected intraperitoneally (IP) into mice and the peritoneal exudates cells (PECs) harvested after 3 hours and gene expression analysed by qRT-PCR. *Isg15*, *Irf7* and *Oas1a* were all significantly induced in response to IFN $\epsilon$  treatment compared to untreated controls (Figure 4.13A-C). *Isg15* was induced 734- fold, *Irf7* induced 117-fold and *Oas1a* induced 18-fold.

As IFN $\epsilon$  is expressed exclusively in the female reproductive tract [13, 114], we felt it was necessary to administer IFN $\epsilon$  at this site and measure gene induction to ensure a more relevant route of administration was possible. 200pmol of IFN $\epsilon$  was injected into the vagina of mice, which were excised 6 hours after treatment, homogenised and gene induction measured by qRT-PCR. IRGs were significantly induced by IFN $\epsilon$  treatment compared to untreated control mice (Figure 4.13D-F). *Isg15* was induced 9.3-fold, *Irf7* was

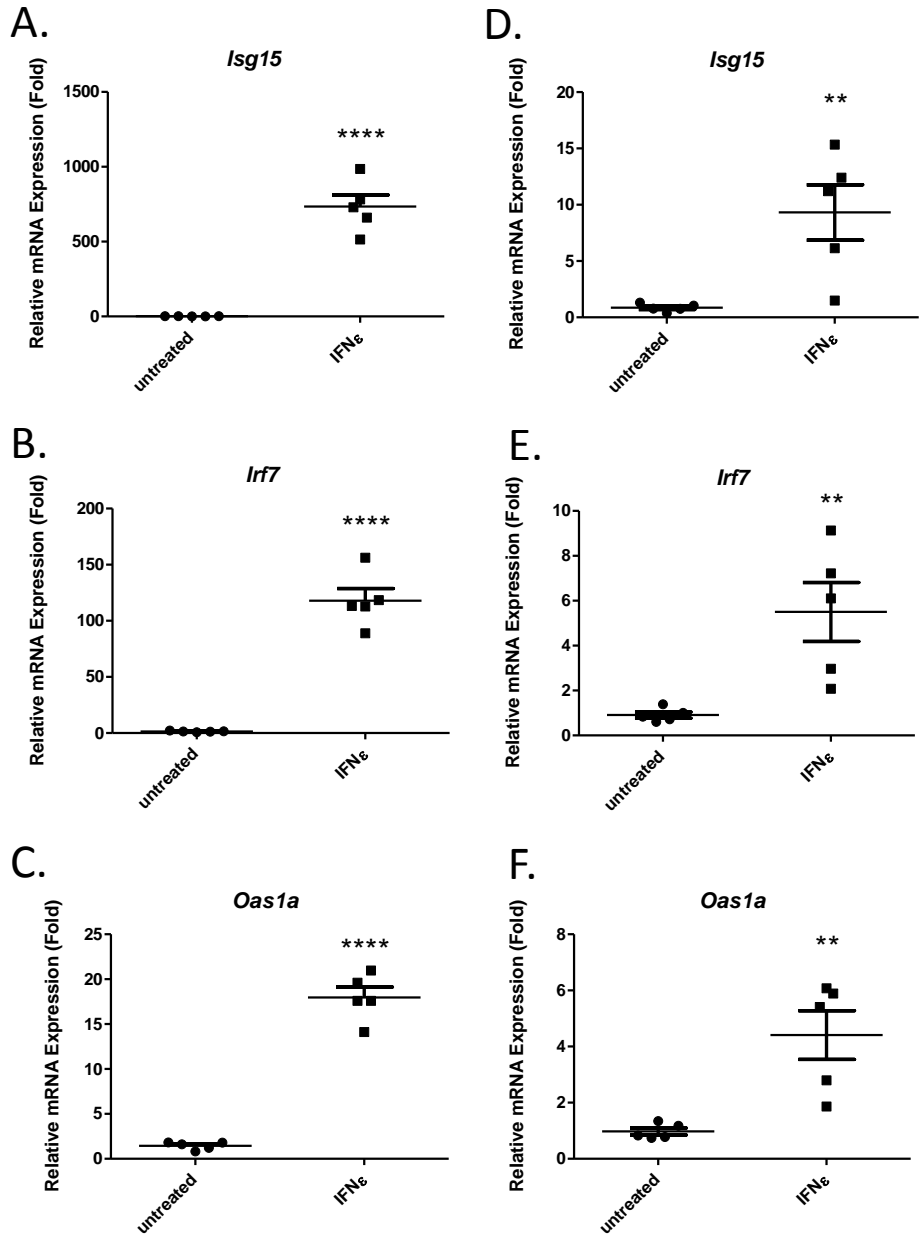


**Figure 4.13 Induction of IRGs by IFN $\epsilon$  treatment *in vivo*.** Dot plots of the relative mRNA levels of IRGs from mice treated with recombinant IFN $\epsilon$ . Wild type C57Bl/6 mice were treated intraperitoneally for 3 hours (A-C) or intravaginally for 6 hours (D-F) with 200pmol (4 $\mu$ g) of recombinant IFN $\epsilon$  and gene induction measured by qRT-PCR in peritoneal exudate cells (A-C) and vagina (D-F). The IRGs *Isg15*, *Irf7* and *Oas1a* were highly and significantly induced in both treatment groups compared to untreated control mice. N = 5 mice per group. Data is presented as mean  $\pm$  SEM. \*\*,  $p < 0.01$ ; \*\*\*\*,  $p < 0.0001$ . Statistical analyses were performed using Student's t-test.

induced 5.5-fold and *Oas1a* induced approximately 4.5-fold over untreated mice.

Interestingly, IP administration of IFN $\epsilon$  led to much higher gene induction compared to intravaginal administration and could reflect the relative difficulty of IFN $\epsilon$  to target cells in the vagina compared to the cells found in the peritoneal cavity. While starting levels of these IRGs in the reproductive tract could differ to those in PECs due to the endogenous expression of IFN $\epsilon$ , IV stimulation of IFN $\epsilon$  deficient animals led to the same levels of gene induction, highlighting that this is unlikely to be responsible for the difference in gene induction observed (Figure 4.14). Irrespective of this difference, these results highlight that IFN $\epsilon$  demonstrates appreciable *in vivo* potency regardless of site of administration.

#### 4.2.13 Antiviral activity of murine IFN $\epsilon$ on human cells

Although type I IFNs are a highly conserved gene family among mammals, their biological activities are species specific [311]. As such, mouse IFN $\beta$  has been shown to demonstrate reduced (if any) antiviral activity on human cells and *vice versa* [312]. In order to determine if mIFN $\epsilon$  exhibited this same species specificity, a cytopathic effect assay was performed on the human amniotic cell line WISH with encephalomyocarditis virus (EMCV). MTT was used to stain viable cells and absorbance measured at 590nm.

Unexpectedly, IFN $\epsilon$  demonstrated remarkably high antiviral activity in this human antiviral assay with an EC<sub>50</sub> of 0.36pmol/ml (95%CI: 0.23 – 0.55) (Figure 4.15A). Expressed as IU per milligram of protein, this equates to a specific activity of  $2.4 \pm 0.6 \times 10^7$  IU/mg (Figure 4.15B), which is approximately 100 times higher than what was measured in the mouse antiviral assay

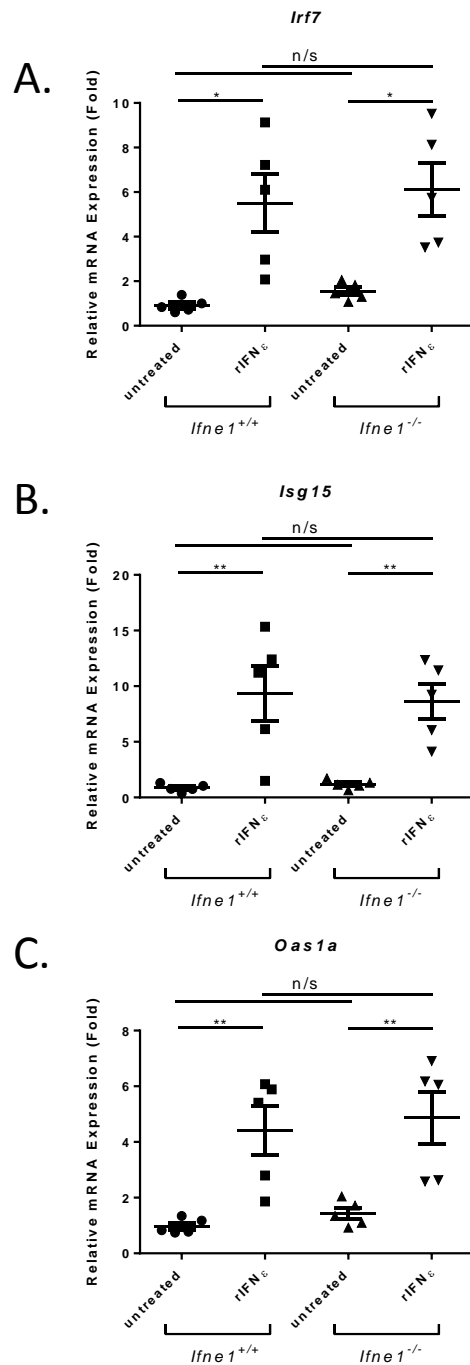
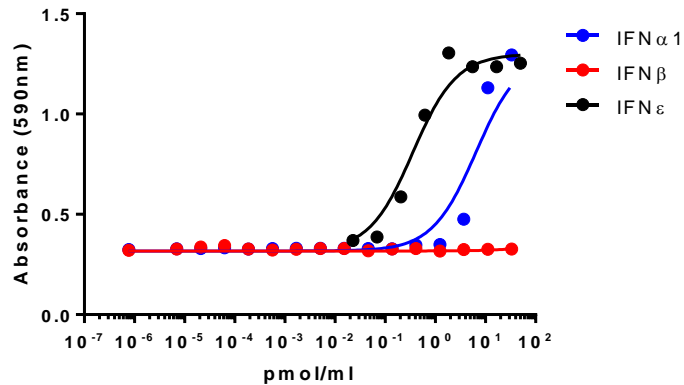


**Figure 4.14 Induction of IRGs in the vagina by IFN $\epsilon$  treatment in WT and IFN $\epsilon$  deficient animals.** Dot plots of the relative mRNA levels of IRGs from mice treated with recombinant IFN $\epsilon$ . Wild type C57Bl/6 mice and *Ifne1*<sup>-/-</sup> were treated intravaginally for 6 hours with 200pmol (4 $\mu$ g) recombinant IFN $\epsilon$  and gene induction measured by qRT-PCR. The IRGs **A) *Irf7***, **B) *Isg15*** and **C) *Oas1a*** were highly and significantly induced in both treatment groups compared to untreated control mice. N = 5 mice per group. Data is presented as mean  $\pm$  SEM. n/s, not significant; \*, p < 0.05; \*\*, p < 0.01. Statistical analyses were performed using one-way ANOVA.

A.



B.

Interferon	Specific Activity (IU/mg)
IFN $\alpha$ 1	$8 \pm 0.4 \times 10^4$
IFN $\beta$	N/D
IFN $\epsilon$	$2.4 \pm 0.6 \times 10^7$

C.

Interferon	Specific Activity (IU/mg)
IFN $\alpha$ 1	$2.4 \pm 0.2 \times 10^7$
IFN $\beta$	$2.2 \pm 0.6 \times 10^8$
IFN $\epsilon$	$2.1 \pm 0.3 \times 10^5$

**Figure 4.15 Antiviral activity of murine type I IFNs on human amniotic cells.** **A)** A dose response curve of human WISH cells stimulated with murine type I IFNs for 16 hours and then challenged with EMCV for 72hours. The inhibition of CPE by IFNs was measured compared to an NIH reference standard. Cell viability was assessed by MTT staining and used to calculate the EC<sub>50</sub>. IFN $\alpha$ 1, 6.44pmol/ml (95%CI: 4.54 – 9.12); IFN $\epsilon$ , 0.36pmol/ml (95%CI: 0.23 – 0.55). The EC<sub>50</sub> of IFN $\beta$  could not be determined. Data points are the mean of an experiment performed in duplicate as a representative of three independent experiments. **B)** A table of antiviral specific activity of investigated murine IFNs on human WISH cells expressed as international units (IU) per milligram of protein. 1IU was the concentration of interferon required to inhibit 50% of the CPE. **C)** A table of the antiviral activities of investigated murine IFNs on murine L929 cells. Data was acquired from at least 3 independent experiments.

(Figure 4.3B and 4.15C). In contrast mouse IFN $\alpha$ 1 demonstrated lower antiviral activity on human cells than mouse cells with an EC<sub>50</sub> of 6.44pmol/ml (95%CI: 4.54 – 9.12) which is equivalent to a specific activity of  $8 \pm 0.4 \times 10^3$  IU/mg. This is approximately 300 times lower than the specific activity in murine cells. Treatment with mouse IFN $\beta$  yielded no protective effect in the human antiviral assay, even at concentrations exceeding 30pmol/ml and thus the specific activity of mIFN $\beta$  on WISH cells was undetectable. These data indicate that IFN $\epsilon$ , unlike IFN $\alpha$ 1 or IFN $\beta$ , exhibits high antiviral activity on human cells and is therefore not species specific.

#### **4.2.14 Antiproliferative activity of murine IFN $\epsilon$ on human cells**

As demonstrated in Chapter 4.2.13, murine IFN $\epsilon$  demonstrated considerable cross-species activity in an antiviral assay. To investigate if the cross-species activity of IFN $\epsilon$  was limited to antiviral activity, the potency of IFN $\epsilon$  in an anti-proliferative assay using the human cervical cancer cell line HeLa was determined. As a positive control, Rebif (a commercial human IFN $\beta$ -1a formulation) was included in all assays. Cells were treated for 72 hours with interferon and then cellular proliferation determined by MTT dye staining.

As demonstrated in Figure 4.16 mouse IFN $\epsilon$  exhibited potent antiproliferative action on HeLa cells where 50% growth inhibition was achieved with 37.47pmol/ml (95%CI: 12.76 - 110.1). To compare, Rebif elicited 50% growth inhibition with 0.029pmol/ml (95%CI: 0.011 - 0.079) and thus shows that mIFN $\epsilon$  is 1300-fold less potent at eliciting an antiproliferative effect in human HeLa cells than human IFN $\beta$  (Rebif). Interestingly, the anti-proliferative activity of mIFN $\epsilon$  on human cells is approximately 8 times higher than on mouse cells (see Chapter 4.2.4), suggesting that the biological activity of murine IFN $\epsilon$  on

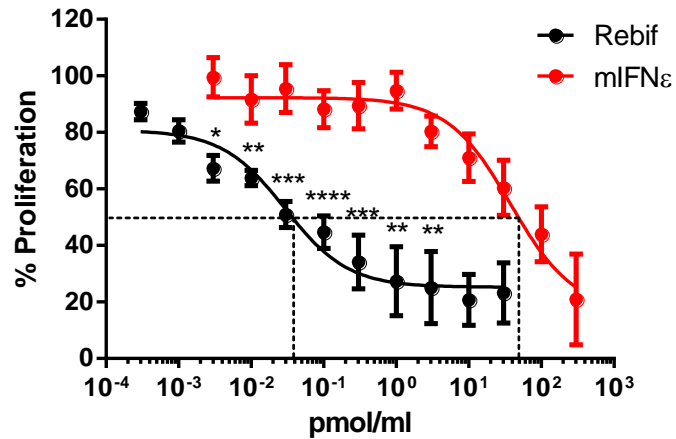


**Figure 4.16 Antiproliferative effect of murine IFN $\epsilon$  on human cells.** A dose response curve of the antiproliferative effect of IFNs on HeLa cells. HeLa human cervical cancer cell line was stimulated with either human IFN $\beta$  (Rebif) or mouse IFN $\epsilon$  for 72 hours and proliferation measured by MTT cell staining. The EC<sub>50</sub>s of interferons are indicated by dashed lines and were: Rebif, 0.029pmol/ml (95%CI: 0.011-0.079); IFN $\epsilon$ , 37.47pmol/ml (95%CI: 12.76-110.1). Data points denote the mean  $\pm$  SEM of 3 independent experiments performed in duplicate. \*, p < 0.05; \*\*, p < 0.01; \*\*\*, p < 0.001; \*\*\*\*, p < 0.0001. Statistical analyses were performed using two way ANOVA and represent significance between mIFN $\epsilon$  and hIFN $\beta$  at the indicated dose.

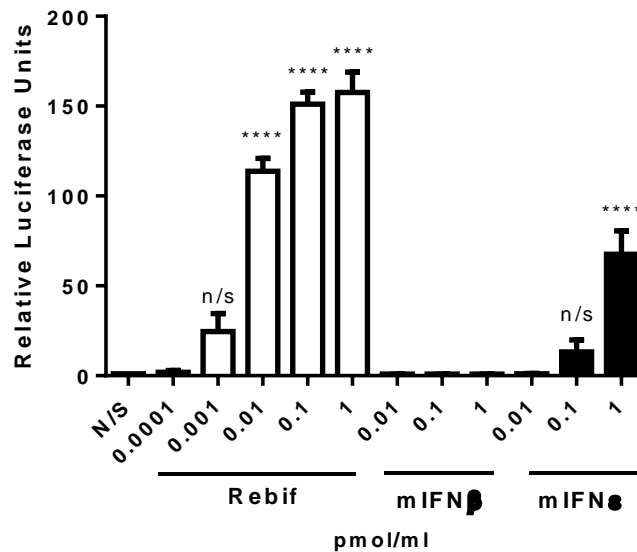
human cells is not restricted to antiviral activity, but that mouse IFNε is also able to elicit antiproliferative actions.

#### **4.2.15 Gene induction of human IRGs by murine IFNε**

As described in 4.2.15 and 4.2.16, murine IFNε was able to elicit biological activities in human cell lines, indicating cross-species activity. To further characterise this finding, it was important to evaluate the ability of IFNε to affect changes at the gene level. This was carried out by measuring luciferase expression under the control of ISRE and also by gene induction directly.

The human embryonic kidney cell line HEK293 stably transfected with an ISRE-luciferase construct was stimulated with Rebif, murine IFNβ or murine IFNε and luciferase activity measured after 16 hours (Figure 4.17A). All values were normalised to unstimulated control cells. Rebif was found to induce luciferase expression in a dose dependent manner from approximately 2-fold induction using 0.0001pmol/ml and up to 150-fold induction with 1pmol/ml. In contrast, murine IFNβ elicited no luciferase response even at the highest concentration of 1pmol/ml, consistent with the antiviral assay from 4.2.13. Consistent with the previously observed cross-reactivity of murine IFNε on human cells, IFNε induced the expression of ISRE driven luciferase in HEK293 cells. 0.01pmol/ml of IFNε did not lead to induction of luciferase however 0.1pmol/ml and 1.0pmol/ml induced luciferase expression approximately 15-fold and 70-fold, respectively. These results suggest that murine IFNε signals via the human cell surface receptors IFNAR1 and IFNAR2 to activate ISGF-3 and induce the expression of genes containing ISRE in their promoters.

A.



B.

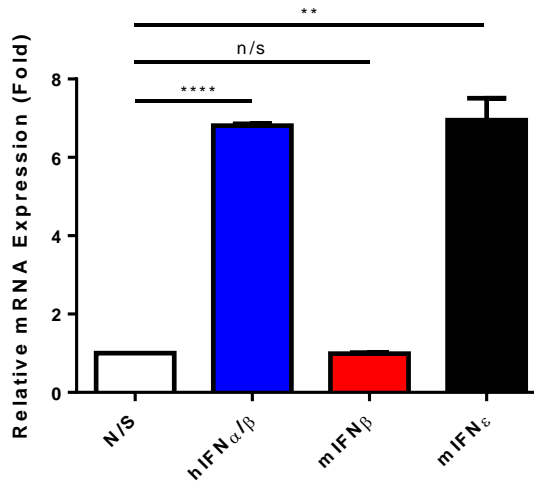


**Figure 4.17 Expression of interferon regulated genes in human cells induced by murine IFNs.** Histograms of the effect of mouse type I IFNs on IRG induction in human cells. **A)** HEK293 cells stably expressing ISRE-Luciferase were stimulated for 16hours with either Rebif (hIFNβ), mIFNβ or mIFNε and luciferase activity measured relative to unstimulated cells. Rebif and mIFNε induced luciferase expression whereas mIFNβ did not. Data are presented as mean ± SEM of three independent experiments performed in triplicate. n/s, not significant; \*\*\*\*,  $p < 0.0001$ . Statistical analyses were performed using one way ANOVA and represent significance of stimulated compared to unstimulated samples. **B)** The human cervical cancer cell line HeLa was stimulated with 1000IU/ml hIFNα/β, 50pmol/ml mIFNβ or 50pmol/ml mIFNε and expression of *OAS2* measured by qRT-PCR. hIFNα/β and mIFNε induced *OAS2* expression whereas mIFNβ did not. Data represents the mean ± SD of two independent experiments performed in triplicate. \*\*,  $p < 0.001$ ; \*\*\*\*,  $p < 0.0001$ . Statistical analyses were performed using student's t-test.

To evaluate if the signalling of murine IFN $\epsilon$  in human cells would lead to successful gene induction, HeLa cells were stimulated with 50pmol/ml of murine IFN $\beta$  or IFN $\epsilon$  (~24,000IU/ml as measured in a human bioassay) and gene induction measured by qRT-PCR. 1000IU/ml of human IFN $\alpha/\beta$  was run alongside as a positive control and all values were normalised to the expression of the housekeeping gene 18S. As seen in Figure 4.17B, human IFN $\alpha/\beta$  was able to induce the expression of the IRG *OAS2* approximately 7-fold. Consistent with the results obtained previously, murine IFN $\beta$  was not able to induce the expression of *OAS2*. As expected, stimulation of HeLa cells with mouse IFN $\epsilon$  led to a 7-fold increase in *OAS2* expression. Collectively, these findings demonstrate that mouse IFN $\epsilon$  is able to signal via the human cell surface receptor and canonical type I IFN pathway to induce the transcription of IRGs in human cells.

### 4.3 Discussion

The type I IFNs were discovered over 50 years ago and since then a vast body of work has led to the identification of additional functions besides antiviral activity [5]. Although belonging to the same gene family and signalling via the same surface receptor, no IFN appears to be identical to another in function or activity [5, 282]. One of the most classic examples is that of human IFN $\alpha$ 7, which is virtually unable to activate NK-cells and proposed to be an antagonist of IFN induced NK-cell activation [229]. Another unique aspect of the type I interferons is that many subtypes also demonstrate unique tissue expression profiles. For example IFN $\kappa$  is selectively expressed from keratinocytes and is strongly induced by viral infection [111] and IFN $\zeta$  was found to be highly expressed in T-lymphocytes of mice [313].

One of the most startling functions of any type I IFN is that of the ungulate IFN $\tau$ , which is expressed by the trophoectoderm of the developing foetus and signals to the maternal uterine environment to maintain pregnancy [24, 38]. IFN $\epsilon$  also demonstrates a unique tissue expression profile as it is constitutively and exclusively expressed in the female reproductive tract and is not induced by classical IFN activators such as TLR agonists or RLH signalling [114]. Although expressed in the female reproductive tract, IFN $\epsilon$  does not appear to have a role in pregnancy or development, as *Ifne1*<sup>-/-</sup> mice produce healthy and viable offspring [114]. Further characterisation of the IFN $\epsilon$  function required the production of recombinant protein as described in Chapter 3. This chapter investigates the characterisation of the novel murine IFN $\epsilon$ , determination of its biological activities and mechanisms of signal transduction.

As biologically active type I IFNs had been expressed from insect cells in the past, the potential for incorrect folding of insect cell expressed IFN $\epsilon$  was not a

major concern [273]. Nevertheless, we still investigated the secondary fold and found that IFN $\epsilon$ , much like the classical IFN $\alpha$ 1 and IFN $\beta$ , adopted an  $\alpha$ -helical fold. Although no crystal structure of IFN $\epsilon$  exists at the time of writing, the data obtained from the CD spectra and the structural modelling performed previously by our lab [13] strongly imply the conserved  $\alpha$ -helical bundle that IFNs adopt [206].

Some, but not all murine IFNs are glycosylated and previous reports confirm our own predictions that IFN $\epsilon$  does not carry any *N*-glycosylation sites [282]. When experimentally verified however, IFN $\epsilon$  did appear to demonstrate light glycosylation as seen by periodic acid-Schiffs staining (PAS). PAS staining of IFN $\epsilon$  was negligible compared to the heavily glycosylated IFN $\alpha$ 1 and IFN $\alpha$ 2, however insect cell expression systems have been shown to produce glycosylated products that differ from those produced in mammalian cells as they do not express the same glycosyltransferases [289, 314, 315]. It is plausible that IFN $\epsilon$  expressed in insect cells, specifically HighFive<sup>TM</sup> cells, carries carbohydrate side chains however IFN $\epsilon$  would need to be produced in mammalian cells to determine if this was an artefact of the expression system or if IFN $\epsilon$  is indeed lightly glycosylated. It is also possible that IFN $\epsilon$  is O-glycosylated as prediction software is only accurate in the context of N-linked glycosylation. Importantly, glycosylation of type I IFNs has been shown to be important for their stability and *in vivo* activity due to increased half-life [288, 316, 317]. Therefore, while glycosylation may not affect *in vitro* bioactivities directly, it may still play a role in terms of *in vivo* administration.

An interesting feature of type I IFNs is their unusual physiochemical stability, namely low pH [263]. This property was also apparent in IFN $\epsilon$ , with reductions in activity comparable to IFN $\alpha$ 1 and IFN $\beta$ . IFN $\beta$  has been reported to be more stable at acidic pH than at high temperatures, which was also evident in my

experiments [263]. While glycosylation of type I IFNs has been linked to their thermal stability [288, 316] the exact biological reason for this high stability is not known, it serves as another characteristic of type I IFNs.

The definitive characteristic of type I IFNs is their antiviral activity and it was the first biological activity of IFNε we investigated. Similar to a reported antiviral activity of human IFNε [248], the antiviral specific activity of mIFNε on L929 cells was demonstrated to be some 100-1000-fold less than IFNα1 or IFNβ. To date, IFNα7/10 has been shown to have the lowest antiviral activity among mouse IFNs [282] yet IFNε appears to be some 10-times less active than IFNα7/10. The low antiviral activity of IFNα7/10 has been attributed to residues between amino acids 68 and 123, specifically Val85 and Ser112, which are unique to IFNα7/10 among IFNαs. Interestingly, IFNε also has the Val85 residue however sequence alignment of IFNs shows little homology of IFNε to other type I IFNs in this region (Figure 4.18) and it is therefore difficult to tell if Val85 is solely responsible for the reduced activity of IFNε. While site directed mutagenesis could aid in discovering residues important for biological activity, investigating the interaction between IFNε, IFNε mutants and the two receptor subunits by surface Plasmon resonance (SPR) would also be required to provide more insightful data into the structure function relationship IFNε has with its receptors.

As IFNs are well characterised for their antiproliferative action, we investigated this activity in mouse fibroblast cells and found that IFNε was almost 300 times less active than IFNα1 and more than 5000-times less active than IFNβ. Previous reports have determined the antiproliferative activity of IFNβ to be higher than IFNα [12, 282], highlighting that our assay is suitable for investigating antiproliferative potential. While direct conclusions regarding the potential antiproliferative activity of IFNε in vivo cannot be drawn from these

		1	10	20	30	40
IFN- $\alpha$ 2	MARLCAFLVMLIVMS-YWSICSL	GC	DLPH	TYNLRN	KRAL	KVLAQMRR
IFN- $\alpha$ 11	MARLCAFLMLILIVMS-YWSTCSL	GC	DLPH	TYNLRN	KRAL	KVLAQMRR
IFN- $\alpha$ 4	MARLCAFLMLIVMMSYWSACSL	GC	DLPH	TYNLRN	GNKRAL	TVLEEMRR
IFN- $\alpha$ 1	MARLCAFLMVLAVMS-YWPTCSL	GC	DLPQ	THNLRN	KKIL	TLVQMR
IFN- $\alpha$ 6T	MARLCAFLMVLAVMS-YWSTCSL	GC	DLPQ	THKLRN	KRAL	TLIIQM
IFN- $\alpha$ 12	MARLCAFLMTLLVMS-YWSTCSL	GC	DLPQ	THNLRN	KRAL	TLLAQMR
IFN- $\alpha$ 14	MARLCAFLMTLLVMS-YWSTCCL	GC	DLPQ	THNLRN	KRAL	TLLVKMR
IFN- $\alpha$ 8/6	MARLCAFLMVLAVLS-YWPTCSL	GC	DLPQ	THNLRN	KRAL	TLLVKMR
IFN- $\alpha$ 5	MARLCAFLMVLAVLS-YWPTCSL	GC	DLPQ	THNLRN	KRAL	TLLVKMR
IFN- $\alpha$ 7/10	MARLCAFLMVLAVMS-YWPTCCL	GC	DLPQ	THNLRN	KRAL	TLLVKMR
IFN- $\alpha$ 13	MARPCAFMLVLVLS-YWSACSL	GC	DLPQ	THNLRN	KRAL	TLLAQMR
IFN- $\alpha$ 9	MARPF AFLMVLVVIS-YWSTCSL	GC	DLPQ	THNLRN	KKIL	TLLAQMR
IFN- $\zeta$	MLPVHLFLVGGVMLS-CSPASSL	DS	GKSD	SLHLER	SETAR	FLAELRS
IFN- $\kappa$	MTPKFLWLVALVALY-IPPIQSL	NC	VYLD	DSILEN	---VK	LLGST
IFN- $\beta$	--MNNRWILHAAFL-FCSTALS	SIN	YKQL	QLQERT	NI	RKQEL
IFN- $\epsilon$	--MVHRQLPETVLLVLSSTIFSL	EP	KRIP	PFQL	WMNR	ESLQL
		50	60	70	80	90
IFN- $\alpha$ 2	DNQIQKAQAIPVLRDLTQQTLN	LFTSK	ASSAA	QATLL	DSFC	NDLHQ
IFN- $\alpha$ 11	DAQQIKKAQAIPVLRDLTQQIL	NLFTS	KASSA	AWNAT	LLDS	FNCND
IFN- $\alpha$ 4	DNQIQKAQAAILVLRDLTQQIL	NLFTS	KDLSA	TWNAT	LLDS	FNCND
IFN- $\alpha$ 1	DAQQIQEAQAIPVLSSELTQQI	LTFSS	KDSSA	AWNAT	LLDS	FNCNE
IFN- $\alpha$ 6T	DTLKIQKEKAIPVLSSEVTQQI	LNIFT	SKDSS	AAWDAT	LLDT	FCNDL
IFN- $\alpha$ 12	DAQQIKKAQVIPVLSSELTQQI	LTFSS	KDSSA	AWNAT	LLDS	FNCND
IFN- $\alpha$ 14	DAQQIKKAQAIPVLSSELTQQI	LTFSS	KDSSA	AWDAT	LLDS	FNCND
IFN- $\alpha$ 8/6	GAQQIQEAQAIPVLTTELTQQI	LTFSS	KDSSA	AWNAT	LLDS	FNCND
IFN- $\alpha$ 5	GAQQIQEAQAIPVLSSELTQQV	LNIFT	SKDSS	AAWNAT	LLDS	FNCNE
IFN- $\alpha$ 7/10	DAQQIQEAQAIPVLSSELTQQI	LNIFT	SKDSS	AAWNAT	LLDS	FNCND
IFN- $\alpha$ 13	DAQQIKKAQAIPFVHELTTQQI	LTFSS	NDSSA	AWNAT	LLDS	FNCND
IFN- $\alpha$ 9	DAQQIQEAQAIPVLSSELTQQI	LTFSS	KDSSA	AWNAT	LLDS	FNCGL
IFN- $\zeta$	NITQMTLGETTSCYSQTLRQV	LHLFD	TEASRA	AHERAL	DQLL	SSLW
IFN- $\kappa$	YIQHMKR-EINAVSYRISSAL	TFNL	KGSIP	PVTEE	HWERI	RISGL
IFN- $\beta$	-TEKMQKSYTAFAIQEMLNQV	FLVFR	NNFST	GWNET	IIVR	LLDEL
IFN- $\epsilon$	SPHQYQEGQKAVVHEILQQI	FTLLQ	THGTM	GIWEE	NHIEK	VLAAL
		120	130	140	150	160
IFN- $\alpha$ 2	TQEDAL---LAVRKYFHRITVYL	REKKH	SPCAW	EVVRAE	VWRAL	SS---SVN
IFN- $\alpha$ 11	TQEDAL---LAVRIYFHSITVFL	REKKH	SPCAW	EVVRAE	VWRAL	SS---SVN
IFN- $\alpha$ 4	TQEDAL---LAVRTYFHSITVYL	RKKKH	SPCAW	EVVRAE	VWRAL	SS---STN
IFN- $\alpha$ 1	TQEDSL---LAVRTYFHRITVYL	REKKH	SPCAW	EVVRAE	VWRTL	SS---SAK
IFN- $\alpha$ 6T	TQEVSL---LAVRKYFHRITVYL	REKKH	SPCAW	EVVRAE	VWRAL	SS---SAN
IFN- $\alpha$ 12	TQEDSL---LAVRKYFHRITVYL	REKKH	SPCAW	EVVRAE	VWRTL	SS---SAK
IFN- $\alpha$ 14	TQEDSL---LAVRKYFHRITVYL	REKKH	SPCAW	EVVRAE	IWRAL	SS---SAK
IFN- $\alpha$ 8/6	TQEDSL---LAVRTYFHRITVFL	REKKH	SPCAW	EVVRAE	VWRAL	SS---SAK
IFN- $\alpha$ 5	TQEDSL---LAVRKYFHRITVYL	REKKH	SPCAW	EVVRAE	VWRAL	SS---SVN
IFN- $\alpha$ 7/10	TQEDSL---LAVRKYFHRITVFL	REKKH	SPCAW	EVVRAE	IWRAL	SS---SAN
IFN- $\alpha$ 13	TQEDSL---LAVRKYFHSITVYL	REKKH	SPCAW	EVVRAE	VQRTL	SS---SAN
IFN- $\alpha$ 9	TQEDSQ---LAMKKYFHRITVYL	REKKH	SPCAW	EVVRAE	VWRAL	SS---SVN
IFN- $\zeta$	CPLPFA---LAIRTYFRGFFRYL	KAKAH	SACSWE	IVRVQ	LQVDLP	---AF
IFN- $\kappa$	HSEDFLTVYLELGYFFRIKKFL	INKKY	SFCAW	KIVTVE	IRRCFI	IFSKR
IFN- $\beta$	TWEMSS-TALHLKSYZWRVQRYL	KLMKY	NSYAW	MVRAE	IFRNFLI	---IRR
IFN- $\epsilon$	SAQBLR---LQIKAFRRIHDFL	ENQRY	SSCAW	IIVQTE	IHRCM	FFVFR

**Figure 4.18 Amino acid sequence alignment of type I IFNs and their conserved residues.** Amino acid sequence alignment of mouse IFN $\alpha$ s, IFN $\beta$ , IFN $\zeta$ , IFN $\kappa$  and IFN $\epsilon$ . The numbering refers to the mature sequence of IFN $\alpha$ 1 and IFN $\alpha$ 2 and excludes the signal peptide. Black boxes show residues absolutely conserved in all type I IFNs aligned. The boxed residues highlight residues Val85 and Ser112. Figure adapted from [281].

experiments, the observation that IFN $\epsilon$  does elicit antiproliferative activity is another strong indicator that the signalling mechanisms activated by IFN $\epsilon$  are common among the type I IFNs.

At the commencement of this project, IFN $\epsilon$  was proposed to be a type I interferon based on chromosomal location, sequence homology and structural prediction only [13]. Type I interferons signal via the canonical type I IFN receptor complex composed of IFNAR1 and IFNAR2 and it is signalling through these receptors which is the defining feature of a type I IFN. Gene induction of the classical IRGs *Isg15*, *Irf7* and *Oas1a* by IFN $\epsilon$  was found to be absolutely dependent on the presence of each interferon receptor subunit as absence of either resulted in a loss of IRG transcription. Thus, IFN $\epsilon$  was demonstrated for the first time to be a member of the type I IFN family, satisfying the criteria of requiring both type I IFN receptor subunits to induce canonical IRGs. Surprisingly, given the reduced antiviral and antiproliferative activities of IFN $\epsilon$ , gene induction in BMDMs was comparable among IFN $\alpha$ 1, IFN $\beta$  and IFN $\epsilon$ . It is possible that the concentration of IFNs used, 0.1 $\mu$ g/ml (or 5pmol/ml) was sufficient to saturate the transcriptional interferon response in these cells and future work needs to determine if this was indeed the case. Further titration of IFNs should discern any differences in gene activation in these cells by each of the IFNs investigated.

Thus far, IFN $\epsilon$  has been shown to signal via the type I IFN receptor to induce classical interferon regulated genes, resulting in antiviral and antiproliferative outcomes. Another unique feature of type I interferons is their ability to signal via the transcription factor complex ISGF-3, which binds ISRE in the promoter of interferon regulated genes [117, 318]. IFN $\epsilon$  was able to induce the ISRE promoter in a luciferase reporter assay, indicating that it signalled via ISGF-3. However, this ISRE signalling was greatly lower than IFN $\beta$  and is consistent

with previous findings of low antiviral and antiproliferative biological activities. To investigate whether this reduced signalling by IFN $\epsilon$  was due to reduced transcription factor activation, STAT1 and 3 were investigated for activation by phosphorylation of tyrosine residues. Somewhat expectedly, STATs were only weakly activated by IFN $\epsilon$  and required much higher concentrations of protein than IFN $\alpha$ 1 and IFN $\beta$ . A hallmark of IFN induced receptor activation is the rapid phosphorylation of STATs 1 and 3 [12, 116]. Indeed, this was seen as early as 5 minutes with the major difference that unlike IFNs - $\alpha$ 1 and - $\beta$ , maximal STAT phosphorylation with IFN $\epsilon$  was not seen until 15-30 minutes after stimulation. This finding would suggest that IFN $\epsilon$  is a more slowly acting IFN, at least initially. However receptor interaction studies need to be performed to investigate whether the slower activation is due to altered receptor binding kinetics or reduced affinity. In the case of the latter, the STAT phosphorylation induced by IFN $\epsilon$  did not appear to differ in duration of activation to the other type I IFNs, which is known to reduce significantly by 2-3 hours [116]. This means that even if IFN $\epsilon$  bound the receptors with reduced affinity, eliciting maximum STAT activation at a later time point compared to IFN $\alpha$ 1 and IFN $\beta$ , it didn't result in a prolonged response. The vast body of work investigating IFN receptor interaction suggests that receptor density, receptor-ligand affinity, receptor-ligand interaction and ligand dissociation time all contribute to biological activity [8-10, 12, 319]. More detailed studies are clearly needed to further elucidate the signalling mechanisms of IFN $\epsilon$ , particularly receptor engagement.

Type I IFNs are potent inducers of MHC class I expression, leading to increased presentation of cellular antigens [178, 320, 321]. IFN $\epsilon$  was shown to increase MHC-I levels in a dose dependent manner however this was 100-300x lower compared to IFN $\alpha$ 1 and IFN $\beta$ .

Further investigation of immunoregulatory activities demonstrated that IFNε was able to activate splenic CD4<sup>+</sup>, CD8<sup>+</sup>, B220<sup>+</sup> and NK1.1<sup>+</sup> positive cells (such as CD4<sup>+</sup> T cells, CD8<sup>+</sup> T cells, B cells and NK-cells, respectively). In particular, IFNε displayed a greater ability to activate NK and B cells than CD4<sup>+</sup> and CD8<sup>+</sup> T cells. Consistent with previous studies, IFNα and IFNβ activated all cell types analysed [181, 322, 323]. Similar to other biological assays performed thus far, IFNε was approximately 300 times less potent than IFNα1 and IFNβ at inducing CD69 expression.

CD69 is a marker on T-cells for early T cell receptor (TCR) signalling and its expression is inducible on B-cells and NK-cells [181, 309, 324]. Importantly CD69 expression has been shown to be upregulated strongly by type I IFNs [308, 325]. Mice infected with vaccinia-virus (VV) designed to express mouse IFNε have previously been reported to demonstrate lower viral burden and disease pathology than control virus in a model of lung infection. This beneficial outcome was found to be due to elevated cytotoxic T lymphocytes expressing CD69 [251]. Critically however, the beneficial outcome in these disease models cannot be directly attributed to IFNε as IFNε protein levels were not measured. In a previous study this group also found that VV-IFNε induced the expression of CD69 on B220<sup>+</sup> cells, which was found to be higher compared to CD8<sup>+</sup> T cells [250]. Our data now shows that recombinant IFNε induces CD69 on the surface of immune cells and that this effect is indeed more pronounced on B220<sup>+</sup> cells compared to CD8<sup>+</sup> cells. While work presented in this thesis and by others [114, 248, 250] suggests that IFNε may be a weaker type I IFN compared to IFNα or IFNβ, reproductive tract specific models of immune function need to be employed to more thoroughly characterise IFNε as a mucosal cytokine.

Given the therapeutic use of other type I IFNs, it was important to investigate the therapeutic potential of IFN $\epsilon$  *in vivo*. Intraperitoneal injection of IFN $\epsilon$  in mice led to a marked upregulation of IRGs in peritoneal exudate cells, indicating *in vivo* pharmacodynamics. However, due to the unique expression of IFN $\epsilon$  in the female reproductive tract [13, 114] we felt it was important to investigate a route of administration reflective of the environment it was naturally expressed in. Intravaginal administration of IFN $\epsilon$  led to significant increases in IRG expression in the vagina. This shows that IFN $\epsilon$  engages the type I IFN receptor of vaginal cells to regulate immunity and that intravaginal treatment could be a viable mode of administration in future studies of reproductive tract disease such as viral and bacterial infection. Importantly, endogenous IFN $\epsilon$  did not appear to affect the potency of exogenously administered IFN $\epsilon$  in this experiment. IRG levels pre-IFN $\epsilon$  treatment between WT and IFN $\epsilon$  deficient animals as well as post-IFN $\epsilon$  treatment did not differ. This is important considering continued basal IFN $\epsilon$  signalling could have negatively affected induction of IRGs.

Further investigations of the use of IFN $\epsilon$  as a treatment *in vivo* need to determine the pharmacokinetics and bioavailability of IFN $\epsilon$  to see if it differs from IFN $\alpha$  and IFN $\beta$ . Given the close structural homology of type I IFN subtypes, it is interesting to note that the pharmacokinetics of IFN $\alpha$ 2 and IFN $\beta$  differ significantly in humans. For instance the terminal half-life of IFN $\alpha$ 2 is 4-16 hours, whereas for IFN $\beta$  it's 1-2 hours [326]. Similarly, the bioavailability of IFN $\alpha$ 2 has been reported to reach 80% after subcutaneous and intramuscular injections [327] while only reaching 27 and 30% respectively for IFN $\beta$  [328]. The much reduced bioavailability of intramuscular injected IFN $\beta$  compared to IFN $\alpha$ 2 has been proposed to be a reason for the lack of a beneficial effect in chronic hepatitis C patients [329]. We have recently shown that intravaginal

administration of equal IU of IFN $\alpha$ 1, IFN $\beta$  and IFN $\epsilon$  resulted in the upregulation of IRGs that wasn't different between IFN treatments [114]. This suggests that at least in the vagina, the pharmacodynamics of IFN $\epsilon$  do not differ to IFN $\alpha$ 1 or  $-\beta$ . Given that the sequence homology of IFN $\epsilon$  is ~30% to either IFN $\alpha$  or  $-\beta$ , and the profound differences in pharmacokinetics between IFN $\alpha$  and  $-\beta$ , it would be interesting to determine the pharmacokinetics and bio-availability of IFN $\epsilon$  to help improve current therapies.

One of the earliest discovered features of IFNs was their species specificity, that is, IFN from one species demonstrates weaker activity on cells of another species [311, 330]. Our results highlight that IFN $\epsilon$  does not appear to be limited by species specificity as are other type I IFNs. In fact, the observed antiviral activity (and also antiproliferative activity) of mouse IFN $\epsilon$  on human cells was greater than that observed for mouse cells. This is not the first report of such an observation, as human leukocyte interferon (IFN $\alpha$ ) was found to exhibit greater activity on bovine cells than human cells [331]. Our experiments have also shown that mouse IFN $\alpha$ 1 demonstrates some, yet weaker, activity on human cells, while mouse IFN $\beta$  does not, which is in agreement with previous studies [312]. Although the precise mechanisms that confer cross-species activity are not elucidated, there are some hints. For one, the type I IFN family as a whole is structurally conserved and alignment of the existing crystal structures of ovine IFN $\tau$ , human IFN $\alpha$ 2 and murine IFN $\beta$  demonstrate remarkable overlap, with only minor differences [210, 332]. These differences however are in critical areas found to be important for receptor binding. In a study by Kumaran *et al* [333], through the use structural modelling it was found that human IFN $\alpha$ 8, an IFN active on mouse cells shared structural similarities in receptor binding areas with mouse IFN $\alpha$ 4 but not the non-cross reactive human IFN $\alpha$ 2. This therefore suggests that there

are residues and/or binding sites on the IFN molecule that confer activity in other species.

Our findings indicate that IFN $\epsilon$  is able to activate the human IFN receptor, whereas IFN $\alpha$  or  $-\beta$  are not, suggesting that IFN $\epsilon$  has some profound structural differences that confer this cross-species activity. Further work involving receptor interaction studies of IFN $\epsilon$  mutants with both human and mouse receptors using surface Plasmon resonance and crystallography could help in determining which residues are responsible for cross-species activity. Mutating these residues would provide a great resource for future IFN structure function studies and rational drug design as currently a number of IFN mutants are used for determining how receptor engagement correlates with biological activity [9, 10, 233].

## 4.4 Conclusion

This chapter outlined the characterisation of murine IFN $\epsilon$  expressed from insect cells alongside IFN $\alpha$ 1 and IFN $\beta$ . We define here for the first time that IFN $\epsilon$  is a type I IFN as it required the cell surface receptors IFNAR1 and IFNAR2 to induce gene transcription via STATs. IFN $\epsilon$  treatment induced an antiviral state in cells much like IFN $\alpha$ 1 and IFN $\beta$ , however at reduced potencies. This reduction in potency was also seen throughout the biological assays investigated, including antiproliferative, transcription factor activation and immunoregulatory activities. Importantly, I have also demonstrated that IFN $\epsilon$  can be used *in vivo* to induce the transcription of IRGs, providing clear evidence of pharmacodynamics.

Although we have not presented data on receptor binding, given published data it is likely that IFN $\epsilon$  engages the receptor complex in a different manner to IFN $\alpha$ 1 and IFN $\beta$ . Future studies into the receptor binding mechanics of IFN $\epsilon$  would aid greatly in strengthening our knowledge of this novel cytokine and its biological function.

## **Chapter 5 – Generation and characterisation of anti-IFN $\epsilon$ mAbs**

### **5.1 – Introduction**

The previous chapters investigated the expression and characterisation of recombinant IFN $\epsilon$  to determine its biological activities and signalling pathways. I found that recombinant IFN $\epsilon$  demonstrates hallmark type I IFN biological activities such as antiviral and antiproliferative activity and that IFN $\epsilon$  could be administered *in vivo* to elicit the induction of interferon regulated genes. Due to the novelty of IFN $\epsilon$  however, reagents for its study are lacking and this thesis aimed to address this shortcoming. Therefore to further characterise IFN $\epsilon$ , I sought to generate monoclonal antibodies against IFN $\epsilon$  and identify their uses in common immunological and biochemical techniques such as immunohistochemistry, immunoprecipitation, affinity chromatography and western blotting. While antibodies are often generated against partial epitopes or synthetic peptides, using the recombinant IFN $\epsilon$  I produced in this thesis allows me to generate antibodies against correctly folded, biologically active protein and thus providing a greater potential for antibodies to conformational epitopes and suitable for the characterisation of this novel cytokine.

Antibodies can be generated in two forms; polyclonal and monoclonal. Polyclonal antibodies (pAbs) are a mixture of antibodies from multiple antibody producing cells and may therefore comprise multiple antibodies recognising different epitopes of the same antigen. A major advantage of polyclonal antibodies is that they can be generated quickly and do not need to be further subcloned or purified. A disadvantage of polyclonal antibodies is

that they are often not specific to a single protein as they can bind epitopes that may be conserved among protein family members. They therefore need to be carefully screened against homologous proteins to ensure specificity.

Monoclonal antibodies (mAbs) can be generated by a number of ways however the strategy employed for this thesis was fusing mouse splenic B-cells with a myeloma cell line. Fusion of an antibody secreting B-cell with a myeloma cell results in the generation of an immortal antibody producing hybridoma cell. Individual hybridoma cell lines are purified and expanded and therefore each hybridoma (cell line) is only capable of producing one antibody. As such, mAbs recognise a specific epitope of a protein and are therefore more specific than polyclonal antibodies. This is advantageous for the study of large protein families where one protein needs to be discerned from others sharing similar amino acid sequence, such as the type I IFNs. Furthermore, hybridomas are stable cells that can be frozen and thawed, and they secrete large amounts of antibody into the supernatant, thus allowing increasing scale of production.

Antibodies are used for a variety of techniques such as western blotting, ELISA, immunoprecipitation, neutralisation of biological activity and immunoaffinity purification. These assays are necessary to fully characterise the function of IFNε. For example western blotting of IFNε protein enables us to monitor expression in our recombinant expression system and also potentially detect IFNε protein in tissue lysates. An IFNε specific ELISA would enable us to monitor quantities of recombinant IFNε during expression and purification and more importantly, an ELISA specific for IFNε is essential in determining the expression levels of IFNε *in vivo*, which so far has not been measured. In addition, while IFNε mRNA has been shown to be highly

expressed in the uterus [13], IFN $\epsilon$  producing cells were only identified using mAb produced in this thesis and will be discussed further herein [114].

The aim of this chapter is to describe the generation and characterisation of anti-IFN $\epsilon$  monoclonal antibodies. Their use in techniques such as western blotting, immunohistochemistry, neutralisation and immunoprecipitation, among others will be investigated. Importantly, I will be able to determine the specificity of these antibodies towards IFN $\epsilon$  as IFN $\beta$  produced in this thesis will be used as a negative control. Overall, the production and characterisation of these novel antibodies against IFN $\epsilon$  will provide another tool with which to study the function of this novel cytokine.

## 5.2 Results

### 5.2.1 Generation of monoclonal antibodies against IFN $\epsilon$

We followed a standard method for immunising mice for the generation of antibodies which is outlined in Figure 5.1. Importantly, while it is possible to elicit an immune response to mouse antigen in a mouse if given at high enough concentration, we used *Ifne1<sup>-/-</sup>* mice because we wanted to generate the most diverse immune response possible and therefore using IFN $\epsilon$  deficient mice would lead to the immunisation with a foreign antigen. A similar strategy was successfully used to generate IFNAR1 mAbs, where a plasmid encoding the extracellular domain of IFNAR1 was injected into *Ifnar1<sup>-/-</sup>* mice [334].

The immunogen was prepared by mixing 16 $\mu$ g of denatured and 16 $\mu$ g of native His<sub>6</sub>-IFN $\epsilon$  protein with CpG DNA, adjuvant and diluted in PBS. Two male C57Bl/6 *Ifne1<sup>-/-</sup>* mice were injected intraperitoneally every two weeks for a total of three injections. All animal injections and subsequent test bleedings were performed by Dr. Niamh Mangan (MIMR, Clayton, Australia).

Following the immunisation cycle, mice were bled and the serum analysed for anti-IFN $\epsilon$  immunogenicity by serum ELISA as described in 2.6.2. Comparing pre-immunisation with post-immunisation sera at either dilution, both mice injected with IFN $\epsilon$  antigen produced high levels of antibodies (Figure 5.2). Overall, mouse P1 demonstrated higher antibody levels than mouse P2. For instance mouse P1 demonstrated antibody levels over 4-fold higher after vaccination compared to pre-vaccination at a serum dilution of 1:250. In contrast, mouse P2 exhibited antibody levels 3-fold higher post-vaccination compared to pre-vaccination at a dilution factor of 1:250. Dilution of the sera to 1:1250 demonstrated that mouse P1 had higher serum antibody levels

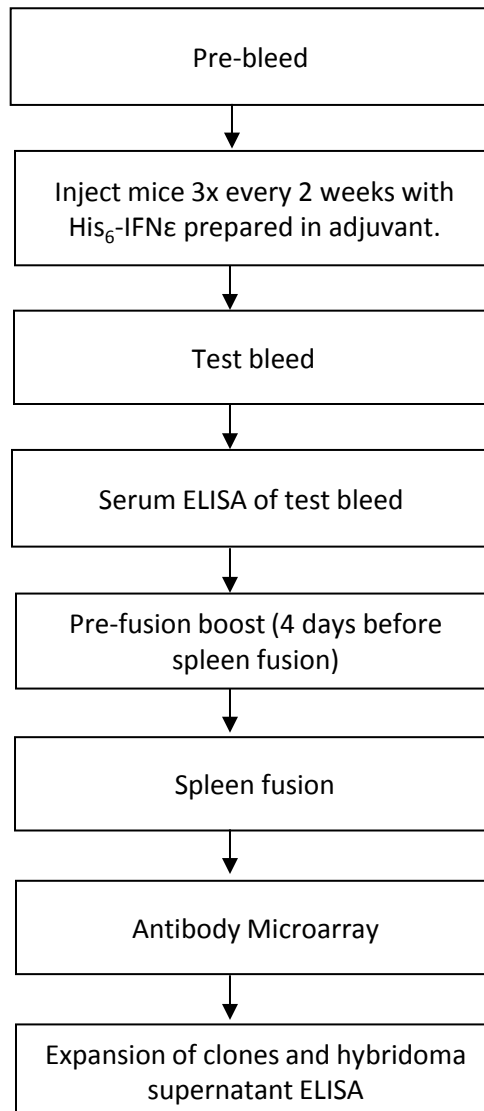


**Figure 5.1 IFNε monoclonal antibody generation strategy.** A flowchart outlining the steps undertaken to generate anti-IFNε monoclonal antibodies by the Monash Antibody Technologies Facility (MATF). Mice were injected intraperitoneally with recombinant His<sub>6</sub>-IFNε protein.

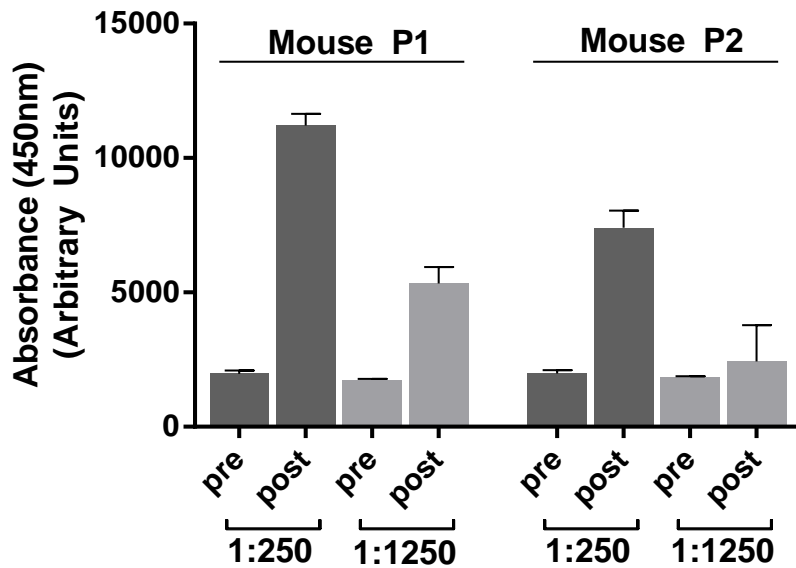


**Figure 5.2 IFN $\epsilon$  Serum ELISA of mice immunised with His<sub>6</sub>-IFN $\epsilon$ .** A bar graph depicting the antibody response from mice bled before and after immunization with His<sub>6</sub>-IFN $\epsilon$  as measured by serum ELISA. C57Bl/6 *Ifne1*<sup>-/-</sup> mice were immunised with recombinant His<sub>6</sub>-IFN $\epsilon$  protein (Mouse P1 and P2) for 6 weeks every second week. Samples were diluted 1:250 or 1:1250 as indicated. Mice immunised with His<sub>6</sub>-IFN $\epsilon$  produced a potent immune response where mouse P1 demonstrated the highest antibody response against IFN $\epsilon$  at both dilutions. Data are the mean  $\pm$  SD of triplicates.

compared to naive sera than mouse P2 and was thus selected for splenic cell fusion.

4 days before spleen fusion, mouse P1 received a pre-fusion boost of His<sub>6</sub>-mIFN $\epsilon$  protein. All antibody work including splenic fusion, hybridoma selection and initial hybridoma screening was performed by the Monash Antibody Technologies Facility (Monash University, Clayton, Australia).

### **5.2.2 Anti-IFN $\epsilon$ hybridoma screening by supernatant ELISA**

At day 11 post-fusion of splenic B-cells with Sp2 myeloma, antigen microarray assay (AMA) was performed by MATF on supernatants using a mixture of Cy3-conjugated goat  $\alpha$ -mouse IgG and Cy5-conjugated goat  $\alpha$ -mouse IgM at 1:1000 dilution. Clones positive for IgG were further expanded and validated by hybridoma supernatant ELISA. Throughout this process, an unrelated N-terminally hexahistidine tagged protein was used as a negative control to select clones only positive for IFN $\epsilon$  and remove clones recognizing the His<sub>6</sub>-tag.

An ELISA was performed by MATF on 46 candidate anti-IFN $\epsilon$  hybridoma clones previously identified by antibody microarray assays (Figure 5.3A). To select hybridomas producing a specific response towards IFN $\epsilon$ , any sample found to exhibit a 3-fold or greater ratio in absorbance against an unrelated hexahistidine tagged protein was considered a positive clone (Figure 5.3A, highlighted in blue). In this initial screen performed by MATF, 12 clones were found to produce IFN $\epsilon$  antibodies with 7 clones producing ratios over 6-fold greater than unrelated antigen. These 7 clones, identified as B5, C3, C4, D6, E6, G5 and H2 were subsequently expanded by MATF for delivery. To increase the potential pool of anti-IFN $\epsilon$  antibodies, the remaining 39 clones

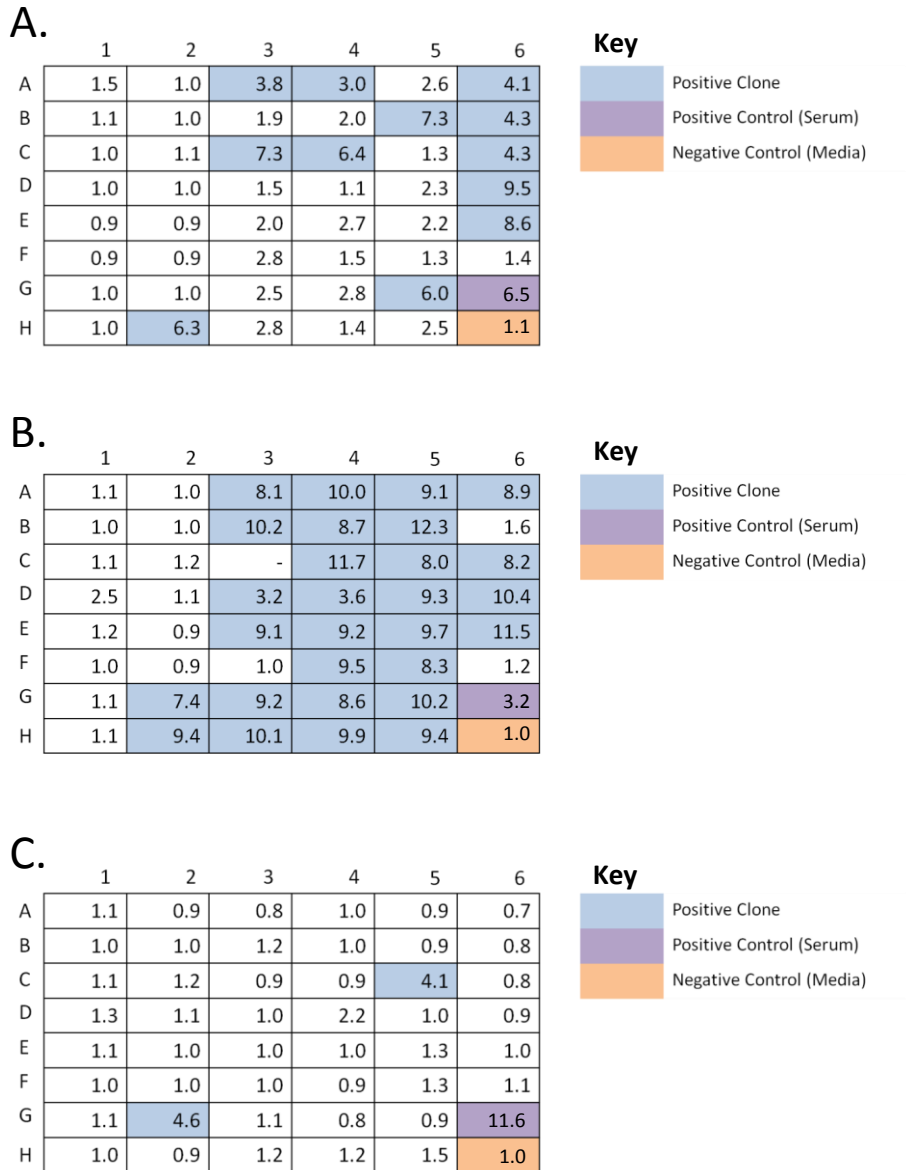


**Figure 5.3 Anti-IFN $\epsilon$  Hybridoma supernatant ELISA.** Tables summarising the ability of antibody clones to detect IFN $\epsilon$  in ELISAs. Values denote the relative fold detection of IFN $\epsilon$  by antibody compared to the indicated control protein. **A)** Supernatant ELISA performed by MATF against His $_6$ -IFN $\epsilon$  and an unrelated protein with N-terminal hexahistidine tag. **B)** Hybridomas were grown to  $\sim 1.3 \times 10^6$  cells/ml and the supernatant assayed for IFN $\epsilon$  antibodies by ELISA against His $_6$ -IFN $\epsilon$  and His $_6$ -IFN $\beta$ . **C)** Supernatant ELISA of hybridoma clones against fresh His $_6$ -IFN $\epsilon$  and 8-week old His $_6$ -IFN $\epsilon$  used at time of immunisation. Positive clones are clones where the ratio of anti-IFN $\epsilon$  compared to negative control protein are above 3.0 and are shaded in blue. Clones with values  $\sim 1.0$  indicate a signal close to baseline for the same clone detecting the control protein. Data are a representative of three independent experiments.

were to be re-assessed by us using the same supernatant ELISA protocol. Microscopic evaluation and trypan blue staining of the microtitre plate containing the hybridoma clones used for ELISA in Figure 5.3A revealed that some wells contained very few live cells (viability ranged from 0 to 80%) while others were confluent and viable. To minimise false negative readings due to low viability or slow growth of individual clones, all 46 hybridomas originally screen by MATF were expanded to  $\sim 1.3 \times 10^6$  cells/ml and the ELISA repeated using His<sub>6</sub>-IFN $\beta$  as the negative control. Like in 5.3a, the assay was analysed by normalising the obtained absorbance value detecting IFN $\epsilon$  against the signal obtained from detecting His<sub>6</sub>-IFN $\beta$ . Any fold-ratio of IFN $\epsilon$  vs. His<sub>6</sub>-IFN $\beta$  greater than 3 was considered a positive signal. After growing up the supernatants at MIMR, we identified more hybridoma clones producing anti-IFN $\epsilon$  antibodies (Figure 5.3B) than originally found in the screening performed by MATF (Figure 5.3A). As such, 28 clones were found to have over 3.0-fold increase in absorbance compared to the negative control with 26 of these clones having a ratio of over 7.0. Indeed, additional clones found in this assay exhibited higher absorbance compared to the original 12 positive clones in Figure 5.3A. For example clone H3, which was not among the positive candidates in the initial screen (Figure 5.3A) demonstrated an absorbance 10.1-fold higher than His<sub>6</sub>-IFN $\beta$  and this was higher than five of the original clones identified by MATF which were believed to be the best candidates for further characterisation. Overall, 28 of the hybridoma cell lines were found to produce a specific signal for IFN $\epsilon$  and did not detect His<sub>6</sub> or His<sub>6</sub>-IFN $\beta$ .

Experiments performed during this thesis indicated that IFN $\epsilon$  lost biological activity after prolonged storage at 4°C. All previous hybridoma supernatant ELISAs (Figure 5.3A and B) were performed on the same batch of His<sub>6</sub>-IFN $\epsilon$  protein to ensure reproducible results. To investigate and account for

potential batch to batch variation of expressed His<sub>6</sub>-IFN $\epsilon$  protein we compared ELISAs from less than a week old His<sub>6</sub>-IFN $\epsilon$  that was stored at 4°C to the preparation that was used for the immunisations and was stored at 4°C for 8 weeks (Figure 5.3C). Interestingly, hybridoma clones C5 and G2 had 4.1 and 4.6-fold increases in absorbance, respectively when comparing the fresh His<sub>6</sub>-IFN $\epsilon$  prep to the 8-week old prep. This suggests that these two antibodies might recognise an epitope of IFN $\epsilon$  that is lost during prolonged storage at 4°C.

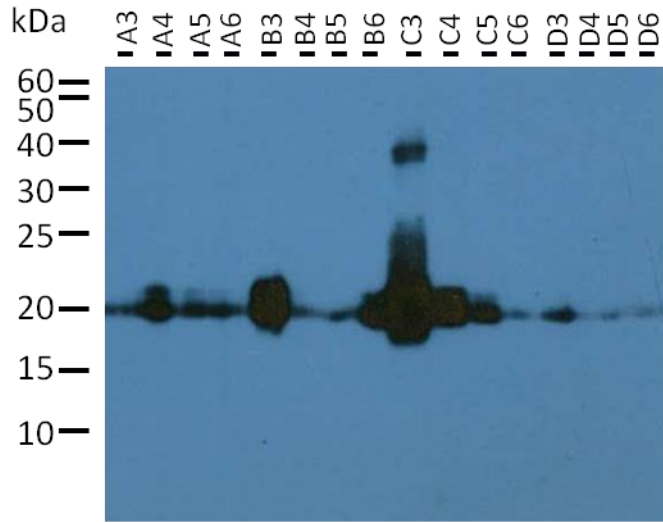
### **5.2.3 Anti-IFN $\epsilon$ mAbs exhibit different abilities to detect His<sub>6</sub>-IFN $\epsilon$ by western blot**

One of the most common applications of antibodies is their use as detection reagents in western blotting. Western blotting is a common method for the detection of a protein in a sample and is often used to determine the approximate Mr (molecular weight approximation of a protein based on mobility) on reducing SDS-PAGE. Furthermore, it is often used for the semi-quantitative estimation of protein levels in a sample (such as tissue lysates) when run alongside known quantities. It is therefore important to screen hybridomas to find antibodies that are able to recognise denatured protein on SDS-PAGE gels.

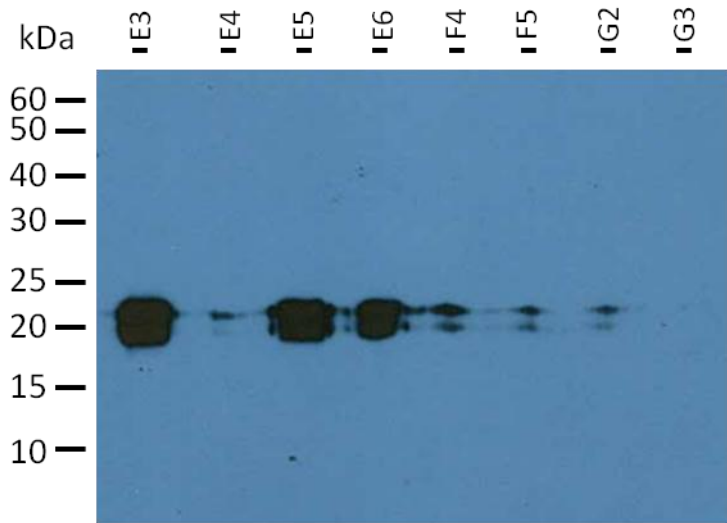
Thirty of the antibody supernatants were investigated for their ability to detect 0.1 $\mu$ g of His<sub>6</sub>-IFN $\epsilon$  by western blot. These thirty supernatants all came from clones found to produce a positive signal towards His<sub>6</sub>-IFN $\epsilon$  by ELISA but not His<sub>6</sub> tagged IFN $\beta$  (see Chapter 5.2.2). Supernatant from clone C3 was found to demonstrate the strongest western blot signal, followed by clone H3 (Figure 5.4). Both antibodies recognised a protein at ~22kDa which corresponds to

**Figure 5.4 Western blotting of recombinant His<sub>6</sub>-IFNε using α-IFNε mAbs.** Hybridomas were grown to ~1.3x10<sup>6</sup> cells/ml and the supernatant assayed for their potential to detect 100ng/well His<sub>6</sub>-IFNε by western blot. **A)** Hybridoma Clones A3 – D6. **B)** Hybridoma clones E3 – G3. **C)** Hybridoma clones G4 – H5. Unconditioned hybridoma media did not produce a positive signal.

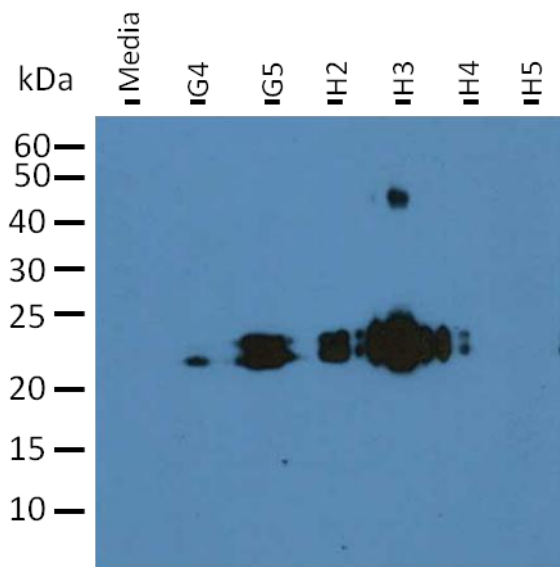
A.



B.



C.



the expected size of His<sub>6</sub>-IFN $\epsilon$ . Although His<sub>6</sub>-IFN $\epsilon$  is expected to only migrate as a single moiety, previous expressions have resulted in the presence of two protein bands (see Figure 3.7), which can also be seen in the western blot data. In addition to this finding, supernatants C3 and H3 recognised a higher molecular weight protein at approximately 40kDa. This band was also on occasion found in His<sub>6</sub>-IFN $\epsilon$  expressions and purifications (See Figures 3.6 and 3.7) and could be the result of protein dimerisation. Interestingly, our laboratory often identifies a high molecular weight isoform of mIFN $\alpha$ 1 at approximately twice the mass of the single mIFN $\alpha$ 1 isoform in highly concentrated samples expressed from *P. pastoris* and suggests that other type I IFNs also have this propensity to dimerise (N.E. de Weerd, unpublished data). Supernatants B3 and E3 were found to demonstrate the next highest signal, followed by B6, C4, E5, E6 and G5. Many of the other clones demonstrated lower levels of western blot signal and supernatants from clones D6, G3 and H5 showed no signal by western blot even though their ELISA signals were highly positive (Figure 5.3). This suggests that an epitope found on native IFN $\epsilon$  is lost during denaturation and is therefore no longer recognised by these particular antibodies. Thus far, ELISA signal strength does not appear to correlate with western blot signal strength.

#### **5.2.4 Identifying IFN $\epsilon$ antibody pairs for ELISA**

Enzyme Linked Immunosorbent Assays (ELISAs) are common assays used both in laboratory work and clinical diagnostics. They rely on the specific interaction formed between an antibody and its antigen. Although ELISAs can be performed with just one antibody to detect antigen (see Chapter 5.2.2 for supernatant ELISA) a much more sensitive and specific application is what is colloquially known as a sandwich ELISA, which utilises a capture antibody to

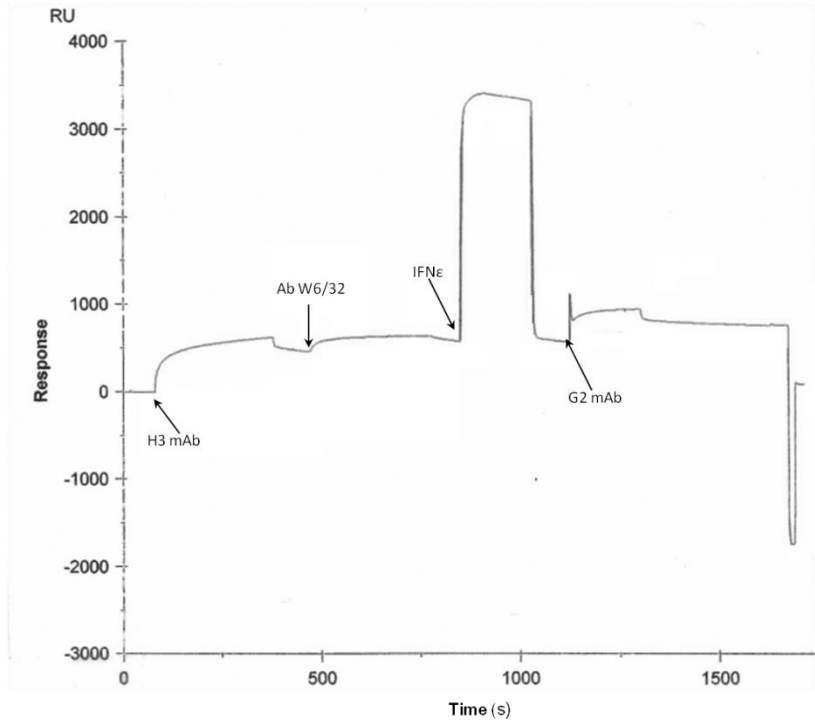
bind the protein of interest and a conjugated detection antibody to detect the protein. Studies examining IFN $\epsilon$  would greatly benefit from the ability to measure protein concentration in biological fluids such as serum and vaginal lavage and we therefore aimed to discover antibody binding pairs suitable for use in ELISA.

A commonly used approach for the identification of antibody binding pairs is the use of Surface Plasmon Resonance (SPR). SPR is a method that measures the non-covalent interaction of a molecule in solution passing over an immobilized ligand on a sensor surface (generally a gold film) in real time. This is achieved by a light source exciting the charged surface of the metal film and a detector measuring the angle of reflected light. Macromolecules adsorbing (or desorbing) the sensor surface, either directly via chemical coupling or via interactions with an immobilised compound result in a measurable change in refractive index. This measurable change in refraction is dependent only on the concentration/mass of analyte and therefore does not require labelling of compounds [335, 336]. Overall, this information allows the calculation of binding affinities between two compounds and their subsequent rate of dissociation. In the context of antibody interactions, SPR can be used to identify antibody binding pairs by the stepwise adsorption of capture antibody, ligand and detection antibody [337].

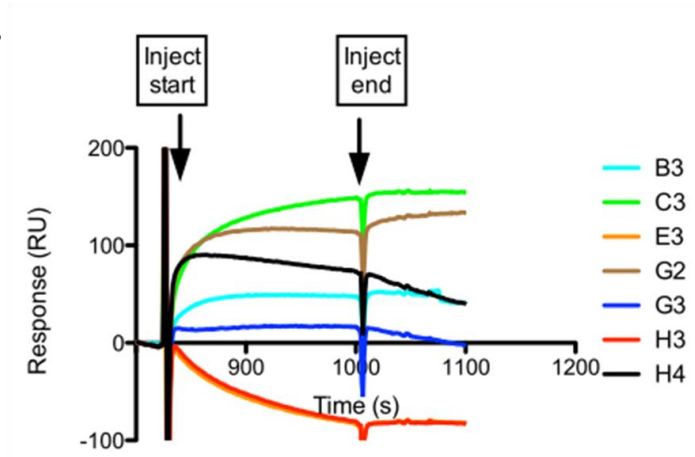
For our purposes, a polyclonal rabbit anti-murine IgG antibody was immobilised to the surface of a BIAcore chip by primary amine linkage. Then protein G-affinity purified H3 anti-IFN $\epsilon$  antibody was washed across and the binding measured (Figure 5.5A). All SPR experiments were carried out by Dr. Travis Beddoe (Monash University, Clayton, Australia). Addition of H3 antibody resulted in a rapid exponential response and is indicative of the antibody H3 binding the immobilised anti-IgG antibody. As more H3 antibody

**Figure 5.5 Identification of IFN $\epsilon$  antibodies binding different epitopes of IFN $\epsilon$ .** Surface plasmon resonance (SPR) traces of response (y-axis) over time (x-axis) when anti-IFN $\epsilon$  antibodies were analysed for their ability to bind separate epitopes of IFN $\epsilon$ . **A)** The SPR trace indicates the response of molecules binding to the BIAcore chip over time. An increase in positive response indicates a molecule binding whereas a reduction in response indicates dissociation of molecules from the BIAcore chip surface. In this experiment, injections of coating antibody (H3 mAb) followed by blocking mAb (Ab W6/32), IFN ligand (IFN $\epsilon$ ) and detection antibody (G2 mAb) are indicated on the graph. **B)** 7  $\alpha$ -IFN $\epsilon$  antibodies were evaluated for their ability to detect immobilised IFN $\epsilon$  using SPR. H3 mAb, Ab W6/32 and His<sub>6</sub>-IFN $\epsilon$  were immobilised as in Part A and subsequently each individual antibody injected to determine the ability to bind “captured” IFN $\epsilon$ . All mAbs with the exception of E3 (orange) and H3 (red) elicited an increase in response, indicating their ability to bind IFN $\epsilon$  once captured by H3 mAb.

A.



B.



is bound by the anti-IgG, the slower the reaction proceeds and is marked by the much slower increase in response seen at around 250s. Ab W6/32 blocking antibody was washed across the chip to block remaining available anti murine Fc sites. Addition of His<sub>6</sub>-IFN $\epsilon$  elicited a sharp secondary response peak, suggesting that His<sub>6</sub>-IFN $\epsilon$  successfully bound to the immobilised H3 antibody. The plateauing seen at approximately 800s is indicative of the equilibrium reached between free IFN $\epsilon$  binding to immobilised H3 and captured IFN $\epsilon$  spontaneously dissociating from H3. The subsequent decrease in signal at around 1000s reflects IFN $\epsilon$  dissociating from the bound H3 antibody. Lastly, injection of protein G-affinity purified G2 antibody was found to elicit an additional signal increase, suggesting binding to the immobilised IFN $\epsilon$ . Thus H3 and G2 antibodies could simultaneously bind IFN $\epsilon$  and is suggestive of the two antibodies binding different epitopes of the protein.

To find additional antibodies binding a different epitope to H3, equal quantities of protein G-affinity purified antibody from hybridoma supernatants B3, C3, E3, G2, G3, H3 and H4 were washed across the immobilised H3/His<sub>6</sub>-IFN $\epsilon$  complex (Figure 5.5B). C3 antibody produced the highest signal with approximately 150 resonance units (RU). G2 antibody produced the second highest response with ~110RU. H4 antibody, although able to bind IFN $\epsilon$  was found to exhibit a rapidly declining signal after binding, suggesting a weaker antigen-antibody interaction. Antibody G3 was found to exhibit the lowest positive signal at ~20RU. Similarly to antibody H4, the signal strength was found to decline rapidly after binding.

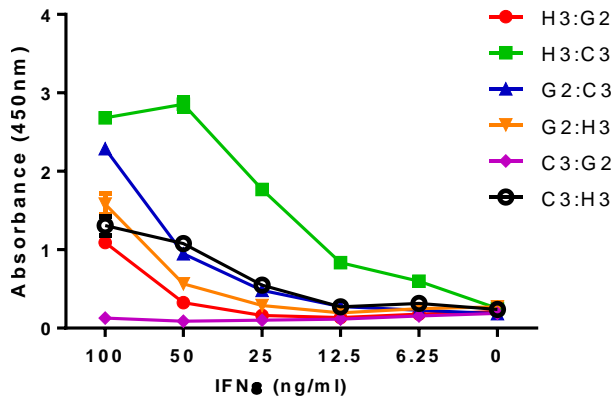
As a negative control, H3 antibody was also tested and found to produce no signal, as expected. Similarly, E3 antibody produced no additional signal, indicating it bound the same epitope as H3 or an epitope masked or sterically

hindered by the binding of H3. Collectively, these data suggest that there are some antibody pairs able to recognise separate epitopes on the surface of IFN $\epsilon$  that could constitute candidates for sandwich ELISA antibody pairs.

### **5.2.5 Optimising IFN $\epsilon$ ELISA**

To further investigate whether some antibodies can be used to establish an IFN $\epsilon$  ELISA, I screened the antibodies with the highest response as found using the BIAcore assay in 5.2.4. Protein G-affinity purified C3, G2 and H3 antibodies were biotinylated as outlined in Chapter 2.4.1 in order to develop the IFN $\epsilon$  ELISA (Chapter 2.5.5). As an initial screen, each antibody was alternated as either capture or detection antibody at a concentration of 4 $\mu$ g/ml and 1 $\mu$ g/ml, respectively allowing me to determine which antibody pairs would produce a high signal with varying concentrations of IFN $\epsilon$  (Figure 5.6A). Although commercial ELISA kits are able to quantify cytokines in the pg/ml range, I assessed IFN $\epsilon$  concentrations from 100ng/ml to 6.25ng/ml as a starting point, as the mAbs were able to detect at least 100ng/ml by western blot (Figure 5.4). As seen in Figure 5.6A, using H3 antibody as capture and C3 as the detection antibody produced the strongest absorbance reading, although at 50ng/ml the assay reached maximum absorbance as 100ng/ml of IFN $\epsilon$  didn't result in a stronger signal. The lowest concentration of IFN $\epsilon$ , 6.25ng/ml still produced a reading of ~0.5AU which was an appreciably higher signal than the baseline of 0.2AU. Different combinations of capture and detection antibody resulted in varying absorbance read-outs, although at much reduced strength compared to H3:C3. Furthermore, checkerboard assays were performed to determine optimal concentrations of H3 and C3 antibodies and to see if sensitivity could be increased. These experiments did not lead to an increase in signal or increase in sensitivity. Thus, while we were

A.



B.

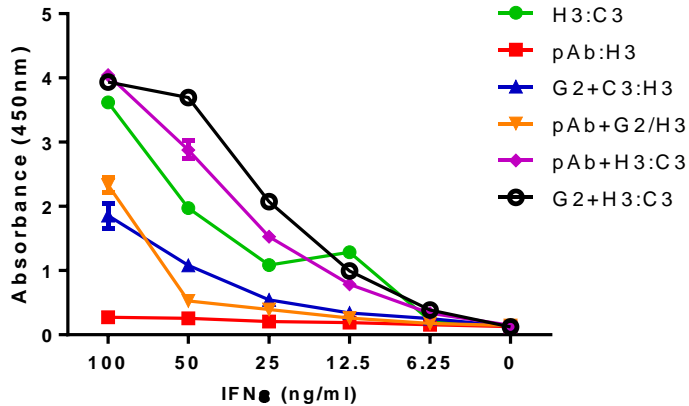


**Figure 5.6 Developing and optimising the IFN $\epsilon$  ELISA.** ELISA curves depicting the ability of antibodies to detect different concentrations of IFN $\epsilon$  (x-axis) as measured by absorbance at 450nm (y-axis). Antibodies found to be able to bind different epitopes of IFN $\epsilon$  as previously determined by SPR were evaluated for their ability to be used in an ELISA assay. The assay was performed using Horse-Raddish peroxidase conjugated detection antibodies and TMB substrate. **A)** Different combinations of IFN $\epsilon$  antibodies were evaluated as capture and detection antibodies. The first antibody is the capture antibody and was added at 4 $\mu$ g/ml. The second antibody is the detection antibody which was added at 1 $\mu$ g/ml. **B)** To increase the working range of the assay, capture antibodies were added in combination in a 1:1 ratio to a final concentration of 4 $\mu$ g/ml. Data are presented as absorbance values at 450nm and denote mean  $\pm$ SD of duplicates. Shown are representative assays from at least 3 independent experiments performed in duplicate. pAb refers to a rabbit polyclonal antibody against IFN $\epsilon$  which was generated previously by Dr Helen Cumming (MIMR).

able to successfully set-up a sandwich ELISA, the sensitivity of the assay was only sufficient to detect high levels of IFN $\epsilon$  in the range of 50ng/ml to 6.25ng/ml.

To increase signal strength and sensitivity at low antigen concentrations, commercial ELISAs often use a combination of capture monoclonal antibodies or even polyclonal antibodies. The premise behind this is that it increases the chance of capturing all available cytokine, therefore increasing the potential signal. In order to investigate this hypothesis, I tested combinations of capture antibodies (Figure 5.6B). Compared to H3:C3, which produced the strongest response in the previous experiment, a combination of G2 and H3 as capture antibodies produced the highest absorbance read out (G2+H3:C3) over the IFN $\epsilon$  concentrations tested. Furthermore, the use of a polyclonal IFN $\epsilon$  antibody (pAb) in combination with H3 as capture antibodies also produced an appreciable increase in the absorbance over H3 alone. In contrast, use of H3 as the detection antibody demonstrated the lower readings than C3, even when the capture antibody was a combination of antibodies. Using H3 and G2 as capture and C3 as the detection antibody resulted in a working detection range from 6.25ng/ml to 100ng/ml. Table 5.1 illustrates the raw absorbance values of conditions H3:C3 and G2+H3:C3 from the assay in Figure 5.6B. Of note, there is a statistically significant difference between IFN $\epsilon$  concentrations of 6.25ng/ml and 0ng/ml for G2+H3:C3 and not for H3:C3, demonstrating that using G2 and H3 in combination as capture antibodies leads to higher sensitivity at the lower end of the detection limit than H3 alone (Table 5.2). As before, checkerboard assays and varying blocking and washing buffers did not lead to any significant increases in detection performance with regards to sensitivity.

**Table 5.1** Mean absorbance readings  $\pm$  SD of the best conditions from Figure 5.6a and b (H3 : C3 data points taken from Figure 5.6b for comparison purposes)

IFN $\epsilon$ (ng/ml)	H3 : C3 Mean $\pm$ SD	G2+H3 : C3 Mean $\pm$ SD
100	2.620 $\pm$ 0.028	3.937 $\pm$ 0.010
50	1.973 $\pm$ 0.014	3.692 $\pm$ 0.009
25	1.088 $\pm$ 0.053	2.073 $\pm$ 0.033
12.5	1.285 $\pm$ 0.0	0.993 $\pm$ 0.004
6.25	0.223 $\pm$ 0.007	0.386 $\pm$ 0.008
0	0.134 $\pm$ 0.004	0.121 $\pm$ 0.001

**Table 5.2** Significance of absorbance readings at 6.25ng/ml compared to 0ng/ml. CI = confidence interval.

IFN $\epsilon$ (ng/ml)	H3 : C3 CI and Significance	G2+H3 : C3 CI and Significance
6.25 vs 0	-0.004 to 0.1821 (Not significant)	0.1719 to 0.3581 ( $p < 0.0001$ )

Overall, these findings demonstrate that using SPR and subsequent ELISA, we were able to find antibody pairs suitable for a sandwich ELISA. This data however also shows low sensitivity of detection as we were not able to attain sensitivity to lower than 6.25ng/ml. Additional study of other antibody pair combinations may therefore improve sensitivity further.

### 5.2.6 Immunohistochemistry using anti-IFN $\epsilon$ mAbs

Monoclonal antibodies are often used for the detection of target protein in tissue sections. In contrast to western blotting, which only indicates the presence of protein in a tissue lysate, immunohistochemistry allows for the localisation of protein of interest in cells in a tissue section. The benefit of this is that one can see where the protein is expressed or how its expression changes under certain conditions. In order to screen the anti-IFN $\epsilon$  antibodies, we decided to use wild-type and *Ifne1<sup>-/-</sup>* mouse uterine sections as the uterus is the primary site of IFN $\epsilon$  expression [114]. Tissues from *Ifne1<sup>-/-</sup>* mice were used as a negative control and would allow us to quickly determine which antibodies specifically stained IFN $\epsilon$  and which produced background signal. As the *Ifne1<sup>-/-</sup>* mouse produces no IFN $\epsilon$  [114], it was an ideal method for screening antibodies for their immunohistochemistry potential. Initial screening of 7 antibodies demonstrated that only C3 mAb produced specific staining in WT uterine sections but not in *Ifne1<sup>-/-</sup>* uterine sections (Figure 5.7) or sections stained with an isotype control antibody (Appendix J).

Potent staining was seen in luminal epithelium and glandular epithelium in WT mice (Figure 5.7, top panel). Positive staining was also seen in some areas of the lamina propria although staining intensity was less than the luminal epithelium. IFN $\epsilon$  staining was absent in the perimetrium. As expected, the

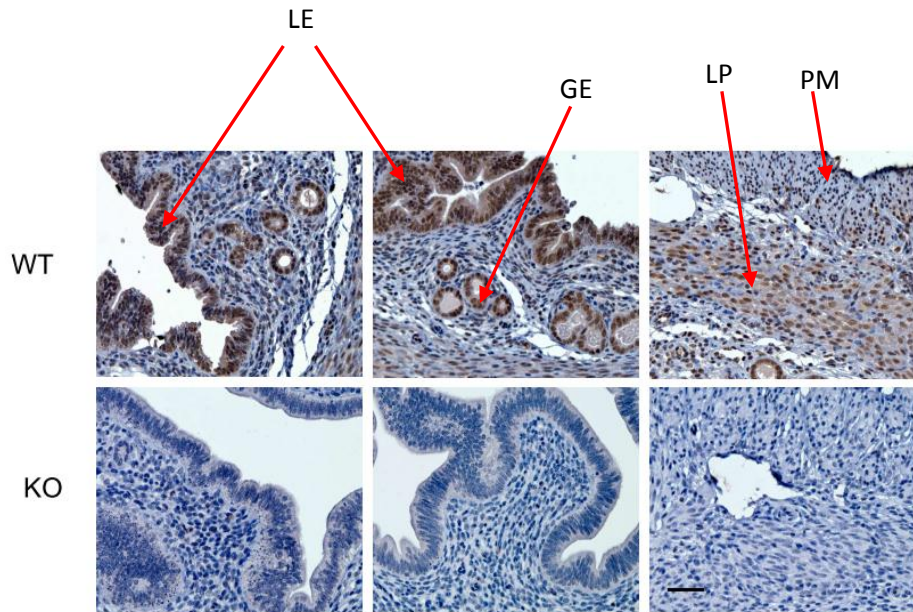


**Figure 5.7 Mouse uterine sections during estrus stage were stained with C3 anti-IFN $\epsilon$  antibody.** The figure shows pictures of immunohistochemical staining of uterine cross sections from C57Bl/6 WT and *Ifne1*<sup>-/-</sup> mice during the estrus stage of the cycle. Sections were stained with C3 anti-IFN $\epsilon$  antibody followed by goat  $\alpha$ -mouse Ig and ABC-HRP. Staining was visualised using DAB substrate. Brown coloration indicates positive staining. Sections were counter-stained with haematoxylin (blue) for clearer morphological analysis. IFN $\epsilon$  producing cells were found to predominantly localise to the luminal epithelium of the uterus. Arrows point to: LE, luminal epithelium; GE, glandular epithelium; LP, lamina propria; PM, perimetrium. Scale bar represents 50 $\mu$ m. Shown is a representative section of n = 5 mice. Appendix J shows staining of the other uterine sections in the experiment.

*Ifne1*<sup>-/-</sup> uterus did not produce any staining (Figure 5.7, bottom panel), indicating that C3  $\alpha$ -IFN $\epsilon$  mAb specifically stains IFN $\epsilon$ .

### 5.2.7 Neutralising activity of IFN $\epsilon$ mAbs

The ability of antibodies to neutralise the biological activity of IFN $\epsilon$  was investigated in interferon inducible luciferase reporter assay as described in Chapter 4. In this assay, I demonstrated that IFN $\epsilon$  induced the expression of luciferase when under the control of an ISG15 promoter (Chapter 4.2.6). The same assay can be used to determine if an antibody has neutralising activity by pre-incubating IFN $\epsilon$  with antibody and then stimulating cells. A loss of luciferase induction would indicate that the antibody was able to neutralise the activity of the cytokine, most likely by preventing the IFN from binding to the IFN receptors.

For this assay, the candidate antibodies were purified by Protein G affinity chromatography and antibody concentrations determined by absorbance at 280nm, taking into account the extinction co-efficient of antibodies. Treatment of cells with 5pmol/ml of IFN $\epsilon$  alone was sufficient to drive the ISG15 promoter 5-fold over unstimulated cells (Figure 5.8A). Pre-incubation of IFN $\epsilon$  with a 5-fold molar excess of H3 antibody resulted in a complete loss of ISG15-promoter activation. Pre incubation of IFN $\epsilon$  with E3 antibody reduced the IFN $\epsilon$  induced ISG15-promoter activation to 2.5-fold, or 50% compared to IFN $\epsilon$  alone. Pre-incubation of C3 antibody with IFN $\epsilon$  conversely did not result in a loss of ISG15-promoter activation, suggesting that it does not neutralise the biological activity of IFN $\epsilon$ .

In order to demonstrate that the neutralising effect observed with H3 antibody was IFN $\epsilon$  specific, ISG15 promoter luciferase expressing cells were stimulated

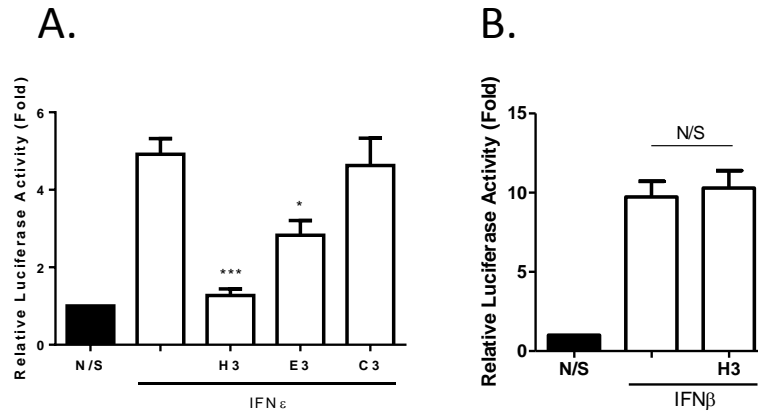


**Figure 5.8 Anti-IFN $\epsilon$  antibodies are able to neutralize the biological activity of IFN $\epsilon$  but not IFN $\beta$ .** Graphs depicting the relative fold induction of an ISG15-promoter driven luciferase reporter following treatment with **A)** 5pmol/ml IFN $\epsilon$  or **B)** 5pmol/ml IFN $\beta$  and indicated  $\alpha$ -IFN $\epsilon$  mAbs (H3, E3 and C3). Protein G affinity purified antibodies were added in a 5-fold molar excess to rIFN for 4 hours and cells stimulated for 16-hours. A reduction in luciferase activity compared to IFN only stimulation indicates neutralisation of biological activity. Data are presented as fold luciferase induction and denote the mean  $\pm$  SEM of at least 3 independent experiments. \*,  $p < 0.5$ ; \*\*\*,  $p < 0.001$ ; NS, not significant.

with 5pmol/ml IFN $\beta$  (Figure 5.8B). A potent luciferase response was observed with an approximately 10-fold increase in relative luciferase activity compared to unstimulated cells. Pre-incubation of IFN $\beta$  with a 5-fold molar excess of H3 antibody did not lead to a loss of ISG15 promoter driven luciferase signal, suggesting that the neutralisation effect is IFN $\epsilon$  specific. Overall, these results demonstrate that at a 5-fold molar excess to IFN $\epsilon$ , H3 antibody is able to fully neutralise the *in vitro* induction of ISG15 promoter driven luciferase and E3 partially neutralises the biological activity of IFN $\epsilon$ .

### 5.2.8 Immunoprecipitation of IFN $\epsilon$ with monoclonal antibodies

Immunoprecipitation is the process by which an antibody is used to selectively bind its protein target in solution, which is then precipitated by Protein A or G coupled to a solid matrix such as sepharose beads. Immunoprecipitation is used to selectively purify the protein antigen from a complex solution such as a cell lysate. This technique also forms the basis of immunoaffinity chromatography, a process in which a target protein can be purified by its specific interaction with the antibody. Importantly, this strategy is widely used for the purification of type I IFNs [5].

In order to test the ability of the IFN $\epsilon$  antibodies to be used for immunoprecipitation experiments, 75 $\mu$ g of Protein G purified antibodies were incubated with 10ml of tagless IFN $\epsilon$  conditioned insect cell culture supernatant and incubated at 4°C on a rotating wheel overnight. The following day, Protein G beads were used to purify the immune complexes and the samples analysed by 15% SDS-PAGE (Figure 5.9). Analysis of the immunoprecipitate samples by 15% SDS-PAGE visualised with Coomassie Brilliant Blue demonstrated a clear band at 25kDa, corresponding to immunoglobulin light

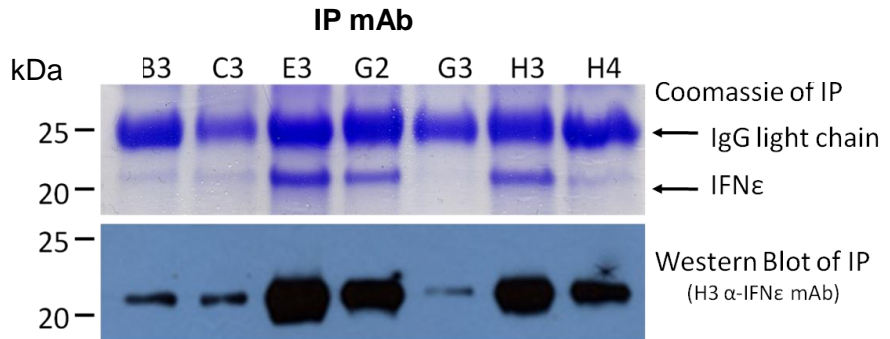


**Figure 5.9 Immunoprecipitation of recombinant tagless IFN $\epsilon$  with monoclonal antibodies.** Coomassie stained SDS-PAGE gel (top) and western blot (bottom) of immunoprecipitated recombinant IFN $\epsilon$  with  $\alpha$ -IFN $\epsilon$  antibody clones. 100 $\mu$ g of affinity purified mAbs were added to 10ml of tagless IFN $\epsilon$  insect cell expression supernatant and subsequently purified by Protein G affinity resin. Protein G Beads were boiled and electrophoresed on 15% SDS-PAGE and stained with CBB. Boiled Protein G beads from each immunoprecipitation reaction were analysed by 15% SDS-PAGE and western blotted for IFN $\epsilon$  using H3 anti-IFN $\epsilon$  mAb. Representative of n=2 experiments.

chain. The intensities of this band were relatively equal among samples and serve as a loading control, with a less prominent band present in samples C3 and G3. A second band was seen at ~21kDa in all samples, corresponding to the approximate molecular weight of untagged IFN $\epsilon$ . This band was most prominent in sample E3 with H3 and G2 having approximately equal protein. Samples B3, C3, G3 and H4 demonstrated only faint bands, suggesting the presence of very little IFN $\epsilon$  protein.

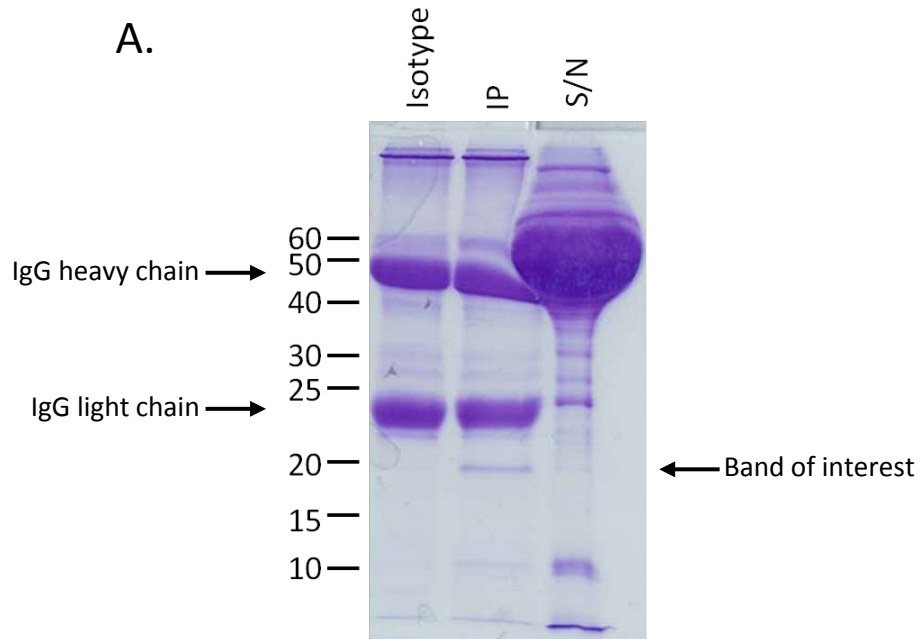
To confirm the presence of IFN $\epsilon$  in the immunoprecipitate samples, IFN $\epsilon$  specific western blotting was performed and demonstrated that E3 was the most efficient in purifying IFN $\epsilon$  from the insect cell culture supernatant as the same volume of antibody added to supernatant resulted in the most intense band. G2 and H3 antibodies demonstrated similar levels of success in purifying IFN $\epsilon$ , while B3, C3 and G3 antibodies showed relatively poor levels of immunoprecipitated material. These results demonstrate that each of the investigated antibodies was able to immunoprecipitate IFN $\epsilon$ , albeit with varying degrees of success.

As discussed previously, IFNs have been purified by immunoaffinity chromatography. As described in Chapter 3, with the difficulties encountered purifying IFN $\epsilon$ , the potential of using monoclonal antibodies for the purification of IFN $\epsilon$  became a major goal of generating the anti-IFN $\epsilon$  antibodies. The successful immunoprecipitation experiments described above lead to the trialling of an anti-IFN $\epsilon$  immunoaffinity chromatography column, which lead to the successful purification of tagless IFN $\epsilon$  as described in Chapter 3.2.6.

Overall, Table 5.3 summarises our finding of 7  $\alpha$ -IFN $\epsilon$  antibodies characterised in this chapter and their potential uses.

### 5.2.9 Immunoprecipitation of IFN $\epsilon$ expressed in mammalian cells and N-terminal sequencing

Due to the novelty of mIFN $\epsilon$  and the difficulty of inducing high level expression *in vitro* or *in vivo* by PAMPs [114], the native N-terminus of mIFN $\epsilon$  has not yet been determined experimentally, only via bioinformatic prediction software [13]. To determine the native N-terminus of mIFN $\epsilon$ , HEK293 cells were transfected with CMV-Ifne-Ires-mCitrine construct (Appendix B) and analysed for protein expression 72 hours later as outlined in Chapter 2.3.20. CMV-Ifne-Ires-mCitrine was a kind gift from Dr. Alec Drew and Dr. Ka Yee Fung (MIMR, Clayton, Australia). This construct was designed for high level expression of IFN $\epsilon$  using a cytomegalovirus promoter and specifically maintaining the native signal sequence of IFN $\epsilon$ . Following this incubation, the conditioned culture supernatant was cleared of endogenous bovine immunoglobulins by pre-incubation with Protein G resin and subsequent centrifugation and collection of cleared supernatant. Anti-IFN $\epsilon$  mAb H3 was then used to immunoprecipitate IFN $\epsilon$  protein and an isotype control antibody used to demonstrate the specificity of immunoprecipitation. Immune complexes were purified from the media by Protein G Sepharose affinity chromatography, washed with PBS, boiled in SDS-PAGE loading dye and separated on a 15% SDS-PAGE gel. Visualising protein bands with Coomassie Brilliant Blue revealed the presence of immunoglobulin light and heavy chains in both isotype control and IFN $\epsilon$  mAb samples (Figure 5.10A). The H3 mAb sample demonstrated the presence of a band at ~20kDa, which was not seen in the isotype control sample and corresponds to the theoretical molecular weight of IFN $\epsilon$ . For N-terminal sequencing, the experiment was repeated and the proteins transferred to PVDF membrane and stained with Coomassie Brilliant Blue. The 20kDa band was excised and sent to the Monash University



**B.**

```

Seq_query                               LEPKRI
                                         | | | | |
mIFNε   MVHRQLPETVLLLLVSSTIFSLEPKRIPFQLWMNRESLQLLKPLPSSSVQOCLAHRKNFLLPQQP
mIFNε   VSPHQYQEGQVLAVVHEILQQIFTLQLQTHGTMGIWEENHIEKVLAALHRQLEYVESLGGLNAAQK
mIFNε   SGGSSAQNLRQLQIKAYFRRIHDYLENQRYSSCAWIIIVQTEIHRMFFVFRFTTWLSRQDPDP

```

**Figure 5.10 Immunoprecipitation of IFN $\epsilon$  expressed in HEK293 cells and N-terminal Sequencing. A)** 15% SDS-PAGE visualised with Coomassie Brilliant Blue of immunoprecipitated samples. HEK293 cells were transfected with CMV-Ifne-Ires-mCitrine and the supernatant collected after 72hours. Conditioned supernatant was pre-cleared with Protein G beads prior to immunoprecipitation of IFN $\epsilon$  with H3 anti-IFN $\epsilon$  mAb. Immune complexes were isolated with Protein G beads **B)** N-terminal sequencing of 20kDa protein moiety from immunoprecipitate and alignment to mIFN $\epsilon$  polypeptide sequence. The N-terminal sequence corresponds to residues 22-27 of mIFN $\epsilon$  indicating the signal peptide is cleaved after residue 21.

Proteomics facility for N-terminal sequencing. The first six amino acid residues of the 20kDa band immunoprecipitated from the cells transfected with CMV-*lfnε-lres-mCitrine* were LEPKRI (Figure 5.10B). Alignment of the sequenced amino acids with the protein coding sequence of mIFN $\epsilon$  revealed 100% sequence identity with residues 22-27, indicating that the IFN $\epsilon$  protein expressed was cleaved after residue 21 to be secreted into the culture supernatant. Thus the signal peptide of mIFN $\epsilon$  is composed of 21 residues and reads MVHRQLPETVLLLLVSSTIFS, with the mature protein beginning at residue 22 with LEPKRI (Figure 5.10B).

**Table 5.3 Summary of 7 investigated monoclonal antibodies.**

	ELISA	W.B.	IP	Neutralisation (Luciferase)	IHC	Comments
<b>B3</b>	+++	+++	++	N/A	-	
<b>C3</b>	++++	++++	++	-	++++	Only mAb shown to work for IHC
<b>E3</b>	+++	+++	++++	+++	-	
<b>G2</b>	++	+	+++	N/A	-	
<b>G3</b>	+++	-	+	N/A	-	
<b>H3</b>	++++	++++	+++	++++	-	Overall best mAb for applications
<b>H4</b>	+++	-	+++	N/A	-	

Scoring was made relative to the highest responding antibody for each assay.

N/A indicates data not available. – indicates no response observed.

### 5.3 Discussion

To aid the characterisation of IFN $\epsilon$ , we produced a panel of monoclonal antibodies and trialled these for a variety of applications. We already had a polyclonal antibody against IFN $\epsilon$  however it was raised against a synthetic peptide of IFN $\epsilon$  and not the full protein antigen (Helen Cumming, unpublished data). To generate monoclonal antibodies, *Ifne1*<sup>-/-</sup> mice were immunised with recombinant His<sub>6</sub>-IFN $\epsilon$  protein, which led to a potent immune response when the mice were bled. After fusion of splenic B-cells with myeloma fusion partners, a number of hybridoma clones were evaluated for their production of anti-IFN $\epsilon$  antibody by supernatant ELISAs. These results indicated that 28 of the clones produced antibody that specifically recognised IFN $\epsilon$  and not IFN $\beta$  nor an unrelated hexahistidine fusion protein. Not all antibody clones were equally capable of detecting IFN $\epsilon$ , as absorbance values differed markedly between the clones. This difference however could be due to the concentration of antibody in the supernatants, which was not determined for supernatant ELISAs and as such all clones responding to IFN $\epsilon$  in the supernatant ELISA were included for further characterisation in western blotting experiments.

Western blotting of IFN $\epsilon$  using hybridoma supernatants demonstrated a varied signal response with C3 and H3 producing the strongest signal. Furthermore, these two hybridomas also detected a second protein moiety at approximately 40kDa. IFN $\alpha$ 1 expressions carried out in our laboratory have often demonstrated a similar protein dimer at high protein concentrations, even after denaturing the sample prior to loading on SDS-PAGE. As this 40kDa protein band is only apparent in C3 and H3, it also appears to correlate with the overall signal strength for the 20kDa band, suggesting that the detection of this moiety is very sensitive. It remains to be tested if other antibodies can be

made to recognise this moiety, by either increasing the IFN $\epsilon$  concentration or increasing the antibody concentration.

So far antibody signal strength from ELISA data does not always correlate with the western blot data. That is, some clones demonstrated high ELISA readings also had low detection by WB (G3 and H4 for example). Interestingly, this was not observed in the reverse (high western blot signal, low ELISA signal). The inability to detect IFN $\epsilon$  following denaturation suggests that the antibodies recognise an epitope only present on correctly folded protein which then disappears when IFN $\epsilon$  is denatured. It is highly likely that many of the antibodies were raised against correctly folded IFN $\epsilon$  as we injected both native and denatured protein. Furthermore, antibodies that detected IFN $\epsilon$  equally well by ELISA and WB it is possible that the epitope is not affected by tertiary fold and thus is not affected by denaturation (such as in the case of C3 and H3 antibody clones). Such antibodies are beneficial in assays where protein fold cannot be maintained, such as during fixation.

In order to develop an ELISA specific for IFN $\epsilon$  we needed to identify two antibodies able to recognise different epitopes of the IFN $\epsilon$  protein and used SPR to determine which of a select number of our antibodies would be able to do so. We identified a number of binding pairs. Antibody C3 produced the highest signal as the detection antibody when H3 was used to capture the IFN $\epsilon$  antigen. As SPR is relative to each experiment, it is difficult to determine if the resonance units achieved in these experiments are a good indicator for subsequent binding affinity and avidity. In subsequent assays however, I was able to demonstrate that at least some of our antibodies recognised different epitopes of IFN $\epsilon$  and could be used in a sandwich ELISA. Furthermore, with the availability of 28 positive hybridoma clones, future studies may potentially identify antibody pairs demonstrating an even higher response in this assay.

Developing the ELISA itself proved difficult in terms of optimisation of the conditions. Even though using H3 as the capture antibody and C3 as the detection antibody was successful, we quickly established that the working range was very limited as using a concentration of 50ng/ml of IFN $\epsilon$  resulted in saturation of signal while IFN $\epsilon$  concentrations lower than 6.25ng/ml were practically undetectable. Commercial ELISAs typically demonstrate a working range of approximately three log units (i.e. 1-1000pg/ml) whereas our assay had a working range of just over one log unit (3-50pg/ml). A lot of time was spent trying to increase the sensitivity of the assay into the 1000-100pg/ml range by performing checkerboard assays and changing buffer conditions however this proved unsuccessful. In addition, we provided C3 and H3 antibodies to MATF for them to attempt increasing sensitivity of the assay. They used high throughput screening ELISA assays and varied coating and detection antibody concentrations however were unable to improve detection to below 2ng/ml (Appendix F). As such, to increase assay sensitivity I tried combining multiple capture antibodies, a practice commonly used in commercial kits. Although I was able to increase the signal strength in the upper working range, using a combination of capture antibodies did not appear to increase sensitivity in the lower range. This would indicate that my detection antibody was not sensitive enough to detect low levels of cytokine, even though more cytokine was captured by the coating antibodies. Screening more antibodies by SPR could potentially lead to the identification of a binding pair with strong enough avidity to detect picogram/ml quantities of IFN $\epsilon$ .

A major finding was that one of the anti-IFN $\epsilon$  antibodies, C3, produced a positive result in immunohistochemistry on formalin fixed, paraffin embedded tissues (FFPE). Not all antibodies work on FFPE, which is often attributed to the way these tissues are treated. Formalin cross-links proteins and can

therefore destroy epitopes. Heat-activated antigen retrieval is most commonly used to restore the antigen however this may not always be successful [338]. Interestingly, antibody C3 was found to bind a different epitope of IFN $\epsilon$  than H3 by SPR, and since the latter was unsuccessful in IHC it suggests that IFN $\epsilon$  is presented in such a way that the C3 epitope is still recognisable whereas the H3 epitope is not. If this is due to the process of fixing with formalin (or subsequent antigen retrieval) or steric hindrance due to *in vivo* components prior to tissue sectioning is not known.

Importantly, the IHC data presented in this thesis represents the first demonstration of this cytokine being expressed in the FRT epithelium. As a proof-of-principle, it is now possible to screen tissues by IHC in order to confirm the gene expression data available which will greatly aid in elucidating the biological role of IFN $\epsilon$ . A method not tested in this thesis is the IHC potential of the antibodies on frozen tissue sections. While frozen tissue sections often suffer from loss of morphology, epitopes remain preserved as there is no formalin fixing involved. Performing IHC on frozen sections may lead to the identification of more antibodies suitable for this particular application. Regardless, the availability of an antibody suitable for IHC will provide a novel tool for analysing the function of IFN $\epsilon$  in the reproductive tract and it will be interesting to evaluate the expression of IFN $\epsilon$  protein during pregnancy and disease models with a reproductive tract phenotype such as chlamydia induced infertility [339]. In addition, the monoclonal antibodies could be evaluated for their ability to detect human IFN $\epsilon$ , which would provide a method for studying IFN $\epsilon$  function in a human setting.

Screening of our monoclonal antibodies for neutralisation potential in an interferon inducible luciferase assay revealed two antibodies able to elicit such an effect. Neutralisation was highest for antibody clone H3, which fully

abolished the ISG15-luciferase inducing ability of IFN $\epsilon$ . Neutralisation was also seen to occur with antibody E3 however to a lesser extent than H3. As expected, the activity of IFN $\beta$  was not inhibited by incubation with anti-IFN $\epsilon$  antibody, indicating an IFN $\epsilon$  specific neutralisation effect. Although it is common to block all type I interferon signalling with a monoclonal antibody directed against IFNAR1 [334, 340], more targeted studies involving IFN $\alpha$  and IFN $\beta$  specific neutralising antibodies would allow for a more careful dissection of specific interferon subtype function [341]. For our studies, IFN $\epsilon$  specific neutralisation is advantageous as it will allow us to discern the precise function of IFN $\epsilon$  in reproductive tract infections while maintaining the normal type I interferon response. This is critical when considering that in a Chlamydia reproductive tract infection model, *Ifnar1*<sup>-/-</sup> mice cleared the infection faster with less pathology than control mice, suggesting that some of the type I interferon members contribute to the pathophysiology of the infection [342]. Utilizing neutralising  $\alpha$ -IFN $\epsilon$  antibodies, it would be interesting to investigate the direct effect IFN $\epsilon$  has on the uterus while maintaining intact pathogen induced IFN signalling. Furthermore, the protective effect IFN $\epsilon$  has on reproductive tract infections [114] could be investigated at different time points after infection to see at what time IFN $\epsilon$  elicits its beneficial effects.

A major step in enabling us to purify untagged IFN $\epsilon$  was the finding that our antibody clones were able to immunoprecipitate IFN $\epsilon$  from insect cell culture media. Interestingly, different antibodies demonstrated varying abilities to IP IFN $\epsilon$ , which suggests different binding affinities among clones, an unsurprising finding given the data presented so far. I used antibody clone H3 to create an immunoaffinity chromatography column specific for IFN $\epsilon$ . Although H3 was not the best IP antibody, it demonstrated high potential for use in western blotting, ELISA and neutralisation and we wanted an antibody

that would be usable across a variety of applications. The results of IFNε specific immunoaffinity chromatography were presented in Chapter 3.2.6. Importantly, this finding enabled us to purify a near native form of IFNε and thus avoids complications that purification tags may introduce.

Another use for IP was to purify IFNε secreted by HEK293 cells transiently transfected with an expression construct to allow us to sequence the N-terminus of the secreted product and determine the native N-terminal. This has been done previously for the novel interferon IFNκ, which also demonstrated a unique tissue expression profile [111]. We found that the signal peptide was cleaved after amino acid residue 21. This corresponded to the predicted cleavage site calculated by Signal P software (Appendix F) [343]. We originally predicted the signal peptide to cleave after residue 19, which was most likely erroneous due to the software available at the time [13]. In all, this data confirms that IFNε is secreted and that the signal peptide is cleaved after residue 21 to result in a mature polypeptide sequence starting with LEPKRI.

## 5.4 Conclusion

This Chapter outlines the production and characterisation of a number of anti-IFN $\epsilon$  monoclonal antibodies. Importantly, I was able to identify antibodies suitable for western blotting, immunohistochemistry, neutralisation and immunoprecipitation. The latter application was of particular importance due to the difficulties encountered in Chapter 3 in regards to purifying His<sub>6</sub>-IFN $\epsilon$ . Furthermore, I was able to show for the first time that IFN $\epsilon$  is secreted from cells and I also defined the mature IFN $\epsilon$  amino acid sequence, an important aspect when considering that this thesis aims to characterise IFN $\epsilon$  as it is expressed in nature.

Lastly, the finding that one of the characterised antibodies demonstrated a use for immunohistochemistry should greatly aid in future studies of IFN $\epsilon$  expression and function. For instance, until the generation of these antibodies, IFN $\epsilon$  could only be measured by mRNA transcript levels. The immunohistochemistry data presented in this thesis not only enabled us to identify which cells in the FRT produced IFN $\epsilon$  but also confirm that mRNA is translated into protein. Not only does this complement the prior observation that *Ifne1* gene expression is highest in the uterus, but it also demonstrates that IFN $\epsilon$  is predominantly expressed in cells of the luminal epithelium and glandular epithelium. To follow up this finding, it will be interesting to investigate if IFN $\epsilon$  is secreted into the lumen or basolaterally and determine which cells are responsive to IFN $\epsilon$ .

Together, this chapter provides an important base for future experiments by providing the necessary tools to fully elucidate the biological activities of novel IFN $\epsilon$ .

## **Chapter 6 – Discussion and Conclusions**

The aim of my PhD project was to express and purify recombinant mouse IFN $\epsilon$  and characterise its biological activities. Due to the difficulties encountered in regards to protein expression and purification, monoclonal antibodies against IFN $\epsilon$  were generated which resulted in the development of a robust protein purification protocol based on immunoaffinity chromatography. Furthermore, the antibodies proved successful in applications such as western blotting, *in vitro* neutralisation and immunohistochemistry. Lastly, I was able to characterise IFN $\epsilon$  as a novel type I IFN by demonstrating the use of the canonical type I IFN receptor and establish its biological specific activities.

The type I IFNs are a large family of alpha helical cytokines conserved in vertebrates and shown to signal via a heterodimeric receptor complex. Importantly, the type I IFNs were among the first cytokines to be identified, characterised, cloned and marketed as biological therapeutics [5]. Specifically, human IFN $\alpha$ 2 and IFN $\beta$  demonstrate considerable pharmaceutical efficacy in the treatment of malignancies and diseases such as chronic hepatitis B and C, hairy cell leukemia, AIDS-related Kaposi's sarcoma, melanoma and multiple sclerosis [344-348]. Interestingly, IFN $\alpha$ 2 is not indicated for the treatment of multiple sclerosis and IFN $\beta$  is not used in the treatment of cancers. Clearly, while the type I IFNs signal via the same cell surface receptor have overlapping downstream signalling cascades, some biological activities may be distinct and non-redundant.

In 2004, our group discovered a novel gene situated in the type I IFN locus and based on sequence homology and structural modelling, designated it as a novel type I IFN, IFN $\epsilon$  [13]. Although subsequent work suggested that IFN $\epsilon$  was a type I IFN by eliciting antiviral and antiproliferative activities [248-250], there was a distinct lack of reagents to definitely characterise it as a type I IFN. Thus, the first aim of my project was to express and purify recombinant mouse IFN $\epsilon$  to a level of purity suitable for definitive biological characterisation. Work performed in Chapter 3 demonstrated that IFN $\epsilon$  is a difficult protein to express. Multiple expression systems yielded little protein and even when sufficient quantities of IFN $\epsilon$  were purified, aggregation, multimerization and instability were encountered by us and others (collaboration work with CSIRO, personal communication). While I was trialling expression systems, we were also expressing the type I IFN receptors IFNAR1 and IFNAR2 using insect cells and we therefore trialled expression of IFN $\epsilon$  in the same system. Unlike bacterial and mammalian expression systems, we were able to consistently produce IFN $\epsilon$  using insect cells, however we still had difficulty in purifying the protein due to the observation that removal of the 6xHis tag with enterokinase led to protein degradation. This appeared to be a problem specific to IFN $\epsilon$  as we were able to express and purify IFN $\beta$  using the same expression system without difficulties.

To overcome the problems encountered with the purification of IFN $\epsilon$ , His<sub>6</sub>-IFN $\epsilon$  was used to immunize *Ifne1*<sup>-/-</sup> mice and differential screening utilised to identify IFN $\epsilon$  specific monoclonal antibodies (Chapter 5). Among the uses of these monoclonal antibodies was the finding that they proved successful in immunoprecipitation and immunoaffinity chromatography. The type I IFNs have a long standing history of being purified by antibody chromatography [349-351] and we felt this would be a suitable method to purify IFN $\epsilon$

expressed without a purification tag. The results shown in Chapter 3 clearly demonstrate immunoaffinity chromatography to be successful for the purification of IFN $\epsilon$ . Furthermore, this purification method has proven robust, with over 20 individual purifications to date, some reaching over 95% purity in just a single step (Appendix K). As such, yields have exceeded 2.5mg of purified protein from a 1L expression volume. We are currently exploring a collaborative effort to increase the scale of IFN $\epsilon$  production with the Commonwealth Scientific and Industrial Research Organisation (CSIRO) with expression volumes exceeding 3L and utilising a 25ml antibody column. The experiments performed in Chapter 3 of this thesis have resulted in the successful production and purification of recombinant mouse IFN $\epsilon$  using an insect cell expression system which is now being performed on a scale large enough to accommodate future scientific research interests. This is particularly important for structural studies, which require large quantities of recombinant protein. Our laboratory has recently demonstrated a novel IFN $\beta$ -IFNAR1 interaction and how this signalling axis exacerbates LPS induced sepsis [234]. Given that IFN $\epsilon$  and IFN $\beta$  share evolutionary origins, it would be interesting to see if IFN $\epsilon$  has a similar interaction with IFNAR1. Furthermore, investigation into the receptor binding interactions on a structural level could further our understanding of how amino acid changes affect IFN affinity and activity. The availability of recombinant IFN $\epsilon$  will not only help in biochemical characterisation. We have already demonstrated that administration of rIFN $\epsilon$  to *C. muridarum* infected animals reduced genital tract bacterial burden and provides evidence of therapeutic potential [114]. We can now investigate other reproductive tract infection models to determine if IFN $\epsilon$  can alleviate infection outcome in those settings as well.

Among the most important findings in this thesis was the identification that uterine luminal epithelium cells stain positive for IFN $\epsilon$ . The immunohistochemistry data presented in this thesis, together with the qRT-PCR data generated by other members of our laboratory (published in [114] and Appendix L) therefore clearly demonstrate that the cells lining the female reproductive tract are the main producers of IFN $\epsilon$ . This was only possible with antibodies that were not only specific for IFN $\epsilon$  but also sensitive enough to work in immunohistochemistry using antigen-retrieval on formalin-fixed, paraffin embedded sections. Importantly, IFN $\epsilon$  has been reported to be expressed in other mucosal tissues such as the lung and small intestine [251]. Now that IFN $\epsilon$  specific antibodies exist, we can investigate the tissue expression of IFN $\epsilon$  more carefully to better define where it is produced and under what circumstances. Furthermore, we can investigate the expression of other type I IFNs using IHC to elucidate whether or not cells in close proximity to IFN $\epsilon$  producing cells demonstrate earlier / more robust IFN $\alpha/\beta$  production due to the proposed priming effect (discussed in more detail further on). Intriguingly, the finding that IFN $\epsilon$  is expressed in uterine luminal epithelium poses the question of where IFN $\epsilon$  elicits its activities. Is it secreted into the uterine lumen or does it act basolaterally? It will be difficult to determine the cellular targets of IFN $\epsilon$  *in vivo* without an IFN signalling reporter mouse strain. The use of such a mouse would allow for the identification of IFN responsive cells in tissue sections and therefore enable us to more closely investigate the effects of IFN $\epsilon$  on this cell type.

Following on from generating anti-IFN $\epsilon$  antibodies and producing highly pure protein, I next characterised IFN $\epsilon$  and demonstrated using circular dichroism that structurally, IFN $\epsilon$  adopts an alpha helical fold like the other type I IFNs. In terms of biological activity, my data shows that IFN $\epsilon$  has antiviral and anti-

proliferative activities, however these specific activities are some 100 to 1000-fold lower compared to IFN $\alpha/\beta$ . Importantly, human rIFN $\epsilon$  was also shown to have lower activity than hIFN $\alpha/\beta$ , suggesting that the lower activity may be a feature evolutionarily conserved and directly linked to its biological function [248]. As I will outline further on in this discussion, it is possible that the lower specific activity of IFN $\epsilon$  could serve to prime cells continuously rather than providing an immediate effect. In addition to this finding, I was for the first time able to definitively determine the use of both interferon receptor subunits to be required for IFN $\epsilon$  signalling. As the requirement to signal via the type I IFN receptor is among the principal features of type I IFNs, we can now classify IFN $\epsilon$  as a bonafide type I IFN.

In addition to the use of the type I IFN receptor, IFN $\epsilon$  stimulation of macrophages led to the phosphorylation of STAT1 and STAT3 transcription factors. In support of the lower antiviral and antiproliferative activities, STAT phosphorylation was lower after treatment with IFN $\epsilon$  than with an equivalent dose of IFN $\alpha$  or IFN $\beta$ . Interestingly, maximal STAT phosphorylation after IFN $\epsilon$  treatment was not seen until 15 minutes after stimulation, indicating that transcription factor activation kinetics are slower for IFN $\epsilon$ . STATs are known to reach maximal phosphorylation 5 minutes after IFN stimulation and then decline back to basal levels [352]. As we did not measure the affinity of IFN $\epsilon$  to the receptors, or the subsequent stability of the ternary complex, it is difficult to propose a theory for the observed changes. Furthermore studies investigating a correlation between receptor affinity and subsequent STAT phosphorylation are inconclusive. For instance the IFN $\alpha$ 2 YNS mutant (Described in Chapter 1) was shown to have an 18-fold increase in binding affinity to the ternary IFN receptor compared to WT IFN $\alpha$ 2, yet STAT1 phosphorylation was only 1.9-fold greater than WT IFN $\alpha$ 2 [10]. In contrast, a

different IFN $\alpha$ 2 mutant with 2.1-fold increase in binding affinity to the ternary receptor was shown to have reduced STAT1 phosphorylation compared to WT IFN $\alpha$ . Thus receptor binding affinity alone may not be a predictor of subsequent signal strength. To better characterise the mechanisms behind differential type I IFN activity, comprehensive studies investigating receptor affinity, tertiary complex stability and STAT phosphorylation kinetics need to be studied in detail. Findings from such studies may reveal the molecular mechanisms responsible for the differences in biological activities seen with IFN $\epsilon$  compared to IFN $\alpha$  and IFN $\beta$ .

Further characterisation of IFN $\epsilon$  also revealed immunoregulatory activities as demonstrated by MHC-I and CD69 upregulation on CD4<sup>+</sup> and CD8<sup>+</sup> cells, NK1.1<sup>+</sup> cells and B220<sup>+</sup> cells. Functionally, these observations have been associated with increased antigen presentation and T-cell activation, respectively [324, 353]. Importantly, given the role of CD4 and CD8 T-cells in controlling HSV-1 [354] and the importance of NK-cells in controlling *C. muridarum* infection [355], the work presented in this thesis demonstrates that these cells are responsive to IFN $\epsilon$ . These data again demonstrated that IFN $\epsilon$  had ~100-1000x lower biological potency compared to IFN $\alpha$ 1 and IFN $\beta$ . Thus far, IFN $\epsilon$  appears to be able to elicit the same functions as other type I IFNs but at reduced potency. It is difficult to speculate on the molecular mechanism of action behind this reduced potency but it is likely the result of altered receptor affinity via the critical receptor interacting residues outlined in Chapter 1. While the molecular mechanisms behind this reduced potency are currently unknown, I have a hypothesis to explain the biological rationale behind this lower activity.

IFN $\epsilon$  is produced predominantly and constitutively in the female reproductive tract [13, 114]. This is in stark contrast to all other type I IFNs which are

produced in response to pathogen recognition receptor signalling and are transient. Therefore, induced IFN $\alpha/\beta$  must elicit their biological activities rapidly to clear infection. It is therefore advantageous for these IFN subtypes to have high activity as their principal role is that of an immediate response to infection. The pro-apoptotic and cytotoxic side effects in this situation are offset by the need to rapidly eliminate the infection to avoid pathology. IFN $\epsilon$  on the other hand is produced throughout the female cycle and only decreases when estrogen is high and also during embryo implantation [114]. Therefore if IFN $\epsilon$  had high biological activity, its constitutive expression could potentially lead to increased cytotoxicity as a result of the anti-proliferative and apoptotic activities of type I IFNs, which may compromise the function of the reproductive tract. Any evidence for a role of type I IFNs in being detrimental during pregnancy is contradictory however. While Sandberg-Wollheim *et al* found no statistical difference in pregnancy rates between women undergoing IFN $\beta$  therapy and healthy control subjects [356], Boskovic *et al* found a significant increase in non-live births and reduction in birth weight in women on IFN $\beta$  therapy [357]. In support of this, the US Food and Drug Administration (FDA) recommend the discontinuation of IFN $\beta$  treatment during pregnancy. Interestingly, as discussed in Chapter 1, IFN $\tau$  is required for the maintenance of pregnancy in ruminants, suggesting that type I IFNs may not be harmful to the developing embryo. With this in mind however, IFN $\tau$  does exhibit lower cytotoxic activity compared to IFN $\alpha$  [358] and could mean that IFN $\tau$  evolved to avoid excessive cytotoxicity that is still present in IFN $\alpha/\beta$ .

While there is insufficient data to implicate IFNs in infertility, the site of IFN $\epsilon$  expression certainly raises the possibility of a role in pregnancy, particularly when considering that *Ifne1* gene expression decreases dramatically at the time of implantation in mice [114]. This suggests that there are homeostatic

mechanisms in place to carefully regulate the expression of IFN $\epsilon$  which warrants further study. We are currently in the process of generating IFN $\epsilon$  over-expressing transgenic mice which together with the reagents produced in this thesis should aid in answering the question of whether or not dysregulated IFN $\epsilon$  expression can affect pregnancy or fertility. Given the diverse biological activities of type I IFNs, it's plausible that the expression of IFN $\epsilon$  during early pregnancy and conception could pose a disadvantage to implantation.

As IFN therapy is associated with debilitating side effects such as nausea, malaise, flu-like symptoms and depression [359], it would be interesting to see if IFN $\epsilon$  treatment in humans results in the same severe side effects as IFN $\alpha$  and IFN $\beta$ . In line with this direction, previous studies found that ovine IFN $\tau$ , although exhibiting high antiviral and antiproliferative activities on human cells, also demonstrated a 50-fold reduction in cytotoxic effects compared to human IFN *in vitro* [358, 360-362]. The proposed mechanism for the lower cytotoxic effect of IFN $\tau$  is the three-fold lower binding affinity to the human receptor compared to IFN $\alpha$  [358]. Furthermore, a form of IFN $\tau$  engineered to be non-cytotoxic was shown to be potent in ameliorating the development of experimental allergic encephalomyelitis (EAE), the mouse model of MS [361]. Intriguingly, this engineered IFN $\tau$  demonstrated low receptor affinity which was shown to be associated with weak antiviral activity on mouse and human cells. This suggests that the beneficial effect of this engineered IFN $\tau$  in EAE may be independent of the molecular pathways inducing antiviral immunity. It would be interesting to investigate whether or not IFN $\epsilon$  displays therapeutic efficacy in diseases that are currently being treated with type I IFNs. At the very least further biological characterisation in combination with structural studies will provide us with a greater knowledge of which factors influence

type I IFN biological activities. We may then be able to produce a “designer” IFN that exhibits higher specific activity with lower cytotoxic side effects.

As far as the *in vivo* role of IFN $\epsilon$  is concerned, we have clearly demonstrated biological relevance as mice lacking IFN $\epsilon$  demonstrate increased severity of reproductive tract infections [114]. While the mechanisms behind the protective role of IFN $\epsilon$  are still unknown, we have demonstrated that the levels of IRGs in the uteri of *Ifne1* null mice are lower than in wild-type mice [114]. Therefore, the presence of IRGs such as STAT1, IRF-1 and IRF-7 at elevated levels could have the effect of priming the immune system, especially for subsequent type I IFN production. The recent finding that low levels of type I IFN induce the expression of unphosphorylated STATs (U-STATs) contribute to this hypothesis [363]. U-STAT1 has been shown to act as a transcription factor in the absence of IFN stimulation and interestingly, after IFN stimulation has been shown to lead to prolonged IRG expression [364]. Given the low biological activities of IFN $\epsilon$  as elucidated in this thesis, it is possible that a major role for IFN $\epsilon$  is as a priming molecule rather than an inducible, highly active principal antiviral/antibacterial effector. Importantly, given that untreated Chlamydia infection can lead to pelvic inflammatory disease (PID) and infertility [365], it would be interesting to measure *IFNE* gene expression in women with PID-induced infertility and see if the two are related. As only 10-15% of untreated Chlamydia infections in women lead to PID, it's possible that those at risk of developing PID and becoming infertile also have lower levels of IFN $\epsilon$  and are thus more susceptible to infection and higher tissue pathology.

While the data presented in this thesis was able to provide clear evidence of the IFN $\epsilon$  producing cells in the FRT, the cellular targets of IFN $\epsilon$  are unknown at this point. Given the large number of immune cells present in the reproductive tract however, it is possible that IFN $\epsilon$  could directly influence their function. Indeed, our data demonstrated that *Ifne1* null mice had lower number of NK-cells compared to control animals after *C. muridarum* infection, suggesting that these cells may be a target of IFN $\epsilon$  [114]. Given the established role of type I IFNs on NK-cells [171, 179], the importance of NK-cells in the female reproductive tract [239, 243, 366] and the function of NK-cells in clearing infected cells [355, 367] these cells could be one of the targets of IFN $\epsilon$  and will require further study.

Overall, the work presented in this thesis highlights that not all type I IFNs are the same. Importantly, IFN $\epsilon$  is unique among the type I IFN family due to its expression profile and induction mechanisms. As such, while the *in vitro* biological activities of IFN $\epsilon$  may be lower than the more classical IFN $\alpha$  and IFN $\beta$ , it still has a profound role in animal models of reproductive tract infection. Therefore, further study of IFN $\epsilon$  will improve our understanding of IFN biology and the work performed in this thesis will enable us to investigate the functions of IFN $\epsilon$  in greater detail.

## **Appendix A - Buffers and Reagents**

### **1% w/v Agarose gel**

0.05g electrophoresis analytical grade agarose LE (Promega) dissolved in 50ml 1 x TAE

### **dNTP**

25µl of each nucleotide (A, T, G, C) stock (100mM) and adjusted to 250µl with MQ dH<sub>2</sub>O.

### **1 x TAE Buffer**

40mM Tris-HCl (pH8.0), 20mM acetic acid, 1mM EDTA (pH8.0) in MQ dH<sub>2</sub>O

### **5 x SDS-PAGE Loading Dye**

60mM Tris (pH6.8), 2% SDS, 10% v/v glycerol, 0.01mM bromophenol blue, 10% β-mercaptoethanol

### **DEPC H<sub>2</sub>O**

MQ dH<sub>2</sub>O containing 0.1% diethyl pyrocarbonate (DEPC)

### **Trypan Blue**

0.4% Trypan Blue dissolved in PBS (Gibco) and filter sterilised.

### **MTT reagent**

3-(4,5-Dimethylthiazol-2-yl)-2,5-diphenyltetrazolium bromide dissolved at a concentration of 5mg/ml in PBS (Gibco) and filter sterilised.

### **Complete RPMI**

RPMI (Gibco) supplemented with 10% v/v FCS, 1% L-glutamine (Gibco) and 1% Penicillin/Streptomycin (Gibco)

### **Complete DMEM**

DMEM (Gibco) supplemented with 10% FCS, 1% L-glutamine (Gibco) and 1% Penicillin/Streptomycin (Gibco)

### **Reduced Serum RPMI**

RPMI (Gibco) supplemented with 3% v/v FCS, 1% v/v L-glutamine (Gibco) and 1% v/v Penicillin/Streptomycin (Gibco)

**20% FCS Hybridoma Media**

DMEM (Gibco) supplemented with 20% v/v FCS, 1% v/v L-Glutamine (Gibco), 1% v/v Penicillin/Streptomycin (Gibco)

**L. cell conditioned media**

L929 cells were seeded at  $5 \times 10^5$  cells per 175cm<sup>2</sup> flask and grown for 4 days in complete RPMI. Supernatant was harvested, filter sterilised and frozen at -80°C.

**10x TBS**

100mM Tris, 1.5M NaCl in MQ dH<sub>2</sub>O, pH8.0

**TBS**

10mM Tris, 150mM NaCl in MQ dH<sub>2</sub>O, pH8.0

**KalB stock solution**

50mM Tris-HCl (pH 7.4), 150mM NaCl, 1% Triton X100, 1mM EDTA

**KalB Lysis Buffer**

1ml KalB stock solution was supplemented with shavings of EDTA-free protease inhibitor cocktail tablet (Roche), 20µl 50mM NaV, 40µl of 50x Ser/Thr phosphatase inhibitors and 20µl 100mM PMSF

**50x Serine/Threonine Phosphatase Inhibitors**

250µl 1M Sodium Fluoride, 6.049g Sodium Molybdate (BDH Chemicals), 11.1526 Sodium Pyrophosphate (Sigma Aldrich) dissolved in 500ml MQ dH<sub>2</sub>O

**1M Sodium Fluoride**

4.2g Sodium Fluoride (Lancaster) dissolved in 2ml of MQ dH<sub>2</sub>O

**10% Ammonium Persulfate (APS)**

10% w/v APS (Bio-Rad) in MQ dH<sub>2</sub>O

**Coomassie Blue SDS-PAGE Stain**

0.1% w/v Coomassie Blue R250, 40% v/v ethanol, 10% v/v glacial acetic acid in MQ dH<sub>2</sub>O

**DNA Loading Dye**

0.2% w/v bromophenol blue, 0.2% w/v xylene cyanol, 10mM EDTA (pH8.0), 20% v/v glycerol

**IMAC Wash Buffer**

10mM Tris, 150mM NaCl, 20mM imidazole, pH8.0 in MQ dH<sub>2</sub>O

**IMAC Elution Buffer**

10mM Tris, 150mM NaCl, 150mM imidazole, pH8.0 in MQ dH<sub>2</sub>O

**Luria-Bertani (LB) Broth**

1% w/v Bacto-tryptone, 1% w/v NaCl, 0.5% w/v Bacto-Yeast Extract, dissolved in MQ dH<sub>2</sub>O

**LB Agar**

LB Broth with 1% w/v agar

**Phosphate Buffered Saline (PBS)**

4.3mM Sodium Phosphate, Dibasic, 137mM NaCl, 2.7mM KCl, 1.4mM Potassium Phosphate, Monobasic in MQ dH<sub>2</sub>O, pH7.4

**PBST (PBS + Tween)**

PBS supplemented with 0.1% Tween20

**Phenylmethylsulphonyl Fluoride (PMSF)**

100mM PMSF dissolved in isopropanol

**SDS-PAGE Running Buffer**

25mM Tris-HCl (pH8.3), 192mM Glycine, 0.1% SDS in MQ dH<sub>2</sub>O

**10x Western Blot Transfer Buffer**

16mM Tris-HCl (pH8.4), 120mM Glycine in MQ dH<sub>2</sub>O

**Western Blot Transfer Buffer**

20% methanol with 1x Western Blot Transfer Buffer diluted in MQ dH<sub>2</sub>O

**10% Ammonium Persulfate (APS)**

1g Ammonium Persulfate dissolved in 10ml MQ dH<sub>2</sub>O.

**5% SDS-PAGE Stacking Gel**

For 4mL

- 2.7ml H<sub>2</sub>O
- 0.67ml 30% Acrylamide
- 40µl 10% SDS
- 40µl 10% APS
- 6µl Temed

**10x Hepes Buffer**

200mM Hepes, 1.5M NaCl dissolved in MQ dH<sub>2</sub>O, pH 6.0

**8% SDS-PAGE Running Gel**

For 10ml

- 4.6ml H<sub>2</sub>O
- 2.7ml 30% Acrylamide
- 2.5ml 1.5M Tris-HCl pH8.8
- 100µl 10% SDS
- 100µl 10% APS
- 6µl TEMED

**15% SDS-PAGE Running Gel**

For 10ml

- 2.3ml H<sub>2</sub>O
- 5ml 30% Acrylamide
- 2.5ml 1.5M Tris-HCl pH8.8
- 100µl 10% SDS
- 100µl 10% APS
- 4µl TEMED

**5% Milk Solution**

1.25g Skim Milk Powder (Diploma) was dissolved in 25ml PBST

**CAPS Transfer Buffer**

10mM CAPS, 15% Methanol, pH11

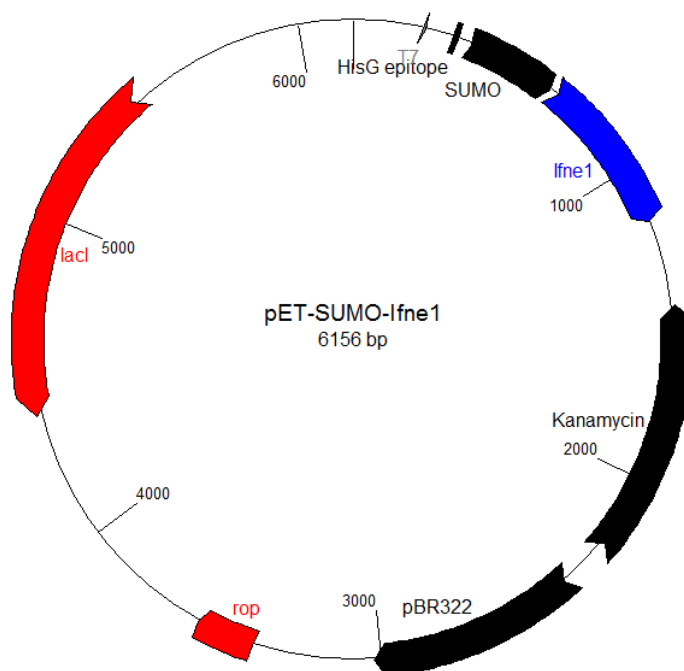
**Red Blood Cell Lysis Buffer**

150mM NH<sub>4</sub>Cl, 10mM KHCO<sub>3</sub>, 0.1mM EDTA, pH7.3

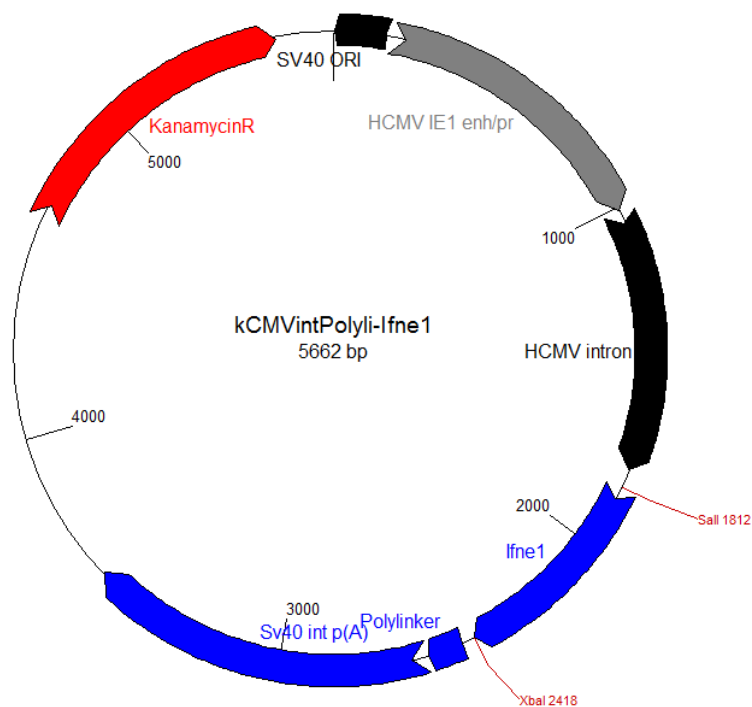
**Glycine Strip Buffer**

3.15 Glycine dissolved in 1L MQ dH<sub>2</sub>O, pH2.0

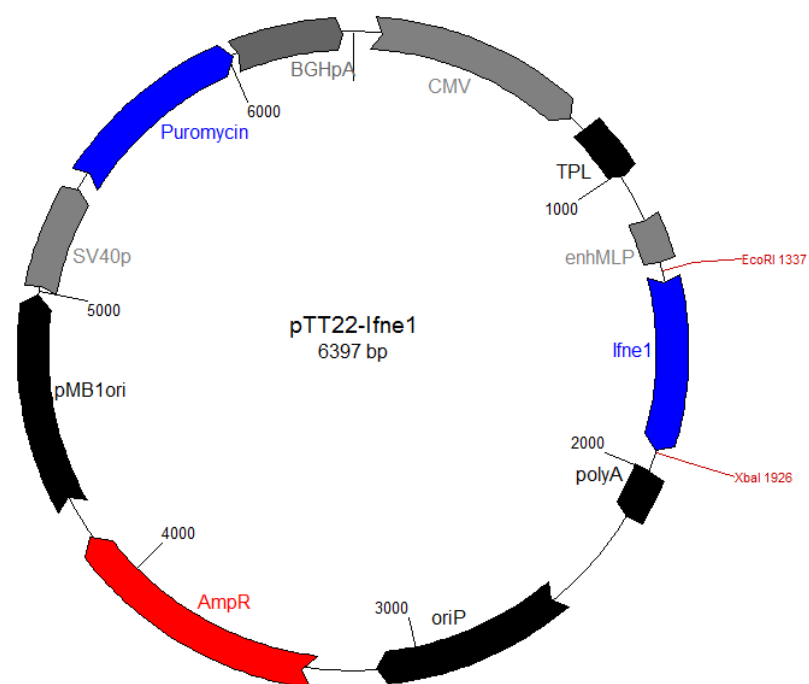
## Appendix B - Vector Maps



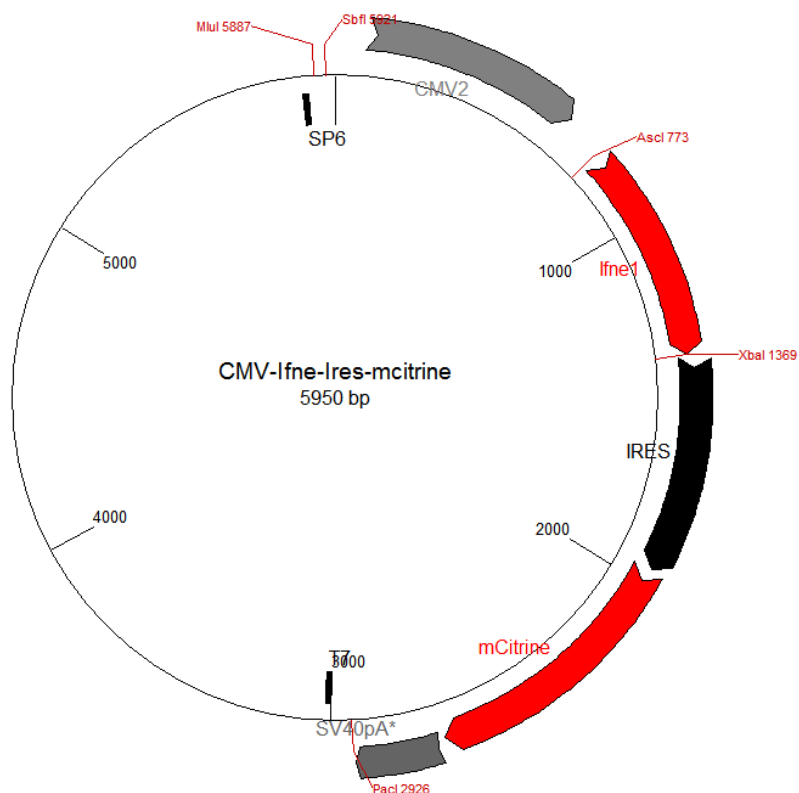
**B.1 Vector Map of pET-SUMO-lfne1.** The mature codon sequence of *lfne1* was cloned into pET-SUMO by TA ligation. Features: T7, T7 promoter; HisG epitope, His<sub>6</sub> sequence; SUMO, open reading frame of SUMO fusion partner; *lfne1*, open reading frame of interferon epsilon gene; Kanamycin, Kanamycin resistance gene; pBR322, pBR322 bacterial origin of replication; *rop*, ROP open reading frame; *lacI*, *lacI* open reading frame. The vector map was generated in GENTle



**B.2 Vector Map of pkCMVintPolyli-lfne1.** The mature codon sequence of *lfne1* was cloned into pkCMVintPolyli with Sall and Xbal restriction enzymes. Features: KanamycinR, Kanamycin resistance gene; SV40 Ori, SV40 origin of replication; HCMV IE1 enh/pr, Human cytomegalovirus (HCMV) enhancer promoter sequence; HCMV intron, intron sequence from HMCV; polylinker, multiple cloning site; SV40int p(A), simian virus-40 polyadenylation signal. pkCMVintPolyli was provided by Cassandra Berry (Murdoch University) with permission of VICAL. Inc (San Diego, USA). The vector map was generated in GENTle



**B.3 Vector Map of pTT22-lfne1.** The complete codon sequence of *lfne1* was cloned into pTT22 with EcoRI and XbaI restriction enzymes. Features: CMV, cytomegalovirus promoter; TPL, tripartite leader sequence; enhMPL; adenovirus major late promoter; *lfne1*, codon sequence coding for murine *lfne1*; polyA, polyadenylation signal; oriP, Epstein Barr virus origin of replication; AmpR, Ampicillin resistance gene; pMB1ori, bacterial origin of replication; SV40p, simian virus-40 promoter; Puromycin, puromycin resistance gene; BGHpA, bovine growth hormone polyadenylation signal. pTT22 vector was generously provided by Yves Durocher (BRI, Montreal, Canada). Vector map was modified from the original provided by Yves Durocher. The vector map was generated in GENTle



**B.4 Vector Map of pCMV-Ifne-Ires-mCitrine.** The complete codon sequence of *Ifne1* was cloned into pCMV with *Ascl* and *XbaI* restriction enzymes. Features: CMV2, cytomegalovirus promoter; *Ifne1*, nucleotide sequence coding for murine *Ifne1*; IRES, internal ribosomal entry site; mCitrine, mCitrine fluorophor; SV40pA, simian virus-40 polyadenylation signal. pCMV-Ifne-Ires-mCitrine vector was generously provided by Dr. Ka Yee Fung and Dr. Alec Drew (MIMR, Clayton, Australia). The vector map was generated in GENTle.

## Appendix C – Monash PPU Report

**PROTEIN PRODUCTION UNIT**

PROJECT REPORT

BLD 16, LEVEL 1  
DEPARTMENT OF  
BIOCHEMISTRY AND  
MOLECULAR BIOLOGY,  
CLAYTON CAMPUS,  
MONASH UNIVERSITY,  
CLAYTON, VICTORIA, 3800

PHONE: 61 3 9902 0019  
FAX: 61 3 9905 3726

MANAGER: DR NOELENE QUINSEY  
PHONE: 61 3 99020020  
EMAIL:  
PROTEINPRODUCTION.BIOCHEMISTRY@MED.MONASH.  
EDU.AU

**PURPOSE**

THE TRIAL EXPRESSION OF THE SUMO IFN  $\epsilon$  CONSTRUCT

**OVERALL SUMMARY**

**EXPRESSION CONDITIONS USED:**  
All transformed cells were selected on the LB agar plates with incubation overnight at 37°C. Individual colonies were selected and grown in autoinduction media with antibiotics at 28°C overnight with shaking at 250rpm. For the 20°C cultures, they were grown for a further 24 hours at 20°C and shaking at 250rpm.

All cultures were lysed by the addition of Popculture + lysonase. Samples were taken after lysis with popculture and after purification using the nickel affinity resin. The lysed sample is mixed with the nickel resin for 20min at room temperature. The resin was washed twice with about 10 column volumes of wash buffer (300mM NaCl, 50mM sodium phosphate buffer, 20mM Imidazole, pH 8.0). The protein was eluted with 300mM NaCl, 50mM sodium phosphate buffer, 250mM Imidazole, pH 8.0 and the eluted protein collected, 150 $\mu$ l of buffer is used to elute the protein.

**EXPRESSION RESULTS**

THERE WERE A NUMBER OF CELL LINES THAT EXPRESSED A PROTEIN OF THE EXPECTED SIZE, ESPECIALLY WHEN GROWN AT 20°C. BECAUSE OF THE LOW LEVELS OF EXPRESSION DETECTED THERE WERE MULTIPLE OTHER BANDS PRESENT. ANALYSIS OF THE VARIOUS FRACTIONS USING A WESTERN BLOT ANALYSIS USING AN ANTI-HIS TAGGED ANTIBODY, SHOWED THAT THERE WAS A PROTEIN OF THE EXPECTED SIZE. IT ALSO DETECTED WHAT LOOKS LIKE SOME BREAKDOWN PRODUCTS, WHICH INDICATE THAT THE FUSION PROTEIN IS BEING DEGRADED AT THE C-TERMINAL END OF THE PROTEIN. THERE WERE NO PROTEASE INHIBITORS ADDED TO ANY OF THE SOLUTIONS USED.

THE BEST CELLS LINES FOR THE EXPRESSION OF THIS CONSTRUCT WERE THE BL21 (DE3) C43 AND THE BL21 (DE3) C41 CELLS WHEN THEY WERE GROWN AT 20°C. THERE WERE DETECTABLE LEVELS OF PROTEIN EXPRESSED IN THE BL21 (DE3) RP AND RIL WHEN THEY WERE GROWN AT 20°C. WHEN THE CELLS WERE GROWN AT 28°C, THE BL21 (DE3) RIL AND BL21 (DE3) C41 CELLS WERE ABLE TO EXPRESS LOW LEVELS OF THE RECOMBINANT PROTEIN AS DETERMINED BY WESTERN BLOT ANALYSIS.

**Appendix C (continued)****PROTEIN PRODUCTION UNIT**

## EXPECTED SIZES OF RECOMBINANT PRODUCT

PROTEIN NAME	ANTIBIOTIC	EXPECTED SIZE (kDA)
SUMO IFN $\epsilon$	KAN	33

CELL LINES USED FOR THE EXPRESSION OF THE CONSTRUCTS AT TWO DIFFERENT TEMPERATURES.

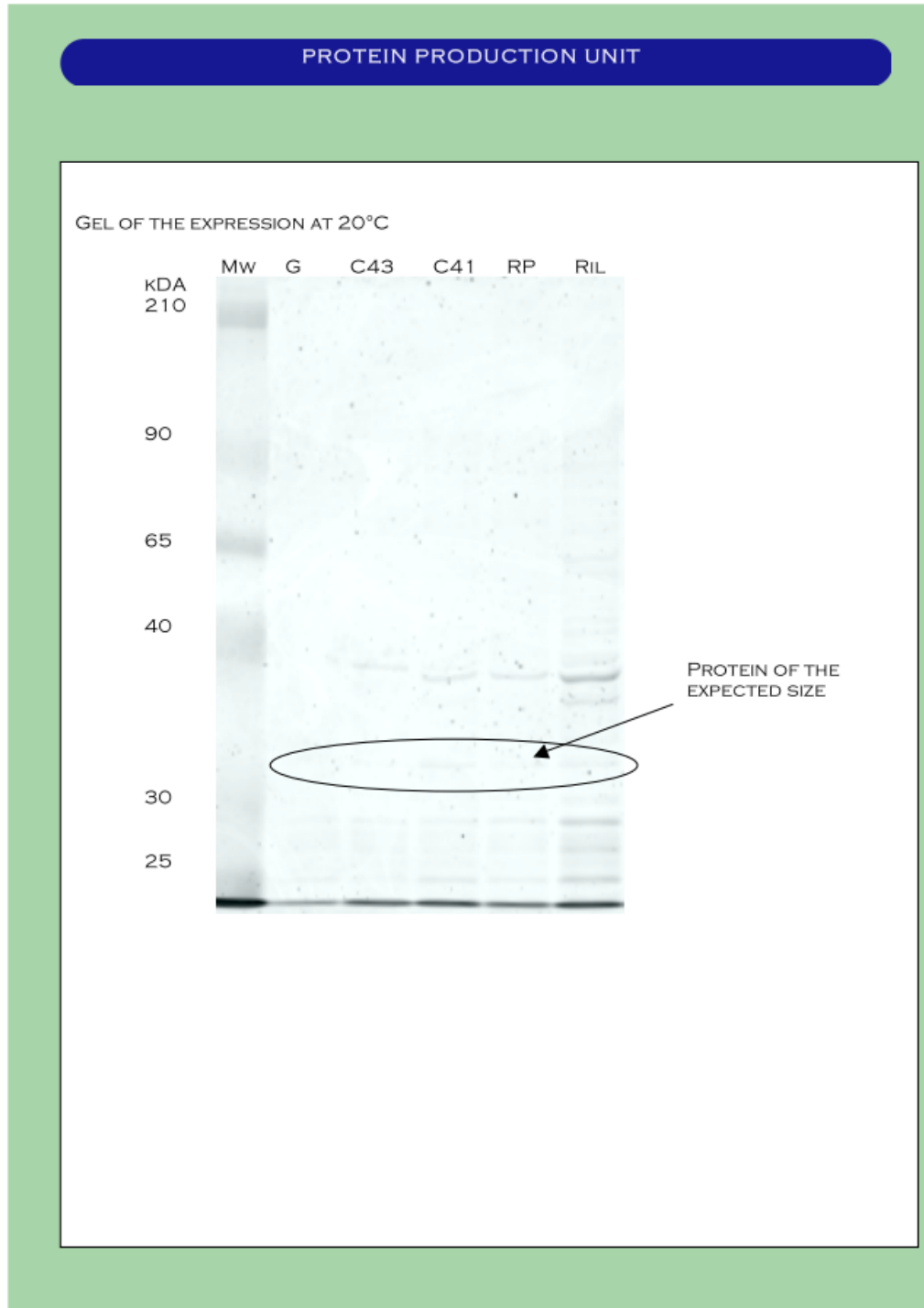
Cell line	SUMO IFN $\epsilon$	
	28°C	20°C
BL21(DE3) GOLD	-	-
BL21(DE3) C43	-	+++
BL21(DE3) C41	+	+++
BL21(DE3) CODON PLUS RP	-	++
BL21(DE3) CODON PLUS RIL	+	++
ROSETTA 2 (DE3)	-	-
GENERATION X	-	-
SG13009	+	+

**KEY**

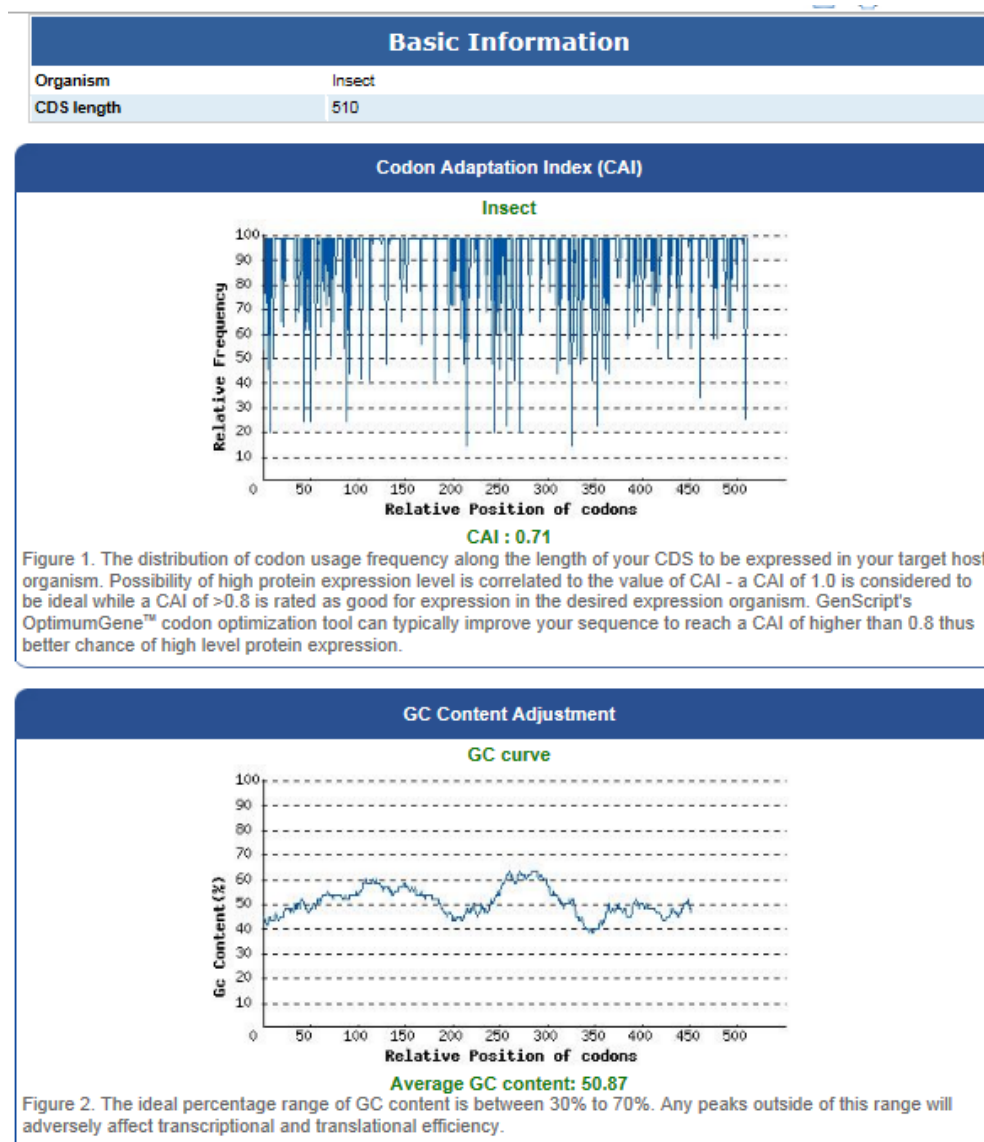
- = NOT DETECTED
- + = FAINT INTENSITY
- ++ = MODERATE INTENSITY
- +++ = HIGH INTENSITY
- ++++ = HIGHEST INTENSITY

EXPRESSION WAS CONFIRMED IN POSITIVE CASES USING AN ANTI-HIS TAGGED ANTIBODY.

**Appendix C (continued)**

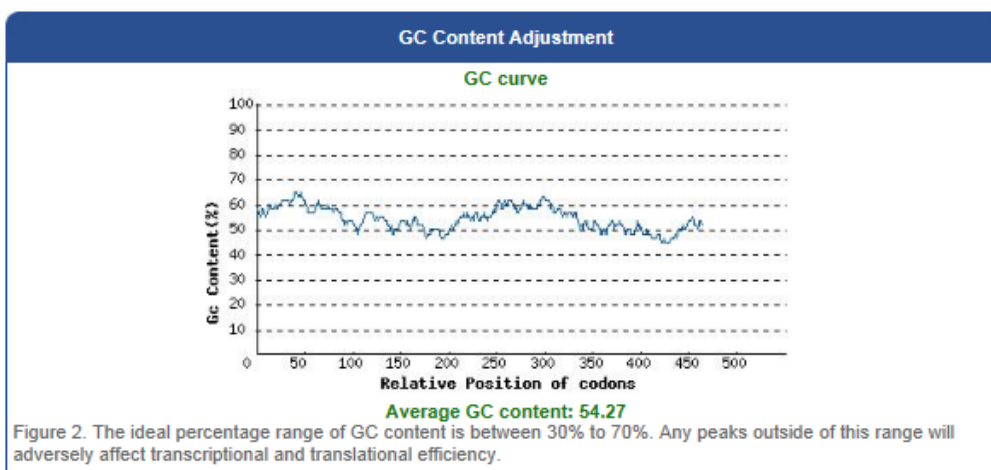
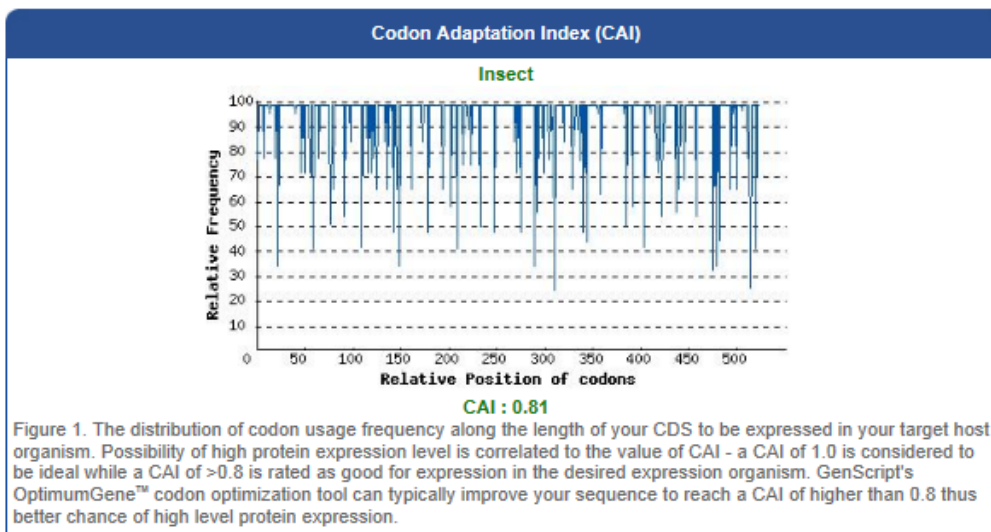


## Appendix D – Codon optimisation of murine *Ifne1*



**D.1 Codon Adaptatin Index (CAI) determination of native mature murine *Ifne1*.** The codon sequence of mature murine *Ifne1* was entered into Genscript's rare codon analysis tool available at [http://www.genscript.com/cgi-bin/tools/rare\\_codon\\_analysis](http://www.genscript.com/cgi-bin/tools/rare_codon_analysis). The CAI was determined to be 0.71.

Basic Information	
Organism	Insect
CDS length	522



**D.2 Codon Adaptatin Index (CAI) determination of codon optimised mature murine *lfne1*.** The codon optimised sequence of mature murine *lfne1* was entered into Genscript's rare codon analysis tool available at [http://www.genscript.com/cgi-bin/tools/rare\\_codon\\_analysis](http://www.genscript.com/cgi-bin/tools/rare_codon_analysis). The CAI was determined to be 0.81 and provide a better chance of high level expression.

## Appendix E - N-terminal amino acid sequencing of tagless IFNε

### Monash University Clayton

Micro Sequencing Service

Date 2/12/2011

Order #

Batch #

Sequence # 5153

Monash Proteomics Facility

Head : Prof. Ian Smith

Monash University

Wellington Road

Clayton

Victoria 3800

Telephone: 9905 1486

email: ian.smith@med.monash.edu.au

### Sequencing Details

Sample Name Sebastian Stifter - IFNE

Sample Preparation

Rinsed blot 3x. Alternating washes of water and 50%Methanol/Water. Cut blot into smaller pieces and loaded onto sequencer cartridge for sequencing on Procise. Sequencing method - Pulsed Liquid PVDF.

Molecular Weight

Enzymic Digestion

Sample Blot

Total Number of Cycles 6

Amount Loaded all

### Amino Acid Sequence

Residue 1 2 3 4 5 6 7 8 9 10

Major Sequence: A E L E P K

Minor Sequence:

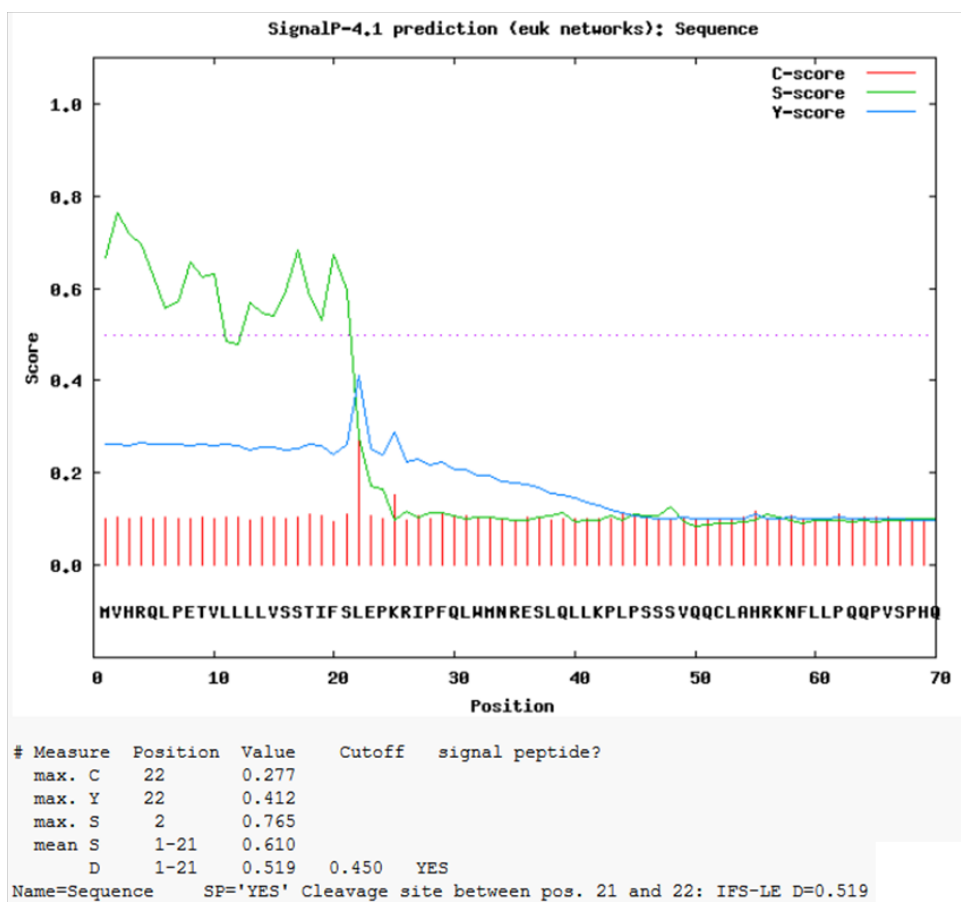
Residue 11 12 13 14 15 16 17 18 19 20

Major Sequence:

Minor Sequence:

### Comments

## Appendix F - Prediction of IFN $\epsilon$ signal peptide cleavage site by SignalP software



## **Appendix G - Primer Sequences**

### **PCR Amplification Primers**

Gapdh fwd	GAACGGGAAGCTTGTCATCAA
Gapdh rev	CTAAGCAGTTGGTGGTGCAG
M13 fwd	GTTTTCCCAGTCACGAC
M13 rev	CAGGAAACAGCTATGAC
pFB-seq	AAATGATAACCATCTCGC
pFB-MSP-Ifne1 fwd	GTACAATTGGAACCAAAGCGCA
pFB-MSP-Ifne1 rev	GCAAGCTTTCATGGGTCAGGGTCT
pFB-Ifnb1 fwd	GGATCCTATAAGCAGCTCCAGCTC
pFB-Ifnb1 rev	GTTAAGCTTAGTTTTGGAAGTTTCTGGTAAG

## TaqMan Gene Expression Assays for RT-PCR

Gene Name	Assay ID
<i>Isg15</i>	Mm01705338_s1
<i>Irf7</i>	Mm00516788_m1
<i>Oas1a</i>	Mm00836412_m1

Eukaryotic 18S rRNA endogenous control (VIC/MGB probe, primer limited)

## SyberGreen Primers for RT-PCR

Gene Name	Primer Sequence (5'-3')
18S fwd	TACACCAGCAGCAGGATCAG
18S rev	CCATCCAATCGGTAGTAGCG
<i>Isg15</i> fwd	TGAGAGCAAGCAGCCAGAAG
<i>Isg15</i> rev	ACGGACACCAGGAAATCGTT
<i>Irf7</i> fwd	ATCTTGCGCCAAGACAATTC
<i>Irf7</i> rev	AGCATTGCTGAGGCTCACTT
<i>Oas1a</i> fwd	CCTGCACAGACAGCTCAGAA
<i>Oas1a</i> rev	AGCCACACATCAGCCTCTTC

**Appendix H – N-terminal sequencing of native IFN $\epsilon$  expressed in HEK293 cells**

**Monash University Clayton**

Micro Sequencing Service		Monash Proteomics Facility
<b>Date</b>	2/5/2012	Head : Prof. Ian Smith
<b>Order #</b>		Monash University
<b>Batch #</b>		Wellington Road
<b>Sequence #</b>	5235	Clayton
		Victoria 3800
		Telephone: 9905 1486
		email: ian.smith@med.monash.edu.au

**Sequencing Details**

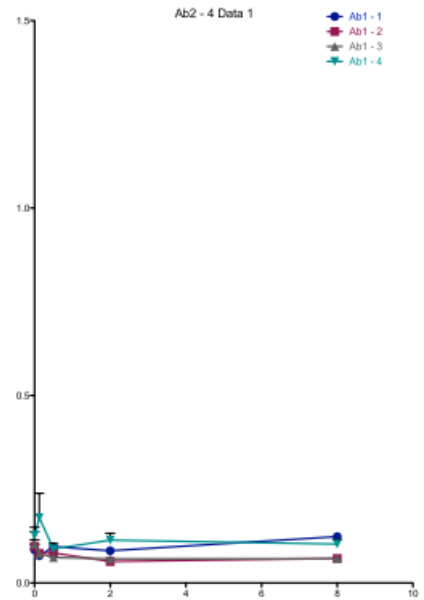
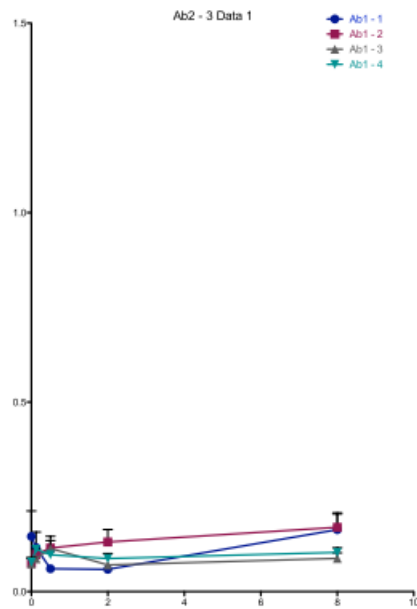
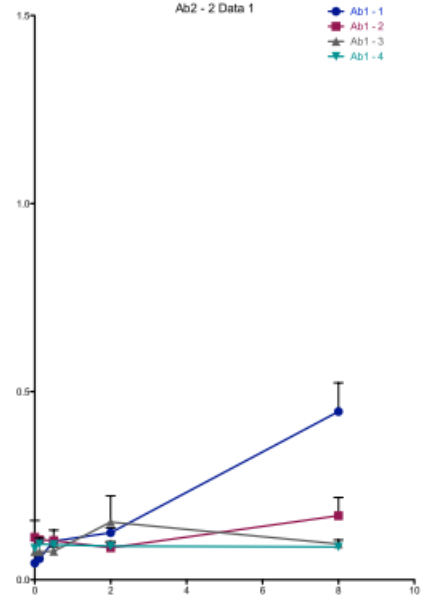
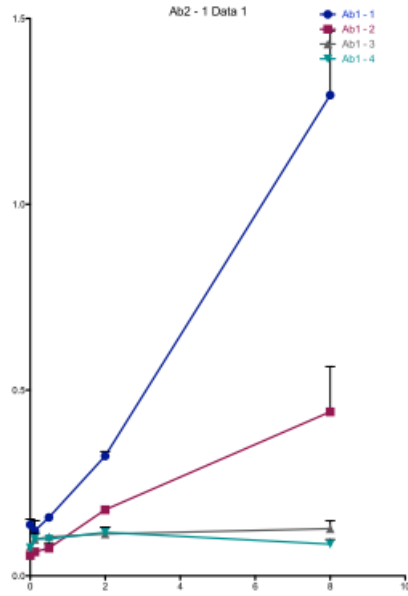
<b>Sample Name</b>	Sebastian - IFNE (top)
<b>Sample Preparation</b>	Rinsed blot 3x. Alternating washes of water and 50%Methanol/Water. Cut blot into smaller pieces and loaded onto sequencer cartridge for sequencing on Procise. Sequencing method - Pulsed Liquid PVDF.
<b>Molecular Weight</b>	
<b>Enzymic Digestion</b>	
<b>Sample</b>	Blot
<b>Total Number of Cycles</b>	6
<b>Amount Loaded</b>	all

**Amino Acid Sequence**

<b>Residue</b>	<b>1</b>	<b>2</b>	<b>3</b>	<b>4</b>	<b>5</b>	<b>6</b>	<b>7</b>	<b>8</b>	<b>9</b>	<b>10</b>
Major Sequence:	L	E	P	K	R	I				
Minor Sequence:										
<b>Residue</b>	<b>11</b>	<b>12</b>	<b>13</b>	<b>14</b>	<b>15</b>	<b>16</b>	<b>17</b>	<b>18</b>	<b>19</b>	<b>20</b>
Major Sequence:										
Minor Sequence:										

**Comments**

## Appendix I – MATF ELISA IFN $\epsilon$ optimisation

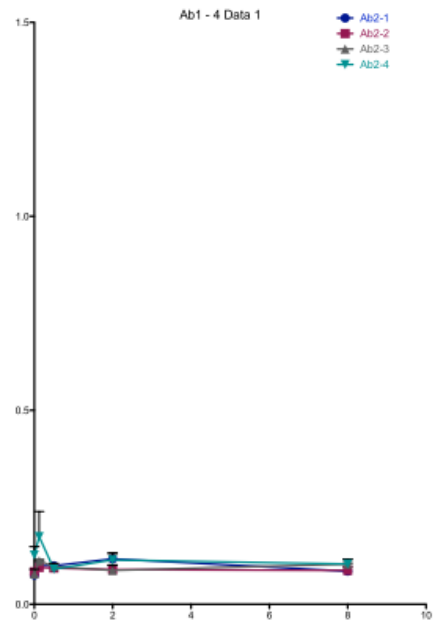
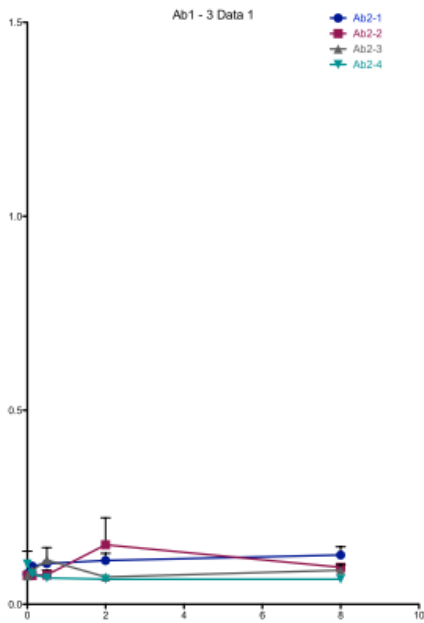
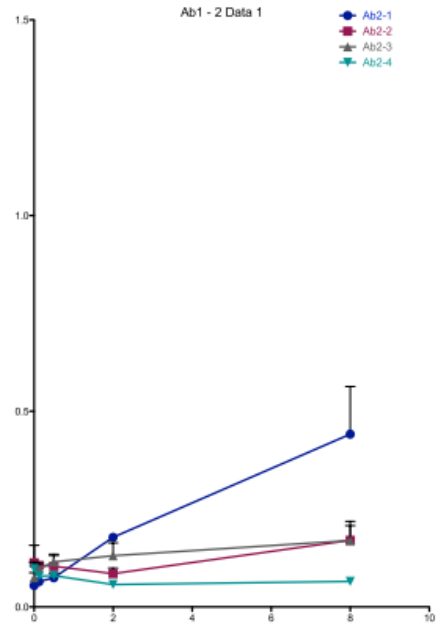
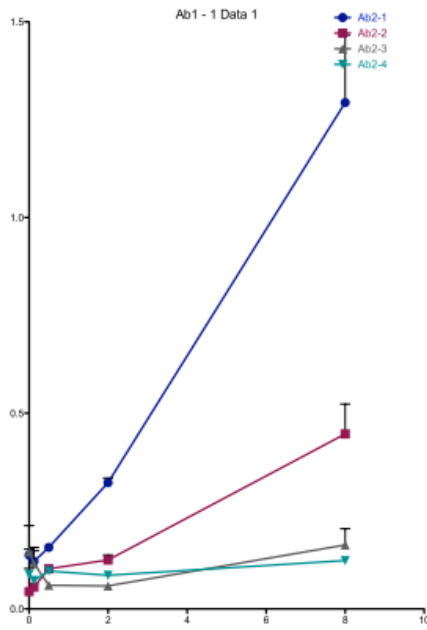


### **F.1 Optimisation of IFN $\epsilon$ ELISA by MATF**

Values on y-axis denote absorbance at 450nm. Values on x-axis denote IFN $\epsilon$  concentration in ng/ml. H3 Coating Ab 1-1, 10 $\mu$ g/mL, H3 Coating Ab 1-2 2.5 $\mu$ g/mL, H3 Coating Ab 1-3 0.625 $\mu$ g/mL, H3 Coating Ab 1-4 0.156 $\mu$ g/mL, C3 Detection Ab 2-1 0.25 $\mu$ g/mL, C3 Detection Ab 2-2 0.0625 $\mu$ g/mL, C3 Detection Ab 2-3 0.0156 $\mu$ g/mL, C3 Detection Ab 2-4 0.039 $\mu$ g/mL. Therefore the top right panel shows detection of IFN $\epsilon$  using H3 coating antibody at a concentration of 10 $\mu$ g/ml and detection with C3 antibody ranging from concentrations of 0.25 $\mu$ g/ml to 0.039 $\mu$ g/ml.

**Appendix I - MATF ELISA IFN $\epsilon$  optimisation**

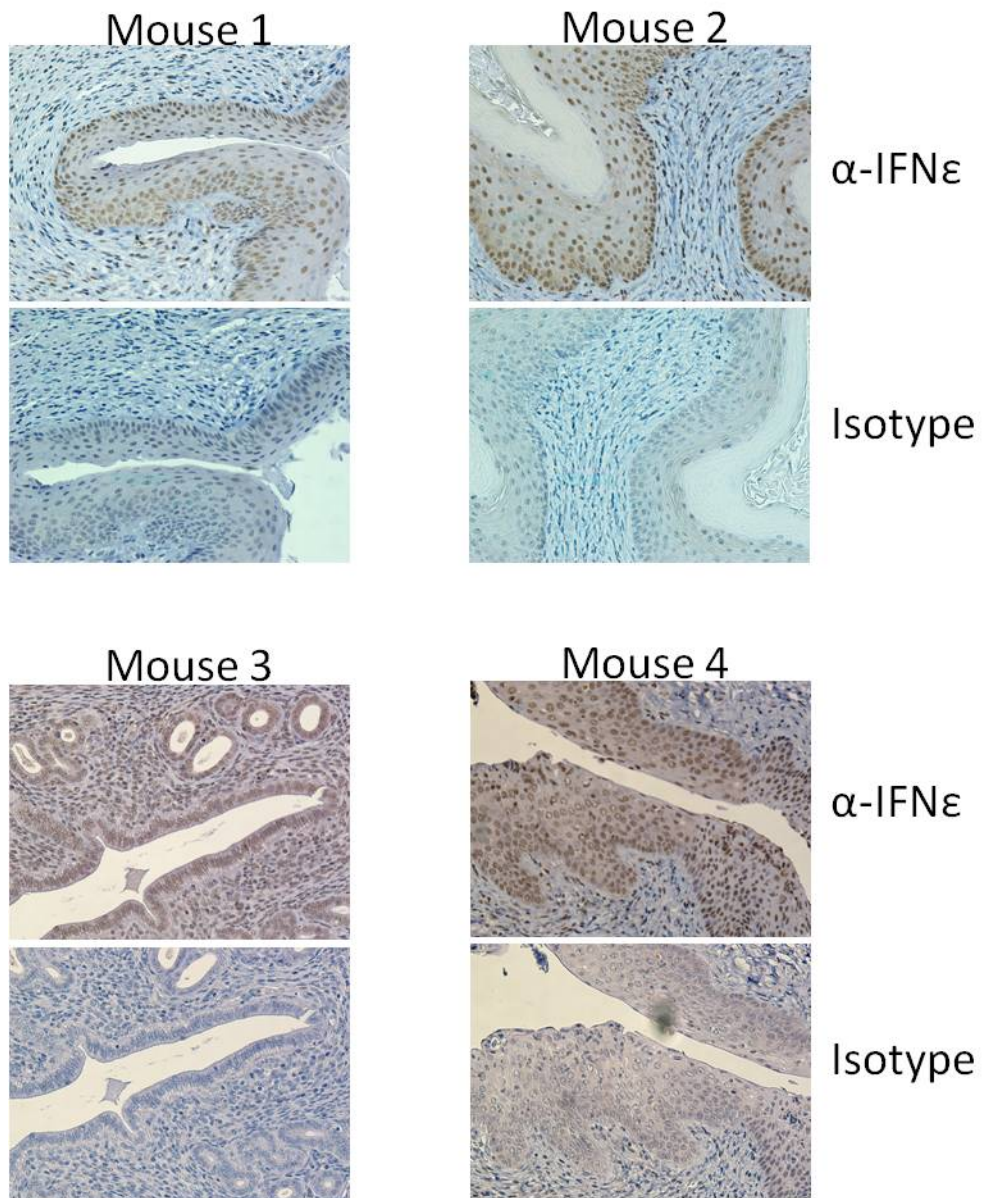
**(continued)**



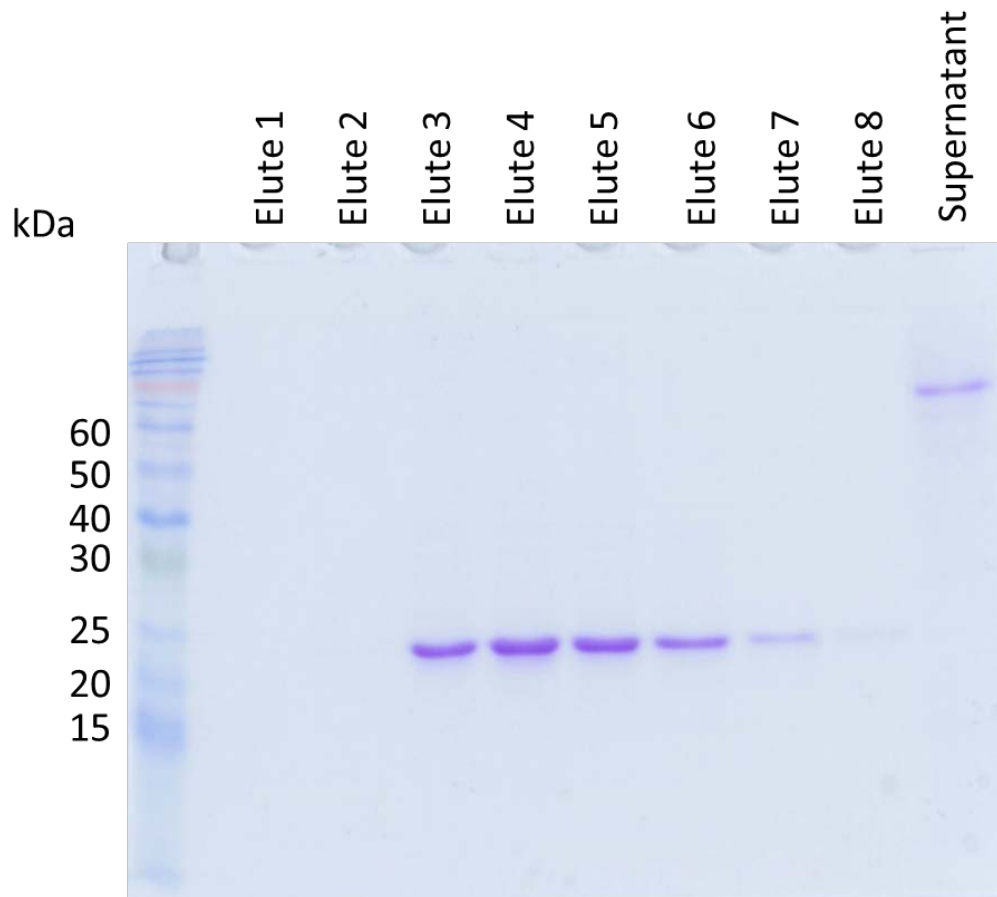
### **F.2 Optimisation of IFN $\epsilon$ ELISA by MATF**

Values on y-axis denote absorbance at 450nm. Values on x-axis denote IFN $\epsilon$  concentration in ng/ml. C3 Coating Ab 2-1, 10 $\mu$ g/mL, C3 Coating Ab 2-2 2.5 $\mu$ g/mL, C3 Coating Ab 2-3 0.625 $\mu$ g/mL, C3 Coating Ab 2-4 0.156 $\mu$ g/mL, H3 Detection Ab 1-1 0.25 $\mu$ g/mL, H3 Detection Ab 1-2 0.0625 $\mu$ g/mL, H3 Detection Ab 1-3 0.0156 $\mu$ g/mL, H3 Detection Ab 1-4 0.039 $\mu$ g/mL. Therefore the top right panel shows detection of IFN $\epsilon$  using C3 coating antibody at a concentration of 10 $\mu$ g/ml and detection with H3 antibody ranging from concentrations of 0.25 $\mu$ g/ml to 0.039 $\mu$ g/ml.

**Appendix J - Immunohistochemistry of uterine sections stained with anti-IFN $\epsilon$  monoclonal antibody C3**



**Appendix K - Highly pure IFN $\epsilon$  obtained from a single immunoaffinity step**



## **Appendix L - Published manuscripts**

Published manuscripts containing work performed in this thesis:

Fung, K.Y., et al., Interferon-epsilon protects the female reproductive tract from viral and bacterial infection. *Science*, 2013. **339**(6123): p. 1088-92.

Stifter, S.A., et al., Purification and biological characterization of soluble, recombinant mouse IFNbeta expressed in insect cells. *Protein Expr Purif*, 2014. **94**: p. 7-14.

The manuscripts are attached.

potential of T cells was altered by these microbiome manipulations, we assessed the ability of T cells from unmanipulated and from M→F recipient females (with or without flutamide) to transfer T1D to lymphocyte-deficient, T1D-resistant NOD.*SCID* (severe combined immunodeficient) recipients. T cells from unmanipulated NOD females transferred T1D to 100% of NOD.*SCID* recipients within 13 weeks (Fig. 4D). In contrast, T cells from M→F mice were delayed in their ability to transfer T1D ( $P < 0.002$ ; Fig. 4D). T cells from M→F + flutamide-treated mice transferred T1D with equivalent kinetics to the T cells from unmanipulated females (Fig. 4D). Thus, testosterone was a key mediator of male microbiota effects on the female metabolome and of the autoimmune response evident in insulinitis progression, Aab production, and the capacity of T cells to transfer diabetes to NOD.*SCID* recipients. Additional studies are needed to define the pro-autoimmune mechanisms conferred by the female intestinal microbiome that likely involve other hormone-regulated pathways.

Our results reveal that alteration of the gut microbiome composition in early life potentially suppresses autoimmunity in animals at high genetic risk for disease. Recent human data demonstrate that puberty and pregnancy shape the intestinal microbiota, provoking metabolic changes that may favor fertility and reproduction (26, 27). Similar to our findings in the NOD model, sex hormones may also modulate sexual dimorphism in human autoimmune diseases. The female-to-male bias in rheumatoid arthritis and multiple sclerosis incidence declines with older age at onset, coincident with a decline in testosterone (28, 29). In contrast, human T1D is not sex-biased, perhaps because the peak age at onset precedes puberty, with a recent rapid rise in incidence reported in children under 5 (30, 31). Our data demonstrate that microbiome alterations in young, commensally colonized mice conferred testosterone and metabolite changes sufficient to oppose genetically programmed autoimmunity while preserving fertility.

Evidence of intestinal dysbiosis in autoimmune disease patients is emerging (32, 33). As shown here and in a recent study of autoimmune demyelination (34), rodent models identify microbiome alterations as a causal factor and not merely a consequence of autoimmune disease. Improved prospective identification of children at high risk for autoimmunity through the use of genetic and immune markers could facilitate the testing of nonpathogenic microbial therapies in disease prevention and treatment.

#### References and Notes

- H. M. Scobie *et al.*, *PLoS Pathog.* **2**, e111 (2006).
- C. C. Whitacre, *Nat. Immunol.* **2**, 777 (2001).
- C. Ober, D. A. Loisel, Y. Gilad, *Nat. Rev. Genet.* **9**, 911 (2008).
- J. F. Bach, *N. Engl. J. Med.* **347**, 911 (2002).
- S. Makino *et al.*, *Jikken Dobutsu* **29**, 1 (1980).
- E. Leiter, M. Atkinson, *NOD Mice and Related Strains: Research Applications in Diabetes, AIDS, Cancer and Other Diseases* (Landes, Austin, TX, 1998), vol. 2.

- D. V. Serreze, E. H. Leiter, *Curr. Dir. Autoimmun.* **4**, 31 (2001).
- P. Miao, L. Yu, G. S. Eisenbarth, *Front. Biosci.* **12**, 1889 (2007).
- M. S. Anderson, J. A. Bluestone, *Annu. Rev. Immunol.* **23**, 447 (2005).
- S. Ghosh *et al.*, *Nat. Genet.* **4**, 404 (1993).
- P. Pozzilli, A. Signore, A. J. Williams, P. E. Beales, *Immunol. Today* **14**, 193 (1993).
- S. Makino, K. Kunitomo, Y. Muraoka, K. Katagiri, *Jikken Dobutsu* **30**, 137 (1981).
- H. S. Fox, *J. Exp. Med.* **175**, 1409 (1992).
- M. Harada, Y. Kishimoto, S. Makino, *Diabetes Res. Clin. Pract.* **8**, 85 (1990).
- H. Y. Qin, M. W. Sadelain, C. Hitchon, J. Lauzon, B. Singh, *J. Immunol.* **150**, 2072 (1993).
- E. A. Ivakine *et al.*, *Diabetes* **55**, 3611 (2006).
- E. A. Ivakine *et al.*, *J. Immunol.* **174**, 7129 (2005).
- See supplementary materials on Science Online.
- J. K. Nicholson *et al.*, *Science* **336**, 1262 (2012).
- T. Koal, H. P. Deigner, *Curr. Mol. Med.* **10**, 216 (2010).
- A. Oberbach *et al.*, *J. Proteome Res.* **10**, 4769 (2011).
- M. W. Sadelain, H. Y. Qin, J. Lauzon, B. Singh, *Diabetes* **39**, 583 (1990).
- E. Slack *et al.*, *Science* **325**, 617 (2009).
- K. Mittelstrass *et al.*, *PLoS Genet.* **7**, e1002215 (2011).
- J. G. Chai, E. James, H. Dewchand, E. Simpson, D. Scott, *Blood* **103**, 3951 (2004).
- O. Koren *et al.*, *Cell* **150**, 470 (2012).
- T. Yatsuneneko *et al.*, *Nature* **486**, 222 (2012).
- M. F. Doran, G. R. Pond, C. S. Crowson, W. M. O'Fallon, S. E. Gabriel, *Arthritis Rheum.* **46**, 625 (2002).
- B. G. Weinschenker, *Ann. Neurol.* **36** (Suppl.), S6 (1994).
- P. R. Burton *et al.*; Wellcome Trust Case Control Consortium, *Nature* **447**, 661 (2007).
- C. C. Patterson, G. G. Dahlquist, E. Gyürüs, A. Green, G. Soltész; EURODIAB Study Group, *Lancet* **373**, 2027 (2009).
- C. T. Brown *et al.*, *PLoS ONE* **6**, e25792 (2011).
- D. N. Frank, W. Zhu, R. B. Sartor, E. Li, *Trends Microbiol.* **19**, 427 (2011).

- K. Berer *et al.*, *Nature* **479**, 538 (2011).
- B. D. Wagner, C. E. Robertson, J. K. Harris, *PLoS ONE* **6**, e20296 (2011).

**Acknowledgments:** We thank S. Bashir for assistance with metabolomic data analysis, C. Vogel Kotter for high-throughput sequencing, and E. Simpson and M. Palmert for helpful discussions. The 16S sequence data have been submitted to the National Center for Biotechnology Information short-read archive project, accession no. SRA064044. Flow cytometry was performed in the SickKids–University Health Network Flow Cytometry Facility with funds from the Ontario Institute for Cancer Research, McEwen Centre for Regenerative Medicine, Canada Foundation for Innovation, and SickKids Foundation. Roche 454 sequencing was performed at the Centre for Applied Genomics, Hospital for Sick Children. Illumina sequencing was performed at the University of Colorado School of Medicine. Supported by Canadian Institutes of Health Research (CIHR) grant 64216 and Juvenile Diabetes Research Foundation (JDRF) grant 17-2011-520 (J.S.D.), Genome Canada (administered by Ontario Genomics Institute) (J.S.D. and A.J.M.), JDRF grant 36-2008-926 and the Genaxen Foundation (A.J.M.), a CIHR Banting and Best fellowship (J.G.M.M.), and NIH grant R21HG005964 (D.N.F. and C.E.R.). J.G.M.M. and J.S.D. designed the study, analyzed data, and wrote the manuscript; J.G.M.M., D.N.F., S.M.-T., C.E.R., M.v.B., K.D.M., and A.J.M. performed experiments and analyzed data; L.M.F. and U.R.-K. performed experiments; and all authors contributed to manuscript editing.

#### Supplementary Materials

www.sciencemag.org/cgi/content/full/science.1233521/DC1

Materials and Methods

Figs. S1 to S4

Tables S1 to S6

References (36–58)

3 December 2012; accepted 9 January 2013

Published online 17 January 2013;

10.1126/science.1233521

## Interferon- $\epsilon$ Protects the Female Reproductive Tract from Viral and Bacterial Infection

Ka Yee Fung,<sup>1\*</sup> Niamh E. Mangan,<sup>1\*</sup> Helen Cumming,<sup>1</sup> Jay C. Horvat,<sup>2</sup> Jemma R. Mayall,<sup>2</sup> Sebastian A. Stifter,<sup>1</sup> Nicole De Weerd,<sup>1</sup> Laila C. Roisman,<sup>1,3</sup> Jamie Rossjohn,<sup>3</sup> Sarah A. Robertson,<sup>4</sup> John E. Schjenken,<sup>4</sup> Belinda Parker,<sup>5,6</sup> Caroline E. Gargett,<sup>7,8</sup> Hong P. T. Nguyen,<sup>7</sup> Daniel J. Carr,<sup>9</sup> Philip M. Hansbro,<sup>2</sup> Paul J. Hertzog<sup>1†</sup>

The innate immune system senses pathogens through pattern-recognition receptors (PRRs) that signal to induce effector cytokines, such as type I interferons (IFNs). We characterized IFN- $\epsilon$  as a type I IFN because it signaled via the *lfnr1* and *lfnr2* receptors to induce IFN-regulated genes. In contrast to other type I IFNs, IFN- $\epsilon$  was not induced by known PRR pathways; instead, IFN- $\epsilon$  was constitutively expressed by epithelial cells of the female reproductive tract (FRT) and was hormonally regulated. *lfn- $\epsilon$* -deficient mice had increased susceptibility to infection of the FRT by the common sexually transmitted infections (STIs) herpes simplex virus 2 and *Chlamydia muridarum*. Thus, IFN- $\epsilon$  is a potent antipathogen and immunoregulatory cytokine that may be important in combating STIs that represent a major global health and socioeconomic burden.

Type I interferons (IFNs) are crucial in host defense because of their antipathogen actions and ability to activate effector cells of the innate and adaptive immune responses (1, 2). The type I IFN locus contains genes encoding 13 IFN- $\alpha$  subtypes, IFN- $\beta$ , and IFN- $\omega$  (3) whose promoters contain acute response elements [such as interferon regulatory factors (IRFs) and

NF- $\kappa$ B in IFN- $\beta$ ], which ensure rapid induction of these genes by pattern-recognition receptor (PRR) pathways (4, 5). This locus also contains a gene, which we previously designated *IFN- $\epsilon$* , but whose function has remained uncharacterized.

Interferon- $\epsilon$  shares only 30% amino acid homology to a consensus IFN- $\alpha$  sequence and to IFN- $\beta$ . Therefore, we first demonstrated that

IFN- $\epsilon$  was a type I IFN by showing that it transduced signals via the *Ifnar1* and *Ifnar2* receptors (see the supplementary materials and methods) (6). Incubation of recombinant *Ifn- $\epsilon$*  with bone marrow-derived macrophages (BMDMs) from wild-type (WT) mice induced IFN-regulated genes (IRGs) such as *Irf-7* and *2'5'oas* (which encodes oligoadenylate synthetase) (Fig. 1, A and B), whereas these IRGs were not induced in BMDMs from *Ifnar1*- or *Ifnar2*-deficient mice. Accordingly, *Ifn- $\epsilon$*  should be classified as a type I IFN.

We next determined whether IFN- $\epsilon$  was induced by PRR pathways. Primary BMDMs, murine embryonic fibroblasts, and the murine macrophage cell line RAW264.7 were treated with synthetic ligands of Toll-like receptors (TLRs) 2, 3, 4, 7/8, and 9; cytosolic DNA sensors or AIM2 inflammasomes potentially induced known PRR response genes such as *Ifn- $\beta$*  and/or *interleukin-6* (*Il-6*) (7–9). By contrast, there was no significant change in the expression of *Ifn- $\epsilon$*  upon stimulation with these activators (Fig. 1C and fig. S1, A and B). Because all PRRs induce type I IFN expression through the activation of the IRF family of transcription factors (5), we then examined whether IRFs could directly regulate the *Ifn- $\epsilon$*  promoter. IRF-3, IRF-7, and IRF-5 induced promoter activity of *Ifn- $\beta$* , *Ifn- $\alpha$* , and *p125* (5) luciferase reporters in human embryonic kidney (HEK) 293 cells (Fig. 1D). By contrast, we did not observe any alteration of *Ifn- $\epsilon$*  promoter activity (Fig. 1D). Semliki Forest virus infection of RAW264.7 cells stimulated the expression of the positive control antiviral response gene *2'5'oas*, but not *Ifn- $\epsilon$*  expression (fig. S1C). Furthermore, *Ifn- $\epsilon$*  expression was not altered during *in vivo* infection with herpes simplex virus 2 (HSV-2) or *Chlamydia muridarum* (see below), nor by stimulation of human endometrial cell lines with PRR ligands (fig. S1D). This lack of regulation of *Ifn- $\epsilon$*  gene expression by conventional PRR pathways is consistent with the lack of response elements for these pathways [IRFs, NF- $\kappa$ B, STAT (signal transducers and activators of transcription), ISRE (interferon-stimulated response element)] in the *Ifn- $\epsilon$*  proximal promoter compared with other type I IFN genes (fig. S1E).

Because *Ifn- $\epsilon$*  was not regulated by PRR pathways, we examined its constitutive expression. The expression of *Ifn- $\alpha$*  and  $\beta$  was undetectable in all organs (Fig. 2A). Similarly, the expression of *Ifn- $\epsilon$*  was not detectable at significant levels in any organ except the uterus, cervix, vagina, and ovary (Fig. 2A). Immunohistochemistry results show that *Ifn- $\epsilon$*  was expressed in the luminal and glandular epithelial cells of the endometrium (Fig. 2B). In support of these data, the uterine expression levels of *Ifn- $\epsilon$*  did not differ in NOD (nonobese diabetic)/SCID (severe combined immunodeficient)/IL-2 $\gamma$ <sup>-/-</sup> mice [which are deficient in mature T, B, and natural killer (NK) cells] relative to WT mice, indicating that the aforementioned cells do not express detectable levels, nor do they regulate this cytokine (fig. S1F). This finding differs from the expression of conventional type I IFNs, which are usually expressed in hemopoietic cells.

We found that *Ifn- $\epsilon$*  expression varied approximately 30-fold at different stages of the estrous cycle, with the lowest levels during diestrus and the highest at estrus (Fig. 2C). During pregnancy, uterine *Ifn- $\epsilon$*  expression was dramatically reduced at day 1.5 postcoitus (pc) and was lowest at day 4.5 pc, coincident with the time of embryo im-

plantation (Fig. 2D). *Ifn- $\epsilon$*  expression was also reduced in pseudo-pregnant mice 4.5 days pc after mating with vasectomized males (Fig. 2D), which suggests that maternal hormones, not the embryo or its products, were required for the reduction in *Ifn- $\epsilon$* . In addition, there was a slight increase in expression of *Ifn- $\epsilon$*  (1.8- to 1.9-fold) 8 hours pc, though expression had returned to normal levels by 16 hours pc, showing that neither seminal fluid nor sperm directly suppress *Ifn- $\epsilon$*  expression (fig. S1G). Because changes in expression occur after mating with vasectomized or intact males, expression fluctuations are likely to be secondary to physiological and hormonal changes, which are known to be comparable at day 4.5 pc whether or not conception occurs. Together, these data are consistent with *Ifn- $\epsilon$*  expression being hormonally regulated. To evaluate this finding, we ovariectomized female mice and administered ovarian sex steroid hormones. Estrogen administration induced *Ifn- $\epsilon$*  expression more than sixfold (Fig. 2E). This hormonal regulation was not observed for expression of other conventional type I IFNs (10).

Expression analysis of a panel of tissues confirmed the lack of basal expression of *IFN- $\epsilon$*  in all organs in women, with the exception of the

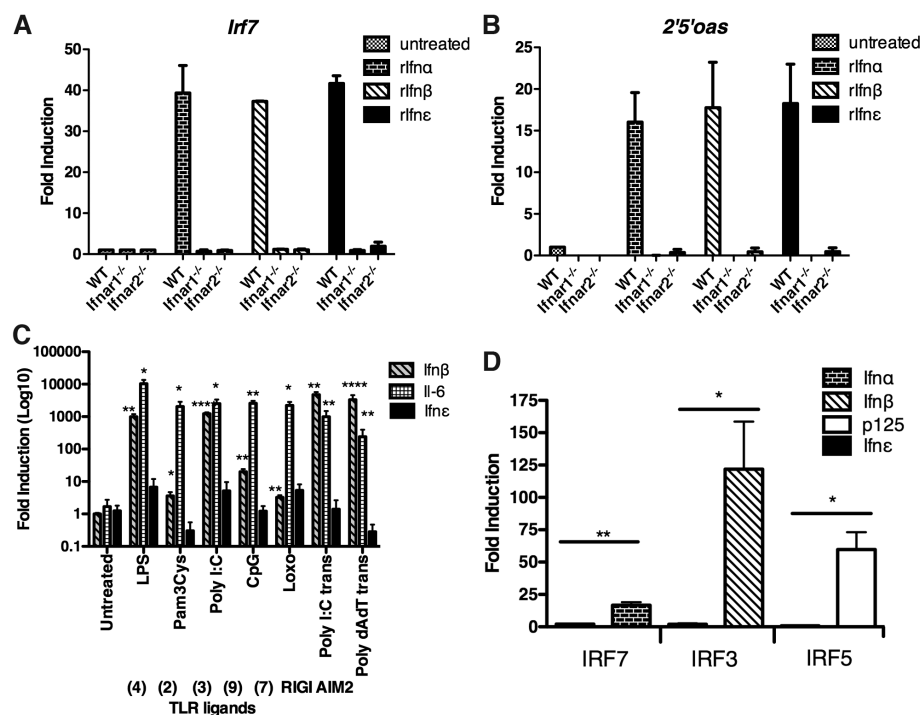


**Fig. 1.** Interferon- $\epsilon$  signals through the type I IFN receptor but is not induced by TLR ligands nor regulated by IRFs. (A and B) BMDMs from WT, *Ifnar1*<sup>-/-</sup>, and *Ifnar2*<sup>-/-</sup> C57BL/6 mice were stimulated with recombinant mouse *Ifn- $\alpha$* 1, *Ifn- $\beta$* , or *Ifn- $\epsilon$*  (0.1  $\mu$ g/ml) for 3 hours. (A) *Irf-7* and (B) *2'5'oas* expression was measured by quantitative real-time fluorescence polymerase chain reaction (qRT-PCR). Data are expressed as mean  $\pm$  SEM (error bars) of at least three independent experiments. (C) BMDMs from C57BL/6 WT mice were treated with a range of TLR ligands or transfected with Poly (I:C) and Poly (dA:dT) for 3 hours at 37°C. *Ifn- $\beta$* , *Il-6*, and *Ifn- $\epsilon$*  were measured by qRT-PCR. Data are expressed as mean  $\pm$  SEM of at least three independent experiments. (D) Luciferase reporter plasmids containing *Ifn- $\alpha$* , *Ifn- $\beta$* , *p125*, or *Ifn- $\epsilon$*  were cotransfected with empty vector or IRF-3, IRF-7, or IRF-5 expression vectors into HEK293 cells. Data are expressed as mean  $\pm$  SEM. All values are means of at least three independent experiments. \**P* < 0.05; \*\**P* < 0.01; \*\*\**P* < 0.001; \*\*\*\**P* < 0.0001 (unpaired Student's *t* test).

<sup>1</sup>Centre for Innate Immunity and Infectious Diseases, Monash Institute of Medical Research, Monash University, Clayton, Victoria, Australia. <sup>2</sup>Centre for Asthma and Respiratory Disease and Hunter Medical Research Institute, The University of Newcastle, Newcastle, New South Wales, Australia. <sup>3</sup>Department of Biochemistry and Molecular Biology, Monash University, Clayton, Victoria, Australia. <sup>4</sup>Robinson Institute and School of Paediatrics and Reproductive Health, University of Adelaide, South Australia, Australia. <sup>5</sup>Peter MacCallum Cancer Centre, East Melbourne, Victoria, Australia. <sup>6</sup>Sir Peter MacCallum Department of Oncology, The University of Melbourne, Parkville, Australia. <sup>7</sup>The Ritchie Centre, Monash Institute of Medical Research, Monash University, Clayton, Victoria, Australia. <sup>8</sup>Department of Obstetrics and Gynaecology, Monash University, Clayton, Victoria, Australia. <sup>9</sup>Department of Ophthalmology and Department of Microbiology and Immunology, University of Oklahoma Health Sciences Center, Oklahoma City, OK, USA.

\*These authors contributed equally to this work.  
 †To whom correspondence should be addressed.

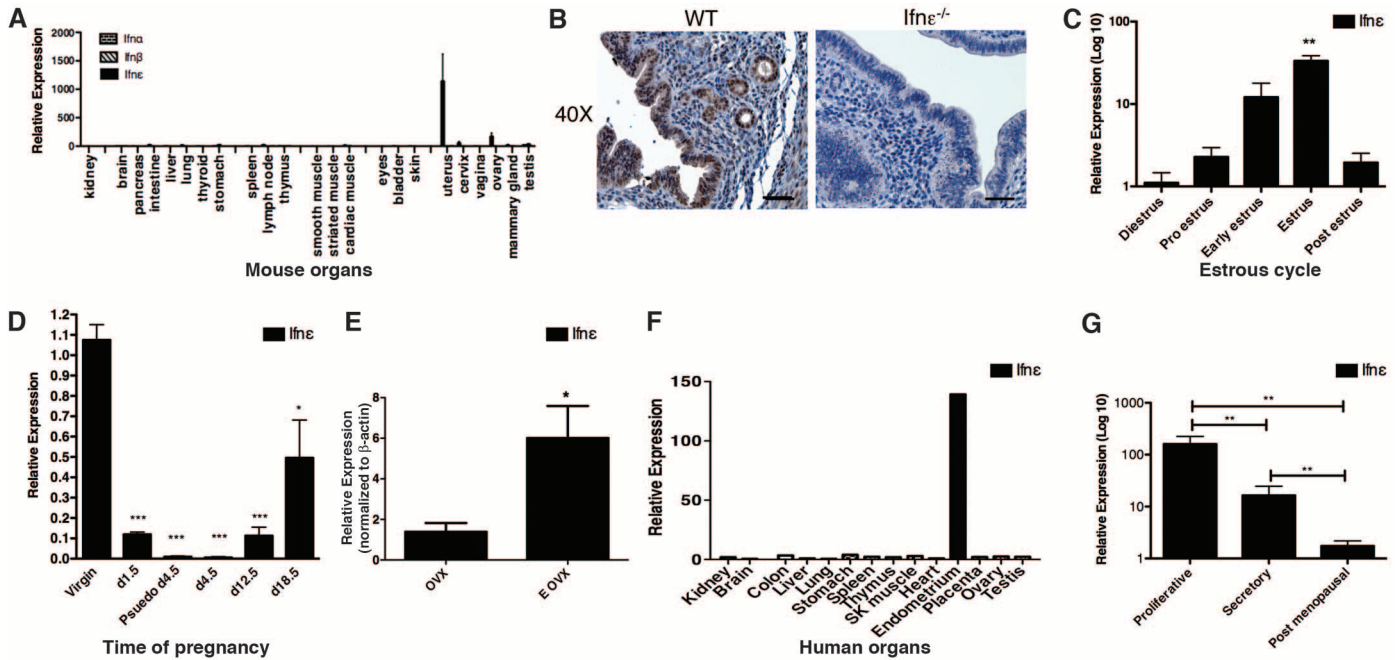


**Fig. 2.** Interferon-ε is expressed in the FRT in both mice and humans. (A) Mouse organs were harvested and *Ifn-ε* expression was measured by qRT-PCR, normalized to 18S RNA and presented relative to *Ifn-ε* expression in kidney. Data are expressed as the mean ± SEM (error bars) of at least three individual mice. (B) Representative images showing *Ifn-ε* localization in uterine tissue (at estrous stage) of WT and *Ifn-ε*<sup>-/-</sup> C57BL/6 mice by immunohistochemistry. Scale bars, 50 μm. These images are representative of at least five individual mice. (C and D) *Ifn-ε* expression was measured by qRT-PCR in mouse uterus at different stages of (C) the estrous cycle and (D) pregnancy. Data are expressed as mean ± SEM of at least three separate experiments. (E) *Ifn-ε* expression was determined by qRT-PCR in ovariectomized (OVX) mice and OVX mice treated with estrogen (E OVX). Data are expressed as mean ± SEM of at least six individual mice and are representative of at least two separate experiments. (F) A cDNA panel of human tissues was examined for *IFN-ε* expression by qRT-PCR, and the results were expressed relative to *IFN-ε* expression in the kidney. (G) Epithelial cells were isolated from endometrial samples of postmenopausal women or those at different stages of the menstrual cycle, and *IFN-ε* expression was measured by qRT-PCR. Values are presented relative to *IFN-ε* expression in the human endometrial cell line ECC-1. Data are expressed as mean ± SEM of six individual patient samples. \**P* < 0.05; \*\**P* < 0.01; \*\*\**P* < 0.001 [(A to F) unpaired Student's *t* test, (G) Mann-Whitney *U* test].

tomized (OVX) mice and OVX mice treated with estrogen (E OVX). Data are expressed as mean ± SEM of at least six individual mice and are representative of at least two separate experiments. (F) A cDNA panel of human tissues was examined for *IFN-ε* expression by qRT-PCR, and the results were expressed relative to *IFN-ε* expression in the kidney. (G) Epithelial cells were isolated from endometrial samples of postmenopausal women or those at different stages of the menstrual cycle, and *IFN-ε* expression was measured by qRT-PCR. Values are presented relative to *IFN-ε* expression in the human endometrial cell line ECC-1. Data are expressed as mean ± SEM of six individual patient samples. \**P* < 0.05; \*\**P* < 0.01; \*\*\**P* < 0.001 [(A to F) unpaired Student's *t* test, (G) Mann-Whitney *U* test].

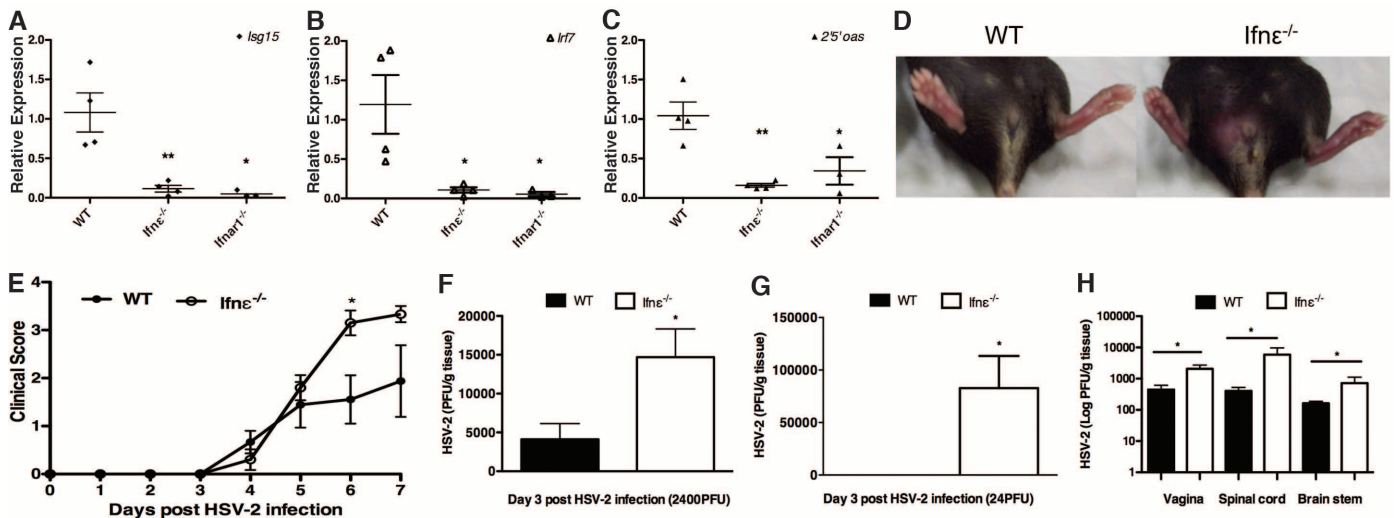


**Fig. 3.** *Ifn-ε*<sup>-/-</sup> mice are more susceptible to HSV-2 vaginal infection. (A) *Isg15*, (B) *Irf-7*, and (C) *2'5'oas* expression between WT and *Ifn-ε*<sup>-/-</sup> C57BL/6 mice was determined by qRT-PCR. The values represent means ± SEM (error bars) of four individual mice. (D to F and H) Mice pretreated with medroxyprogesterone acetate (Depo-Ralovera, Pfizer) at day -5 were infected with HSV-2 (D, E, H) at a level of 2400 or (F) 24 pfu per mouse on day 0. (D) Representative images demonstrating overt genital lesions, redness, and swelling in HSV-2-infected *Ifn-ε*<sup>-/-</sup> mice at day 7 pi; these qualities are absent in C57BL/6 WT mice. (E) Clinical scores of WT and *Ifn-ε*<sup>-/-</sup> C57BL/6 mice during the 7-day course of

infection. Data are means ± SEM of five individual mice and are representative of at least three separate experiments. (F and G) HSV-2 titers (pfu) from vaginal tissue of WT and *Ifn-ε*<sup>-/-</sup> C57BL/6 mice infected with (F) 2400 and (G) 24 pfu, respectively, at day 3 pi were determined by titration of clarified vaginal tissue samples on Vero cell monolayers by plaque assay. Data are expressed as mean ± SEM of five individual mice. (H) HSV-2 titers from homogenates of vaginal tissue, spinal cord, and brain stem of infected WT and *Ifn-ε*<sup>-/-</sup> C57BL/6 mice at day 7 pi were determined as in (F) and (G). Data are expressed as mean ± SEM of five individual mice. \**P* < 0.05; \*\**P* < 0.01 (unpaired Student's *t* test).

endometrium (Fig. 2F). To determine whether human *IFN-ε* was also regulated in different hormonal states, we tested epithelial cells isolated from uterine endometrium from six women in secretory or proliferative stages of the menstrual cycle or after menopause. *IFN-ε* expression was highest in the proliferative phase when estrogen levels were high and was approximately 10-fold lower in the secretory phase when estrogen levels were low and progesterone was high. *IFN-ε* levels were virtually undetectable in samples from postmenopausal women (Fig. 2G) (11). Consistent with the epithelial cell origin of this cytokine, several endometrial cancer-derived cell lines were found to express *IFN-ε* (fig. S1H).

Next, we generated *Ifn-ε*<sup>-/-</sup> mice to characterize the pathophysiological functions of this gene (fig. S2, A to E, and table S1). No differences were detected in male and female fertility (fig. S3A), or in the reproductive organs from male and female mice (fig. S3B) and immune organs characterized by immunophenotyping (fig. S3, C to H).

The basal levels of *2'5'oas*, *Irf-7*, and *Isg15* were significantly reduced in uteri from *Ifn-ε*<sup>-/-</sup> mice, similar to the very low levels observed in *Ifnar1*<sup>-/-</sup> mice (Fig. 3, A to C), indicating that *Ifn-ε* did signal in vivo. IRG levels in other organs were the same between WT and *Ifnε*<sup>-/-</sup> mice (fig. S3I). Furthermore, this difference in IRG levels resulting from constitutive *Ifn-ε* expres-

sion was similar in magnitude to the induction of these IRGs in WT mice that were given *Ifn-α*, *-β*, or *-ε* intravaginally (fig. S4) and to the degree of altered expression observed after *Chlamydia* or HSV-2 infection (see below). These data demonstrate that expression of *IFN-ε* in the female reproductive tract (FRT) is required for maintaining basal levels of IRGs, which play an important role in innate immunity.

To determine whether *Ifn-ε* is important in protecting the FRT from viral infection, we examined the effect of genital HSV-2 infection in *Ifn-ε*<sup>-/-</sup> mice. After a sublethal dose of a clinical isolate of HSV-2 strain 186 (12), *Ifn-ε*<sup>-/-</sup> mice had significantly more severe clinical scores of disease [day 6 and 7 postinfection (pi)] with severe epidermal lesions evident compared with WT mice (Fig. 3, D and E). These effects were observed at virus doses of 24 and 2400 plaque-forming units (pfu) per mouse (Fig. 3, F and G) and were consistent with elevated viral titers in infected vaginal tissues of *Ifn-ε*<sup>-/-</sup> mice at day 3 pi, compared with WT animals. At the low dose of 24 pfu, *Ifn-ε* was protective, as virus was only detectable in the null mice and not in WT animals. In addition, *Ifn-ε*<sup>-/-</sup> mice had significantly higher viral titers in the spinal cord and brain stem 7 days pi, consistent with either increased replication or retrograde transport of virus (Fig. 3H). Notably, there was no significant change in

the expression of *Ifn-ε* in the first 3 days after viral infection, consistent with our in vitro data showing that this gene is not pathogen induced (fig. S5A). The susceptibility of *Ifn-ε*<sup>-/-</sup> was less than that of *Ifnar1*<sup>-/-</sup> mice, which cannot respond to *Ifn-α*, *-β*, or *-ε* (fig. S5B). However, because *Ifn-β* and IRGs were not induced less in *Ifn-ε*<sup>-/-</sup> mice, the protective effects of *Ifn-ε* in this model of a prevalent sexually transmitted infection (STI) were independent of other type I IFNs (fig. S5, C to F).

We next investigated the role of *Ifn-ε* in a murine model of FRT infection by *Chlamydia*, the most prevalent bacterial STI (13, 14). After a sublethal, intravaginal infection of WT and *Ifn-ε*<sup>-/-</sup> mice with *C. muridarum* (15), *Ifn-ε*<sup>-/-</sup> mice displayed more severe clinical signs of disease from 7 until 30 days pi (Fig. 4A). More bacteria were detected in vaginal swabs of *Ifn-ε*<sup>-/-</sup> mice throughout the course of infection (Fig. 4B). *C. muridarum* recovery from vaginal lavage 3 days pi in WT mice had not increased from day 1 inoculum levels, but there was a 40-fold increase in the levels of bacteria in *Ifn-ε*<sup>-/-</sup> mice (Fig. 4C). We also observed significantly increased levels of *Chlamydia* at 30 days pi, indicative of increased chlamydial growth in the upper FRT (uterine horns) of *Ifn-ε*<sup>-/-</sup> mice compared with very low levels in WT mice (Fig. 4D). This finding in particular indicates that *Ifn-ε*<sup>-/-</sup> mice are

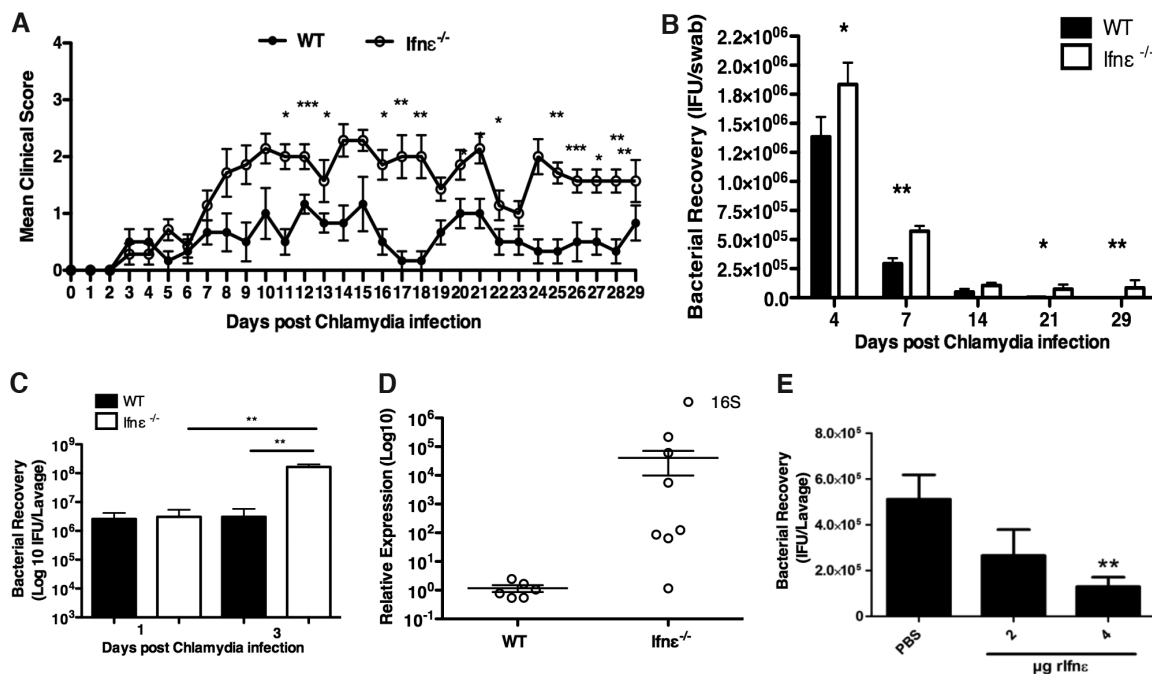


**Fig. 4.** *Ifn-ε*<sup>-/-</sup> mice are more susceptible to *Chlamydia muridarum* vaginal infection. (A to D) Mice were pretreated with progesterone at day -7 and infected intravaginally with  $5 \times 10^4$  inclusion-forming units (IFU) of *C. muridarum*. (A) Clinical scores were recorded daily for 30 days. Data are means  $\pm$  SEM (error bars) of at least six individual mice. (B) Bacterial recovery from vaginal swabs of WT and *Ifn-ε*<sup>-/-</sup> C57BL/6 mice at different time points, as determined by qRT-PCR for bacterial major outer membrane protein. Data are means  $\pm$  SEM of at least six individual mice. (C) Bacterial recovery, as measured by qRT-PCR from vaginal lavage at days 1 and 3 pi.

Data are means  $\pm$  SEM of at least six individual mice. (D) Bacterial 16S RNA from the uterine horns of WT and *Ifn-ε*<sup>-/-</sup> C57BL/6 mice at 30 days pi was examined by qRT-PCR. Data are means  $\pm$  SEM of at least six individual mice. (E) WT C57BL/6 mice were pretreated with progesterone at day -7 and treated intravaginally with *rIfn-ε* (2 or 4  $\mu$ g) 6 hours before *C. muridarum* infection. Bacterial recovery from the vaginal lavage at day 3 pi was measured by qRT-PCR. PBS, phosphate-buffered saline. Data are means  $\pm$  SEM of at least six individual mice. \**P* < 0.05; \*\**P* < 0.01; \*\*\**P* < 0.001 (unpaired Student's *t* test).

substantially more susceptible to (and less able to clear) an ascending infection in the FRT than WT mice. Because NK cells have a protective role against this infection (16), we measured their levels at 3 days pi. Notably, both the percentage and total numbers of these cells were decreased in the uteri of *Ifn-ε*<sup>-/-</sup> mice (fig. S6, A and B). Importantly, there were no changes in *Ifn-ε* RNA expression at the early or late stages of the infection (fig. S6C), consistent with our in vitro data showing that *Ifn-ε* is not regulated by PRR pathways. Furthermore, production of *Ifn-β* and IRGs was higher than the levels in WT mice (fig. S7, A to D), indicating that the protective effects of *Ifn-ε* were not solely due to priming for the production of other type I IFNs. To demonstrate that *Ifn-ε* could directly mediate protection against infection, we observed a dose-dependent reduction in bacteria (Fig. 4E), demonstrating that reconstitution of (progesterone) lowered *Ifn-ε* levels protected against this bacterial infection.

The distinct properties of IFN-ε, compared with other type I IFNs (table S2), make IFN-ε the only one that protects against *Chlamydia*, whereas the others exacerbate disease (17–20). All type I IFNs protect against HSV-2 infection (21, 22), with IFN-ε likely contributing because its constitutive expression by epithelial cells offers immediate efficacy at the site of first contact of mucosal pathogens. Interestingly, the increased susceptibility to FRT infections of women on progestagen-containing contraception (23, 24) may be explained by the lowering of *Ifn-ε* levels (fig. S8A) during progestin pretreatment that is required for all FRT infection models (25, 26). The local effect of

IFN-ε is supported by our observation that IFN-ε makes no difference in a systemic model (fig. S8, B to D). Consistent with the importance of IFN-ε in FRT immunity, IFN-ε is evolutionarily conserved in eutherian mammals, particularly in residues predicted to contact the two receptor components (fig. S9) (27). Because STIs are major global health and socioeconomic problems, the distinctive regulatory and protective properties of IFN-ε may facilitate the development of new strategies for preventing and treating STIs and, perhaps, other diseases.

#### References and Notes

1. S. Hervas-Stubbis *et al.*, *Clin. Cancer Res.* **17**, 2619 (2011).
2. A. Isaacs, J. Lindenmann, *Proc. R. Soc. London Ser. B Biol. Sci.* **147**, 258 (1957).
3. M. P. Hardy, C. M. Owczarek, L. S. Jermini, M. Ejdebäck, P. J. Hertzog, *Genomics* **84**, 331 (2004).
4. K. Honda, A. Takaoka, T. Taniguchi, *Immunity* **25**, 349 (2006).
5. M. Sato *et al.*, *Immunity* **13**, 539 (2000).
6. N. A. de Weerd, S. A. Samarajiva, P. J. Hertzog, *J. Biol. Chem.* **282**, 20053 (2007).
7. L. Alexopoulou, A. C. Holt, R. Medzhitov, R. A. Flavell, *Nature* **413**, 732 (2001).
8. S. E. Doyle *et al.*, *J. Immunol.* **170**, 3565 (2003).
9. V. Hornung, E. Latz, *Nat. Rev. Immunol.* **10**, 123 (2010).
10. M. V. Patel, M. Ghosh, J. V. Fahey, C. R. Wira, *PLoS ONE* **7**, e35654 (2012).
11. L. A. Salamonsen, in *The Endometrium*, J. D. Aplin, A. T. Fazleabas, S. R. Glasser, L. C. Giudice, Eds. (Informa Healthcare, London, ed. 2, 2008), pp. 25–45.
12. M. Thapa, D. J. Carr, *J. Virol.* **83**, 9486 (2009).
13. K. W. Beagley, W. M. Huston, P. M. Hansbro, P. Timms, *Crit. Rev. Immunol.* **29**, 275 (2009).
14. World Health Organization (WHO), *Global Prevalence and Incidence of Selected Curable Sexually Transmitted Infections Overview and Estimates* (WHO, Geneva, 2001).
15. K. L. Asquith *et al.*, *PLoS Pathog.* **7**, e1001339 (2011).
16. C. T. Tseng, R. G. Rank, *Infect. Immun.* **66**, 5867 (1998).
17. A. Devitt, P. A. Lund, A. G. Morris, J. H. Pearce, *Infect. Immun.* **64**, 3951 (1996).
18. S. P. Lad, E. Y. Fukuda, J. Li, L. M. de la Maza, E. Li, *J. Immunol.* **174**, 7186 (2005).
19. U. M. Nagarajan, D. M. Ojcius, L. Stahl, R. G. Rank, T. Darville, *J. Immunol.* **175**, 450 (2005).
20. U. M. Nagarajan *et al.*, *Infect. Immun.* **76**, 4642 (2008).
21. B. A. Austin, C. M. James, P. Härle, D. J. Carr, *Biol. Proced. Online* **8**, 55 (2006).
22. C. D. Conrady, W. P. Halford, D. J. Carr, *J. Virol.* **85**, 1625 (2011).
23. J. M. Baeten *et al.*, *Am. J. Obstet. Gynecol.* **185**, 380 (2001).
24. C. C. Wang, J. K. Kreiss, M. Reilly, *J. Acquir. Immune Defic. Syndr.* **21**, 51 (1999).
25. R. P. Morrison, H. D. Caldwell, *Infect. Immun.* **70**, 2741 (2002).
26. M. B. Parr *et al.*, *Lab. Invest.* **70**, 369 (1994).
27. C. Thomas *et al.*, *Cell* **146**, 621 (2011).



**Acknowledgments:** We thank A. Mansell, R. Ferrero, and L. Salamonsen for their contributions; N. Bourke and S. Forster for helpful discussions and reading of the manuscript; K. Fitzgerald for reagents; and C. Berry for assistance with viral plaque assays. The data presented in this paper are tabulated in the main text and in the supplementary materials. This work was supported by funding from Australian National Health and Medical Research Council (P.J.H., N.E.M., P.M.H., J.R., C.E.G., and B.P.), the Australian Research Council (P.J.H., N.E.M., J.R.), the NIH via grant R01 AI053108 (D.J.C.), and the Victorian Government's Operational Infrastructure Support Program. P.J.H., N.E.M., K.Y.F., H.C., S.A.S., and N.D.W. hold International Patent Application number PCT/AU2011/000715, "Use of interferon epsilon in methods of diagnosis and treatment."

#### Supplementary Materials

www.sciencemag.org/cgi/content/full/339/6123/1088/DC1  
Materials and Methods

Figs. S1 to S9

Tables S1 and S2

References (28–33)

28 November 2012; accepted 8 January 2013

10.1126/science.1233321

## Spreading Depression Triggers Headache by Activating Neuronal Panx1 Channels

Hulya Karatas,<sup>1,2</sup> Sefik Evren Erdener,<sup>1,2</sup> Yasemin Gursoy-Ozdemir,<sup>1,2</sup> Sevda Lule,<sup>1</sup> Emine Eren-Koçak,<sup>1,3</sup> Zümüt Duygu Sen,<sup>1,3</sup> Turgay Dalkara<sup>1,2\*</sup>

The initial phase in the development of a migraine is still poorly understood. Here, we describe a previously unknown signaling pathway between stressed neurons and trigeminal afferents during cortical spreading depression (CSD), the putative cause of migraine aura and headache. CSD caused neuronal Pannexin1 (Panx1) megachannel opening and caspase-1 activation followed by high-mobility group box 1 (HMGB1) release from neurons and nuclear factor κB activation in astrocytes. Suppression of this cascade abolished CSD-induced trigeminovascular activation, dural mast cell degranulation, and headache. CSD-induced neuronal megachannel opening may promote sustained activation of trigeminal afferents via parenchymal inflammatory cascades reaching glia limitans. This pathway may function to alarm an organism with headache when neurons are stressed.

There is agreement that activation of the trigeminocervical complex mediates migraine headache, whereas the brain event that initiates migraine is unclear (1–3). Cortical spreading depression (CSD) thought to cause the migraine aura may activate perivascular trigeminal nerves (4–10) by way of potassium, protons, nitric oxide (NO), arachidonic acid, and adenosine

5'-triphosphate released during CSD (3, 8, 11). However, sufficient concentrations of these mediators may not be sustained in the perivascular space for trigeminal sensitization and hours-lasting headache (10, 12) because of the glia limitans barrier and continuous cerebrospinal fluid (CSF) flow. Trigeminal meningeal nociceptors and central neurons also start firing ~14 and 25 min after CSD in

the rat (10, 13). Similarly, there is a 20- to 30-min delay between the end of the aura and the headache (14). Such time lags may be required for transduction of algogenic signals over glia limitans via inflammatory mediators. Intense depolarization and *N*-methyl-D-aspartate (NMDA) receptor over-activation opens neuronal Pannexin1 (Panx1) megachannels (15–17). These conditions are present during CSD and suggest that CSD, by activating Panx1 and downstream inflammasome formation, may trigger inflammation (17, 18). We therefore hypothesize that stress-induced Panx1 activation may cause headache by releasing pro-inflammatory mediators such as high-mobility group box 1 (HMGB1) from neurons, which initiates a parenchymal inflammatory response, leading to sustained release of inflammatory mediators from glia limitans and, hence, prolonged trigeminal stimulation.

Propidium iodide (PI) is a membrane-impermeable fluorochrome used to monitor activity as it passes through megachannels such as

<sup>1</sup>Institute of Neurological Sciences and Psychiatry, Hacettepe University, Ankara 06100, Turkey. <sup>2</sup>Department of Neurology, Faculty of Medicine, Hacettepe University, Ankara 06100, Turkey. <sup>3</sup>Department of Psychiatry, Faculty of Medicine, Hacettepe University, Ankara 06100, Turkey.

\*To whom correspondence should be addressed.



## Purification and biological characterization of soluble, recombinant mouse IFN $\beta$ expressed in insect cells



Sebastian A. Stifter<sup>a</sup>, Jodee A. Gould<sup>a</sup>, Niamh E. Mangan<sup>a</sup>, Hugh H. Reid<sup>b</sup>, Jamie Rossjohn<sup>b,c</sup>, Paul J. Hertzog<sup>a</sup>, Nicole A. de Weerd<sup>a,\*</sup>

<sup>a</sup> Centre for Innate Immunity and Infectious Diseases, Monash Institute of Medical Research, Monash University, Clayton, Victoria 3800, Australia

<sup>b</sup> Department of Biochemistry and Molecular Biology, School of Biomedical Sciences, Monash University, Clayton, Victoria 3800, Australia

<sup>c</sup> Institute of Infection and Immunity, Cardiff University, School of Medicine, Heath Park, Cardiff CF14 4XN, UK

### ARTICLE INFO

#### Article history:

Received 14 September 2013  
and in revised form 28 October 2013  
Available online 6 November 2013

#### Keywords:

Interferon beta  
Insect cell expression  
Soluble protein  
Natively folded  
Endotoxin-free  
Biologically active

### ABSTRACT

Interferon  $\beta$  (IFN $\beta$ ) is a member of the type I interferon family of cytokines widely recognised for their anti-viral, anti-proliferative and immunomodulatory properties. Recombinant, biologically active forms of this cytokine are used clinically for the treatment of multiple sclerosis and in laboratories to study the role of this cytokine in health and disease. Established methods for expression of IFN $\beta$  utilise either bacterial systems from which the insoluble recombinant proteins must be refolded, or mammalian expression systems in which large volumes of cell culture are required for recovery of acceptable yields. Utilising the baculovirus expression system and *Trichoplusia ni* (Cabbage Looper) BTI-TN-5B1-4 cell line, we report a reproducible method for production and purification of milligram/litre quantities of biologically active murine IFN $\beta$ . Due to the design of our construct and the eukaryotic nature of insect cells, the resulting soluble protein is secreted allowing purification of the Histidine-tagged natively-folded protein from the culture supernatant. The IFN $\beta$  purification method described is a two-step process employing immobilised metal-ion affinity chromatography (IMAC) and reverse-phase high performance liquid chromatography (RP-HPLC) that results in production of significantly more purified IFN $\beta$  than any other reported eukaryotic-based expression system. Recombinant murine IFN $\beta$  produced by this method was natively folded and demonstrated hallmark type I interferon biological effects including antiviral and anti-proliferative activities, and induced genes characteristic of IFN $\beta$  activity *in vivo*. Recombinant IFN $\beta$  also had specific activity levels exceeding that of the commercially available equivalent. Together, our findings provide a method for production of highly pure, biologically active murine IFN $\beta$ .

© 2013 Elsevier Inc. All rights reserved.

### Introduction

The type I interferons (IFNs)<sup>1</sup> were discovered by virtue of their antiviral activity and have since been shown to also possess

\* Corresponding author. 

<sup>1</sup> Abbreviations used: ACN, acetonitrile; CD, circular dichroism; CPE, cytopathic effect; DMSO, dimethyl sulfoxide; EC<sub>50</sub>, effective concentration (to give 50% effect); EK, enterokinase; EU, endotoxin units; HRP, horseradish peroxidase; IFN, interferon; IMAC, immobilized metal affinity chromatography; ISG, interferon stimulated gene; MTT, 3-(4,5-dimethylthiazol-2-yl)-2,5-diphenyltetrazolium bromide; MWCO, molecular weight cut-off; PCR, polymerase chain reaction; PMSF, phenylmethanesulfonyl fluoride; PVDF, polyvinylidene fluoride; qRT-PCR, quantitative real time PCR; RP-HPLC, reverse phase-HPLC; SDS-PAGE, sodium dodecyl sulphate polyacrylamide electrophoresis; SEM, standard error of the mean; Sf, *Spodoptera frugiperda*; TBS, tris buffered saline; TFA, trifluoroacetic acid.

anti-proliferative and immunoregulatory functions [1,2]. In humans this multi-gene family comprises 12 IFN $\alpha$  subtypes and individual IFN $\beta$ ,  $\epsilon$ ,  $\omega$ ,  $\kappa$ ,  $\delta$ ,  $\tau$  and  $\zeta$  proteins, that signal via a heterodimeric receptor complex composed of two subunits, IFNAR1 and IFNAR2 [3]. Ligand engagement of the receptor initiates an intracellular signalling cascade involving the JAK-STAT signalling pathway, which subsequently activates numerous interferon stimulated genes (ISGs) resulting in the generation of an immune response [4]. While showing considerable sequence and structural homology across different species, the type I IFNs are highly species specific in regards to receptor interactions and subsequent signalling events.

IFN $\beta$  is an inducible component of the host immune response to viral and bacterial infections, and is also used clinically for the treatment of multiple sclerosis [5]. This cytokine is also pivotal to various processes in the body, including lymphoid development, myelopoiesis [6] and the toxicity induced by septic shock [7]. Compared to the IFN $\alpha$  subtypes, IFN $\beta$  is also more effective at activating anti-proliferative responses, pro-apoptotic pathways in tumour

cells [8–10] and has a vital role in the control of macrophage differentiation and osteoclastogenesis [11,12]. Recently we established a structural basis for the unique properties of IFN $\beta$  [13].

Before the availability of recombinant DNA technology, commercial or laboratory quantities of type I IFNs were extracted from virally infected white blood cells via a single step purification protocol. Thus, early clinical trials used crude protein preparations, in which active IFN was less than 0.1% of the total protein [14]. Based on the acid-stable nature of the type I IFNs, a protocol utilising reverse-phase high performance liquid chromatography (RP-HPLC) was later developed which enabled the production of homogeneous and highly purified preparations of IFN [15]. For the first time, the biological activities of type I IFNs could be precisely demonstrated and characterised, paving the way for future researchers to clearly demonstrate the multipotent activities attributable to these cytokines.

Baculoviral expression systems have been used successfully for the production of biologically-active cytokines including human and canine IFNs [16–18]. These systems are ideal for the production of recombinant mammalian-derived cytokines as, due to their eukaryotic nature, insect cells produce soluble, natively folded proteins. Also, since these cells are not prokaryotic in origin, there is no risk of contaminating endotoxin, an impurity of bacterial expression systems.

To investigate the functions of IFN $\beta$  in mouse models and cell culture, requires a high-yielding source of biologically-active, endotoxin-free protein. We therefore developed an insect cell-based expression and purification protocol for the large scale production of highly-purified, endotoxin-free murine IFN $\beta$ . The cytokine produced in this system displays comparable levels of *in vitro* and *in vivo* biological activity to a commercial IFN $\beta$ , but has a higher specific activity, thus demonstrating greater purity of the functional protein.

## Materials and methods

### Plasmid construction

The *mlfnb1* gene was amplified from C57BL/6 genomic DNA using *Pfu* polymerase with amplification directed by specific forward (GGATCCTATAAGCAGCTCCAGCTC) and reverse primers (GTAAAGCTTAGTTTTGGAAGTTCTGGAAG). IFN $\beta$ 1 expressed during this study corresponds to residues 24–182 of murine IFN $\beta$  (RefSeq Acc No. NP\_034640.1). The 490 bp polymerase chain reaction (PCR) product was cloned into a modified pFastBac<sup>TM</sup>1 vector (Life Technologies) and contained the gp67 signal sequence of the *Autographa californica* nucleopolyhedrovirus followed by the His<sub>6</sub> tag, enterokinase (EK) cleavage site and a flexible linker. After transformation of competent JM109 cells (BioLine), transformants were screened for inserts by colony PCR using the *mlfnb1* forward and reverse primers above with positive clones sequenced with the polyhedrin sequencing primer (AAATGATAACCATCTCGC).

### Generation of recombinant bacmid and baculoviral stocks

For expression in insect cells using the Bac-to-Bac Baculoviral Expression System (Life Technologies), recombinant bacmids incorporating pFastBac-*mlfnb1* were generated in the AcBac $\Delta$ CC bacmid [19] following the manufacturer's instructions (Life Technologies). Transformed clones were identified by blue/white colour selection and screened by colony PCR using M13 forward (GTTTCCAGTCACGAC) and reverse (CAGGAAACAGCTATGAC) primers. Positive clones were isolated using a Qiagen EndoFree Maxi-Prep kit according to the manufacturer's instructions (Qiagen). Recombinant baculovirus was generated by transient trans-

fection of the recombinant bacmid into *Spodoptera frugiperda* (Sf)-9 insect cells according to the manufacturer's instructions (Life Technologies). To generate high titre viral stocks, the viral supernatants from these transient transfections were amplified in two rounds of low multiplicity of infection (MOI of  $\sim$ 0.1) of  $1 \times 10^6$  Sf9 cells mL<sup>-1</sup> for 4–5 days.

### Insect and mammalian cell culture and reagents

The mouse L929 fibroblast cell line was purchased from the American Type Culture Collection. Mouse macrophage RAW 264.7 cells were a kind gift from Dr. Ashley Mansell (Monash Institute of Medical Research, Victoria, Australia). Both L929 and RAW 264.7 cell lines were maintained in RPMI 1640 medium supplemented with 10% fetal calf serum (ICP, New Zealand), 1% L-glutamine (Life Technologies) and 1% Penicillin/Streptomycin (Life Technologies) at 37 °C, 5% CO<sub>2</sub>. Serum free adapted insect cell lines Sf9 and High Five<sup>TM</sup> (BTI-TN-5B1-4 from *Trichoplusia ni*) were purchased from Life Technologies and maintained in Sf900-II media (Life Technologies) supplemented with 1  $\mu$ g mL<sup>-1</sup> Gentamicin (Sigma-Aldrich) in a shaking incubator at 27 °C, 120 rpm. For expression cultures, High Five<sup>TM</sup> cells were diluted in serum-free Express Five media (Life Technologies) supplemented with 20 mM L-Glutamine and 1  $\mu$ g mL<sup>-1</sup> Gentamicin (Sigma-Aldrich) and incubated as above. Recombinant murine IFN $\beta$  (containing 0.1% (w/v) bovine serum albumin) was purchased from Sigma Aldrich. The certificate of analysis for each batch of this reagent details the batch-specific IFN activity (given as international units (IU) mL<sup>-1</sup>) and its specific activity in relation to IFN content (given as IU mg<sup>-1</sup> of protein).

### Expression of recombinant IFN $\beta$

IFN $\beta$  was expressed as a soluble protein secreted into the culture supernatant. For recombinant protein expression, cells at  $2 \times 10^6$  cells mL<sup>-1</sup> were infected with the amplified high-titre recombinant IFN $\beta$  baculoviral stocks at a ratio of 1 mL virus to 10 mL cells (a multiplicity of infection of  $\sim$ 10). Expression was carried out at 27 °C for 48 h on an orbital shaker rotating at 120 rpm. Cultures were transferred to sterile 50 mL conical falcon tubes (Becton–Dickinson), the cells pelleted by centrifugation at 160 g 4 °C for 20 min, followed by a second centrifugation step at 6000 g, 4 °C for 20 min. The cell pellet was discarded and the supernatant retained for protein purification.

### Purification of recombinant His<sub>6</sub>-IFN $\beta$

Soluble His<sub>6</sub>-IFN $\beta$  was purified from the insect cell culture supernatant. After the addition of the serine protease inhibitor phenylmethanesulfonyl fluoride (PMSF; to 1 mM final concentration), the supernatant was dialysed against TBS (10 mM Tris-HCl, 150 mM NaCl, pH8.0) overnight at 4 °C using 12.5 kDa cut-off dialysis tubing (Sigma Aldrich). To reduce non-specific interactions with the resin, 20 mM imidazole was then added to the dialysate which was then recirculated at least three times over Nickel Sepharose FastFlow 6 resin (GE Healthcare Life Sciences) to capture His-tagged proteins. Bound proteins were eluted under native conditions using TBS supplemented with 150 mM Imidazole, pH8.0. Fractions that contained IFN $\beta$  were pooled, acidified with 1  $\mu$ l mL<sup>-1</sup>, 0.1% (v/v) trifluoroacetic acid (TFA) (Merck), filtered (0.2  $\mu$ m syringe-driven filter; Sartorius) to remove particulates and then injected onto a Phenomenex Jupiter C5 prep and guard column (Phenomenex) attached to an Agilent 1100 modular RP-HPLC. All recombinant IFN $\beta$  proteins were resolved using a linear gradient of Buffer A (0% acetonitrile (ACN), 0.1% TFA, pH2.0) into Buffer B (90% ACN, 0.1% TFA, pH2.0) at 3 mL min<sup>-1</sup> for 60 min.

1 mL fractions were collected using an Agilent 1100 Series fraction collector into 96-well fraction collection plates (Axygen). Peak-containing fractions were dried using a vacuum pump at room temperature for 16 h. Fractions were fully resuspended in 0.05% TFA, MilliQ H<sub>2</sub>O and then neutralised with 10xHepes Buffer (200 mM HEPES, 1.5 M NaCl, pH6.0). All protein preparations were subsequently stored at 4 °C. The concentration of all protein preparations was measured by standard Bradford colorimetric assay [20].

#### Removal of His<sub>6</sub> tag by EK digestion

To remove the His<sub>6</sub> tag, affinity purified His<sub>6</sub>-IFN $\beta$ , was digested with enterokinase (EK) (EK-Max; Life Technologies) according to the manufacturer's instructions. Optimised digestion conditions were established using 0.5U of EK-Max per 10  $\mu$ g of recombinant His<sub>6</sub>-IFN $\beta$  in 1xHEPES buffer (20 mM HEPES, 150 mM NaCl, pH6.0) for 16 h rotating at 4 °C. Digestion was halted by the addition of imidazole to 100 mM followed by centrifugation at 7,500 g for 5mins, 4 °C to remove particulates. After confirmation of His<sub>6</sub> tag removal by SDS-PAGE and Western blotting, tagless IFN $\beta$  (herein referred to as IFN $\beta$ ) was subjected to RP-HPLC as outlined above.

#### Determination of endotoxin levels

Endotoxin contamination levels in all protein samples were assayed using a ToxinSensor Endotoxin Assay kit according to the manufacturer's instructions (Genscript). His<sub>6</sub>-IFN $\beta$  and IFN $\beta$  samples were diluted to 10  $\mu$ g mL<sup>-1</sup> and the endotoxin concentration of each sample was determined as Endotoxin Units (EU)  $\mu$ g<sup>-1</sup> of protein.

#### Sodium dodecyl sulphate–polyacrylamide gel electrophoresis (SDS–PAGE) and Western blotting

All SDS–PAGE (15% w/v) was carried out under reducing conditions by the method of Laemmli [21]. For analysis of antibody binding, gels were blotted to PVDF membrane, blocked with 5% (w/v) skim milk powder in PBS and incubated with either an anti-mIFN $\beta$  polyclonal antibody (Ab) (diluted 1:1000 in blocking buffer; PBL) or an anti His-tag monoclonal Ab (diluted 1:1000 in blocking buffer; Cell Signalling Technologies) for up to 16 h. After washing, the primary Abs were detected by incubation with a horseradish peroxidase (HRP)-conjugated anti-rabbit IgG Ab (diluted 1:1000 in blocking buffer; DAKO) or a HRP-conjugated anti-mouse IgG Ab (diluted 1:1000 in blocking buffer; DAKO), respectively. Bound HRP-conjugated secondary antibodies were detected using the SuperSignal West Pico Chemiluminescence kit (Pierce).

#### Circular Dichroism (CD) spectral analysis

CD spectra were measured at room temperature in a Jasco J815 CD spectrophotometer. All scans were run on proteins concentrated to 130  $\mu$ g mL<sup>-1</sup> in TBS. Triplicate scans were run between 190 and 260 nm. Data was collected and converted to mean residue ellipticity by the equation of Correa and Ramos [22].

#### Measurement of anti-viral activities

Antiviral activity was determined by cytopathic effect (CPE) inhibition assay using mouse L929 cells. Activity was measured against a National Institutes of Health reference standard (GU-02-901-511) as published previously [23] and is reported as the concentration of IFN that is required to provide protection to 50% of the exposed cells (ED<sub>50</sub>).

#### Measurement of anti-proliferative activity

Anti-proliferative activity was measured in RAW 264.7 cells. His<sub>6</sub>-IFN $\beta$  and commercial IFN $\beta$  were titrated out in a 96-well flat bottom plate in duplicate and  $2 \times 10^3$  cells added to each well. After 72 h incubation at 37 °C in 5%CO<sub>2</sub>, 3-(4,5-Dimethylthiazol-2-yl)-2,5-diphenyltetrazolium bromide (MTT) was added at 0.5 mg mL<sup>-1</sup> and the plate was incubated for a further 3 h at 37 °C. The supernatant was aspirated and MTT crystals were dissolved in dimethyl sulfoxide (DMSO). The absorbance was measured at 590 nm using a FluoStar OPTIMA plate reader (BMG Labtech) and proliferation was calculated using the following formula: % proliferation = (stimulated cells A<sub>590</sub> –  $2 \times 10^3$  cells A<sub>590</sub>) / (unstimulated cells A<sub>590</sub> –  $2 \times 10^3$  cells A<sub>590</sub>)  $\times$  100. Data are represented as mean  $\pm$  SEM of triplicate experiments.

#### Bioactivity of recombinant IFN $\beta$ in vivo

All animal experimentations were compliant with guidelines set by the institutional ethics committee (Monash Medical Centre AEC-A, Monash University, Clayton, Australia). Six to eight week old female wildtype mice (C57Bl/6  $\times$  129) (3 per group) were injected via the intra-peritoneal route with 10,000 IU per mouse of either recombinant His<sub>6</sub>-IFN $\beta$  or commercial IFN $\beta$ . Three hours after injection, the mice were euthanized, the peritoneal cavity flushed with sterile PBS and the peritoneal exudate cells (PECs) harvested in the PBS. PECs were concurrently harvested from three untreated mice for use as matched untreated control samples. RNA was purified using the RNeasy column purification kit (Qiagen); all cDNA synthesis was prepared using MMLV polymerase (Promega) and random hexamers (Promega) following the manufacturer's protocol. Quantitative real-time polymerase chain reaction (qRT-PCR) was performed on an Applied Biosystems 7900HT Fast Real-Time PCR system (ABI) using Sybr reagents (ABI) and the following forward (f) and reverse (r) primer pairs: 18S-f GTAACCCG TTGAACCCATT; 18S-r CCATCCAATCGGTAGTAGCG; Oas1a-f CCTGCACAGACTCAGAA; Oas1a-r AGCCACACATCAGCCTCTTC; ISG15-f TGAGAGCAAGCAGCCAGAAG; ISG15-r ACGGACACCAG-GAAATCGTT; IRF7-f ATCTTGCCCAAGACAATTC; IRF7-r AGCATTG CTGAGGCTCACTT. All experiments were carried out in triplicate. Data were normalised relative to the expression of 18S and transformed using the  $\Delta\Delta C_T$  method [24]. Data are presented as fold induction relative to unstimulated control samples with mean  $\pm$  SEM indicated. Student's *t*-test was applied to all data groups to determine significance.

## Results

#### Design of the IFN $\beta$ expression construct

The construct for protein expression used in this study was modified from pFastBac<sup>TM</sup>1 (Life Technologies) and was designed to express a tagged IFN $\beta$  protein under the control of the polyhedrin promoter (Fig. 1). The signal sequence used to direct secretion of recombinant proteins into the culture media was that from the *A. californica* nucleopolyhedrovirus glycoprotein gp67, reportedly the most effective baculovirus-encoded signal sequence [25]. Expressed recombinant IFN $\beta$  was linked via an EK cleavage site (Asp-Asp-Asp-Asp-Lys) to an amino-terminal six residue histidine tag (His<sub>6</sub>) to facilitate purification of recombinant proteins by IMAC (Fig. 1). The position of the EK cleavage site was designed to allow removal of the His<sub>6</sub> tag from purified IFN $\beta$  with the resultant protein retaining two (Gly-Ser) amino acid residues on the amino-terminal of the native IFN $\beta$  protein.

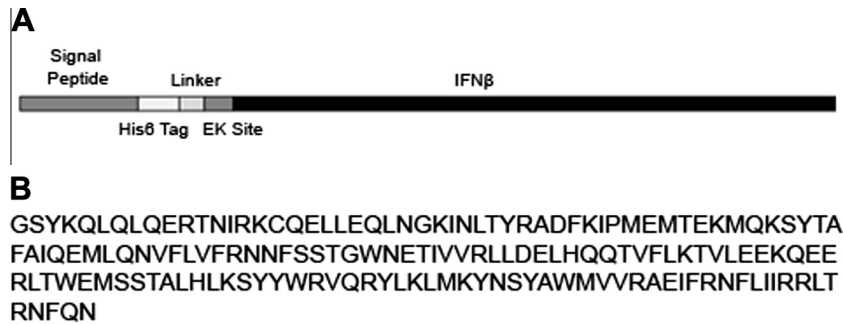


**Fig. 1.** Cloning of *Ifnb1* into the baculoviral expression vector. (A) Design of the IFN $\beta$  expression construct showing the location of the gp67 signal peptide, His $_6$  purification tag, linker region and the EK cleavage site upstream of the coding sequence for murine IFN $\beta$ . (B) Amino acid sequence of the final protein product after removal of the His $_6$  tag by EK digestion.

Since the *mlfnb1* gene is intron-less the *mlfnb1* coding sequence was obtained by amplifying genomic DNA from C57BL/6 mice (Fig. 1) [26]. The amplified product was sequenced fully in the modified pFastBac shuttle vector and, after taking into account the position of the His $_6$ -tag, linker and EK site, was shown to encode a protein that would be expected to translate to the sequence of the mature protein shown in Fig. 1B. The Bac to Bac baculoviral expression system used in this study is designed to incorporate the coding sequence for the His $_6$ -linker-EK site-*mlfnb1* sequence via site-specific transposition into the genome of the AcBac $\Delta$ CC bacmid. Thus the recombinant protein expressed in insect cells using this construct would produce a protein comprising Signal sequence-His $_6$ -GSGS-DDDDD-IFN $\beta$  protein (Fig. 1).

#### Expression and purification of recombinant IFN $\beta$

The expression and purification strategy outlined in this report is shown as a flow chart in Fig. 2. The His $_6$  tag on the recombinant protein facilitated the purification of a protein corresponding to the size of His $_6$ -IFN $\beta$  (~24 kDa) from the cell culture supernatant (Fig. 3A). Since proteins with a higher molecular weight than the protein of interest were also detectable in the pooled eluted fractions, a second purification step was required to fully purify the recombinant protein. Acidification and RP-HPLC purification of the preparation resulted in the resolution of two major overlapping protein peaks at 93% and 96% buffer B (Fig. 3B). Proteins under both peaks were subsequently shown to be equally biologically active via the CPE assay (data not shown). To demonstrate whether the presence of the His $_6$  tag had an effect on biological activity, the affinity purified His $_6$ -IFN $\beta$  was subjected to EK digestion prior to RP-HPLC purification. EK digestion reduced the size of the major protein product by ~2 kDa, the size predicted for the His $_6$ -linker-EK site peptide (16 amino acids) (Fig. 4A). Removal of the His $_6$  tag from recombinant IFN $\beta$  was confirmed by lack of recognition of the digested protein by an anti-His tag monoclonal antibody (Fig. 4B).

The purification protocol reported herein yielded overall 0.31 mg of purified recombinant IFN $\beta$  per 200 mL expression volume (Table 1). This equates to a yield of >1.5 mg or  $3 \times 10^8$  IU of IFN for a 1 litre expression, a yield which we were able to achieve reproducibly using the protocol described.

#### Biochemical characterization of recombinant IFN $\beta$

Circular Dichroism (CD) spectroscopic analysis was carried out on His $_6$ -IFN $\beta$  to confirm the nature of its structural fold. The far-UV spectral scan of His $_6$ -IFN $\beta$  shows mean residue ellipticity minima at 208 and 222 nm and a maximum at ~195 nm (Fig. 5A), features characteristic of an  $\alpha$ -helical protein such as IFN $\beta$

which is composed of five  $\alpha$ -helices [27]. To verify that we had recombinantly expressed and purified murine-derived IFN $\beta$  from the insect cell culture supernatant, the fully purified protein was subjected to SDS-PAGE analysis and western blotting. A band corresponding to the size of IFN $\beta$  (~23 kDa) was purified by RP-HPLC (Fig. 5B). This protein was subsequently shown to bind a commercially available anti-mouse IFN $\beta$  polyclonal antibody suggesting that the purified protein retained epitopes of murine IFN $\beta$ .

#### Endotoxin testing

Although expressed in endotoxin-free insect cells, endotoxins can be introduced into preparations from the laboratory environment through poor handling and endotoxin-contaminated equipment. We thus assayed our preparations to confirm the absence of endotoxin contamination. All RP-HPLC purified recombinant His $_6$ -IFN $\beta$  and IFN $\beta$  preparations were assayed for the presence of endotoxins, immunomodulatory molecules associated with the presence of bacterial contamination. All preparations produced by this procedure were found to have less than 0.01 EU  $\mu$ g $^{-1}$  of protein. These levels are up to 100 fold lower than what is guaranteed by commercial companies, where a range of 0.1–1.0 EU  $\mu$ g $^{-1}$  is often quoted.

#### Anti-viral activity of recombinant IFN $\beta$

To determine whether recombinant IFN $\beta$  prepared via our expression and purification protocol was functionally active, the ability of our preparations to protect L929 cells against infection by Semliki Forest Virus was assessed. This is the standard procedure used by both research laboratories and commercial companies to assess the biological activity of type I IFNs [28]. The specific activity of recombinant IFNs is a measure of the anti-viral activity of the protein as a function of protein content and is given as IU mg $^{-1}$  of protein. Compared to a NIH reference standard, the specific antiviral activity of recombinant His $_6$ -IFN $\beta$  and IFN $\beta$  purified from our insect cell expression system was reproducibly  $\sim 2 \times 10^8$  IU mg $^{-1}$  protein (Table 1) which exceeded that reported for the commercially available equivalent that ranged between 0.05 and  $0.7 \times 10^8$  IU mg $^{-1}$  (mean  $0.29 \pm 0.20 \times 10^8$  IU mg $^{-1}$ ; of triplicate batches).

#### Anti-proliferative activity of recombinant IFN $\beta$

To measure and compare the anti-proliferative activities of His $_6$ -IFN $\beta$ , IFN $\beta$  and the commercial form of IFN $\beta$ , the mouse macrophage RAW 264.7 cell line was stimulated with increasing doses of protein. His $_6$ -IFN $\beta$  and IFN $\beta$  had comparable anti-proliferative activity in this assay across the range of doses compared

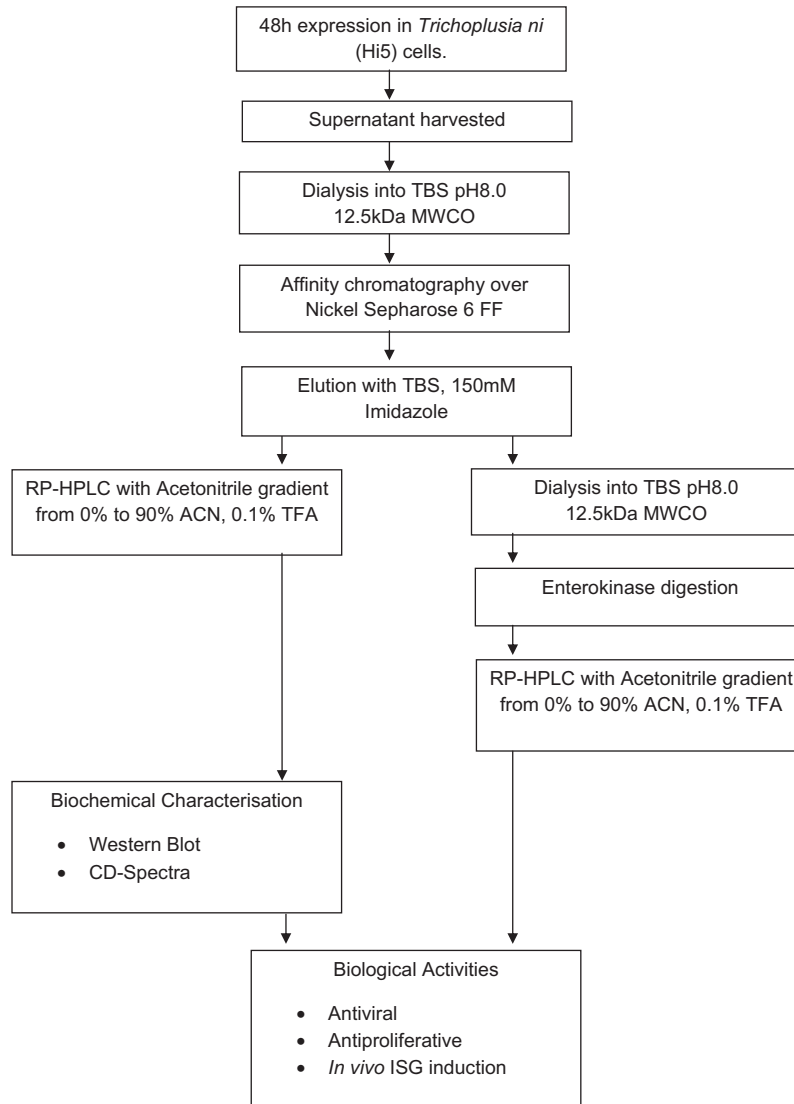


Fig. 2. Flow chart of IFN $\beta$  expression strategy in insect cells.

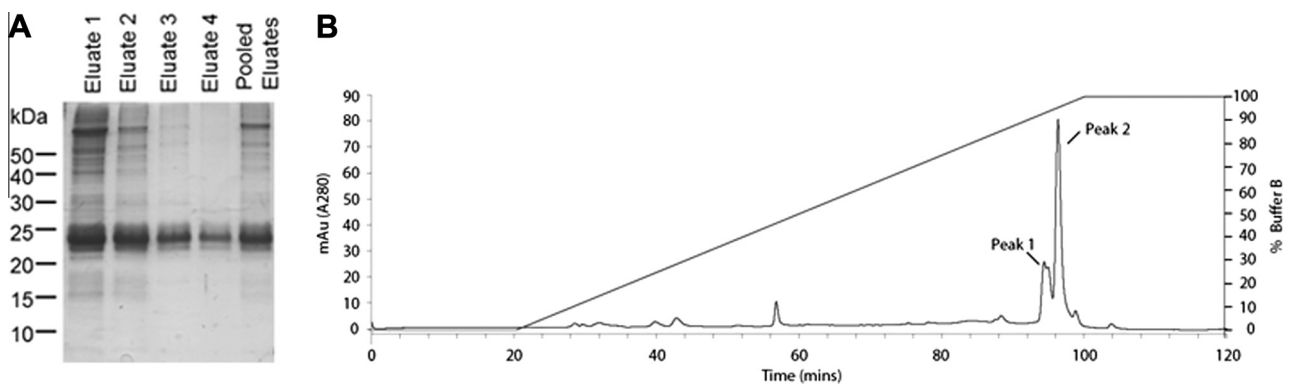
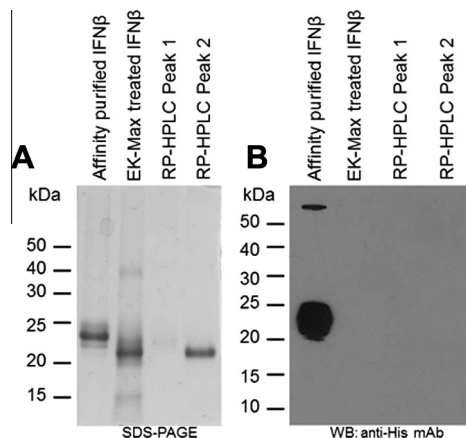


Fig. 3. The purification of recombinant IFN $\beta$  produced in insect cells by a two-step method. (A) SDS-PAGE analysis of affinity purified His<sub>6</sub>-IFN $\beta$  from insect cell supernatant. Lanes 1–4, Eluates 1–4; Lane 5, Pooled eluates. (B) RP-HPLC chromatogram of IFN $\beta$  purification. Nickel affinity purified and EK-Max treated IFN $\beta$  was injected onto a Phenomenex C5 RP-HPLC column and the protein resolved using a linear gradient of Acetonitrile, 0.1% TFA (Buffer B).

(Fig. 6A). The concentration of each protein at which they effectively inhibited cell proliferation by 50% (EC<sub>50</sub>) was interpreted from the graphs. With EC<sub>50</sub> values of 0.03 pmol mL<sup>-1</sup> and 0.031 pmol mL<sup>-1</sup>, respectively, the anti-proliferative activities of

His<sub>6</sub>-IFN $\beta$  and IFN $\beta$  were determined to be not significantly different. The anti-proliferative activity of IFN $\beta$  prepared via our protocol was also compared to that of the commercial IFN $\beta$ . These two proteins also have similar anti-proliferative activities over a range



**Fig. 4.** Analysis of enterokinase digestion and RP-HPLC purification of IFN $\beta$ . (A) SDS-PAGE analysis of EK-Max digested His $_6$ -IFN $\beta$  and RP-HPLC purified IFN $\beta$ . Lane 1, affinity purified His $_6$ -IFN $\beta$ ; Lane 2, affinity purified and EK-Max treated His $_6$ -IFN $\beta$ ; Lane 3, RP-HPLC Peak 1; Lane 4, RP-HPLC Peak 2. (B) Gel identical to that in part A western blotted and treated with an anti-His monoclonal antibody. Lane 1, affinity purified His $_6$ -IFN $\beta$ ; Lane 2, EK-Max treated His $_6$ -IFN $\beta$ ; Lane 3, RP-HPLC Peak 1; Lane 4, RP-HPLC Peak 2.

of IU mL $^{-1}$  concentrations (Fig. 6B). Using the respective dose response curves, the EC $_{50}$  of IFN $\beta$  and the commercial IFN $\beta$  were determined to be similar at 95.46 and 112.5 IU mL $^{-1}$ , respectively.

#### Ability of recombinant IFN $\beta$ to induce expression of interferon stimulated genes *in vivo*

To investigate the capacity of His $_6$ -IFN $\beta$  to stimulate the induction of interferon stimulated gene (ISG) expression *in vivo*, wild type mice were stimulated with 10,000 IU per mouse of either His $_6$ -IFN $\beta$  or the commercial IFN $\beta$  (triplicate mice in each group). Using qRT-PCR we found that the level of mRNA for three well-characterised ISGs, *Isg15*, *Irf7* and *Oas1a*, were equivalent in PECs extracted from mice treated with either His $_6$ -IFN $\beta$  or the commercial IFN $\beta$  (Fig. 6C). These results suggest that the His $_6$ -IFN $\beta$  prepared via the protocol described herein has an equivalent capacity to induce ISGs *in vivo* as the commercial equivalent.

## Discussion

We have developed a protocol for the large scale expression and purification of recombinant mouse IFN $\beta$ . Using insect cells as the host, the soluble recombinant protein was successfully expressed and secreted into the culture media allowing harvesting of the cytokine under native conditions. Since the recombinant IFN $\beta$  carried an amino-terminal His $_6$  tag, the initial purification step was a relatively straight-forward procedure using IMAC. Due to the acid-stable nature of the type I IFNs and the successful application of RP-HPLC for their purification by other laboratories in the past [29], we used this technique as the second chromatography step in our purification protocol.

**Table 1**  
Results of IFN $\beta$  expressed and purified from insect cell expression system.

Purification step	Total Protein (mg)	Volume (ml)	Activity (IU mL $^{-1}$ )	Specific activity (IU mg $^{-1}$ )	Total activity (IU)	Fold enrichment	Yield (%)
Supernatant	40	200	$7.9 \times 10^5$	$3.95 \times 10^6$	$1.58 \times 10^8$	1.00	100
Dialysed supernatant	34.65	210	$6.3 \times 10^5$	$3.82 \times 10^6$	$1.32 \times 10^8$	0.97	84
Ni Sepharose FF	0.31	4	$2.57 \times 10^7$	$3.32 \times 10^8$	$1.03 \times 10^8$	83.95	65
RP-HPLC His $_6$ -IFN $\beta$	0.31	0.5	$1.31 \times 10^8$	$2.11 \times 10^8$	$6.55 \times 10^7$	53.49	41
RP-HPLC, EK treated IFN $\beta^a$	0.28	0.8	$7.25 \times 10^7$	$2.07 \times 10^8$	$5.80 \times 10^7$	52.44	37

<sup>a</sup> Independent, non-consecutive purification step.

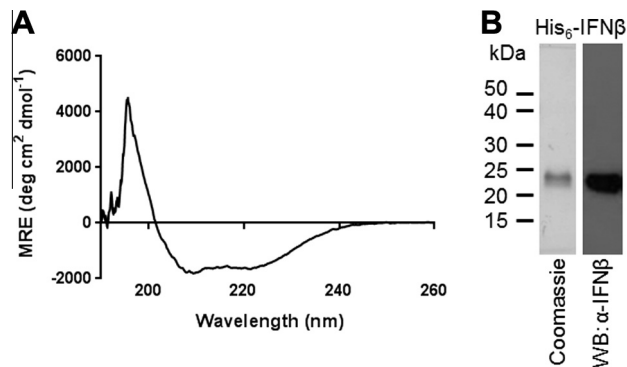


**Fig. 5.** Recombinant His $_6$ -IFN $\beta$  has the correct conformation for an  $\alpha$ -helical protein and retains epitopes of murine IFN $\beta$ . (A) Far-UV CD spectral analysis of purified recombinant His $_6$ -IFN $\beta$ . A representative scan from triplicate experiments is shown. (B) SDS-PAGE analysis of purified His $_6$ -IFN $\beta$  (left) and a similar reducing SDS-PAGE gel western blotted to PVDF and immunoblotted with an anti-mIFN $\beta$  polyclonal antiserum (right).

Insect cell culture has been used previously for the expression of human and canine IFN $\alpha$  and IFN $\beta$  [16–18,30]. Using similarly designed constructs, expression of the human proteins and canine IFN $\beta$  was also driven by the polyhedrin promoter and the products were secreted into the culture supernatant. While significant IFN activity was detected in the culture supernatant, in all three cases the proteins contained no affinity tags and no purification protocol was reported. More recently, canine IFN $\alpha$  was expressed in live *Bombyx mori* silkworm larvae using a similarly designed His $_6$  tagged IFN expression construct [30]. This expression system produced appreciably high recombinant protein yields, demonstrating the utility of insect cells for IFN production. However, as this study used live, whole larvae, multiple purification steps were required to isolate the proteins from larval debris and lipids prior to affinity chromatography. Furthermore, as an expression system, the growth and maintenance of live silkworm larvae may be difficult in many laboratory settings. Overall, that other IFNs have also been successfully expressed in insect cells demonstrates that perhaps the purification protocol reported herein may be more widely applicable to other members of this family of cytokines. From the literature we note that the amount of mammalian IFN expressed in an insect cell host greatly exceeds that reported in mammalian cell culture. For example, in Chinese hamster ovary cells, the maximal IFN activity detected in the culture supernatant represents  $\sim 2500$  fold lower activity than that detected in the supernatant of our system, thus demonstrating the increased yield benefit of an insect expression system [31].

As failure to fold biologically active proteins correctly generally produces inactive reagents, we strived to follow an expression and purification protocol that would produce natively folded proteins. Being eukaryotic, insect cells were the ideal choice for expression of mouse-derived IFN $\beta$  since they produce natively folded proteins. Indeed, the structural fold and functional integrity of the IFN $\beta$  expressed and purified by our protocol was verified using

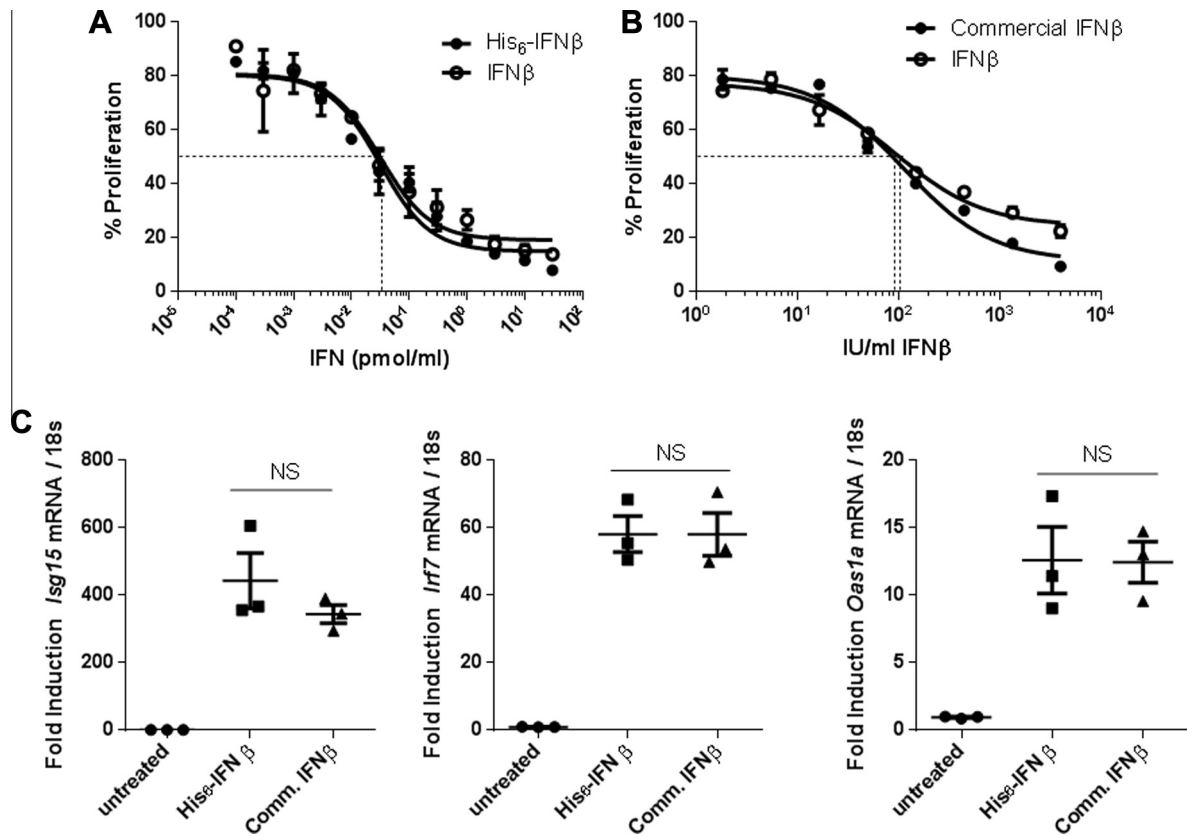


**Fig. 6.** The biological activities of recombinant IFN $\beta$  were investigated. (A) The anti-proliferative activity of His<sub>6</sub>-IFN $\beta$  and IFN $\beta$  were determined in RAW 264.7 mouse macrophage cell line and quantified by an MTT assay. Percentage proliferation is calculated as described in the methods section. The EC<sub>50</sub> of His<sub>6</sub>-IFN $\beta$  and IFN $\beta$  were determined and are indicated by overlapping hashed lines. (B) The anti-proliferative activity of IFN $\beta$  was also compared to a commercially available IFN $\beta$  using RAW 264.7 mouse macrophage cell line and quantified by an MTT assay. Percentage proliferation was calculated as for above. The EC<sub>50</sub> of IFN $\beta$  and the commercial IFN $\beta$  were determined (indicated by the hashed lines). Data points were generated from three independent experiments; mean  $\pm$  SEM are indicated. (C) Induction of *Isg15*, *Irf7* and *Oas1a* gene expression in peritoneal exudates cells extracted from wild type mice untreated or following *in vivo* stimulation with His<sub>6</sub>-IFN $\beta$  or commercial IFN $\beta$  (Comm. IFN $\beta$ ). Mean  $\pm$  SEM relative to gene levels in untreated mice are indicated. Three independent mice were used in each group.

biochemical techniques and functional assays. CD spectral analysis revealed ellipticity minima characteristic of  $\alpha$ -helical proteins, as expected for a type I IFN [32]. Recognition of the recombinant protein by an anti-mIFN $\beta$  polyclonal antiserum confirmed that mIFN $\beta$  had indeed been expressed and purified. Since the two overlapping peaks resolved by RP-HPLC had comparable anti-viral activity, and since insect cells have previously been shown to differentially glycosylate recombinant proteins, these peaks were predicted to contain different glyco-forms of IFN $\beta$  [17]. As it had been shown previously that the presence of a His<sub>6</sub> tag could affect protein activity [33,34], we anticipated that removal of the tag would be required to maximise biological activity. However, in functional assays in which the tagged (His<sub>6</sub>-IFN $\beta$ ) and non-tagged IFN $\beta$  proteins were directly compared, the presence of the His<sub>6</sub> tag had no detrimental effect on IFN $\beta$  activity. Indeed, His<sub>6</sub>-IFN $\beta$  and IFN $\beta$  had similar anti-viral and anti-proliferative potencies in these standard IFN activity assays.

We compared the functional quality of tagged (His<sub>6</sub>-IFN $\beta$ ), non-tagged IFN $\beta$  and the commercial preparation in anti-proliferative and *in vivo* experiments. Due to the fact that the commercial IFN $\beta$  was supplied containing bovine serum albumin and with concentration given only in IU mL<sup>-1</sup>, it was not possible to calculate its molarity. Thus, we compared tagged (His<sub>6</sub>-IFN $\beta$ ) and non-tagged IFN $\beta$  activity to that of the commercial preparation on an IU mL<sup>-1</sup> basis. While recombinant IFN $\beta$  expressed and purified by our protocol had similar functional capabilities as the commercial IFN $\beta$ , our product had a higher specific activity indicating a more active protein on a per milligram basis. Indeed, the specific activity of

IFN $\beta$  produced by our protocol is identical to that of IFN $\beta$  purified from native sources ( $2 \times 10^8$  IU mL<sup>-1</sup> [35]) validating the accuracy of our protocol to produce recombinant IFN $\beta$  most similar to the native form. In comparison, the commercial murine IFN $\beta$  which is purified from a bacterial over-expression system, and is therefore most likely refolded to acquire activity, has an average specific activity of  $0.29 \pm 0.20 \times 10^8$  IU mg<sup>-1</sup> (from triplicate batches) which is 10-fold less than native IFN $\beta$  suggesting the presence of inactive protein.

As bacterial endotoxins stimulate an immune response that leads to inflammation and sepsis in humans and in animal models [36], and since IFNs are often used *in vivo*, it is vital that contaminating endotoxins are minimized in reagent preparations to remove confounding biological effects of the cytokine by contaminants. With careful handling and minimal purification steps, our protocol succeeded in generating IFN $\beta$  with endotoxin levels of  $<0.01$  EU  $\mu$ g<sup>-1</sup>, below the industry recognised limit. Importantly, we have developed an expression and purification procedure to produce endotoxin-free reagents for laboratory use which is not only important for our research but may also be broadly applicable to the purification of other type I IFNs.

In summary, we describe an expression and purification protocol for the production of highly purified IFN $\beta$ . Using a two-step purification strategy, we have demonstrated that the IFN $\beta$  produced by this protocol is natively folded and possesses hallmark type I IFN anti-viral and anti-proliferative activities *in vitro* and *in vivo*. Furthermore, based on previous reports from the literature, we expect that this expression and purification protocol could be

widely applicable to other mammalian type I IFNs. The IFN $\beta$  produced via this protocol should be suitable for animal models investigating the immunomodulatory function of this cytokine or its role in therapeutic applications.

### Author contributions

SS carried out experiments, analysed data, contributed to preparing the manuscript; JAG carried out experiments, analysed data; NEM carried out *in vivo* mouse experiments, analysed data; HHR generated the expression vector and optimized protein expression conditions; JR supervised protein expression experiments; PJH supervised all biological assays and *in vitro* experimentation; NAD oversaw all aspects of this study and contributed to preparation of the manuscript.

### Acknowledgments

The authors thank Dr. Ashley Mansell of MIMR for the gift of RAW 264.7 cell line and Dr. Rebecca Smith of MIMR for manuscript and submission assistance. This work is supported by funding from the National Health and Medical Research Council (NHMRC) and the Victorian Government's Operational Infrastructure Support Program. NEM is supported by funding from the NHMRC and Australian Research Council (ARC). HHR is supported by funding from NHMRC. JR is supported by an NHMRC Australia Fellowship. PJH is supported by an NHMRC Senior Principal Research Fellowship.

### References

- [1] A. Isaacs, J. Lindenmann, Virus interference. I. The interferon, *Proc. R. Soc. Lond. B Biol. Sci.* 147 (1957) 258–267.
- [2] S. Pestka, C.D. Krause, M.R. Walter, Interferons, interferon-like cytokines, and their receptors, *Immunol. Rev.* 202 (2004) 8–32.
- [3] N.A. de Weerd, T. Nguyen, The interferons and their receptors—distribution and regulation, *Immunol. Cell Biol.* 90 (2012) 483–491.
- [4] G.R. Stark, I.M. Kerr, B.R. Williams, R.H. Silverman, R.D. Schreiber, How cells respond to interferons, *Annu. Rev. Biochem.* 67 (1998) 227–264.
- [5] R.A. Rudick, S.E. Goelz, Beta-interferon for multiple sclerosis, *Exp. Cell Res.* 317 (2011) 1301–1311.
- [6] M. Chawla-Sarkar, D.W. Leaman, E.C. Borden, Preferential induction of apoptosis by interferon (IFN)-beta compared with IFN-alpha2: correlation with TRAIL/Apo2L induction in melanoma cell lines, *Clin. Cancer Res.* 7 (2001) 1821–1831.
- [7] K.E. Thomas, C.L. Galligan, R.D. Newman, E.N. Fish, S.N. Vogel, Contribution of interferon-beta to the murine macrophage response to the toll-like receptor 4 agonist, lipopolysaccharide, *J. Biol. Chem.* 281 (2006) 31119–31130.
- [8] P.M. van Koetsveld, G. Vitale, W.W. de Herder, R.A. Feelders, K. van der Wansem, M. Waaijers, C.H. van Eijck, E.J. Speel, E. Croze, A.J. van der Lely, S.W. Lamberts, L.J. Hofland, Potent inhibitory effects of type I interferons on human adrenocortical carcinoma cell growth, *J. Clin. Endocrinol. Metab.* 91 (2006) 4537–4543.
- [9] G. Vitale, W.W. de Herder, P.M. van Koetsveld, M. Waaijers, W. Schoorlijk, E. Croze, A. Colao, S.W. Lamberts, L.J. Hofland, IFN-beta is a highly potent inhibitor of gastroenteropancreatic neuroendocrine tumor cell growth *in vitro*, *Cancer Res.* 66 (2006) 554–562.
- [10] B. Damdinsuren, H. Nagano, H. Wada, M. Kondo, H. Ota, M. Nakamura, T. Noda, J. Natsag, H. Yamamoto, Y. Doki, K. Umeshita, K. Dono, S. Nakamori, M. Sakon, M. Monden, Stronger growth-inhibitory effect of interferon (IFN)-beta compared to IFN-alpha is mediated by IFN signaling pathway in hepatocellular carcinoma cells, *Int. J. Oncol.* 30 (2007) 201–208.
- [11] J.A. Hamilton, G.A. Whitty, I. Kola, P.J. Hertzog, Endogenous IFN-alpha beta suppresses colony-stimulating factor (CSF)-1-stimulated macrophage DNA synthesis and mediates inhibitory effects of lipopolysaccharide and TNF-alpha, *J. Immunol.* 156 (1996) 2553–2557.
- [12] L.F. Coelho, G. Magno de Freitas Almeida, F.J. Mennechet, A. Blangy, G. Uze, Interferon-alpha and -beta differentially regulate osteoclastogenesis: role of differential induction of chemokine CXCL11 expression, *Proc. Natl. Acad. Sci. USA* 102 (2005) 11917–11922.
- [13] N.A. de Weerd, J.P. Vivian, T.K. Nguyen, N.E. Mangan, J.A. Gould, S.J. Braniff, L. Zaker-Tabrizi, K.Y. Fung, S.C. Forster, T. Beddoe, H.H. Reid, J. Rossjohn, P.J. Hertzog, Structural basis of a unique interferon-beta signaling axis mediated via the receptor IFNAR1, *Nat. Immunol.* 14 (2013) 901–907.
- [14] S. Pestka, The interferons: 50 years after their discovery, there is much more to learn, *J. Biol. Chem.* 282 (2007) 20047–20051.
- [15] M. Rubinstein, S. Rubinstein, P.C. Familletti, M.S. Gross, R.S. Miller, A.A. Waldman, S. Pestka, Human leukocyte interferon purified to homogeneity, *Science* 202 (1978) 1289–1290.
- [16] A. Iwata, T. Saito, N. Mizukoshi-Iwata, M. Fujino, A. Katsumata, K. Hamada, Y. Sokawa, S. Ueda, Cloning and expression of the canine interferon-beta gene, *J. Interferon Cytokine Res.* 16 (1996) 765–770.
- [17] G.E. Smith, M.D. Summers, M.J. Fraser, Production of human beta interferon in insect cells infected with a baculovirus expression vector, *Mol. Cell. Biol.* 3 (1983) 2156–2165.
- [18] S. Maeda, T. Kawai, M. Obinata, H. Fujiwara, T. Horiuchi, Y. Saeki, Y. Sato, M. Furusawa, Production of human alpha-interferon in silkworm using a baculovirus vector, *Nature* 315 (1985) 592–594.
- [19] S.A. Kaba, A.M. Salcedo, P.O. Wafula, J.M. Vlaskovic, M.M. van Oers, Development of a chitinase and v-cathepsin negative bacmid for improved integrity of secreted recombinant proteins, *J. Virol. Methods* 122 (2004) 113–118.
- [20] M.M. Bradford, A rapid and sensitive method for the quantitation of microgram quantities of protein utilizing the principle of protein-dye binding, *Anal. Biochem.* 72 (1976) 248–254.
- [21] U.K. Laemmli, Cleavage of structural proteins during the assembly of the head of bacteriophage T4, *Nature* 227 (1970) 680–685.
- [22] D.H.A. Correa, C.H.I. Ramos, The use of circular dichroism spectroscopy to study protein folding, form and function, *Afr. J. Biochem. Res.* 3 (2009) 164–173.
- [23] S.Y. Hwang, P.J. Hertzog, K.A. Holland, S.H. Sumarsono, M.J. Tymms, J.A. Hamilton, G. Whitty, I. Bertonecchio, I. Kola, A null mutation in the gene encoding a type I interferon receptor component eliminates antiproliferative and antiviral responses to interferons alpha and beta and alters macrophage responses, *Proc. Natl. Acad. Sci. USA* 92 (1995) 11284–11288.
- [24] J.S. Yuan, A. Reed, F. Chen, C.N. Stewart Jr., Statistical analysis of real-time PCR data, *BMC Bioinformatics* 7 (2006) 85–96.
- [25] L.M. Stewart, M. Hirst, M. Lopez Ferber, A.T. Merryweather, P.J. Cayley, R.D. Possee, Construction of an improved baculovirus insecticide containing an insect-specific toxin gene, *Nature* 352 (1991) 85–88.
- [26] R.M. Roberts, L. Liu, Q. Guo, D. Leaman, J. Bixby, The evolution of the type I interferons, *J. Interferon Cytokine Res.* 18 (1998) 805–816.
- [27] G. Holzwarth, P. Doty, The ultraviolet circular dichroism of polypeptides, *J. Am. Chem. Soc.* 87 (1965) 218–228.
- [28] E.P. Knight Jr., Purification of native interferons, *J. Interferon Cytokine Res.* 28 (2008) 637–638.
- [29] R.J. Salo, D.K. Bleam, V.L. Greer, A.P. Ortega, Interferon production in murine macrophage-like cell lines, *J. Leukoc. Biol.* 37 (1985) 395–406.
- [30] Z. Na, Y. HuiPeng, L. Lipan, C. Cuiping, M.L. Umashankar, L. Xingmeng, W. Xiaofeng, W. Bing, C. Weizheng, J.L. Cen, Efficient production of canine interferon-alpha in silkworm *Bombyx mori* by use of a BmNPV/Bac-to-Bac expression system, *Appl. Microbiol. Biotechnol.* 78 (2008) 221–226.
- [31] P. Zago, M. Baralle, Y.M. Ayala, N. Skoko, S. Zacchigna, E. Buratti, S. Tisminetzky, Improving human interferon-beta production in mammalian cell lines by insertion of an intronic sequence within its naturally uninterrupted gene, *Biotechnol. Appl. Biochem.* 52 (2009) 191–198.
- [32] R. Hu, J. Bekisz, H. Schmeisser, P. McPhie, K. Zoon, Human IFN-alpha protein engineering: the amino acid residues at positions 86 and 90 are important for antiproliferative activity, *J. Immunol.* 167 (2001) 1482–1489.
- [33] H. Schmeisser, P. Kontsek, D. Esposito, W. Gillette, G. Schreiber, K.C. Zoon, Binding characteristics of IFN-alpha subvariants to IFNAR2-EC and influence of the 6-histidine tag, *J. Interferon Cytokine Res.* 26 (2006) 866–876.
- [34] C.M. Halliwell, G. Morgan, C.P. Ou, A.E. Cass, Introduction of a (poly)histidine tag in L-lactate dehydrogenase produces a mixture of active and inactive molecules, *Anal. Biochem.* 295 (2001) 257–261.
- [35] E. Knight Jr., Interferon: purification and initial characterization from human diploid cells, *Proc. Natl. Acad. Sci. USA* 73 (1976) 520–523.
- [36] M.P. Glauser, G. Zanetti, J.D. Baumgartner, J. Cohen, Septic shock: pathogenesis, *Lancet* 338 (1991) 732–736.

## **Bibliography**

1. Stark, G.R., et al., *How cells respond to interferons*. Annu Rev Biochem, 1998. **67**: p. 227-64.
2. Noppert, S.J., K.A. Fitzgerald, and P.J. Hertzog, *The role of type I interferons in TLR responses*. Immunol Cell Biol, 2007. **85**(6): p. 446-457.
3. Samarajiwa, S.A., et al., *INTERFEROME: the database of interferon regulated genes*. Nucleic Acids Res, 2009. **37**(Database issue): p. D852-7.
4. Rusinova, I., et al., *Interferome v2.0: an updated database of annotated interferon-regulated genes*. Nucleic Acids Res, 2013. **41**(Database issue): p. D1040-6.
5. Pestka, S., C.D. Krause, and M.R. Walter, *Interferons, interferon-like cytokines, and their receptors*. Immunol Rev, 2004. **202**: p. 8-32.
6. Bekisz, J., et al., *Human interferons alpha, beta and omega*. Growth Factors, 2004. **22**(4): p. 243-51.
7. Domanski, P., et al., *Differential use of the betaL subunit of the type I interferon (IFN) receptor determines signaling specificity for IFNalpha2 and IFNbeta*. J Biol Chem, 1998. **273**(6): p. 3144-7.
8. Jaks, E., et al., *Differential receptor subunit affinities of type I interferons govern differential signal activation*. J Mol Biol, 2007. **366**(2): p. 525-39.
9. Thomas, C., et al., *Structural linkage between ligand discrimination and receptor activation by type I interferons*. Cell, 2011. **146**(4): p. 621-32.
10. Kalie, E., et al., *The stability of the ternary interferon-receptor complex rather than the affinity to the individual subunits dictates differential biological activities*. J Biol Chem, 2008. **283**(47): p. 32925-36.
11. Moraga, I., et al., *Receptor density is key to the alpha2/beta interferon differential activities*. Mol Cell Biol, 2009. **29**(17): p. 4778-87.
12. Levin, D., D. Harari, and G. Schreiber, *Stochastic receptor expression determines cell fate upon interferon treatment*. Mol Cell Biol, 2011. **31**(16): p. 3252-66.
13. Hardy, M.P., et al., *Characterization of the type I interferon locus and identification of novel genes*. Genomics, 2004. **84**(2): p. 331-45.
14. Isaacs, A. and J. Lindenmann, *Virus interference. I. The interferon*. Proc R Soc Lond B Biol Sci, 1957. **147**(927): p. 258-67.
15. Domanski, P., et al., *Cloning and expression of a long form of the beta subunit of the interferon alpha beta receptor that is required for signaling*. J Biol Chem, 1995. **270**(37): p. 21606-11.
16. Decker, T., M. Muller, and S. Stockinger, *The yin and yang of type I interferon activity in bacterial infection*. Nat Rev Immunol, 2005. **5**(9): p. 675-87.
17. Kotenko, S.V., et al., *IFN-lambdas mediate antiviral protection through a distinct class II cytokine receptor complex*. Nat Immunol, 2003. **4**(1): p. 69-77.
18. Sheppard, P., et al., *IL-28, IL-29 and their class II cytokine receptor IL-28R*. Nat Immunol, 2003. **4**(1): p. 63-8.
19. Schroder, K., et al., *Interferon-gamma: an overview of signals, mechanisms and functions*. J Leukoc Biol, 2004. **75**(2): p. 163-89.
20. Weigent, D.A., G.J. Stanton, and H.M. Johnson, *Interleukin 2 enhances natural killer cell activity through induction of gamma interferon*. Infect Immun, 1983. **41**(3): p. 992-7.

21. Ank, N., et al., *An important role for type III interferon (IFN-lambda/IL-28) in TLR-induced antiviral activity*. Journal of immunology, 2008. **180**(4): p. 2474-85.
22. Ank, N., et al., *Lambda interferon (IFN-lambda), a type III IFN, is induced by viruses and IFNs and displays potent antiviral activity against select virus infections in vivo*. J Virol, 2006. **80**(9): p. 4501-9.
23. Oritani, K., et al., *Limitin: An interferon-like cytokine that preferentially influences B-lymphocyte precursors*. Nature medicine, 2000. **6**(6): p. 659-66.
24. Roberts, R.M., *Interferon-tau, a Type 1 interferon involved in maternal recognition of pregnancy*. Cytokine Growth Factor Rev, 2007. **18**(5-6): p. 403-8.
25. Goeddel, D.V., et al., *The structure of eight distinct cloned human leukocyte interferon cDNAs*. Nature, 1981. **290**(5801): p. 20-6.
26. Todokoro, K., D. Kioussis, and C. Weissmann, *Two non-allelic human interferon alpha genes with identical coding regions*. EMBO J, 1984. **3**(8): p. 1809-12.
27. Hughes, A.L., *The evolution of the type I interferon gene family in mammals*. J Mol Evol, 1995. **41**(5): p. 539-48.
28. Hughes, A.L. and R.M. Roberts, *Independent origin of IFN-alpha and IFN-beta in birds and mammals*. J Interferon Cytokine Res, 2000. **20**(8): p. 737-9.
29. Chen, J., E. Baig, and E.N. Fish, *Diversity and relatedness among the type I interferons*. J Interferon Cytokine Res, 2004. **24**(12): p. 687-98.
30. Woelk, C.H., et al., *Evolution of the interferon alpha gene family in eutherian mammals*. Gene, 2007. **397**(1-2): p. 38-50.
31. Zou, J., et al., *Identification of a second group of type I IFNs in fish sheds light on IFN evolution in vertebrates*. J Immunol, 2007. **179**(6): p. 3859-71.
32. Xu, L., L. Yang, and W. Liu, *Distinct evolution process among type I interferon in mammals*. Protein Cell, 2013. **4**(5): p. 383-92.
33. Levraud, J.P., et al., *Identification of the zebrafish IFN receptor: implications for the origin of the vertebrate IFN system*. J Immunol, 2007. **178**(7): p. 4385-94.
34. Fox, B.A., P.O. Sheppard, and P.J. O'Hara, *The role of genomic data in the discovery, annotation and evolutionary interpretation of the interferon-lambda family*. PLoS One, 2009. **4**(3): p. e4933.
35. Qi, Z., et al., *Intron-containing type I and type III IFN coexist in amphibians: refuting the concept that a retroposition event gave rise to type I IFNs*. Journal of immunology, 2010. **184**(9): p. 5038-46.
36. Hamming, O.J., et al., *Crystal structure of Zebrafish interferons I and II reveals conservation of type I interferon structure in vertebrates*. J Virol, 2011. **85**(16): p. 8181-7.
37. Manry, J., et al., *Evolutionary genetic dissection of human interferons*. J Exp Med, 2011. **208**(13): p. 2747-59.
38. Demmers, K.J., K. Derecka, and A. Flint, *Trophoblast interferon and pregnancy*. Reproduction, 2001. **121**(1): p. 41-9.
39. Nourbakhsh, M., K. Hoffmann, and H. Hauser, *Interferon-beta promoters contain a DNA element that acts as a position-independent silencer on the NF-kappa B site*. EMBO J, 1993. **12**(2): p. 451-9.
40. Fujita, T., et al., *Delimitation and properties of DNA sequences required for the regulated expression of human interferon-beta gene*. Cell, 1985. **41**(2): p. 489-96.

41. Ryals, J., et al., *A 46-nucleotide promoter segment from an IFN-alpha gene renders an unrelated promoter inducible by virus*. Cell, 1985. **41**(2): p. 497-507.
42. Fujita, T., et al., *Evidence for a nuclear factor(s), IRF-1, mediating induction and silencing properties to human IFN-beta gene regulatory elements*. Embo J, 1988. **7**(11): p. 3397-405.
43. Fujita, T., et al., *Interferon-beta gene regulation: tandemly repeated sequences of a synthetic 6 bp oligomer function as a virus-inducible enhancer*. Cell, 1987. **49**(3): p. 357-67.
44. Visvanathan, K.V. and S. Goodbourn, *Double-stranded RNA activates binding of NF-kappa B to an inducible element in the human beta-interferon promoter*. EMBO J, 1989. **8**(4): p. 1129-38.
45. Hiscott, J., et al., *Induction of human interferon gene expression is associated with a nuclear factor that interacts with the NF-kappa B site of the human immunodeficiency virus enhancer*. J Virol, 1989. **63**(6): p. 2557-66.
46. Hoffmann, A., T.H. Leung, and D. Baltimore, *Genetic analysis of NF-kappaB/Rel transcription factors defines functional specificities*. Embo J, 2003. **22**(20): p. 5530-9.
47. Kirchhoff, S., et al., *NFkappaB activation is required for interferon regulatory factor-1-mediated interferon beta induction*. European journal of biochemistry / FEBS, 1999. **261**(2): p. 546-54.
48. Verstrepen, L., et al., *TLR-4, IL-1R and TNF-R signaling to NF-kappaB: variations on a common theme*. Cellular and molecular life sciences : CMLS, 2008. **65**(19): p. 2964-78.
49. Honda, K., A. Takaoka, and T. Taniguchi, *Type I interferon [corrected] gene induction by the interferon regulatory factor family of transcription factors*. Immunity, 2006. **25**(3): p. 349-60.
50. Braganca, J., et al., *Synergism between multiple virus-induced factor-binding elements involved in the differential expression of interferon A genes*. J Biol Chem, 1997. **272**(35): p. 22154-62.
51. Bisat, F., N.B. Raj, and P.M. Pitha, *Differential and cell type specific expression of murine alpha-interferon genes is regulated on the transcriptional level*. Nucleic Acids Res, 1988. **16**(13): p. 6067-83.
52. Au, W.C., et al., *Distinct activation of murine interferon-alpha promoter region by IRF-1/ISFG-2 and virus infection*. Nucleic Acids Res, 1992. **20**(11): p. 2877-84.
53. Raj, N.B., et al., *Virus infection and interferon can activate gene expression through a single synthetic element, but endogenous genes show distinct regulation*. J Biol Chem, 1989. **264**(28): p. 16658-66.
54. Doly, J., et al., *Type I interferons: expression and signalization*. Cell Mol Life Sci, 1998. **54**(10): p. 1109-21.
55. Civas, A., et al., *Repression of the murine interferon alpha 11 gene: identification of negatively acting sequences*. Nucleic Acids Res, 1991. **19**(16): p. 4497-502.
56. Genin, P., et al., *Differential regulation of human interferon A gene expression by interferon regulatory factors 3 and 7*. Mol Cell Biol, 2009. **29**(12): p. 3435-50.
57. Harada, H., et al., *Regulation of IFN-alpha/beta genes: evidence for a dual function of the transcription factor complex ISGF3 in the production and action of IFN-alpha/beta*. Genes Cells, 1996. **1**(11): p. 995-1005.
58. Sato, M., et al., *Positive feedback regulation of type I IFN genes by the IFN-inducible transcription factor IRF-7*. FEBS Lett, 1998. **441**(1): p. 106-10.

59. Fujii, Y., et al., *Crystal structure of an IRF-DNA complex reveals novel DNA recognition and cooperative binding to a tandem repeat of core sequences*. *Embo J*, 1999. **18**(18): p. 5028-41.
60. Juang, Y.T., et al., *Primary activation of interferon A and interferon B gene transcription by interferon regulatory factor 3*. *Proc Natl Acad Sci U S A*, 1998. **95**(17): p. 9837-42.
61. Tanaka, N., T. Kawakami, and T. Taniguchi, *Recognition DNA sequences of interferon regulatory factor 1 (IRF-1) and IRF-2, regulators of cell growth and the interferon system*. *Mol Cell Biol*, 1993. **13**(8): p. 4531-8.
62. Izaguirre, A., et al., *Comparative analysis of IRF and IFN-alpha expression in human plasmacytoid and monocyte-derived dendritic cells*. *J Leukoc Biol*, 2003. **74**(6): p. 1125-38.
63. Honda, K. and T. Taniguchi, *IRFs: master regulators of signalling by Toll-like receptors and cytosolic pattern-recognition receptors*. *Nat Rev Immunol*, 2006. **6**(9): p. 644-58.
64. Bjorck, P., H.X. Leong, and E.G. Engleman, *Plasmacytoid dendritic cell dichotomy: identification of IFN-alpha producing cells as a phenotypically and functionally distinct subset*. *Journal of immunology*, 2011. **186**(3): p. 1477-85.
65. Nguyen, H., J. Hiscott, and P.M. Pitha, *The growing family of interferon regulatory factors*. *Cytokine Growth Factor Rev*, 1997. **8**(4): p. 293-312.
66. Miyamoto, M., et al., *Regulated expression of a gene encoding a nuclear factor, IRF-1, that specifically binds to IFN-beta gene regulatory elements*. *Cell*, 1988. **54**(6): p. 903-13.
67. Schoggins, J.W. and C.M. Rice, *Interferon-stimulated genes and their antiviral effector functions*. *Current opinion in virology*, 2011. **1**(6): p. 519-25.
68. Kimura, T., et al., *Essential and non-redundant roles of p48 (ISGF3 gamma) and IRF-1 in both type I and type II interferon responses, as revealed by gene targeting studies*. *Genes Cells*, 1996. **1**(1): p. 115-24.
69. Matsuyama, T., et al., *Targeted disruption of IRF-1 or IRF-2 results in abnormal type I IFN gene induction and aberrant lymphocyte development*. *Cell*, 1993. **75**(1): p. 83-97.
70. Schoggins, J.W., et al., *A diverse range of gene products are effectors of the type I interferon antiviral response*. *Nature*, 2011. **472**(7344): p. 481-5.
71. Schafer, S.L., et al., *Regulation of type I interferon gene expression by interferon regulatory factor-3*. *J Biol Chem*, 1998. **273**(5): p. 2714-20.
72. Au, W.C., et al., *Identification of a member of the interferon regulatory factor family that binds to the interferon-stimulated response element and activates expression of interferon-induced genes*. *Proc Natl Acad Sci U S A*, 1995. **92**(25): p. 11657-61.
73. Sato, M., et al., *Distinct and essential roles of transcription factors IRF-3 and IRF-7 in response to viruses for IFN-alpha/beta gene induction*. *Immunity*, 2000. **13**(4): p. 539-48.
74. Honda, K., et al., *IRF-7 is the master regulator of type-I interferon-dependent immune responses*. *Nature*, 2005. **434**(7034): p. 772-7.
75. Sato, M., et al., *Involvement of the IRF family transcription factor IRF-3 in virus-induced activation of the IFN-beta gene*. *FEBS Lett*, 1998. **425**(1): p. 112-6.

76. Steinhagen, F., et al., *IRF-5 and NF-kappaB p50 co-regulate IFN-beta and IL-6 expression in TLR9-stimulated human plasmacytoid dendritic cells*. Eur J Immunol, 2013. **43**(7): p. 1896-906.
77. Pelka, K. and E. Latz, *IRF5, IRF8, and IRF7 in human pDCs - the good, the bad, and the insignificant?* Eur J Immunol, 2013. **43**(7): p. 1693-7.
78. Darnell, J.E., Jr., I.M. Kerr, and G.R. Stark, *Jak-STAT pathways and transcriptional activation in response to IFNs and other extracellular signaling proteins*. Science, 1994. **264**(5164): p. 1415-21.
79. Medzhitov, R., P. Preston-Hurlburt, and C.A. Janeway, Jr., *A human homologue of the Drosophila Toll protein signals activation of adaptive immunity*. Nature, 1997. **388**(6640): p. 394-7.
80. Lang, T. and A. Mansell, *The negative regulation of Toll-like receptor and associated pathways*. Immunol Cell Biol, 2007. **85**(6): p. 425-34.
81. Kawai, T., et al., *Interferon-alpha induction through Toll-like receptors involves a direct interaction of IRF7 with MyD88 and TRAF6*. Nat Immunol, 2004. **5**(10): p. 1061-8.
82. Kawai, T. and S. Akira, *Toll-like receptors and their crosstalk with other innate receptors in infection and immunity*. Immunity, 2011. **34**(5): p. 637-50.
83. Keating, S.E., M. Baran, and A.G. Bowie, *Cytosolic DNA sensors regulating type I interferon induction*. Trends Immunol, 2011. **32**(12): p. 574-81.
84. Hemmi, H., et al., *The roles of two I kappa B kinase-related kinases in lipopolysaccharide and double stranded RNA signaling and viral infection*. J Exp Med, 2004. **199**(12): p. 1641-50.
85. McWhirter, S.M., et al., *IFN-regulatory factor 3-dependent gene expression is defective in Tbk1-deficient mouse embryonic fibroblasts*. Proc Natl Acad Sci U S A, 2004. **101**(1): p. 233-8.
86. Sakaguchi, S., et al., *Essential role of IRF-3 in lipopolysaccharide-induced interferon-beta gene expression and endotoxin shock*. Biochem Biophys Res Commun, 2003. **306**(4): p. 860-6.
87. Liljeroos, M., et al., *Bacterial ligand of TLR2 signals Stat activation via induction of IRF1/2 and interferon-alpha production*. Cell Signal, 2008. **20**(10): p. 1873-81.
88. Yoneyama, M., et al., *The RNA helicase RIG-I has an essential function in double-stranded RNA-induced innate antiviral responses*. Nat Immunol, 2004. **5**(7): p. 730-7.
89. Loo, Y.M. and M. Gale, Jr., *Immune signaling by RIG-I-like receptors*. Immunity, 2011. **34**(5): p. 680-92.
90. Kato, H., et al., *Length-dependent recognition of double-stranded ribonucleic acids by retinoic acid-inducible gene-1 and melanoma differentiation-associated gene 5*. J Exp Med, 2008. **205**(7): p. 1601-10.
91. Takahashi, K., et al., *Nonself RNA-sensing mechanism of RIG-I helicase and activation of antiviral immune responses*. Mol Cell, 2008. **29**(4): p. 428-40.
92. Kato, H., et al., *Differential roles of MDA5 and RIG-I helicases in the recognition of RNA viruses*. Nature, 2006. **441**(7089): p. 101-5.
93. Kumar, H., et al., *Essential role of IPS-1 in innate immune responses against RNA viruses*. J Exp Med, 2006. **203**(7): p. 1795-803.
94. Yoneyama, M. and T. Fujita, *Structural mechanism of RNA recognition by the RIG-I-like receptors*. Immunity, 2008. **29**(2): p. 178-81.

95. Desmet, C.J. and K.J. Ishii, *Nucleic acid sensing at the interface between innate and adaptive immunity in vaccination*. Nat Rev Immunol, 2012. **12**(7): p. 479-91.
96. Saito, T. and M. Gale, Jr., *Differential recognition of double-stranded RNA by RIG-I-like receptors in antiviral immunity*. J Exp Med, 2008. **205**(7): p. 1523-7.
97. Girardin, S.E., et al., *Peptidoglycan molecular requirements allowing detection by Nod1 and Nod2*. J Biol Chem, 2003. **278**(43): p. 41702-8.
98. Pandey, A.K., et al., *NOD2, RIP2 and IRF5 play a critical role in the type I interferon response to Mycobacterium tuberculosis*. PLoS Pathog, 2009. **5**(7): p. e1000500.
99. Herskovits, A.A., V. Auerbuch, and D.A. Portnoy, *Bacterial ligands generated in a phagosome are targets of the cytosolic innate immune system*. PLoS Pathog, 2007. **3**(3): p. e51.
100. Leber, J.H., et al., *Distinct TLR- and NLR-mediated transcriptional responses to an intracellular pathogen*. PLoS Pathog, 2008. **4**(1): p. e6.
101. Ishikawa, H. and G.N. Barber, *STING is an endoplasmic reticulum adaptor that facilitates innate immune signalling*. Nature, 2008. **455**(7213): p. 674-8.
102. Ishikawa, H., Z. Ma, and G.N. Barber, *STING regulates intracellular DNA-mediated, type I interferon-dependent innate immunity*. Nature, 2009. **461**(7265): p. 788-92.
103. Zhong, B., et al., *The adaptor protein MITA links virus-sensing receptors to IRF3 transcription factor activation*. Immunity, 2008. **29**(4): p. 538-50.
104. Nazmi, A., et al., *STING mediates neuronal innate immune response following Japanese encephalitis virus infection*. Sci Rep, 2012. **2**: p. 347.
105. Choubey, D., et al., *Interferon-inducible p200-family proteins as novel sensors of cytoplasmic DNA: role in inflammation and autoimmunity*. J Interferon Cytokine Res, 2010. **30**(6): p. 371-80.
106. Unterholzner, L., et al., *IFI16 is an innate immune sensor for intracellular DNA*. Nat Immunol, 2010. **11**(11): p. 997-1004.
107. Sun, L., et al., *Cyclic GMP-AMP synthase is a cytosolic DNA sensor that activates the type I interferon pathway*. Science, 2013. **339**(6121): p. 786-91.
108. Ablasser, A., et al., *cGAS produces a 2'-5'-linked cyclic dinucleotide second messenger that activates STING*. Nature, 2013. **498**(7454): p. 380-4.
109. Takaoka, A., et al., *DAI (DLM-1/ZBP1) is a cytosolic DNA sensor and an activator of innate immune response*. Nature, 2007. **448**(7152): p. 501-5.
110. Yang, P., et al., *The cytosolic nucleic acid sensor LRRFIP1 mediates the production of type I interferon via a beta-catenin-dependent pathway*. Nat Immunol, 2010. **11**(6): p. 487-94.
111. LaFleur, D.W., et al., *Interferon-kappa, a novel type I interferon expressed in human keratinocytes*. J Biol Chem, 2001. **276**(43): p. 39765-71.
112. Nardelli, B., et al., *Regulatory effect of IFN-kappa, a novel type I IFN, on cytokine production by cells of the innate immune system*. J Immunol, 2002. **169**(9): p. 4822-30.
113. Harley, I.T., et al., *The role of genetic variation near interferon-kappa in systemic lupus erythematosus*. J Biomed Biotechnol, 2010. **2010**.

114. Fung, K.Y., et al., *Interferon-epsilon protects the female reproductive tract from viral and bacterial infection*. Science, 2013. **339**(6123): p. 1088-92.
115. Brierley, M.M. and E.N. Fish, *Review: IFN-alpha/beta receptor interactions to biologic outcomes: understanding the circuitry*. J Interferon Cytokine Res, 2002. **22**(8): p. 835-45.
116. Darnell, J.E., Jr., *STATs and gene regulation*. Science, 1997. **277**(5332): p. 1630-5.
117. Heim, M.H., *The Jak-STAT pathway: cytokine signalling from the receptor to the nucleus*. J Recept Signal Transduct Res, 1999. **19**(1-4): p. 75-120.
118. Gough, D.J., et al., *IFNgamma signaling-does it mean JAK-STAT?* Cytokine Growth Factor Rev, 2008. **19**(5-6): p. 383-94.
119. Plataniias, L.C., *Mechanisms of type-I- and type-II-interferon-mediated signalling*. Nat Rev Immunol, 2005. **5**(5): p. 375-86.
120. Durbin, J.E., et al., *Targeted disruption of the mouse Stat1 gene results in compromised innate immunity to viral disease*. Cell, 1996. **84**(3): p. 443-50.
121. Kristensen, I.A., et al., *Novel STAT1 alleles in a patient with impaired resistance to mycobacteria*. J Clin Immunol, 2011. **31**(2): p. 265-71.
122. Chagier, A., et al., *A partial form of recessive STAT1 deficiency in humans*. J Clin Invest, 2009. **119**(6): p. 1502-14.
123. Park, C., et al., *Immune response in Stat2 knockout mice*. Immunity, 2000. **13**(6): p. 795-804.
124. Takeda, K., et al., *Targeted disruption of the mouse Stat3 gene leads to early embryonic lethality*. Proc Natl Acad Sci U S A, 1997. **94**(8): p. 3801-4.
125. Levy, D.E. and C.K. Lee, *What does Stat3 do?* J Clin Invest, 2002. **109**(9): p. 1143-8.
126. Yang, C.H., A. Murti, and L.M. Pfeffer, *STAT3 complements defects in an interferon-resistant cell line: evidence for an essential role for STAT3 in interferon signaling and biological activities*. Proc Natl Acad Sci U S A, 1998. **95**(10): p. 5568-72.
127. Zhu, H., et al., *STAT3 induces anti-hepatitis C viral activity in liver cells*. Biochem Biophys Res Commun, 2004. **324**(2): p. 518-28.
128. Wang, W.B., D.E. Levy, and C.K. Lee, *STAT3 negatively regulates type I IFN-mediated antiviral response*. J Immunol, 2011. **187**(5): p. 2578-85.
129. Meinke, A., et al., *Activation of different Stat5 isoforms contributes to cell-type-restricted signaling in response to interferons*. Mol Cell Biol, 1996. **16**(12): p. 6937-44.
130. Seegert, D., et al., *A novel interferon-alpha-regulated, DNA-binding protein participates in the regulation of the IFP53/tryptophanyl-tRNA synthetase gene*. J Biol Chem, 1994. **269**(11): p. 8590-5.
131. Uddin, S., et al., *Role of Stat5 in type I interferon-signaling and transcriptional regulation*. Biochem Biophys Res Commun, 2003. **308**(2): p. 325-30.
132. Fish, E.N., et al., *Activation of a CrkL-stat5 signaling complex by type I interferons*. J Biol Chem, 1999. **274**(2): p. 571-3.
133. Lekmine, F., et al., *The CrkL adapter protein is required for type I interferon-dependent gene transcription and activation of the small G-protein Rap1*. Biochem Biophys Res Commun, 2002. **291**(4): p. 744-50.
134. Tough, D.F., *Modulation of T-cell function by type I interferon*. Immunology and cell biology, 2012.

135. Borden, E.C., T.F. Hogan, and J.G. Voelkel, *Comparative antiproliferative activity in vitro of natural interferons alpha and beta for diploid and transformed human cells*. Cancer research, 1982. **42**(12): p. 4948-53.
136. Malmgaard, L., et al., *Promotion of alpha/beta interferon induction during in vivo viral infection through alpha/beta interferon receptor/STAT1 system-dependent and -independent pathways*. J Virol, 2002. **76**(9): p. 4520-5.
137. Jewell, N.A., et al., *Differential type I interferon induction by respiratory syncytial virus and influenza A virus in vivo*. J Virol, 2007. **81**(18): p. 9790-800.
138. Li, W., B. Moltedo, and T.M. Moran, *Type I interferon induction during influenza virus infection increases susceptibility to secondary Streptococcus pneumoniae infection by negative regulation of gamma delta T cells*. J Virol, 2012. **86**(22): p. 12304-12.
139. Meurs, E.F., et al., *Constitutive expression of human double-stranded RNA-activated p68 kinase in murine cells mediates phosphorylation of eukaryotic initiation factor 2 and partial resistance to encephalomyocarditis virus growth*. J Virol, 1992. **66**(10): p. 5805-14.
140. Garcia, M.A., et al., *Impact of protein kinase PKR in cell biology: from antiviral to antiproliferative action*. Microbiol Mol Biol Rev, 2006. **70**(4): p. 1032-60.
141. Khabar, K.S., et al., *Effect of deficiency of the double-stranded RNA-dependent protein kinase, PKR, on antiviral resistance in the presence or absence of ribonuclease L: HSV-1 replication is particularly sensitive to deficiency of the major IFN-mediated enzymes*. J Interferon Cytokine Res, 2000. **20**(7): p. 653-9.
142. Rebouillat, D. and A.G. Hovanessian, *The human 2',5'-oligoadenylate synthetase family: interferon-induced proteins with unique enzymatic properties*. J Interferon Cytokine Res, 1999. **19**(4): p. 295-308.
143. Skaug, B. and Z.J. Chen, *Emerging role of ISG15 in antiviral immunity*. Cell, 2010. **143**(2): p. 187-90.
144. Lu, G., et al., *ISG15 enhances the innate antiviral response by inhibition of IRF-3 degradation*. Cellular and molecular biology, 2006. **52**(1): p. 29-41.
145. Zhang, D. and D.E. Zhang, *Interferon-stimulated gene 15 and the protein ISGylation system*. Journal of interferon & cytokine research : the official journal of the International Society for Interferon and Cytokine Research, 2011. **31**(1): p. 119-30.
146. Zhao, C., et al., *Human ISG15 conjugation targets both IFN-induced and constitutively expressed proteins functioning in diverse cellular pathways*. Proc Natl Acad Sci U S A, 2005. **102**(29): p. 10200-5.
147. Lenschow, D.J., et al., *IFN-stimulated gene 15 functions as a critical antiviral molecule against influenza, herpes, and Sindbis viruses*. Proc Natl Acad Sci U S A, 2007. **104**(4): p. 1371-6.
148. Strandén, A.M., P. Staeheli, and J. Pavlovic, *Function of the mouse Mx1 protein is inhibited by overexpression of the PB2 protein of influenza virus*. Virology, 1993. **197**(2): p. 642-51.
149. Staeheli, P., et al., *Influenza virus-susceptible mice carry Mx genes with a large deletion or a nonsense mutation*. Mol Cell Biol, 1988. **8**(10): p. 4518-23.
150. Roos, G., T. Leanderson, and E. Lundgren, *Interferon-induced cell cycle changes in human hematopoietic cell lines and fresh leukemic cells*. Cancer research, 1984. **44**(6): p. 2358-62.

151. Sangfelt, O., S. Erickson, and D. Grander, *Mechanisms of interferon-induced cell cycle arrest*. Front Biosci, 2000. **5**: p. D479-87.
152. Matsuoka, M., K. Tani, and S. Asano, *Interferon-alpha-induced G1 phase arrest through up-regulated expression of CDK inhibitors, p19Ink4D and p21Cip1 in mouse macrophages*. Oncogene, 1998. **16**(16): p. 2075-86.
153. Sangfelt, O., et al., *Molecular mechanisms underlying interferon-alpha-induced G0/G1 arrest: CKI-mediated regulation of G1 Cdk-complexes and activation of pocket proteins*. Oncogene, 1999. **18**(18): p. 2798-810.
154. Pelengaris, S., M. Khan, and G. Evan, *c-MYC: more than just a matter of life and death*. Nature reviews. Cancer, 2002. **2**(10): p. 764-76.
155. Einat, M., D. Resnitzky, and A. Kimchi, *Close link between reduction of c-myc expression by interferon and, G0/G1 arrest*. Nature, 1985. **313**(6003): p. 597-600.
156. Pape, K.A. and G. Floyd-Smith, *Effects of interferon-beta on Daudi cells and on small cell lung carcinoma cells which over-express the c-myc oncogene*. Anticancer research, 1989. **9**(6): p. 1737-42.
157. Jaitin, D.A. and G. Schreiber, *Upregulation of a small subset of genes drives type I interferon-induced antiviral memory*. J Interferon Cytokine Res, 2007. **27**(8): p. 653-64.
158. Subramaniam, P.S., et al., *Type I interferon induction of the Cdk-inhibitor p21WAF1 is accompanied by ordered G1 arrest, differentiation and apoptosis of the Daudi B-cell line*. Oncogene, 1998. **16**(14): p. 1885-90.
159. Yen, J.H. and D. Ganea, *Interferon beta induces mature dendritic cell apoptosis through caspase-11/caspase-3 activation*. Blood, 2009. **114**(7): p. 1344-54.
160. Thyrell, L., et al., *Mechanisms of Interferon-alpha induced apoptosis in malignant cells*. Oncogene, 2002. **21**(8): p. 1251-62.
161. Chen, Q., et al., *Apo2L/TRAIL and Bcl-2-related proteins regulate type I interferon-induced apoptosis in multiple myeloma*. Blood, 2001. **98**(7): p. 2183-92.
162. Panaretakis, T., et al., *Interferon-alpha-induced apoptosis in U266 cells is associated with activation of the proapoptotic Bcl-2 family members Bak and Bax*. Oncogene, 2003. **22**(29): p. 4543-56.
163. Takaoka, A., et al., *Integration of interferon-alpha/beta signalling to p53 responses in tumour suppression and antiviral defence*. Nature, 2003. **424**(6948): p. 516-23.
164. Porta, C., et al., *Interferons alpha and gamma induce p53-dependent and p53-independent apoptosis, respectively*. Oncogene, 2005. **24**(4): p. 605-15.
165. Chawla-Sarkar, M., et al., *Apoptosis and interferons: role of interferon-stimulated genes as mediators of apoptosis*. Apoptosis : an international journal on programmed cell death, 2003. **8**(3): p. 237-49.
166. Kayagaki, N., et al., *Type I interferons (IFNs) regulate tumor necrosis factor-related apoptosis-inducing ligand (TRAIL) expression on human T cells: A novel mechanism for the antitumor effects of type I IFNs*. J Exp Med, 1999. **189**(9): p. 1451-60.
167. Chawla-Sarkar, M., D.W. Leaman, and E.C. Borden, *Preferential induction of apoptosis by interferon (IFN)-beta compared with IFN-alpha2: correlation with TRAIL/Apo2L induction in melanoma cell lines*. Clinical cancer research : an official journal of the American Association for Cancer Research, 2001. **7**(6): p. 1821-31.

168. Selleri, C., et al., *Involvement of Fas-mediated apoptosis in the inhibitory effects of interferon-alpha in chronic myelogenous leukemia*. Blood, 1997. **89**(3): p. 957-64.
169. Pokrovskaja, K., T. Panaretakis, and D. Grander, *Alternative signaling pathways regulating type I interferon-induced apoptosis*. Journal of interferon & cytokine research : the official journal of the International Society for Interferon and Cytokine Research, 2005. **25**(12): p. 799-810.
170. Garcin, G., et al., *Differential activity of type I interferon subtypes for dendritic cell differentiation*. PLoS One, 2013. **8**(3): p. e58465.
171. Gidlund, M., et al., *Enhanced NK cell activity in mice injected with interferon and interferon inducers*. Nature, 1978. **273**(5665): p. 759-61.
172. Le Bon, A., et al., *Type I interferons potently enhance humoral immunity and can promote isotype switching by stimulating dendritic cells in vivo*. Immunity, 2001. **14**(4): p. 461-70.
173. Lee, C.K., et al., *Distinct requirements for IFNs and STAT1 in NK cell function*. Journal of immunology, 2000. **165**(7): p. 3571-7.
174. Senik, A., et al., *Enhancement by interferon of natural killer cell activity in mice*. Cell Immunol, 1979. **44**(1): p. 186-200.
175. Biron, C.A., et al., *Natural killer cells in antiviral defense: function and regulation by innate cytokines*. Annu Rev Immunol, 1999. **17**: p. 189-220.
176. Swann, J.B., et al., *Type I IFN contributes to NK cell homeostasis, activation, and antitumor function*. Journal of immunology, 2007. **178**(12): p. 7540-9.
177. Nguyen, K.B., et al., *Coordinated and distinct roles for IFN-alpha beta, IL-12, and IL-15 regulation of NK cell responses to viral infection*. Journal of immunology, 2002. **169**(8): p. 4279-87.
178. Lindahl, P., et al., *Interferon treatment of mice: enhanced expression of histocompatibility antigens on lymphoid cells*. Proc Natl Acad Sci U S A, 1976. **73**(4): p. 1284-7.
179. Hervas-Stubbs, S., et al., *Direct effects of type I interferons on cells of the immune system*. Clin Cancer Res, 2011. **17**(9): p. 2619-27.
180. Oganesyan, G., et al., *IRF3-dependent type I interferon response in B cells regulates CpG-mediated antibody production*. J Biol Chem, 2008. **283**(2): p. 802-8.
181. Braun, D., I. Caramalho, and J. Demengeot, *IFN-alpha/beta enhances BCR-dependent B cell responses*. Int Immunol, 2002. **14**(4): p. 411-9.
182. Brunner, T., et al., *Cell-autonomous Fas (CD95)/Fas-ligand interaction mediates activation-induced apoptosis in T-cell hybridomas*. Nature, 1995. **373**(6513): p. 441-4.
183. Marrack, P., J. Kappler, and T. Mitchell, *Type I interferons keep activated T cells alive*. J Exp Med, 1999. **189**(3): p. 521-30.
184. Scheel-Toellner, D., et al., *Inhibition of T cell apoptosis by IFN-beta rapidly reverses nuclear translocation of protein kinase C-delta*. European journal of immunology, 1999. **29**(8): p. 2603-12.
185. Tough, D.F., P. Borrow, and J. Sprent, *Induction of bystander T cell proliferation by viruses and type I interferon in vivo*. Science, 1996. **272**(5270): p. 1947-50.
186. Zhang, X., et al., *Potent and selective stimulation of memory-phenotype CD8+ T cells in vivo by IL-15*. Immunity, 1998. **8**(5): p. 591-9.
187. Kolumam, G.A., et al., *Type I interferons act directly on CD8 T cells to allow clonal expansion and memory formation in response to viral infection*. J Exp Med, 2005. **202**(5): p. 637-50.

188. Shiow, L.R., et al., *CD69 acts downstream of interferon-alpha/beta to inhibit S1P1 and lymphocyte egress from lymphoid organs*. Nature, 2006. **440**(7083): p. 540-4.
189. Kalaaji, A.N., et al., *Recombinant bovine interferon-alpha 1 inhibits the migration of lymphocytes from lymph nodes but not into lymph nodes*. Regional immunology, 1988. **1**(1): p. 56-61.
190. Matloubian, M., et al., *Lymphocyte egress from thymus and peripheral lymphoid organs is dependent on S1P receptor 1*. Nature, 2004. **427**(6972): p. 355-60.
191. Martal, J.L., et al., *IFN-tau: a novel subtype I IFN1. Structural characteristics, non-ubiquitous expression, structure-function relationships, a pregnancy hormonal embryonic signal and cross-species therapeutic potentialities*. Biochimie, 1998. **80**(8-9): p. 755-77.
192. Chenna, R., et al., *Multiple sequence alignment with the Clustal series of programs*. Nucleic Acids Res, 2003. **31**(13): p. 3497-500.
193. Roberts, R.M., J.C. Cross, and D.W. Leaman, *Unique features of the trophoblast interferons*. Pharmacol Ther, 1991. **51**(3): p. 329-45.
194. Lefevre, F., et al., *Interferon-delta: the first member of a novel type I interferon family*. Biochimie, 1998. **80**(8-9): p. 779-88.
195. Ezashi, T., et al., *Control of interferon-tau gene expression by Ets-2*. Proc Natl Acad Sci U S A, 1998. **95**(14): p. 7882-7.
196. Zaldumbide, A., et al., *The role of the Ets2 transcription factor in the proliferation, maturation, and survival of mouse thymocytes*. Journal of immunology, 2002. **169**(9): p. 4873-81.
197. Spencer, T.E., et al., *Pregnancy recognition and conceptus implantation in domestic ruminants: roles of progesterone, interferons and endogenous retroviruses*. Reprod Fertil Dev, 2007. **19**(1): p. 65-78.
198. Hansen, T.R., et al., *Mechanism of action of interferon-tau in the uterus during early pregnancy*. J Reprod Fertil Suppl, 1999. **54**: p. 329-39.
199. Pontzer, C.H., et al., *Antiviral activity of the pregnancy recognition hormone ovine trophoblast protein-1*. Biochem Biophys Res Commun, 1988. **152**(2): p. 801-7.
200. Gray, C.A., et al., *Identification of endometrial genes regulated by early pregnancy, progesterone, and interferon tau in the ovine uterus*. Biol Reprod, 2006. **74**(2): p. 383-94.
201. Aboagye-Mathiesen, G., et al., *Human trophoblast interferons*. Antiviral research, 1993. **22**(2-3): p. 91-105.
202. Aboagye-Mathiesen, G., et al., *Production of interferons in human placental trophoblast subpopulations and their possible roles in pregnancy*. Clin Diagn Lab Immunol, 1994. **1**(6): p. 650-9.
203. Zidovec Lepej, S., et al., *Interferon-alpha-like biological activity in human seminal plasma, follicular fluid, embryo culture medium, amniotic fluid and fetal blood*. Reprod Fertil Dev, 2003. **15**(7-8): p. 423-8.
204. Ebbesen, P., et al., *Concurrence of high levels of interferons alpha and beta in cord and maternal blood and simultaneous presence of interferon in trophoblast in an African population*. Journal of interferon & cytokine research : the official journal of the International Society for Interferon and Cytokine Research, 1995. **15**(2): p. 123-8.
205. Zdravkovic, M., et al., *High interferon alpha levels in placenta, maternal, and cord blood suggest a protective effect against intrauterine herpes simplex virus infection*. J Med Virol, 1997. **51**(3): p. 210-3.

206. Kontsek, P., *Human type I interferons: structure and function*. Acta Virol, 1994. **38**(6): p. 345-60.
207. Karpusas, M., et al., *The crystal structure of human interferon beta at 2.2-A resolution*. Proc Natl Acad Sci U S A, 1997. **94**(22): p. 11813-8.
208. Radhakrishnan, R., et al., *Zinc mediated dimer of human interferon-alpha 2b revealed by X-ray crystallography*. Structure, 1996. **4**(12): p. 1453-63.
209. Senda, T., S. Saitoh, and Y. Mitsui, *Refined crystal structure of recombinant murine interferon-beta at 2.15 A resolution*. J Mol Biol, 1995. **253**(1): p. 187-207.
210. Klaus, W., et al., *The three-dimensional high resolution structure of human interferon alpha-2a determined by heteronuclear NMR spectroscopy in solution*. J Mol Biol, 1997. **274**(4): p. 661-75.
211. Roisman, L.C., et al., *Mutational analysis of the IFNAR1 binding site on IFNalpha2 reveals the architecture of a weak ligand-receptor binding-site*. J Mol Biol, 2005. **353**(2): p. 271-81.
212. Morehead, H., P.D. Johnston, and R. Wetzel, *Roles of the 29-138 disulfide bond of subtype A of human alpha interferon in its antiviral activity and conformational stability*. Biochemistry, 1984. **23**(11): p. 2500-7.
213. Wu, D., et al., *Incomplete formation of intramolecular disulfide bond triggers degradation and aggregation of human consensus interferon-alpha mutant by Pichia pastoris*. Appl Microbiol Biotechnol, 2010. **85**(6): p. 1759-67.
214. Waive, G.J., et al., *Structure-function study of the region encompassing residues 26-40 of human interferon-alpha 4: identification of residues important for antiviral and antiproliferative activities*. J Interferon Res, 1992. **12**(1): p. 43-8.
215. Fish, E.N., *Definition of receptor binding domains in interferon-alpha*. J Interferon Res, 1992. **12**(4): p. 257-66.
216. Piehler, J., L.C. Roisman, and G. Schreiber, *New structural and functional aspects of the type I interferon-receptor interaction revealed by comprehensive mutational analysis of the binding interface*. J Biol Chem, 2000. **275**(51): p. 40425-33.
217. Day, C., et al., *Engineered disulfide bond greatly increases specific activity of recombinant murine interferon-beta*. J Interferon Res, 1992. **12**(2): p. 139-43.
218. Evinger, M., M. Rubinstein, and S. Pestka, *Antiproliferative and antiviral activities of human leukocyte interferons*. Arch Biochem Biophys, 1981. **210**(1): p. 319-29.
219. Hu, R., et al., *Human IFN-alpha protein engineering: the amino acid residues at positions 86 and 90 are important for antiproliferative activity*. J Immunol, 2001. **167**(3): p. 1482-9.
220. Pestka, S., *The human interferon alpha species and receptors*. Biopolymers, 2000. **55**(4): p. 254-87.
221. Foster, G.R., et al., *Different relative activities of human cell-derived interferon-alpha subtypes: IFN-alpha 8 has very high antiviral potency*. J Interferon Cytokine Res, 1996. **16**(12): p. 1027-33.
222. Weck, P.K., et al., *Comparison of the antiviral activities of various cloned human interferon-alpha subtypes in mammalian cell cultures*. J Gen Virol, 1981. **57**(Pt 1): p. 233-7.
223. Lavoie, T.B., et al., *Binding and activity of all human alpha interferon subtypes*. Cytokine, 2011. **56**(2): p. 282-9.

224. Ozes, O.N., et al., *A comparison of interferon-Con1 with natural recombinant interferons-alpha: antiviral, antiproliferative, and natural killer-inducing activities*. J Interferon Res, 1992. **12**(1): p. 55-9.
225. Keeffe, E.B. and F.B. Hollinger, *Therapy of hepatitis C: consensus interferon trials*. Consensus Interferon Study Group. Hepatology, 1997. **26**(3 Suppl 1): p. 101S-107S.
226. Kumaran, J., et al., *A structural basis for interferon-{alpha}-receptor interactions*. Faseb J, 2007.
227. Hu, K.Q., J.M. Vierling, and A.G. Redeker, *Viral, host and interferon-related factors modulating the effect of interferon therapy for hepatitis C virus infection*. J Viral Hepat, 2001. **8**(1): p. 1-18.
228. Moll, H.P., et al., *The differential activity of interferon-alpha subtypes is consistent among distinct target genes and cell types*. Cytokine, 2011. **53**(1): p. 52-9.
229. Ortaldo, J.R., et al., *A species of human alpha interferon that lacks the ability to boost human natural killer activity*. Proc Natl Acad Sci U S A, 1984. **81**(15): p. 4926-9.
230. Jaitin, D.A., et al., *Inquiring into the differential action of interferons (IFNs): an IFN-alpha2 mutant with enhanced affinity to IFNAR1 is functionally similar to IFN-beta*. Mol Cell Biol, 2006. **26**(5): p. 1888-97.
231. Sanceau, J., et al., *IFN-beta induces serine phosphorylation of Stat-1 in Ewing's sarcoma cells and mediates apoptosis via induction of IRF-1 and activation of caspase-7*. Oncogene, 2000. **19**(30): p. 3372-83.
232. Tsuno, T., et al., *IRF9 is a key factor for eliciting the antiproliferative activity of IFN-alpha*. J Immunother, 2009. **32**(8): p. 803-16.
233. Kalie, E., et al., *An interferon alpha2 mutant optimized by phage display for IFNAR1 binding confers specifically enhanced antitumor activities*. J Biol Chem, 2007. **282**(15): p. 11602-11.
234. de Weerd, N.A., et al., *Structural basis of a unique interferon-beta signaling axis mediated via the receptor IFNAR1*. Nat Immunol, 2013. **14**(9): p. 901-7.
235. Mangan, N.E. and K.Y. Fung, *Type I interferons in regulation of mucosal immunity*. Immunology and cell biology, 2012. **90**(5): p. 510-9.
236. Schaefer, T.M., et al., *Innate immunity in the human female reproductive tract: antiviral response of uterine epithelial cells to the TLR3 agonist poly(I:C)*. Journal of immunology, 2005. **174**(2): p. 992-1002.
237. Wira, C.R., K.S. Grant-Tschudy, and M.A. Crane-Godreau, *Epithelial cells in the female reproductive tract: a central role as sentinels of immune protection*. Am J Reprod Immunol, 2005. **53**(2): p. 65-76.
238. Iijima, N., J.M. Thompson, and A. Iwasaki, *Dendritic cells and macrophages in the genitourinary tract*. Mucosal immunology, 2008. **1**(6): p. 451-9.
239. Croy, B.A., et al., *Uterine natural killer cells: insights into their cellular and molecular biology from mouse modelling*. Reproduction, 2003. **126**(2): p. 149-60.
240. Givan, A.L., et al., *Flow cytometric analysis of leukocytes in the human female reproductive tract: comparison of fallopian tube, uterus, cervix, and vagina*. American journal of reproductive immunology, 1997. **38**(5): p. 350-9.
241. Hunt, J.S., M.G. Petroff, and T.G. Burnett, *Uterine leukocytes: key players in pregnancy*. Seminars in cell & developmental biology, 2000. **11**(2): p. 127-37.

242. Manaster, I. and O. Mandelboim, *The unique properties of uterine NK cells*. American journal of reproductive immunology, 2010. **63**(6): p. 434-44.
243. Zhang, J., B.A. Croy, and Z. Tian, *Uterine natural killer cells: their choices, their missions*. Cellular & molecular immunology, 2005. **2**(2): p. 123-9.
244. Sentman, C.L., C.R. Wira, and M. Eriksson, *NK cell function in the human female reproductive tract*. American journal of reproductive immunology, 2007. **57**(2): p. 108-15.
245. Zhao, X., et al., *Vaginal submucosal dendritic cells, but not Langerhans cells, induce protective Th1 responses to herpes simplex virus-2*. J Exp Med, 2003. **197**(2): p. 153-62.
246. Keenihan, S.N. and S.A. Robertson, *Diversity in phenotype and steroid hormone dependence in dendritic cells and macrophages in the mouse uterus*. Biol Reprod, 2004. **70**(6): p. 1562-72.
247. Kaul, R., et al., *The genital tract immune milieu: an important determinant of HIV susceptibility and secondary transmission*. J Reprod Immunol, 2008. **77**(1): p. 32-40.
248. Peng, F.W., et al., *Purification of recombinant human interferon-epsilon and oligonucleotide microarray analysis of interferon-epsilon-regulated genes*. Protein Expr Purif, 2007. **53**(2): p. 356-62.
249. Huang, J., et al., *Inhibition of type I and type III interferons by a secreted glycoprotein from Yaba-like disease virus*. Proc Natl Acad Sci U S A, 2007. **104**(23): p. 9822-7.
250. Day, S.L., et al., *Differential Effects of the Type I Interferons {alpha}4, {beta}, and {epsilon} on Antiviral Activity and Vaccine Efficacy*. J Immunol, 2008. **180**(11): p. 7158-66.
251. Xi, Y., et al., *Role of novel type I interferon epsilon in viral infection and mucosal immunity*. Mucosal immunology, 2012.
252. Knight, E.P., Jr., *Purification of native interferons*. Journal of interferon & cytokine research : the official journal of the International Society for Interferon and Cytokine Research, 2008. **28**(11): p. 637-8.
253. Pestka, S., *Purification and cloning of interferon alpha*. Current topics in microbiology and immunology, 2007. **316**: p. 23-37.
254. Knight, E., Jr., *Heterogeneity of purified mouse interferons*. J Biol Chem, 1975. **250**(11): p. 4139-44.
255. Knight, E., Jr., *Antiviral and cell growth inhibitory activities reside in the same glycoprotein of human fibroblast interferon*. Nature, 1976. **262**(5566): p. 302-3.
256. Rubinstein, M., et al., *Human leukocyte interferon: production, purification to homogeneity, and initial characterization*. Proc Natl Acad Sci U S A, 1979. **76**(2): p. 640-4.
257. Zoon, K.C., et al., *Purification and partial characterization of human lymphoblast interferon*. Proc Natl Acad Sci U S A, 1979. **76**(11): p. 5601-5.
258. Shi, L., et al., *Efficient expression and purification of human interferon alpha2b in the methylotrophic yeast, Pichia pastoris*. Protein Expr Purif, 2007. **54**(2): p. 220-6.
259. Loignon, M., et al., *Stable high volumetric production of glycosylated human recombinant IFNalpha2b in HEK293 cells*. BMC biotechnology, 2008. **8**: p. 65.
260. Maeda, S., et al., *Construction and identification of bacterial plasmids containing nucleotide sequence for human leukocyte interferon*. Proc Natl Acad Sci U S A, 1980. **77**(12): p. 7010-3.

261. Goeddel, D.V., et al., *Synthesis of human fibroblast interferon by E. coli*. Nucleic Acids Res, 1980. **8**(18): p. 4057-74.
262. Goeddel, D.V., et al., *Human leukocyte interferon produced by E. coli is biologically active*. Nature, 1980. **287**(5781): p. 411-6.
263. Salo, R.J., et al., *Interferon production in murine macrophage-like cell lines*. J Leukoc Biol, 1985. **37**(4): p. 395-406.
264. Kaba, S.A., et al., *Development of a chitinase and v-cathepsin negative bacmid for improved integrity of secreted recombinant proteins*. Journal of virological methods, 2004. **122**(1): p. 113-8.
265. Livak, K.J. and T.D. Schmittgen, *Analysis of relative gene expression data using real-time quantitative PCR and the 2(-Delta Delta C(T)) Method*. Methods, 2001. **25**(4): p. 402-8.
266. Stifter, S.A., et al., *Purification and biological characterization of soluble, recombinant mouse IFNbeta expressed in insect cells*. Protein Expr Purif, 2014. **94**: p. 7-14.
267. Hardy, M.P., et al., *The soluble murine type I interferon receptor Ifnar-2 is present in serum, is independently regulated, and has both agonistic and antagonistic properties*. Blood, 2001. **97**(2): p. 473-82.
268. Piganis, R.A., et al., *Suppressor of cytokine signaling (SOCS) 1 inhibits type I interferon (IFN) signaling via the interferon alpha receptor (IFNAR1)-associated tyrosine kinase Tyk2*. J Biol Chem, 2011. **286**(39): p. 33811-8.
269. Millen, S.H., et al., *Identification and characterization of the carbohydrate ligands recognized by pertussis toxin via a glycan microarray and surface plasmon resonance*. Biochemistry, 2010. **49**(28): p. 5954-67.
270. Butt, T.R., et al., *SUMO fusion technology for difficult-to-express proteins*. Protein Expr Purif, 2005. **43**(1): p. 1-9.
271. Cull, V.S., E.J. Bartlett, and C.M. James, *Type I interferon gene therapy protects against cytomegalovirus-induced myocarditis*. Immunology, 2002. **106**(3): p. 428-37.
272. Iwata, A., et al., *Cloning and expression of the canine interferon-beta gene*. Journal of interferon & cytokine research : the official journal of the International Society for Interferon and Cytokine Research, 1996. **16**(10): p. 765-70.
273. Maeda, S., et al., *Production of human alpha-interferon in silkworm using a baculovirus vector*. Nature, 1985. **315**(6020): p. 592-4.
274. Smith, G.E., M.D. Summers, and M.J. Fraser, *Production of human beta interferon in insect cells infected with a baculovirus expression vector*. Mol Cell Biol, 1983. **3**(12): p. 2156-65.
275. Pikaart, M.J. and G. Felsenfeld, *Expression and codon usage optimization of the erythroid-specific transcription factor cGATA-1 in baculoviral and bacterial systems*. Protein Expr Purif, 1996. **8**(4): p. 469-75.
276. Yang, M., S.C. Johnson, and P.P. Murthy, *Enhancement of alkaline phytase production in Pichia pastoris: Influence of gene dosage, sequence optimization and expression temperature*. Protein Expr Purif, 2012. **84**(2): p. 247-54.
277. Retnoningrum, D.S., et al., *Codon optimization for high level expression of human bone morphogenetic protein - 2 in Escherichia coli*. Protein Expr Purif, 2012. **84**(2): p. 188-94.
278. Davis, T.R., et al., *Comparative recombinant protein production of eight insect cell lines*. In vitro cellular & developmental biology. Animal, 1993. **29A**(5): p. 388-90.

279. Gasteiger E., H.C., Gattiker A., Duvaud S., Wilkins M.R., Appel R.D., Bairoch A., ed. *Protein Identification and Analysis Tools on the ExPASy Server*. The Proteomics Protocols Handbook, ed. J.M. Walker. 2005, Humana Press. 571-607.
280. Shahravan, S.H., et al., *Enhancing the specificity of the enterokinase cleavage reaction to promote efficient cleavage of a fusion tag*. Protein Expr Purif, 2008. **59**(2): p. 314-9.
281. Vagenende, V., M.G. Yap, and B.L. Trout, *Mechanisms of protein stabilization and prevention of protein aggregation by glycerol*. Biochemistry, 2009. **48**(46): p. 11084-96.
282. van Pesch, V., et al., *Characterization of the murine alpha interferon gene family*. J Virol, 2004. **78**(15): p. 8219-28.
283. Tamassia, N., et al., *IFN-beta expression is directly activated in human neutrophils transfected with plasmid DNA and is further increased via TLR-4-mediated signaling*. Journal of immunology, 2012. **189**(3): p. 1500-9.
284. Croset, A., et al., *Differences in the glycosylation of recombinant proteins expressed in HEK and CHO cells*. J Biotechnol, 2012. **161**(3): p. 336-48.
285. Brooks, S.A., *Protein glycosylation in diverse cell systems: implications for modification and analysis of recombinant proteins*. Expert Rev Proteomics, 2006. **3**(3): p. 345-59.
286. Kirkpatrick, R.B., et al., *Bacterial production of biologically active canine interleukin-1beta by seamless SUMO tagging and removal*. Protein Expr Purif, 2006. **50**(1): p. 102-10.
287. Matsumiya, T., S.M. Prescott, and D.M. Stafforini, *IFN-epsilon mediates TNF-alpha-induced STAT1 phosphorylation and induction of retinoic acid-inducible gene-1 in human cervical cancer cells*. J Immunol, 2007. **179**(7): p. 4542-9.
288. Runkel, L., et al., *Structural and functional differences between glycosylated and non-glycosylated forms of human interferon-beta (IFN-beta)*. Pharmaceutical research, 1998. **15**(4): p. 641-9.
289. Misaki, R., et al., *N-linked glycan structures of mouse interferon-beta produced by Bombyx mori larvae*. Biochem Biophys Res Commun, 2003. **311**(4): p. 979-86.
290. Utsumi, J., et al., *Stability of human interferon-beta 1: oligomeric human interferon-beta 1 is inactive but is reactivated by monomerization*. Biochimica et biophysica acta, 1989. **998**(2): p. 167-72.
291. Wu, J. and M. Filutowicz, *Hexahistidine (His6)-tag dependent protein dimerization: a cautionary tale*. Acta Biochim Pol, 1999. **46**(3): p. 591-9.
292. Arnau, J., et al., *Reprint of: Current strategies for the use of affinity tags and tag removal for the purification of recombinant proteins*. Protein Expr Purif, 2011.
293. Waugh, D.S., *An overview of enzymatic reagents for the removal of affinity tags*. Protein Expr Purif, 2011. **80**(2): p. 283-93.
294. Pestka, S., *The human interferons--from protein purification and sequence to cloning and expression in bacteria: before, between, and beyond*. Arch Biochem Biophys, 1983. **221**(1): p. 1-37.
295. Blomkalns, A.L., et al., *Low level bacterial endotoxin activates two distinct signaling pathways in human peripheral blood mononuclear cells*. J Inflamm (Lond), 2011. **8**: p. 4.
296. Kelly, S.M., T.J. Jess, and N.C. Price, *How to study proteins by circular dichroism*. Biochim Biophys Acta, 2005. **1751**(2): p. 119-39.

297. De Maeyer-Guignard, J., et al., *Purification of mouse interferon by sequential affinity chromatography on poly(U)--and antibody--agarose columns.* Nature, 1978. **271**(5646): p. 622-5.
298. Gupta, R.J., E.; Brunak, S., *Prediction of N-glycosylation sites in human proteins.* in preparation, 2004.
299. Stromqvist, M. and H. Gruffman, *Periodic acid/Schiff staining of glycoproteins immobilized on a blotting matrix.* Biotechniques, 1992. **13**(5): p. 744-6, 749.
300. Hwang, S.Y., et al., *A null mutation in the gene encoding a type I interferon receptor component eliminates antiproliferative and antiviral responses to interferons alpha and beta and alters macrophage responses.* Proc Natl Acad Sci U S A, 1995. **92**(24): p. 11284-8.
301. Loveland, B.E., et al., *Validation of the MTT dye assay for enumeration of cells in proliferative and antiproliferative assays.* Biochem Int, 1992. **27**(3): p. 501-10.
302. Berger Rentsch, M. and G. Zimmer, *A vesicular stomatitis virus replicon-based bioassay for the rapid and sensitive determination of multi-species type I interferon.* PLoS One, 2011. **6**(10): p. e25858.
303. de Veer, M.J., et al., *Functional classification of interferon-stimulated genes identified using microarrays.* J Leukoc Biol, 2001. **69**(6): p. 912-20.
304. Kugel, D., et al., *Novel nonviral bioassays for mouse type I and type III interferon.* Journal of interferon & cytokine research : the official journal of the International Society for Interferon and Cytokine Research, 2011. **31**(4): p. 345-9.
305. Kiessling, R., et al., *Genetic variation of in vitro cytolytic activity and in vivo rejection potential of non-immunized semi-syngeneic mice against a mouse lymphoma line.* Int J Cancer, 1975. **15**(6): p. 933-40.
306. Welsh, R.M., et al., *Interferon-mediated protection of normal and tumor target cells against lysis by mouse natural killer cells.* J Immunol, 1981. **126**(1): p. 219-25.
307. Piontek, G.E., et al., *YAC-1 MHC class I variants reveal an association between decreased NK sensitivity and increased H-2 expression after interferon treatment or in vivo passage.* J Immunol, 1985. **135**(6): p. 4281-8.
308. Radulovic, K., et al., *CD69 regulates type I IFN-induced tolerogenic signals to mucosal CD4 T cells that attenuate their colitogenic potential.* Journal of immunology, 2012. **188**(4): p. 2001-13.
309. Benlahrech, A., et al., *Human NK Cell Up-regulation of CD69, HLA-DR, Interferon gamma Secretion and Cytotoxic Activity by Plasmacytoid Dendritic Cells is Regulated through Overlapping but Different Pathways.* Sensors, 2009. **9**(1): p. 386-403.
310. Borrego, F., J. Pena, and R. Solana, *Regulation of CD69 expression on human natural killer cells: differential involvement of protein kinase C and protein tyrosine kinases.* European journal of immunology, 1993. **23**(5): p. 1039-43.
311. Merigan, T.C., *Purified Interferons: Physical Properties and Species Specificity.* Science, 1964. **145**(3634): p. 811-3.
312. Samuel, C.E. and D.A. Farris, *Mechanism of interferon action. Species specificity of interferon and of the interferon-mediated inhibitor of translation from mouse, monkey, and human cells.* Virology, 1977. **77**(2): p. 556-65.
313. Oritani, K., et al., *T lymphocytes constitutively produce an interferonlike cytokine limitin characterized as a heat- and acid-stable and heparin-binding glycoprotein.* Blood, 2003. **101**(1): p. 178-85.

314. Harrison, R.L. and D.L. Jarvis, *Protein N-glycosylation in the baculovirus-insect cell expression system and engineering of insect cells to produce "mammalianized" recombinant glycoproteins*. *Advances in virus research*, 2006. **68**: p. 159-91.
315. Jarvis, D.L. and E.E. Finn, *Modifying the insect cell N-glycosylation pathway with immediate early baculovirus expression vectors*. *Nature biotechnology*, 1996. **14**(10): p. 1288-92.
316. Johnston, M.J., et al., *O-linked glycosylation leads to decreased thermal stability of interferon alpha 2b as measured by two orthogonal techniques*. *Pharmaceutical research*, 2011. **28**(7): p. 1661-7.
317. Dissing-Olesen, L., et al., *The function of the human interferon-beta 1a glycan determined in vivo*. *J Pharmacol Exp Ther*, 2008. **326**(1): p. 338-47.
318. Fu, X.Y., et al., *ISGF3, the transcriptional activator induced by interferon alpha, consists of multiple interacting polypeptide chains*. *Proc Natl Acad Sci U S A*, 1990. **87**(21): p. 8555-9.
319. Pan, M., et al., *Mutation of the IFNAR-1 receptor binding site of human IFN-alpha2 generates type I IFN competitive antagonists*. *Biochemistry*, 2008. **47**(46): p. 12018-27.
320. Yang, I., et al., *Modulation of major histocompatibility complex Class I molecules and major histocompatibility complex-bound immunogenic peptides induced by interferon-alpha and interferon-gamma treatment of human glioblastoma multiforme*. *Journal of neurosurgery*, 2004. **100**(2): p. 310-9.
321. Halloran, P.F., et al., *Regulation of MHC expression in vivo. II. IFN-alpha/beta inducers and recombinant IFN-alpha modulate MHC antigen expression in mouse tissues*. *Journal of immunology*, 1989. **142**(12): p. 4241-7.
322. Atzeni, F., et al., *Induction of CD69 activation molecule on human neutrophils by GM-CSF, IFN-gamma, and IFN-alpha*. *Cell Immunol*, 2002. **220**(1): p. 20-9.
323. Borrego, F., et al., *CD69 is a stimulatory receptor for natural killer cell and its cytotoxic effect is blocked by CD94 inhibitory receptor*. *Immunology*, 1999. **97**(1): p. 159-65.
324. Ziegler, S.F., F. Ramsdell, and M.R. Alderson, *The activation antigen CD69*. *Stem cells*, 1994. **12**(5): p. 456-65.
325. Sun, S., et al., *Type I interferon-mediated stimulation of T cells by CpG DNA*. *J Exp Med*, 1998. **188**(12): p. 2335-42.
326. Wills, R.J., *Clinical pharmacokinetics of interferons*. *Clinical pharmacokinetics*, 1990. **19**(5): p. 390-9.
327. Wills, R.J., et al., *Interferon kinetics and adverse reactions after intravenous, intramuscular, and subcutaneous injection*. *Clinical pharmacology and therapeutics*, 1984. **35**(5): p. 722-7.
328. Buchwalder, P.A., et al., *Pharmacokinetics and pharmacodynamics of IFN-beta 1a in healthy volunteers*. *Journal of interferon & cytokine research : the official journal of the International Society for Interferon and Cytokine Research*, 2000. **20**(10): p. 857-66.
329. Villa, E., et al., *Alpha but not beta interferon is useful in chronic active hepatitis due to hepatitis C virus. A prospective, double-blind, randomized study*. *Digestive diseases and sciences*, 1996. **41**(6): p. 1241-7.
330. Wagner, R.R., *Biological studies of interferon. I. Suppression of cellular infection with eastern equine encephalomyelitis virus*. *Virology*, 1961. **13**: p. 323-37.

331. Gresser, I., et al., *Pronounced antiviral activity of human interferon on bovine and porcine cells*. Nature, 1974. **251**(5475): p. 543-5.
332. Radhakrishnan, R., et al., *Crystal structure of ovine interferon-tau at 2.1 Å resolution*. J Mol Biol, 1999. **286**(1): p. 151-62.
333. Kumaran, J., et al., *A structural basis for interferon-alpha-receptor interactions*. FASEB journal : official publication of the Federation of American Societies for Experimental Biology, 2007. **21**(12): p. 3288-96.
334. Sheehan, K.C., et al., *Blocking monoclonal antibodies specific for mouse IFN-alpha/beta receptor subunit 1 (IFNAR-1) from mice immunized by in vivo hydrodynamic transfection*. Journal of interferon & cytokine research : the official journal of the International Society for Interferon and Cytokine Research, 2006. **26**(11): p. 804-19.
335. Guo, X., *Surface plasmon resonance based biosensor technique: a review*. Journal of biophotonics, 2012. **5**(7): p. 483-501.
336. Schuck, P., *Use of surface plasmon resonance to probe the equilibrium and dynamic aspects of interactions between biological macromolecules*. Annu Rev Biophys Biomol Struct, 1997. **26**: p. 541-66.
337. Lin, S., et al., *Determination of Binding Constant and Stoichiometry for Antibody-Antigen Interaction with Surface Plasmon Resonance*. Current Proteomics, 2006. **3**(4): p. 271-282.
338. Hsi, E.D., *A practical approach for evaluating new antibodies in the clinical immunohistochemistry laboratory*. Archives of pathology & laboratory medicine, 2001. **125**(2): p. 289-94.
339. Pal, S., et al., *Factors influencing the induction of infertility in a mouse model of Chlamydia trachomatis ascending genital tract infection*. J Med Microbiol, 1998. **47**(7): p. 599-605.
340. Li, Q., et al., *Interferon-alpha initiates type 1 diabetes in nonobese diabetic mice*. Proc Natl Acad Sci U S A, 2008. **105**(34): p. 12439-44.
341. Poovassery, J.S. and G.A. Bishop, *Type I IFN receptor and the B cell antigen receptor regulate TLR7 responses via distinct molecular mechanisms*. Journal of immunology, 2012. **189**(4): p. 1757-64.
342. Nagarajan, U.M., et al., *Type I interferon signaling exacerbates Chlamydia muridarum genital infection in a murine model*. Infect Immun, 2008. **76**(10): p. 4642-8.
343. Petersen, T.N., et al., *SignalP 4.0: discriminating signal peptides from transmembrane regions*. Nature methods, 2011. **8**(10): p. 785-6.
344. Rudick, R.A. and S.E. Goelz, *Beta-interferon for multiple sclerosis*. Experimental cell research, 2011. **317**(9): p. 1301-11.
345. Volberding, P.A., et al., *Treatment of Kaposi's sarcoma with interferon alfa-2b (Intron A)*. Cancer, 1987. **59**(3 Suppl): p. 620-5.
346. Tarhini, A.A., H. Gogas, and J.M. Kirkwood, *IFN-alpha in the treatment of melanoma*. Journal of immunology, 2012. **189**(8): p. 3789-93.
347. Vedantham, S., H. Gamliel, and H.M. Golomb, *Mechanism of interferon action in hairy cell leukemia: a model of effective cancer biotherapy*. Cancer research, 1992. **52**(5): p. 1056-66.
348. Manns, M.P., H. Wedemeyer, and M. Cornberg, *Treating viral hepatitis C: efficacy, side effects, and complications*. Gut, 2006. **55**(9): p. 1350-9.
349. Novick, D., et al., *Affinity chromatography of human fibroblast interferon (IFN-beta 1) by monoclonal antibody columns*. The Journal of general virology, 1983. **64** (Pt 4): p. 905-10.

350. Allen, G., et al., *Analysis and purification of human lymphoblastoid (Namalwa) interferon using a monoclonal antibody*. The Journal of general virology, 1982. **63 (Pt 1)**: p. 207-12.
351. Anfinsen, C.B., et al., *Partial purification of human interferon by affinity chromatography*. Proc Natl Acad Sci U S A, 1974. **71(8)**: p. 3139-42.
352. Marchetti, M., et al., *Stat-mediated signaling induced by type I and type II interferons (IFNs) is differentially controlled through lipid microdomain association and clathrin-dependent endocytosis of IFN receptors*. Mol Biol Cell, 2006. **17(7)**: p. 2896-909.
353. Hewitt, E.W., *The MHC class I antigen presentation pathway: strategies for viral immune evasion*. Immunology, 2003. **110(2)**: p. 163-9.
354. Koelle, D.M. and L. Corey, *Recent progress in herpes simplex virus immunobiology and vaccine research*. Clinical microbiology reviews, 2003. **16(1)**: p. 96-113.
355. Tseng, C.T. and R.G. Rank, *Role of NK cells in early host response to chlamydial genital infection*. Infect Immun, 1998. **66(12)**: p. 5867-75.
356. Sandberg-Wollheim, M., et al., *Pregnancy outcomes during treatment with interferon beta-1a in patients with multiple sclerosis*. Neurology, 2005. **65(6)**: p. 802-6.
357. Boskovic, R., et al., *The reproductive effects of beta interferon therapy in pregnancy: a longitudinal cohort*. Neurology, 2005. **65(6)**: p. 807-11.
358. Subramaniam, P.S., et al., *Differential recognition of the type I interferon receptor by interferons tau and alpha is responsible for their disparate cytotoxicities*. Proc Natl Acad Sci U S A, 1995. **92(26)**: p. 12270-4.
359. Chon, T.W. and S. Bixler, *Interferon-tau: current applications and potential in antiviral therapy*. Journal of interferon & cytokine research : the official journal of the International Society for Interferon and Cytokine Research, 2010. **30(7)**: p. 477-85.
360. Pontzer, C.H., et al., *Potent anti-feline immunodeficiency virus and anti-human immunodeficiency virus effect of IFN-tau*. Journal of immunology, 1997. **158(9)**: p. 4351-7.
361. Alexenko, A.P., A.D. Ealy, and R.M. Roberts, *The cross-species antiviral activities of different IFN-tau subtypes on bovine, murine, and human cells: contradictory evidence for therapeutic potential*. Journal of interferon & cytokine research : the official journal of the International Society for Interferon and Cytokine Research, 1999. **19(12)**: p. 1335-41.
362. Khan, O.A., et al., *Immunomodulating functions of recombinant ovine interferon tau: potential for therapy in multiple sclerosis and autoimmune disorders*. Multiple sclerosis, 1998. **4(2)**: p. 63-9.
363. Yang, J. and G.R. Stark, *Roles of unphosphorylated STATs in signaling*. Cell research, 2008. **18(4)**: p. 443-51.
364. Cheon, H. and G.R. Stark, *Unphosphorylated STAT1 prolongs the expression of interferon-induced immune regulatory genes*. Proc Natl Acad Sci U S A, 2009. **106(23)**: p. 9373-8.
365. Paavonen, J. and M. Lehtinen, *Chlamydial pelvic inflammatory disease*. Human reproduction update, 1996. **2(6)**: p. 519-29.
366. Croy, B.A., et al., *Uterine natural killer cells: insights into lineage relationships and functions from studies of pregnancies in mutant and transgenic mice*. Natural immunity, 1996. **15(1)**: p. 22-33.
367. Brandstadter, J.D. and Y. Yang, *Natural killer cell responses to viral infection*. J Innate Immun, 2011. **3(3)**: p. 274-9.

